USGS
science for a changing world

Prepared in cooperation with the Fort Irwin National Training Center

Geohydrology, Geochemistry, and Numerical Simulation of Groundwater Flow and Land Subsidence in the Bicycle Basin, Fort Irwin National Training Center, California

Scientific Investigations Report 2018–5067

U.S. Department of the Interior
U.S. Geological Survey

Cover photographs:

Front cover: Aerial view of the Bicycle Basin and Bicycle Lake (dry) playa. (Photograph from Fort Irwin National Training Center, 2007)

Back cover: Bicycle Lake playa inundated following several winter storms. View looking east across the playa at Tiefort Mountain. (Photo taken on December 23, 2010, J.N. Densmore, U.S. Geolgical Survey.)

Geohydrology, Geochemistry, and Numerical Simulation of Groundwater Flow and Land Subsidence in the Bicycle Basin, Fort Irwin National Training Center, California

By Jill N. Densmore, Linda R. Woolfenden, Diane L. Rewis, Peter M. Martin, Michelle Sneed, Kevin M. Ellett, Michael Solt, and David M. Miller

Prepared in cooperation with the Fort Irwin National Training Center

Scientific Investigations Report 2018–5067

U.S. Department of the Interior
U.S. Geological Survey

U.S. Department of the Interior
RYAN K. ZINKE, Secretary

U.S. Geological Survey
James F. Reilly II, Director

U.S. Geological Survey, Reston, Virginia: 2018

Suggested citation:
Densmore, J.N., Woolfenden L.R., Rewis, D.L., Martin, P.M., Sneed, M., Ellett, K.M., Solt, M., and Miller, D.M., 2018, Geohydrology, geochemistry, and numerical simulation of groundwater flow and land subsidence in the Bicycle Basin, Fort Irwin National Training Center, California: U.S. Geological Survey Scientific Investigations Report 2018–5067, 176 p., https://doi.org/10.3133/sir20185067.

ISSN 2328-0328 (online)

Contents

Contents—Continued

Figures

Figures—Continued

Figures—Continued

Tables

Tables—Continued

Tables—Continued

Conversion Factors

U.S. customary units to International System of Units

Multiply	By	To obtain
	Length	
inch (in.)	25.4	millimeter (mm)
inch (in.)	12	foot (ft)
inch (in.)	25,400	micrometer (µm)
foot (ft)	0.3048	meter (m)
mile (mi)	1.609	kilometer (km)
	Area	
square foot (ft^2)	0.09290	square meter (m^2)
square mile (mi^2)	2.590	square kilometer (km^2)
	Volume	
cubic foot (ft^3)	0.02832	cubic meter (m^3)
ounce, fluid (fl. oz)	29.5735	milliliter (mL)
acre-foot (acre-ft)	43,560	cubic feet (ft^3)
acre-foot (acre-ft)	1,233	cubic meter (m^3)
	Flow rate	
acre-foot per year (acre-ft/yr)	1,233	cubic meter per year (m^3/yr)
foot per day (ft/d)	0.3048	meter per day (m/d)
foot per year (ft/yr)	0.3048	meter per year (m/yr)
inch per second (in/s)	6.675	millimeter per month (mm/mo)
inch per month (in/mo)	9.66513	millimeter per second (mm/s)
inch per year (in/yr)	25.4	millimeter per year (mm/yr)
	Mass	
pound, avoirdupois (lb)	0.4536	kilogram (kg)
	Specific capacity	
gallon per minute per foot [gpm/ft]	0.2070	liter per second per meter ([L/s]/m)
	Hydraulic conductivity	
foot per day (ft/d)	0.3048	meter per day (m/d)
	Transmissivity	
foot squared per day (ft^2/d)	0.09290	meter squared per day (m^2/d)

Temperature in degrees Celsius (°C) may be converted to degrees Fahrenheit (°F) as follows:

$$°F = (1.8 \times °C) + 32.$$

Temperature in degrees Fahrenheit (°F) may be converted to degrees Celsius (°C) as follows:

$$°C = (°F - 32) / 1.8.$$

Datum

Vertical coordinate information is referenced to the North American Vertical Datum of 1988 (NAVD 88).

Horizontal coordinate information is referenced to the North American Datum of 1983 (NAD 83).

Altitude, as used in this report, refers to distance above the vertical datum.

Supplemental Information

Transmissivity: The standard unit for transmissivity is cubic foot per day per square foot times foot of aquifer thickness ($[ft^3/d]/ft^2$)ft. In this report, the mathematically reduced form, foot squared per day (ft^2/d), is used for convenience.

Specific conductance is given in microsiemens per centimeter at 25 degrees Celsius (µS/cm at 25 °C).

Concentrations of chemical constituents in water are given in either milligrams per liter (mg/L) or micrograms per liter (µg/L).

Activities for radioactive constituents in water are given in picocuries per liter (pCi/L).

Results for measurements of stable isotopes of an element (with symbol E) in water, solids, and dissolved constituents commonly are expressed as the relative difference in the ratio of the number of the less abundant isotope (iE) to the number of the more abundant isotope of a sample with respect to a measurement standard.

Abbreviations

As	arsenic
bls	below land surface
^{14}C	carbon-14
Cl	chloride
D	deuterium
F	fluoride
H	hydrogen
^{2}H	deuterium
^{3}H	tritium

Abbreviations—Continued

HCO_3	bicarbonate
Hchar	Hydraulic characteristic
HK	horizontal hydraulic conductivity
InSAR	interferometric synthetic aperture radar
Na	sodium
NO_3	nitrate
NTC	National Training Center
O	oxygen
^{18}O	oxygen-18
pmC	percent modern carbon
PVC	polyvinyl chloride
PET	potential evapotranspiration
RMSE	root-mean-squared error
SO_4	sulfate
SP	spontaneous potential
Ske	elastic skeletal specific storage (for instantaneous compaction)
Sske	elastic skeletal specific storage (for delayed compaction)
Skv	inelastic skeletalspecific storage (for instantaneous compaction)
Sskv	inelastic skeletalspecific storage (for delayed compaction)
SS	specific storage
SY	specific yield
TEM	transient electromagnetic
TDS	total dissolved solids
TU	tritium units
USEPA	U.S. Environmental Protection Agency
USGS	U.S. Geological Survey
VANI	vertical anisotropy, defined as ratio of HK to VK
Vki	vertical hydraulic conductivity (for delayed compaction)
VK	vertical hydraulic conductivity
VSMOW	Vienna Standard Mean Ocean Water
Bc	basement complex
Qoa	Quaternary older alluvium
Qp	Quaternary playa deposits
Qya	Quaternary younger alluvial deposits

Abbreviations—Continued

QToa	Quaternary-Tertiary older alluvium
QTol	Quaternary-Tertiary older clay lacustrine
Tog	Tertiary older alluvium
Tv	Tertiary volcanic rocks
Tyg	Tertiary younger alluvium

Well-numbering System

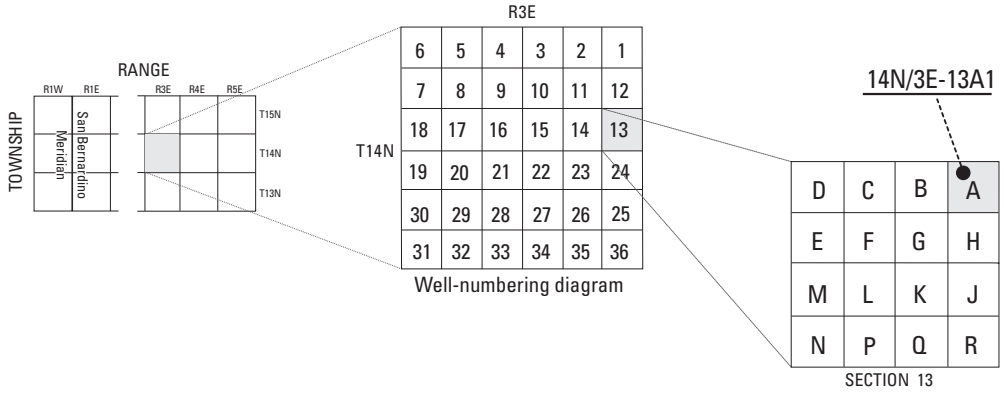

Wells are assigned a state well number (station name) by the California Department of Water Resources according to the location in the rectangular township and range grid system for the subdivision of public lands. Station names consist of the township number, north or south; the range number, east or west; and the section number. Each section is divided into sixteen 40-acre tracts lettered consecutively (except "I" and "O"), beginning with "A" in the northeast corner of the section and progressing in a sinusoidal manner to "R" in the southeast corner. Within the 40-acre tract, numbers are assigned sequentially in the order the wells are inventoried. The next letter within the station name refers to the base line and meridian. California has three base lines and meridians—Humboldt (H), Mount Diablo (M), and San Bernardino (S). Wells in the study area are referenced to the San Bernardino and Mount Diablo base line and meridian (S and M). Well numbers consist of 15 characters and follow the format 012N003E01M001S. In this report, wells are abbreviated and written as 12N/03E-01M1S. Wells are abbreviated in figures by their section number, tract letter, and sequence number (for example, 1M1). In addition to a station name assigned by the California Department of Water Resources, wells were assigned a common name derived from the basin in which they were installed and a sequence number. Wells were also assigned a 15-digit site identification number in the U.S. Geological Survey National Water Information System database.

Geohydrology, Geochemistry, and Numerical Simulation of Groundwater Flow and Land Subsidence in the Bicycle Basin, Fort Irwin National Training Center, California

By Jill N. Densmore, Linda R. Woolfenden, Diane L. Rewis, Peter M. Martin, Michelle Sneed, Kevin M. Ellett[1], Michael Solt[2], and David M. Miller

Abstract

Groundwater pumping from Bicycle Groundwater Basin (referred to as Bicycle Basin) in the Fort Irwin National Training Center, California, began in 1967. From 1967 to December 2010, about 46,000 acre-feet of water had been pumped from the basin and transported to the Irwin Basin. During this time, not only did water levels in the basin decline by as much as 100 feet, the quality of the groundwater pumped from the basin also deteriorated in some wells.

The U.S. Geological Survey collected geohydrologic data from existing wells, test holes, and 16 additional monitoring wells installed at 6 sites in Bicycle Basin during 1992–2011 to determine the quantity and quality of groundwater available in the basin. Geophysical surveys, including electrical, gravity, and seismic refraction surveys, were completed to help determine the geometry of the structural basin, delineate depths to the interface between Quaternary and Tertiary rocks, map the depth to the water table, and used to develop a geohydrologic framework and groundwater-flow model for Bicycle Basin.

Water samples were used to determine the groundwater quality in the basin and to delineate potential sources of poor-quality groundwater. Analysis of stable isotopes of oxygen and hydrogen in groundwater indicated that present-day precipitation is not a major source of recharge to the basin. Tritium and carbon-14 data indicated that most of the groundwater in the basin was recharged prior to 1952 and had an apparent age of 15,625–39,350 years. Natural recharge to the basin was not sufficient to replenish the groundwater pumped from the basin. Interferograms from synthetic aperture radar data (InSAR), analyzed to evaluate land-surface subsidence between 1993 and 2010, showed 0.23 to 1.1 feet of subsidence during this period near one production well north of Bicycle Lake (dry) playa.

A groundwater-flow model of Bicycle Basin was developed and calibrated using groundwater levels for 1964–2010, and a subsidence model using land-surface deformation data for 1993–2010. Between January 1967 and December 2010, the simulated total recharge from precipitation runoff and underflow from adjacent basins was about 5,100 acre-feet and pumpage from the Bicycle Basin was about 47,000 acre-feet of water. Total outflows exceeded natural recharge during this period, resulting in a net loss of about 42,100 acre-feet of groundwater storage in the basin.

The Fort Irwin National Training Center is considering various groundwater-management options in the Bicycle Basin. The groundwater-flow model was used to (1) evaluate changes in groundwater levels and subsidence with the addition of capture and recharge of simulated runoff in retention basins (scenario 1) for predevelopment through 2010; (2) simulate a base case (scenario 2) for reference; and (3) compare projections of alternative future pumping strategies for 2011–60 (scenarios 3–5).

Model results from the runoff-capture simulation (scenario 1) indicated that total recharge, including runoff captured using retention basins, locally increased water levels, which partially offset, but did not mitigate, groundwater depletion associated with pumping. Groundwater-storage depletion in scenario 1 was about 14 percent less than without runoff capture. Simulated-drawdown results in model layer 1 in the eastern part of the basin indicated that, because of the captured runoff, simulated heads were as much as 100 feet higher in December 2010 than prior to the onset of development in 1967. In contrast, simulated drawdown for model without runoff capture indicated that, without captured runoff, simulated heads for December 2010 in this area were 80–90 feet lower than during the predevelopment period. Subsidence was mitigated slightly in scenario 1 compared to without runoff capture; the largest decrease in subsidence at observation sites was about 0.07 feet.

[1]Indiana Geological and Water Survey, Indiana University.

[2]Langan Engineering and Environmental Services.

Scenario 2 results indicated that simulated drawdown in model layer 6 at the end of 2060 ranged from about 46 to 135 feet. Subsidence at observation sites at the end of 2060 ranged from 0.83 to 2.8 feet. Reducing the base case pumping rate by 25 percent in the existing production well in the subsidence area and redistributing the pumpage to the other two production wells (scenario 3) resulted in a reduction of drawdown in the subsidence area compared with the base case (scenario 2). The difference in subsidence at the end of 2060 between scenario 3 and the base case was small (less than 0.07 feet) for all observation locations. Repeating the simulation scenario 3 but additionally reducing the basin-wide pumpage by 3 percent per year from 2011 through 2020 (scenario 4) resulted in about 60 feet less drawdown in the subsidence area than for the base case. Subsidence at observation sites ranged from 0.12 to 0.43 feet less than for the base case. Reducing the pumpage in the existing production well in the subsidence area to zero, while continuing the base case pumping rate in the other two existing production wells (scenario 5), resulted in more than 100 feet less drawdown in the subsidence area than in the base case. The simulated subsidence at the end of 2060 ranged from about 0.19 to about 1.16 feet less than in the base case, indicating that the discontinuation of pumpage at well 14N/3E-14P1 would result in substantially reduced subsidence.

Overall, continued water-table declines dewatered the more productive upper layers of the aquifer, causing more groundwater to be withdrawn from deeper, lower yielding layers and resulting in faster declines in the water table and greater vertical gradients in the future. If the water table declines into the perforated intervals of wells, increased maintenance costs and altered well-water quality could potentially result. Water-management scenario 1 indicated that adding managed recharge resulted in a modest decrease (4–5 percent) in the rate of subsidence compared with historical conditions. The reduction of pumpage in the area of subsidence and redistribution of the amount of reduced pumpage to wells in other parts of the basin (scenario 3) resulted in modest decreases (5–6 percent) in the rate of subsidence compared with continuation of historical pumpage. Including either a basin-wide reduction of pumpage of 3 percent annually (cumulatively, a 24 percent decrease) as well as redistribution of the pumpage (scenario 4) or discontinuing pumping in the area of greatest subsidence (scenario 5), however, demonstrated that subsidence could be reduced substantially (22–26 percent for scenario 4 and 62–68 percent for scenario 5) compared with subsidence for continuing historical pumpage.

Introduction

Fort Irwin National Training Center (NTC) in the Mojave Desert of southern California has been used as a military training facility almost continuously since August 1940. Fort Irwin NTC obtains its potable water (as of 2018) from groundwater in the Irwin, Bicycle, and Langford Groundwater Basins (fig. 1). Groundwater pumpage exceeds natural recharge, resulting in water-level declines in these basins. Several production wells have been abandoned or destroyed because of water-quality concerns. To effectively manage the water resources and plan for future water needs at Fort Irwin NTC, a complete understanding of the geohydrologic and geochemical framework of Irwin, Langford, and Bicycle Basins is needed.

In 1992, the U.S. Geological Survey (USGS) entered into an agreement with Fort Irwin NTC to monitor and evaluate the groundwater resources of the Fort Irwin NTC. The reader is referred to Densmore and Londquist (1997), Densmore (2003), Voronin and others (2013), and Voronin and others (2014) for more information. The work presented in this report was completed under a continuation of this agreement. The objectives of the study are to describe the geohydrologic and geochemical framework of the groundwater basins that supply water to the Fort Irwin NTC, to develop groundwater-flow models that help refine the understanding of the geohydrology of these basins, and to use this information to evaluate the long-term availability of groundwater for the Fort Irwin NTC.

Purpose and Scope

This report describes the geohydrologic and geochemical framework of Bicycle Basin and how the information was utilized to develop a groundwater-flow model for Bicycle Basin to evaluate the long-term availability of groundwater in the basin.

Available geohydrologic and geochemical data were compiled for the Bicycle Basin, and new data were collected from existing wells. Additional work included geophysical surveys (gravity, seismic refraction, and time-domain electromagnetic induction) to refine understanding of the size and shape of the basin and provide additional information about the stratigraphy. Monitoring wells were installed during 1993–2011 to provide depth-dependent geohydrologic and geochemical data.

Water-quality samples were collected and analyzed for major ions and trace elements to evaluate possible sources of groundwater-quality degradation. Samples also were analyzed for the stable isotopes oxygen-18 (^{18}O) and deuterium (D) to determine the source of groundwater and for the radioactive isotopes of tritium (^{3}H) and carbon-14 (^{14}C) to evaluate the relative age of groundwater (years since the water entered the groundwater system) in the basin.

A conceptual model of the geohydrologic system was developed using data compiled and collected for this study, including lithologic and geophysical data from available boreholes (data shown in appendix 1). The conceptual model and groundwater-level data were used to develop and calibrate a groundwater-flow model of the Bicycle Basin.

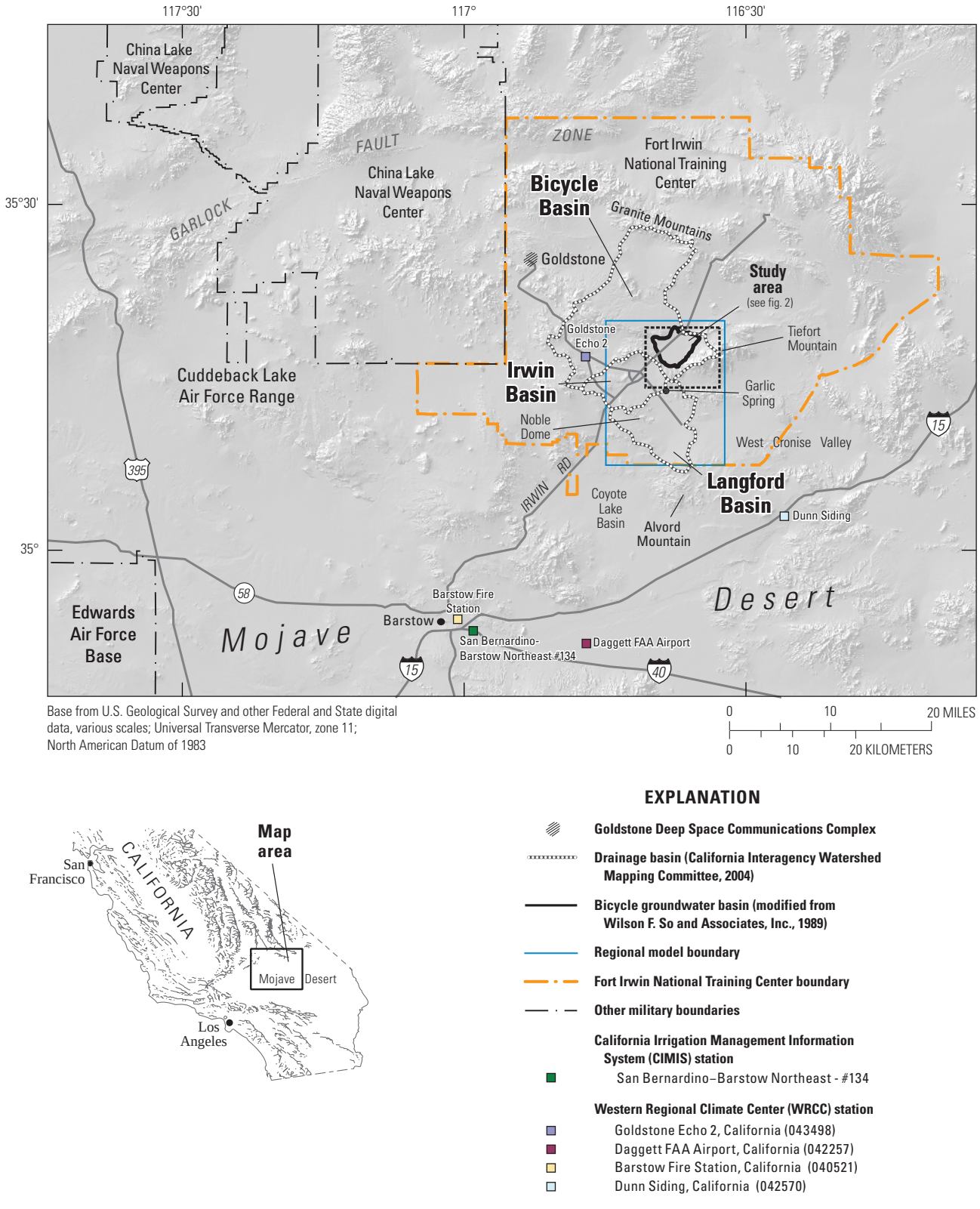

Figure 1. Location of study area, Fort Irwin National Training Center, California.

The groundwater-flow model is intended to provide a better understanding of the geohydrology of the basin and to help estimate the long-term availability of groundwater from the basin by evaluating changes in groundwater-level altitudes (or hydraulic heads) under different runoff-capture and pumping scenarios. The model also was used to evaluate the subsidence caused by continued pumping and its effect on fissuring that has developed on Bicycle Lake (dry) playa.

Location and Description of Study Area

Fort Irwin NTC is about 130 miles (mi) northeast of Los Angeles in the Mojave Desert region of southern California (fig. 1). The NTC covers an area of about 1,177 square miles (mi^2) that contain several surface-water drainage basins, including Irwin, Bicycle, and Langford Basins. Bicycle Basin is near the center of Fort Irwin NTC, about 35 mi northeast of Barstow, California.

Bicycle Groundwater Basin (fig. 1), referred to as Bicycle Basin in this report, lies in the southeastern part of the much larger Bicycle Valley drainage basin (about 140 mi^2); the Bicycle Basin covers an area of about 10.5 mi^2 (fig. 1). Bicycle Basin, typical of desert basins in the Mojave Desert, is a closed basin with a relatively flat floor surrounded by generally rugged mountains or low-lying hills. Bicycle Valley drainage basin is bounded to the north by the Granite Mountains, to the east by Tiefort Mountain, to the south by low-lying hills that separate Bicycle Basin from Irwin Basin, and to the west by low-lying hills that separate Bicycle Basin from the highlands near Goldstone (fig. 1). Bicycle Lake (dry), a playa, lies in the southern part of Bicycle Basin (fig. 2). The floor of Bicycle Basin ranges in altitude from about 2,350 feet (ft) North American Vertical Datum of 1988 (NAVD 88) at the playa to about 2,600 ft at the base of Tiefort Mountain. No perennial streams are present in the basin, but the washes can flow for several days after large storms. Surface water in Bicycle Basin drains to the playa, the lowest part of the basin. No vegetation grows on Bicycle Lake (dry) playa or on its margins; however, a small, vegetated area that might be supported by a localized, shallow perched zone or a buried well described in Mendenhall (1909, p. 54), is in the northeastern part of the playa.

The climate of Bicycle Basin, typical of the Mojave Desert region, is characterized by low precipitation, hot summers, and cool winters. Sporadic weather records for 2003–08 were available for Bicycle Basin. Weather records were available for nearby Goldstone, about 11 mi west of the basin, for 1973–2006 (Western Region Climate Center, 2009) and for Barstow for 1943–2013 (National Oceanic and Atmospheric Administration, 1994, 2010, 2013), which indicated average annual precipitation was about 7 inches (in.) and ranged from 2 to 15 in. between 1950 and 2013). Most precipitation falls during the winter, but some precipitation from isolated thunderstorms falls during the summer months. The average annual temperature at Barstow between 1940 and 2009 was 64 degrees Fahrenheit (°F), and temperatures ranged from 3 to 121 °F (EarthInfo, Inc., 1995, 2000; California Irrigation Management Information System, station 134, 1997–2013, accessed February 17, 2009, at http://wwwcimis.water.ca.gov/Stations.aspx, replaced by station 234, 2015–16, accessed June 26, 2016). The average annual potential evapotranspiration was about 140 in. for Death Valley (1961–2005, accessed July 26, 2016, at https://wrcc.dri.edu/Climate/comp_table_show.php?stype=pan_evap_avg), about 35 mi northeast of the basin, and about 78 in. at Newberry Springs (not shown on fig. 1), about 25 mi to the south (1987–99, California Department of Water Resources, p. 25, accessed July 26, 2016, at http://www.water.ca.gov/wateruseefficiency/docs/MWELO09-10-09.pdf).

Previous Studies

Previous studies of Bicycle Basin have been completed by the USGS and by several consulting and engineering companies. Kunkel and Riley (1959) reported on a geological reconnaissance of the basin. Yount and others (1994) and Schermer and others (1996) published detailed geologic maps. Groundwater-availability studies were published by C.F. Hostrup and Associates (1955), James M. Montgomery and Associates (1981), and Wilson F. So and Associates (1989). In conjunction with the present study, gravity data collected during 1999 and 2010–11 were used to develop a depth-to-basement map and the subsequent altitude of the basement complex (Jachens and Langenheim, 2014). A seismic-refraction survey was used to provide information about different lithologic layers (David Berger, U.S. Geological Survey, written commun., 1996).

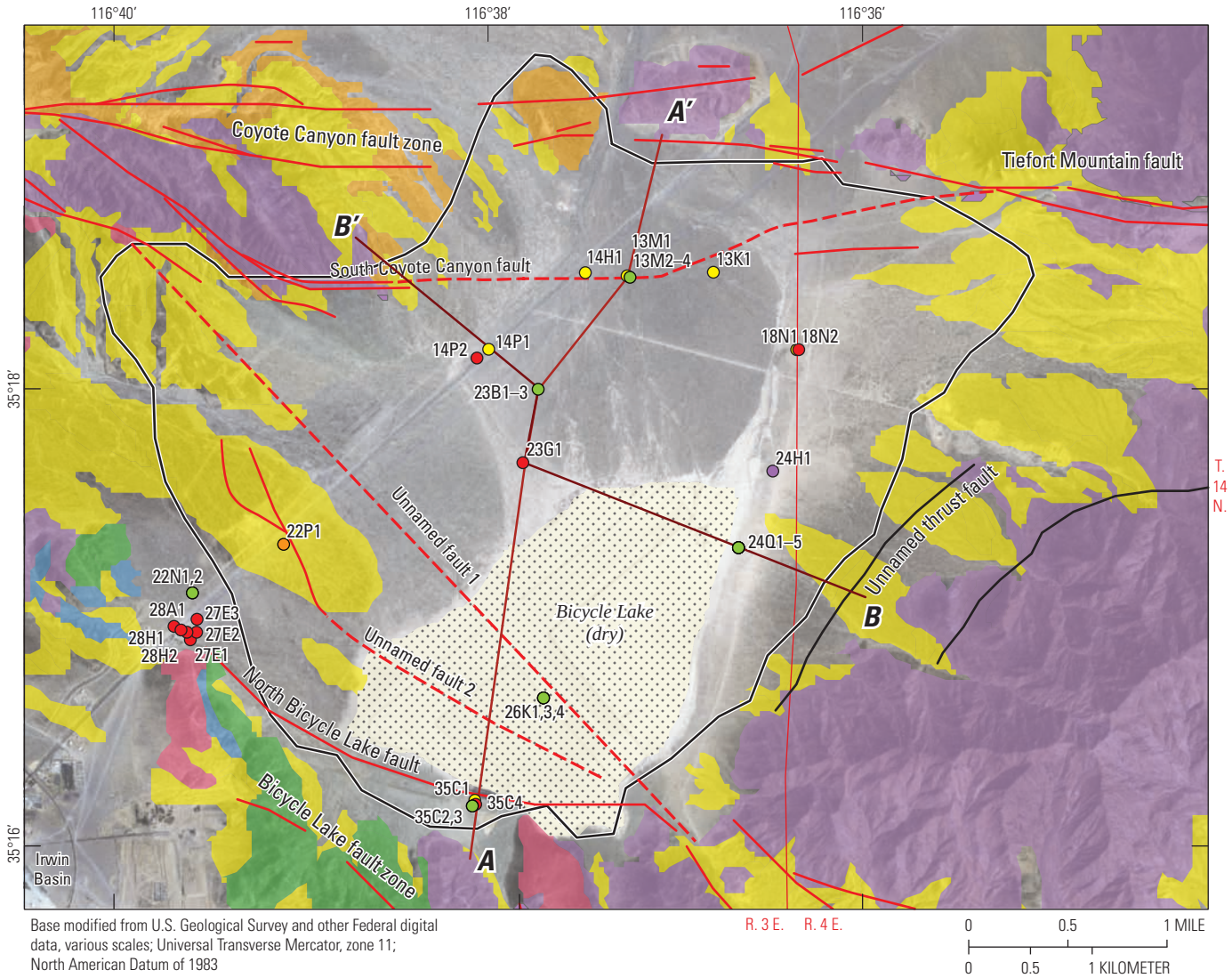

Figure 2. Generalized surficial geology, major faults, locations of groundwater monitoring sites and production wells, and geologic section lines in Bicycle Basin, Fort Irwin National Training Center, California.

Geohydrologic Framework

The geohydrologic framework of the Bicycle Basin was developed by evaluating information from previously published reports, by doing geophysical surveys, and by collecting geologic and hydrologic data from existing and newly drilled wells. Table 1 lists the local well name, state well number, and well-construction data for all wells used in this report.

Geology

The geology of Bicycle Basin was previously described by C.F. Hostrup and Associates (1955), Kunkel and Riley (1959), James M. Montgomery and Associates (1981), Wilson F. So and Associates (1989), Yount and others (1994), Schermer and others (1996), and Miller and Yount (2002). The geologic discussion presented in this report summarizes information from these reports and updates the geology on the basis of work completed as part of this study.

Geologic Units

For this study, the geologic units are grouped into five generalized units: (1) pre-Tertiary basement complex (Bc), (2) Tertiary volcanic rocks (Tv), (3) Tertiary sedimentary deposits (Tog, Tp, and Tyg), (4) Quaternary-Tertiary older alluvium and lacustrine deposits (QToa and QTol), and (5) Quaternary older and younger alluvium and playa deposits (Qoa, Qya, and Qp). The older and younger Tertiary sedimentary deposits and Quaternary-Tertiary lacustrine deposits (Tog, Tyg, and QTol) are in the subsurface, but not mapped at the surface. The structural and stratigraphic relationships in Bicycle Basin are presented in figures 2 and 3. The basin fill represents the water-bearing deposits that consist of Tertiary sedimentary deposits (Tog and Tyg), Quaternary-Tertiary older alluvium and lacustrine deposits (QToa and QTol), Quaternary older alluvium and clay, Quaternary younger alluvium, and Quaternary playa deposits (Qoa, Qya, and Qp). These deposits are unconsolidated at land surface and become moderately to well consolidated with depth.

The basement complex is exposed in the hills surrounding Bicycle Basin and underlies the basin (figs. 2, 3). The pre-Tertiary basement complex consists of mostly felsic and mafic plutonic rocks; metamorphic rocks consisting of marble, quartzite, and schist; carbonate rock consisting of dolomite or limestone; and metasedimentary and metavolcanic rocks (Yount and others, 1994; Schermer and others, 1996; Miller and Yount, 2002). Volcanic rocks (Yount and others, 1994) crop out in the hills to the northwest, west, and southwest of Bicycle Basin (Schermer and others, 1996; Miller and Yount, 2002). Although it is possible that these volcanic rocks underlie at least part of the basin fill, no boreholes have penetrated them. The basement complex has low permeability, and water generally is contained only where these rocks are extensively jointed, fractured, or weathered. Although the "weathered" zone of the basement complex might contain water, it was considered non-water-bearing because it is likely that only small amounts of groundwater are stored in the fractures (Densmore and Londquist, 1997).

Tertiary volcanic rocks (Tv) are exposed south and west of Bicycle Basin along an approximately north-trending, low-lying ridge in the Bicycle Lake fault zone as well as northwest of the basin in several fault blocks on the south side of and in the Coyote Canyon fault zone (fig. 2). This distribution correlates with lava that flowed from the southeast, through what is now Bicycle Basin, and to the northwest (Miller and Yount, 2002, fig. 11). Time-domain or transient electromagnetic (TEM) surveys (Burgess and Bedrosan, 2014) in the southwestern part of the basin and west of Bicycle Lake (dry) playa showed higher resistivity at depth, and seismic surveys showed layers with higher seismic wave velocity at depth, as described in the next section. These geophysical data indicated a different layer with higher resistivity and seismic wave velocity is present at depth; this layer could represent buried volcanic rock, although no boreholes were present west of the playa to confirm. The Tertiary volcanic rocks (Tv) generally have low permeability, and water generally is contained only where these rocks are extensively jointed, fractured, or weathered.

Tertiary sedimentary deposits are exposed in the low-lying hills to the north, west, and south of Bicycle Basin; they overlie the basement complex and partially fill the basin (Miller and Yount, 2002; figs. 2, 3). These deposits include older gravels (Tog), younger gravels (Tyg), and paludal deposits (Tp, which are typically fine-grained evaporates, clay, silt, and fine sand deposited in spring or marsh environments; Yount and others, 1994). The older and younger gravels (Tog and Tyg) are moderately to well consolidated, poorly sorted coarse sands and gravels to boulder-sized clasts, primarily derived of granitic and volcanic material; the older gravels (Tog), which are more consolidated, are much less permeable than the overlying younger gravels (Tyg; see "Aquifer System Definitions" section). The paludal deposits (Tp) tend to coarsen upward and laterally to sand and pebble conglomerate of the Tertiary younger gravel (Tyg). Where sand and gravel predominate, the Tertiary deposits might yield moderate amounts of groundwater to wells.

Table 1. Summary of construction data for production and monitoring wells in the Bicycle Basin, Fort Irwin Training Center, California.

[Location of wells are shown in figure 2. **Abbreviations**: Bc, basement complex; D, well destroyed; ft, feet; ID, identification; M, monitoring well; NA, well not in model domain; NAVD 88, North American Vertical Datum of 1988; P, production well; Qoa, Quaternary older alluvium; QToa, QToa1, QToa2, Quaternary-Tertiary older alluvium; QTol, Qaternary-Tertiary older lacustrine; Qya, Quaternary younger alluvium; Tog, Tertiary older gravels; TW, test well; Tyg, Tertiary younger gravels; U, unused well; —, data not available]

State well number	Short ID	Local ID	Well type	Date drilled	Geology	Land-surface altitude, in feet, NAVD 88 (ft)	Hole depth (ft)	Well depth (ft)	Screen top (ft)	Screen bottom (ft)	Screen thickness (ft)	Model layers	Area
14N/3E-13K1S	-13K1	B-1	P[1]	January 1955	QToa, Tyg	2,398	600	600	180	580	400	1–7	Central
14N/3E-13M1S	-13M1	B-4	P	May 1965	QToa, Tyg	2,419	614	600	226	594	368	2–7	North
14N/3E-13M2S	-13M2	BLA2-1	M	June 1997	Tyg	2,418	600	600	580	600	20	7	North
14N/3E-13M3S	-13M3	BLA2-2	M	June 1997	QToa2, 1	2,418	600	440	420	440	20	5	North
14N/3E-13M4S	-13M4	BLA2-3	M	June 1997	QToa2	2,418	600	330	310	330	20	3	North
14N/3E-14H1S	-14H1	B-2	P[1]	November 1964	QToa	2,423	602	602	230	585	355	2–7	North
14N/3E-14P1S	-14P1	B-6	P	January 1988	QToa	2,380	540	535	380	525	145	5–6	Central
14N/3E-14P2S	-14P2	TH-7	TW	January 1988	QToa	2,380	800	535	380	525	145	5–6	Central
14N/4E-18N1S	-18N1	B-5	P	March 1983	QToa, Tyg, Tog	2,378	803	800	300	780	480	3–8	Central
14N/4E-18N2S	-18N2	B-5A	TW	February 1983	QToa	2,380	803	803	302	305	3	3	Central
14N/3E-22N1S	-22N1	BA1-1	M[1]	March 1993	Bc	2,418	—	260	240	260	20	NA	South
14N/3E-22N2S	-22N2	BA1-2	M[1]	March 1993	QToa	2,418	—	170	150	170	20	NA	South
14N/3E-22P1S	-22P1	B-3	D	—	QToa	2,432	532	478	—	—	0	1–3	South
14N/3E-23B1S	-23B1	BLA4-1	M	December 2007	Tyg	2,377	865	850	710	730	20	7	Central
14N/3E-23B2S	-23B2	BLA4-2	M	December 2007	QToa1	2,377	865	460	440	460	20	6	Central
14N/3E-23B3S	-23B3	BLA4-3	M	December 2007	QToa2	2,377	865	280	260	280	20	2–3	Central
14N/3E-23G1S	-23G1	BX-2	TW	October 1980	QToa, QTol, Tyg	2,361	748	747	178	737	559	1–8	Central
14N/3E-24H1S	-24H1	BX-1	TW[2]	October 1980	Qoa, QToa	2,362	414	413	183	403	220	1–4	Central
14N/3E-24Q1S	-24Q1	BLA3-1	M	July 1997	Tog	2,356	900	898	878	898	20	8	Central
14N/3E-24Q2S	-24Q2	BLA3-2	M	July 1997	Tog	2,356	900	745	725	745	20	8	Central
14N/3E-24Q3S	-24Q3	BLA3-3	M	July 1997	Tyg	2,356	900	610	590	610	20	7	Central
14N/3E-24Q4S	-24Q4	BLA3-4	M	July 1997	QToa1	2,356	900	450	430	450	20	6	Central
14N/3E-24Q5S	-24Q5	BLA3-5	M	July 1997	QToa2	2,356	900	310	290	310	20	3–4	Central
14N/3E-26K1S	-26K1	BLA5-1	M	March 2011	Tyg	2,345	370	360	320	340	20	3	South
14N/3E-26K2S[3]	-26K2	BLA5-2	M	March 2011	QToa	2,345	370	210	190	210	20	2	—
14N/3E-26K3S	-26K3	BLA5-3	M	March 2011	QToa	2,345	370	210	190	210	20	3	South
14N/3E-26K4S	-26K4	BLA5B- 1	M	March 2011	QToa	2,345	280	270	250	270	20	NA	South
14N/3E-27E1S	-27E1	BP-2, MW-12	TW	—	Tog	2,401	—	—	—	—	—	NA	South
14N/3E-27E2S	-27E2	BP-3, MW-13	TW	—	Tog	2,401	—	—	—	—	—	NA	South

Table 1. Summary of construction data for production and monitoring wells in the Bicycle Basin, Fort Irwin Training Center, California.—Continued

[Location of wells are shown in figure 2. **Abbreviations**: Bc, basement complex; D, well destroyed; ft, feet; ID, identification; M, monitoring well; NA, well not in model domain; NAVD 88, North American Vertical Datum of 1988; P, production well; Qoa, Quaternary older alluvium; QToa, QToa1, QToa2, Quaternary-Tertiary older alluvium; QTol, Qaternary-Tertiary older lacustrine; Qya, Quaternary younger alluvium; Tog, Tertiary older gravels; TW, test well; Tyg, Tertiary younger gravels; U, unused well; —, data not available]

State well number	Short ID	Local ID	Well type	Date drilled	Geology	Land-surface altitude, in feet, NAVD 88 (ft)	Hole depth (ft)	Well depth (ft)	Screen top (ft)	Screen bottom (ft)	Screen thickness (ft)	Model layers	Area
14N/3E-27E3S	-27E3	BP-4, MW-14	TW	—	Tog	2,401	—	—	—	—	—	NA	South
14N/3E-28A1S	-28A1	BP-MW22	TW	—	Tog	2,411	—	151.28	—	—	—	NA	South
14N/3E-28H1S	-28H1	BP-1, MW-11	TW	—	Tog	2,407	—	—	—	—	—	NA	South
14N/3E-28H2S	-28H2	BP-MW21	TW	—	Tog	2,401	—	164.32	—	—	—	NA	South
14N/3E-35C1S	-35C1	B-9_Aprt	U	March 1963	Bc	2,352	250	245	125	245	120	NA	South
14N/3E-35C2S	-35C2	BLA1-1	M	May 1994	Bc	2,357	200	175	155	175	20	NA	South
14N/3E-35C3S	-35C3	BLA1-2	M	May 1994	Qya	2,357	200	25	15	25	10	NA	South
14N/3E-35C4S	-35C4	W3	TW	August 1997	Bc	2,350	300	300	200	300	100	NA	South

[1]The well has been destroyed.

[2]The well was obstructed.

[3]The well was sealed and abandoned; it was replaced by site BLA5B.

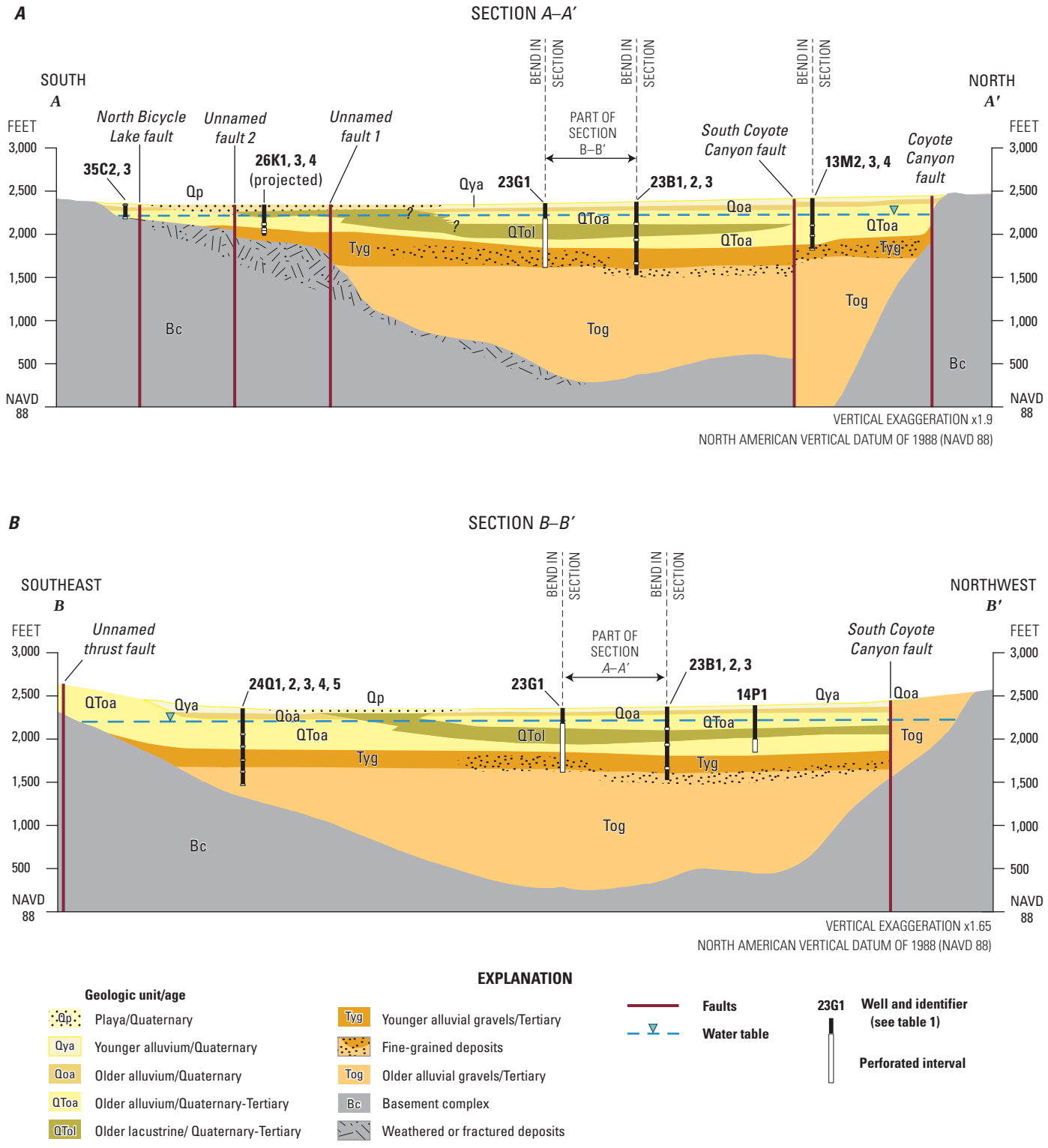

Figure 3. Generalized geologic sections across Bicycle Basin, Fort Irwin National Training Center, California: *A*, A–A′ and *B*, B–B′.

Quaternary-Tertiary deposits surround and partially fill Bicycle Basin (figs. 2, 3); these deposits were divided into Quaternary-Tertiary older alluvium and lacustrine deposits (QToa and QTol, respectively) that overlie the Tertiary sedimentary deposits and underlie Quaternary older and younger deposits. The Quaternary-Tertiary deposits represent a transitional unit during the Pliocene to Pleistocene; the Quaternary deposits roughly represent the Pleistocene and Holocene (Yount and others, 1994; Schermer and others, 1996). The Quaternary-Tertiary older alluvium (QToa) is generally coarse-grained interbedded sands and gravels, whereas Quaternary-Tertiary lacustrine deposits (QTol) are fine-grained sandy clays and silts. The Quaternary-Tertiary older alluvium (QToa) grades into lakebed clays (QTol) north and northwest of Bicycle Lake (dry) playa. A considerable amount of clay, interbedded with sands and gravels, was described at depths of 200–420 ft below land surface (bls) in geologic logs from wells in this area (14N/3E-23B1–3, 14N/3E-14P1, 14N/3E-14P2, and 14N/3E-23G1). These wells are adjacent to and along a dry wash, where large-storm runoff drains to the playa. The presence of extensive clay layers indicates that the wash and lakebed clays most likely were north and northwest of the present playa historically. The Quaternary-Tertiary older alluvium (QToa) generally is more consolidated and slightly less permeable than the overlying Quaternary alluvium, but still yields moderate amounts of water.

Quaternary deposits overlie the Quaternary-Tertiary deposits; these deposits were divided into Quaternary older and younger deposits. Quaternary older (Pleistocene) deposits include older colluvial, eolian, wash, and alluvial fan deposits (Qoc, Qoe, Qow, and Qoa, respectively; Yount and others, 1994; Schermer and others, 1996); these deposits were grouped into undifferentiated older alluvium (Qoa) in this report. The Quaternary older alluvium (Qoa) consists of interbedded sand and gravel. The clasts in these deposits vary with nearby source rocks. Near the base of Tiefort Mountain, the older alluvium is coarse grained and derived primarily from quartzite and granite. The Quaternary older alluvium (Qoa) typically is cemented by calcite in its upper 10–20 ft where exposed at the surface. The older alluvium generally is more consolidated and slightly less permeable than the overlying younger alluvium, but still yields moderate amounts of water. Quaternary younger (Holocene) deposits include younger colluvial, eolian, playa, wash, and alluvial fan deposits (Qyc, Qye, Qp, Qyw, and Qya, respectively; Yount and others, 1994; Schermer and others, 1996); these deposits were grouped into undifferentiated younger alluvium (Qya) and playa deposits (Qp). The younger alluvium (Qya) and playa deposits (Qp) overlie the older alluvium throughout the basin (figs. 2, 3) and are composed of unconsolidated sand and gravel with some pedogenic silt and clay. The Quaternary younger alluvium (Qya) is coarser grained near the base of the hills surrounding Bicycle Basin and becomes finer grained and better sorted toward the Bicycle Lake (dry) playa. The Quaternary younger alluvium (Qya) generally is less than 20 ft thick near the margins of the valley and is generally thicker in the alluvial fans at the foot of Tiefort Mountain, but could be as thick as 130 ft in the central part of the basin (fig. 3*A*, B). The Quaternary younger alluvium (Qya) generally lies above the water table; however, it is more permeable than the underlying deposits and, if saturated, is capable of yielding large quantities of water to wells.

Quaternary playa deposits (Qp; fig. 2) form the surface of Bicycle Lake (dry) in the southeastern part of the basin. These deposits consist of moderately to well-sorted clay, silt, and fine sand and could be as much as 50 ft thick. These deposits interfinger with the surrounding Quaternary younger alluvium (Qya) and generally lie above the water table. Because these deposits are fine grained and much less permeable than the Quaternary younger alluvium (Qya), they tend to impede infiltration of surface water that ponds on the playa after occasional storms.

Structure and Depth to the Basement Complex

Gravity, seismic-refraction, and TEM data were collected for this study to help understand the three-dimensional structure and estimate the depth and shape of the Bicycle Basin. A gravity survey was used to understand the three-dimensional structure and estimate the depth to the granitic basement (thickness of basin fill) in the study area. Data originally were collected in 1999 for only Bicycle Basin; additional data were collected NTC wide in 2010 (Jachens and Langenheim, 2014). The original gravity survey covers about 15 mi^2 and includes measurements at 350 gravity stations (R.C. Jachens, written commun., 2000). Estimating the depth to the basement complex using a gravity survey requires knowledge of the residual gravity field of the exposed geology and knowledge of the vertical density variation in the basin deposits. Data from boreholes that penetrate the surface of the basement complex and geophysical data, including seismic refraction (David Berger, U.S. Geological Survey, written commun., 1996) and TEM data (Burgess and Bedrosian, 2014), were used to provide constraints on the thickness of the basin fill. For detailed information regarding how gravity data were analyzed, see Jachens and Langenheim (2014).

The estimated altitude of the basement complex in the Bicycle Basin, based on gravity data, showed that the deepest part of the basin is north of Bicycle Lake (dry) playa near monitoring wells 14N/3E-13M2–4, at an altitude below 0 ft relative to NAVD 88 (or about 2,300 ft bls; fig. 4). To the north, the basin appears to become shallower over a short lateral distance, indicating the existence of one or more unnamed east–west trending faults. To the southwest, the basin also becomes shallower, but more gradually than to the north.

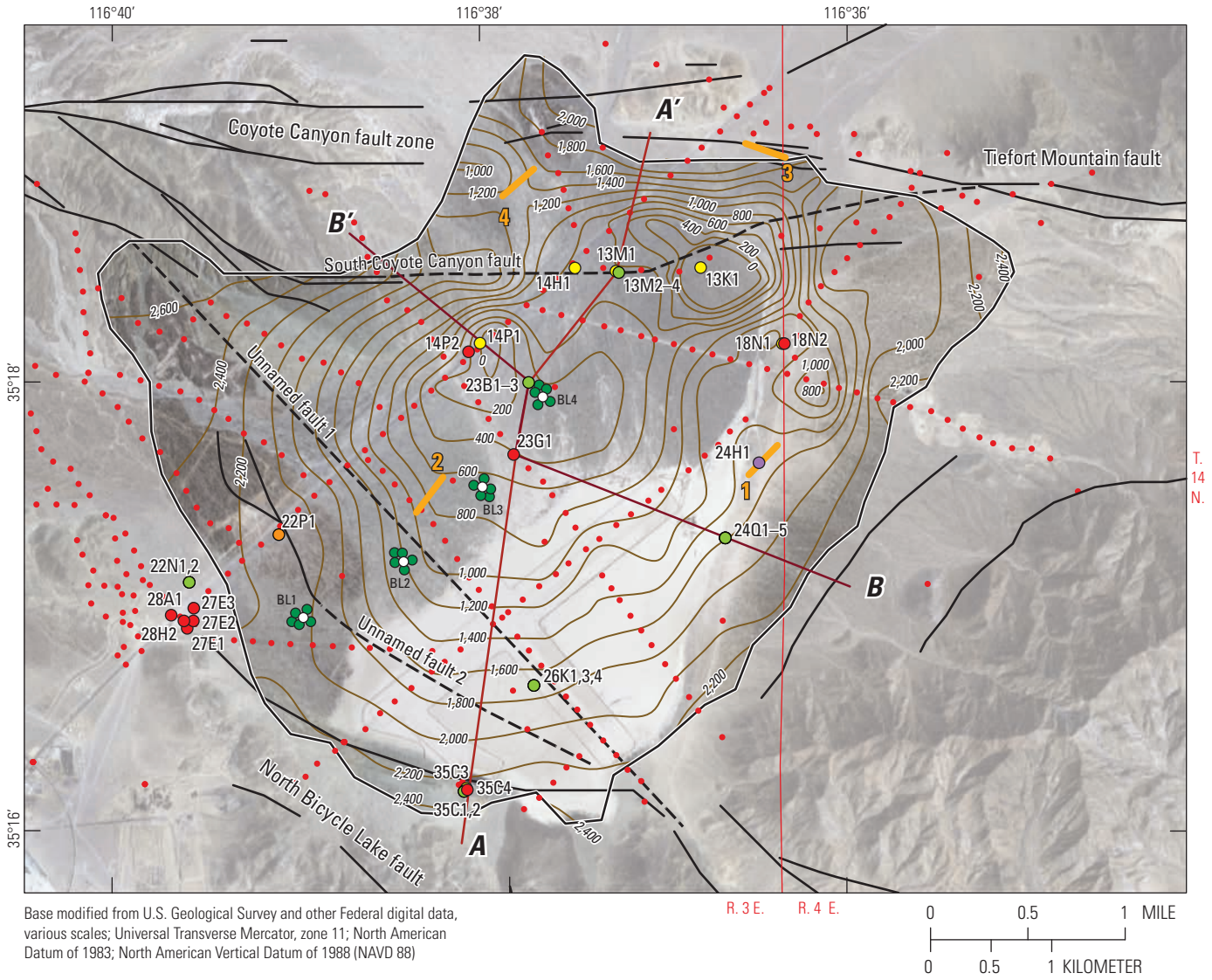

Base modified from U.S. Geological Survey and other Federal digital data, various scales; Universal Transverse Mercator, zone 11; North American Datum of 1983; North American Vertical Datum of 1988 (NAVD 88)

EXPLANATION

- Bicycle groundwater basin
- Section *A–A′*
- Section *B–B′*
- 1 Seismic line and identifier
- Township/range
- Faults
- Bicycle model inferred faults
- 1,600 Altitude of basement, in feet above NAVD 88. Contour interval is 200 feet.

Well type and identifier (see table 1)

- 14P1 Production
- 23B1–3 Multiple-well monitoring site
- 22P1 Destroyed
- 23G1 Test well
- 24H1 Obstructed

- BL2 TEM array and identifier
- Gravity station
  - Jachens and Langenheim, 2014

Figure 4. Altitude of the basement complex, wells, transient electromagnetic survey (TEM) locations, and location of seismic lines in Bicycle Basin, Fort Irwin National Training Center, California.

The altitude of the basement complex estimated from gravity data also was compared with the altitudes estimated from the seismic-refraction data collected in four locations and from the TEM data at four soundings in the basin (fig. 4). The seismic-refraction method uses a seismic source to generate compression-wave energy (P-waves) and a seismograph to measure and collect the timing of the first arrival of a refracted wave at an array of geophones. Different geologic layers typically have different refracted wave velocities. These velocity differences are used to determine the depth to the refracting layer in the subsurface. Transient electromagnetic surveys, or TEM, are a technique that provides a measure of subsurface resistivity by passing a current through a wire loop, which, as explained by Ampere's law, generates a primary magnetic field. The primary current is turned off rapidly, thereby causing a time-varying change in magnetic flux, which induces voltages and, hence, eddy currents in conductive bodies according to Faraday's law. In TEM, a secondary magnetic field is produced by the decay of these subsurface eddy currents, and the time derivative of this secondary magnetic field commonly is measured as a voltage with time after primary current turnoff at one or more surface receivers. An apparent resistivity is calculated from the measured voltage at the receiver coil and the time elapsed after turnoff (Fitterman and Labson, 2005).

With the exception of the southwestern seismic line (fig. 4, line 2), the estimated bedrock-surface altitudes from three of the four seismic lines agreed well with the estimated altitude based on the gravity data. The northern seismic lines (fig. 4, lines 3, 4) crossed two topographic divides between granitic outcrops to evaluate subsurface structure across potential groundwater-flow boundaries. The seismic data indicated that a buried valley in the bedrock surface exists beneath the western section (fig. 4, line 4) that connects areas of thicker sediments overlying bedrock to the northeast and southwest. Such a buried valley through a bedrock ridge could allow increased subsurface flow between deeper portions of the basin if there is a head gradient between them. The southwestern seismic line (fig. 4, line 2) was collected in the area of the projected trace of one or more faults through the basin to evaluate the possible location of the faults. The estimated altitude of the basement complex, based on the seismic data, ranged from 1,450 to 1,280 ft above NAVD 88 (or a depth of 920–1,100 ft bls) from southwest to northeast. The estimated altitudes based on seismic data were about 350–620 ft shallower than the estimate of 1,100–650 ft based on the gravity data; the apparent discrepancy could reflect the presence of volcanic or conglomerate bedrock that has a less pronounced density contrast, affecting the interpreted depth to bedrock from gravity data. The seismic data also suggested that projected fault traces cross the basin in a stepwise manner near this line.

Results from the TEM surveys were used to refine the depth-to-basement estimates in the southwestern part of the basin. The modeled apparent resistivity from these surveys also supported the shallowing of basement to the southwest, although the depths were as much as several hundred feet shallower than estimated using gravity data. The altitude of the basement complex was estimated using various density-depth functions in the gravity inversion equation. Changes in this density function or rock type can result in shallower or deeper estimates of depth to basement, which is why estimates from these methods do not agree exactly. In any case, the interpreted overall shape of the basin was consistent.

Faults

Faults play a large role in the physiography of Fort Irwin and control the shape of Bicycle Basin (Yount and others, 1994; Morin, 2000). Many faults in Bicycle Basin have been active during the Quaternary although few have demonstrated Holocene rupture; none are considered a seismic risk (Miller and others, 1994). The sinistral faults that strike northwest and east can be shown to have last moved during the Quaternary, whereas thrust faults that strike northeast last moved before the Quaternary (fig. 2). Several faults have been mapped in the bedrock hills around Bicycle Basin; the most prominent ones are the Bicycle Lake and Coyote Canyon fault zones (Yount and others, 1994; Schermer and others, 1996; Miller and Yount, 2002). The precise locations of these faults, or splays off the faults, where they cross Bicycle Basin and are buried by sediment, are uncertain. The locations of these buried faults were approximated by projecting mapped faults into the basin. Additionally, the location of mapped and other potential faults in Bicycle Basin were refined using data collected for this study, including geophysical and gravity surveys, groundwater-level measurements, and groundwater-flow model calibration.

The Bicycle Lake fault zone is made up of east-trending faults that cross the southern part of the basin and form the southern boundary of the basin (fig. 2). The Bicycle Lake fault zone uplifts and offsets rocks of the basement complex between Bicycle Basin and Irwin Basin to the south. Uplift and offset across the Bicycle Lake fault zone prevents groundwater flow between Bicycle and Irwin Basins; this hypothesis is supported by differences in water level between the basins. One fault splay borders the southern edge of Bicycle Lake (dry) playa and lies just north of wells 14N/3E-35C1–3 (fig. 2). This fault is referred to as the North Bicycle Lake fault by Yount and others (1994).

The Coyote Canyon fault zone is made up of east-west trending faults that cross the northern part of the basin and form the northern boundary of the basin (fig. 2). Offset Quaternary-Tertiary sedimentary deposits and basement complex appear on the north side of the Coyote Canyon fault zone at the north end of Bicycle Basin. Either this offset or the fault itself could act as a barrier preventing groundwater flow at depth from the Granite Mountains in the north toward Bicycle Basin to the south. On the basis of data collected for this study, an east-west trending fault splay of the Coyote Canyon fault zone was projected to extend into Bicycle Basin, just south of wells 14N/3E-14H1 and 14N/3E-13M1–4, which is referred to as the South Coyote Canyon fault in this report.

Two additional faults were identified in Bicycle Basin based on water-level, geophysical- and gravity-survey data, and calibration of the groundwater-flow model. Unnamed fault 1 (fig. 2) trends northwest-southeast and is a projected continuation of mapped faults in bedrock areas to the southeast and northwest. Unnamed fault 1 was projected to cross Bicycle Lake (dry) playa approximately parallel to the cross-runway that bisects the main runway (fig. 4) and connects to the southernmost of two northwest–southeast trending parallel faults mapped near the southeastern edge of playa. It was unknown whether the northernmost of these parallel faults crosses the basin. One multiple-well monitoring site (14N/3E-26K1, 3, 4) was drilled south of the unnamed fault 1 projection. Water-level altitudes measured in three wells at this site were about 6–20 ft higher than in wells (14N/3E-24Q5 and 14N/3E-23B3, respectively) north of unnamed fault 1. Unnamed fault 2 trends west-northwest–east-southeast and is a projected continuation of mapped faults in Tertiary older alluvium along the west side of the basin. Historical water levels in wells (14N/3E-22N1, 14N/3E-22P1, 14N/3E-27E2, 14N/3E-28A1, and 14N/3E-28H2) south of unnamed fault 2 were more than 40 ft higher than water levels in wells north of unnamed fault 2. Unfortunately, wells 14N/3E-22N1–2 and 14N/3E-22P1 were destroyed in the late 1990s–early 2000, so more recent water levels were unavailable. Water levels in wells 14N/3E-28A1 and 14N/3E-27E3, near 14N/3E-22N1–2, had risen slightly, however, probably as a result of water leaking from nearby infrastructure (from an overhead water pipe used to fill water tanks or from buried water pipes transferring water from Bicycle Basin to Irwin Basin). Depth to basement is shallow in well 14N/3E-22P1, indicating offset south of unnamed faults 1 and 2 similar to that observed south of North Bicycle Lake fault. These data indicated that unnamed faults 1 and 2 impede groundwater flow from the southern part of the basin to some extent.

Hydrologic Framework

The aquifer system in Bicycle Basin was delineated from information contained in previous studies and supplemented with geophysical investigations of the basin and with geohydrologic data collected from existing and newly installed wells in the basin. As part of this project, several multiple-well monitoring sites were installed to update and refine the understanding of the geohydrologic framework of Bicycle Basin. During 1993–2011, six multiple-well monitoring sites were drilled (table 1; fig. 2). Two piezometers each were installed at multiple-well monitoring sites BA1 (14N/3E-22N1–2) and BLA1 (14N/3E-35C2–3) during 1993 and 1994, respectively. During 1997, three piezometers were installed at multiple-well monitoring site BLA2 (14N/3E-13M2–4), and five piezometers at BLA3 (14N/3E-24Q1–5). During 2007, three piezometers were installed at a multiple-well monitoring site BLA4 (14N/3E-23B1–3). During 2011, three piezometers were installed at a multiple-well monitoring site BLA5 (14N/3E-26K1, 2, 4). A typical multiple-well monitoring site in Bicycle Basin consisted of two to five 2-in.-diameter polyvinyl chloride (PVC) piezometers with 20-ft screen intervals installed at different depths in the same borehole. The actual design of each multiple-well monitoring site was determined during well construction by examining the drill cuttings collected during drilling and the borehole geophysical logs. The lithologic logs of the drill cuttings and the geophysical logs from each borehole are presented in appendix 1, figures 1–1 through 1–6.

Aquifer System Definitions

The aquifer system in Bicycle Basin consists of two aquifers, referred to as the upper aquifer and lower aquifer in this report. The upper aquifer is generally unconfined and is composed of the saturated part of the younger Quaternary alluvium (Qya and Qp), the Quaternary older alluvium (Qoa), and the Quaternary-Tertiary older alluvium and lacustrine deposits (QToa and QTol). The saturated thickness of the upper aquifer was about 300 ft near well 14N/3E-23B1–3; it thins at the margins of the basin (fig. 3). The lower aquifer is composed of Tertiary younger sedimentary deposits (Tyg) and older sedimentary deposits (Tog) and generally is confined or partly confined. This aquifer is as much as 1,500 ft thick and generally is less permeable than the upper aquifer. The base of the aquifer system was considered to be the top of the basement complex, although the deepest part of the older Tertiary sedimentary deposits did not appear to produce much water. For this study, the areal extent of Bicycle Basin was based on the altitude where the basement complex is intersected by the 1965 groundwater-level altitude of about 2,225 ft, which was estimated from water levels in wells 14N/3E-13K1, -14H1, and -13M1, measured in 1955, 1964, and 1965, respectively. The resulting areal extent of Bicycle Basin used for this study differs somewhat in that it is smaller than that of previous studies (for example, Wilson F. So and Associates, 1989).

Hydraulic conductivities for the upper aquifer were estimated from aquifer tests (table 2) and slug tests (Nawikas and others, written commun., 2011). Several aquifer tests were done at specified wells perforated solely in the upper aquifer in Bicycle Basin by C.F. Hostrup and Associates (1955), U.S. Army Corps of Engineers (written commun., 1965), James M. Montgomery and Associates (1981), Wilson F. So and Associates (1989), and the U.S. Geological Survey (unpublished data, 1997, 2008; Nawikas, written commun., 2011). For wells that did not have aquifer tests, the transmissivities of the saturated interval of wells were approximated using the relation between specific capacity and transmissivity reported by Thomasson and others (1960). The specific capacity measured at wells in the basin ranged from about 6.4 to 22.5 gallons per minute per foot (gpm/ft) of drawdown. Specific capacities (in gpm/ft) were multiplied by 230 (Thomasson and others, 1960) to yield transmissivities ranging from about 1,740 to 10,630 square feet per day (ft^2/d).

Transmissivities were divided by the estimated saturated thicknesses of the aquifer to yield hydraulic conductivities for the upper aquifer ranging from about 3 to 35 feet per day (ft/d). The hydraulic conductivity estimated from slug tests performed in monitoring well 14N/3E-26K4, perforated from 250 to 270 ft bls in the upper aquifer (table 1), was 28 ft/d (Joseph Nawikas, U.S. Geological Survey, written commun., 2011), which was within the previously estimated range.

Limited data about the hydraulic properties for the lower aquifer were available. The specific-capacity test in well 14N/4E-18N1, with perforations spanning from the Quaternary-Tertiary older alluvium (QToa) to Tertiary older gravels (Tog), should have reflected, at least partially, the properties of the lower aquifer; it showed the lowest hydraulic conductivity of any of the specific capacity tests at 3 ft/d (table 2). On the basis of grain size from lithologic cuttings and characteristics during drilling, age, and consolidation, the hydraulic properties for the lower aquifer were assumed to be low (1–5 ft/d). The horizontal hydraulic conductivity estimated from a slug test performed in monitoring well 14N/3E-26K1, perforated from 320 to 340 ft in a sand and gravel layer of the Tertiary younger gravels (Tyg) in the lower aquifer, was 6.8 ft/d (Nawikas and others, U.S. Geological Survey, written commun., 2011). Vertical hydraulic conductivities were estimated by evaluating test results, analyzed by the USGS Hydrologic Research Laboratory in Sacramento for core samples collected from three depths (310–315 ft, 660–665 ft, and 860–865 ft) during the drilling of the borehole for wells 14N/3E-23B1–3 (fig. 2, appendix fig. 1–3). The shallow

Table 2. Summary of aquifer-test results from various studies in Bicycle Basin, Fort Irwin National Training Center, California, 1955–2008.

[Location of wells shown in figure 2. **Abbreviations**: CoE, Corp of Engineers; ft, feet; ft/d, feet per day; ft²/d, feet squared per day; gpm/ft, gallons per minute per foot of drawdown; M, maximum drawdown; m, minimum drawdown; USGS, U.S. Geological Survey; *, average hydraulic conductivity shown, hydraulic conductivities estimated from specific depths in aquifer-test data archived at the USGS office; —, no data]

State well number	Local name	Date tested	Tested by	Specific capacity (gpm/ft)	Transmissivity (ft²/d)	Saturated thickness (ft)	Hydraulic conductivity (ft/d)	Drawdown	Specific yield (percent)
14N/3E-13K1S	B-1	January 1955	Hostrup[1]	8.08	[2]1,858	270	6.9	M*	—
14N/3E-13K1S	B-1	January 1955	Hostrup[1]	15.73	[2]3,549	270	13.1	m*	—
14N/3E-13K1S	B-1	November 1978	Montgomery[3]	—	—	270	—	—	12.5
14N/3E-13M1S	B-4	June 1965	CoE[6]	22.50	[2]5,175	300	17.3	M*	—
14N/3E-13M1S	B-4	June 1965	CoE[6]	21.00	[2]4,830	300	16.1	m*	—
14N/3E-13M1S	B-4	January 1988	So[4]	7.53	2,005	300	6.7	—	—
14N/3E-13M1S	B-4	September 1997	USGS[5]	—	10,630	300	35.4	—	—
14N/3E-13M1S	B-4	November 1978	Montgomery[3]	—	—	330	—	—	23.6
14N/3E-14H1S	B-2	November 1964	CoE[6]	13.00	[2]2,990	300	10.0	M*	—
14N/3E-14H1S	B-2	November 1964	CoE[6]	20.00	[2]4,600	300	15.3	m*	—
14N/3E-14H1S	B-2	November 1978	Montgomery[3]	—	2,000	330	6.1	—	21.0
14N/3E-14P1S	B-6	March 1988	So[4]	8.46	2,741	349	7.9	—	—
14N/3E-14P2S	TH-7	March 1988	So[4]	—	3,090	359	8.6	—	—
14N/3E-14P2S	TH-7	January 2008	USGS[5]	—	4,310	359	12.0	—	—
14N/3E-22P1S	B-3	November 1978	Montgomery[2]	—	—	—	—	—	5.0
14N/3E-24H1S	BX-1	October 1980	Montgomery	—	—	—	—	—	8.2
14N/4E-18N1S	B-5	January 1988	So[4]	6.40	1,738	580	3.0	—	—
14N/4E-18N2S	B-5A	January 2008	USGS[5]	—	7,500	580	12.9	—	—

[1]C.F. Hostrup and Associates, 1955.

[2]Transmissivity calculated by multiplying specific capacity by 230 (Thomasson and others, 1960).

[3]James M. Montgomery and Associates, 1981.

[4]Wilson F. So and Associates, Inc., 1989.

[5]U.S. Geological Survey, continuous water-level data collected during 2008–09; multiple dates were used to estimate transmissivity.

[6]U.S. Army Corps of Engineers, wells drilled during 1964–65.

core consisted of sandy, silty clay of the Quaternary-Tertiary lacustrine deposits (QTol) unit; the middle core consisted of sandy, silty clay of the Tertiary younger gravels (Tyg) unit; and the deep core consisted of fine-grained deposits of the Tertiary older gravels (Tog) unit. Analyses of the cores (Kevin Ellett, U.S. Geological Survey, written commun., 2008) indicated that vertical hydraulic conductivities varied and were 0.0009 ft/d for the shallow core (Quaternary-Tertiary lacustrine deposits, QTol), 0.01 ft/d for the middle core (Tertiary younger gravels, Tyg), and 0.0004 ft/d for the deeper core (Tertiary older gravels, Tog). These values were measured on low-volume samples, subsampled from cores that generally were less than 2 ft in length, and were likely not representative of hydraulic conductivities in the lower aquifer as a whole because of the heterogeneous nature of the deposits.

Natural Recharge and Discharge

Previous investigators estimated annual natural recharge to be low, ranging from negligible (James M. Montgomery and Associates, 1981) to more than 300 acre feet per year (acre-ft/yr) for the Bicycle Basin (Wilson F. So and Associates, 1989). As previously stated, annual precipitation in the region of Bicycle Basin is about 2–15 inches, and potential evapotranspiration is about 70 inches. Except during extended storms, recharge derived from direct precipitation is minimal. Natural recharge to the basin is only from infiltration of accumulated storm runoff, primarily in the winter or after short summer thunderstorms, along normally dry washes and near the base of the surrounding hills (fig. 1). Groundwater discharges from Bicycle Basin as groundwater underflow to the south, along the southeast side of the playa (fig. 2).

Natural recharge in Bicycle Basin was assumed primarily to be from infiltration and underflow of precipitation runoff along the major washes that drain watersheds, including the upland area near Goldstone and the Granite Mountains to the west and north of Bicycle Basin (fig. 1). Additional groundwater recharges along smaller drainages in the northwestern and northeastern parts of the basin and at the base of Tiefort Mountains (fig. 2). Although surface runoff collects on the Bicycle Lake (dry) playa, recharge of this water on the playa was assumed to be negligible. After large storms, ponded water can remain on the playa for several months before evaporating because of the fine-grained texture and extremely low permeability of the playa deposits. Some water could recharge the aquifer system along the edge of the playa deposits where the sediment is coarser grained.

A range of modeled estimates of natural recharge for Bicycle Basin from infiltration of runoff from precipitation and underflow was developed using the Basin Characterization Model (BCM; Flint and Flint 2007a, b). The BCM is a regional, physically based model of the southwestern United States that calculates monthly water-balance fractions and changes in soil moisture, runoff, and recharge on the basis of topography; vegetation density; soil composition, depth, and water storage; underlying bedrock geology; and spatially distributed transient values (measured or estimated) of air temperature, precipitation, and potential evapotranspiration (PET; Flint and Flint 2007a, b). The climate data used to drive the BCM are available as monthly gridded maps of precipitation and air temperature at a 2.5-mi (4-kilometer [km]) spatial resolution from PRISM (the empirically based Parameter-Elevation Regressions on Independent Slopes Model; Daly and others 2004). Because a finer resolution of BCM simulations was needed for this study, the data were downscaled to a 885-ft (270-meter [m]) spatial resolution following Flint and Flint (2007a). These data were compared to the nearby climate stations “Goldstone Echo 2”, “Daggett FAA Airport”, “Barstow Fire Station” and “Dunn Siding” (Western Regional Climate Center of the Desert Research Institute, WRCC-DRI, 2009, http://www.wrcc.dri.edu) and “San Bernardino–Barstow NE - #134” (California Irrigation Management Information System, 2009). The average monthly measured precipitation between 1948 and 2010 for stations near Bicycle Basin ranged from about 0.03 inches in June to about 1.2 inches in February. Figure 5*A* shows high variability in monthly precipitation for December through March for the five climate stations in the region, indicating the variability in winter storm patterns that track through the region. Except for sporadic tropical storms, precipitation in the warmer months was regionally distributed. Area-averaged minimum and maximum monthly temperatures ranged from about 34 to 60 °F in December and from about 70 °F to more than 103 °F in July. Temperature variability among the three climate stations was small (fig. 5*B*). Generally, the minimum and maximum temperatures at the Daggett FAA Airport station were slightly higher than those at the other two stations. Average monthly potential evapotranspiration rates ranged from about 2.0 in. for December to about 10.2 in. for June (fig. 5*C*). Results of the BCM simulations of runoff and recharge are described in the “Simulation of Natural Recharge and Discharge” section.

Groundwater discharges from Bicycle Basin by underflow through fractured volcanic material and granitic bedrock southeast of the Bicycle Lake (dry) playa. Discharge in this part of the basin was inferred because (1) long-term runoff and recharge into the basin were greater than zero, (2) there are no outflows from the basin other than subsurface flow in the southeast, and (3) the estimated predevelopment water level, as discussed in “Groundwater Altitudes and Movement” section, was higher than the estimated bedrock elevation at this point. Evaporative loss of groundwater from the Bicycle Lake (dry) playa was negligible because the depth to groundwater under predevelopment conditions was more than 30 ft bls. Prior to groundwater development in 1967, Bicycle Basin was considered to be in a steady-state condition, where discharge is equivalent to recharge to the basin with no appreciable change in storage.

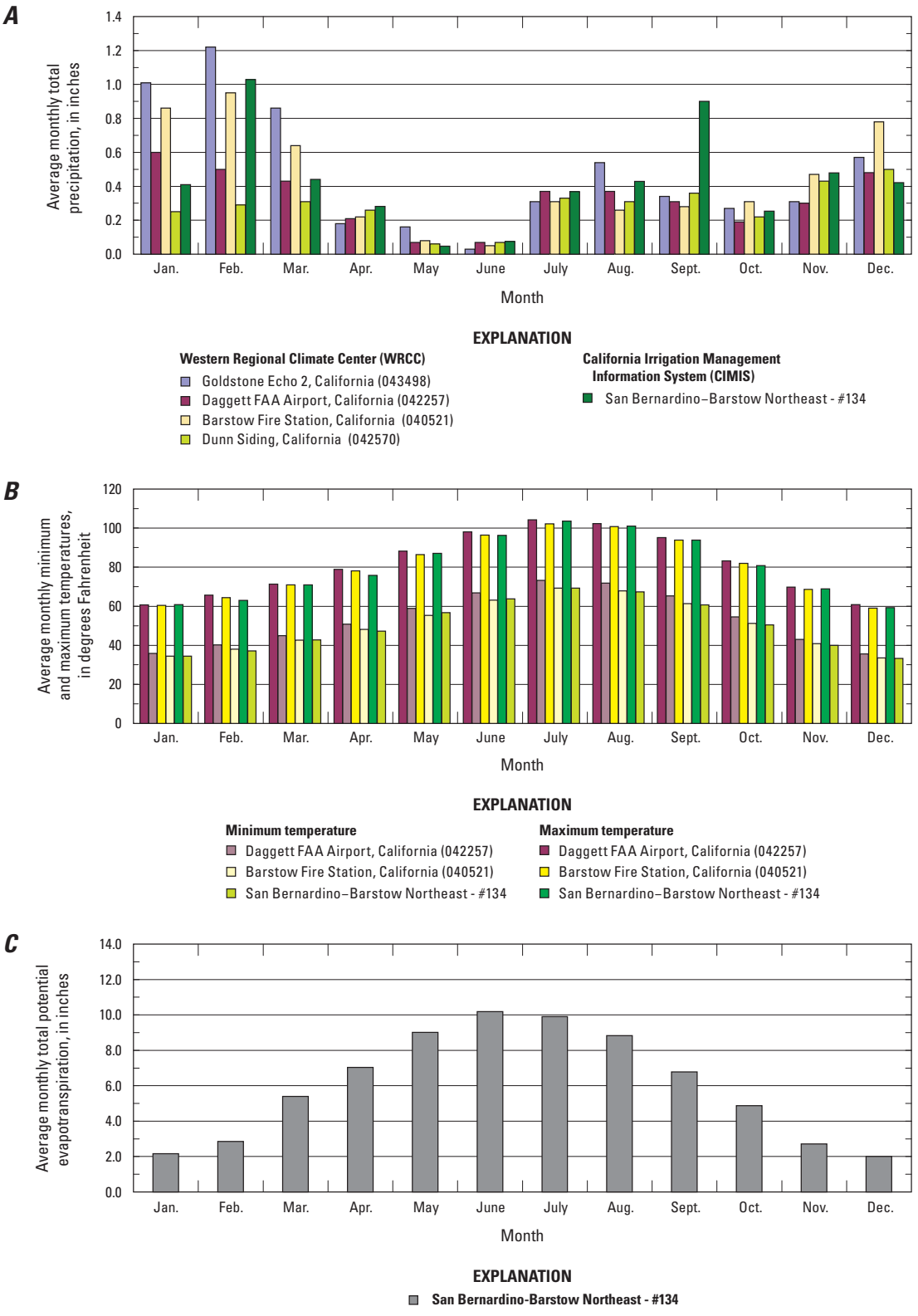

Figure 5. Comparisons of average monthly climate variables for the Fort Irwin National Training Center, San Bernardino County, California: *A*, average monthly total precipitation (1948–2010); *B*, minimum and maximum temperatures for three climate stations; and *C*, averaged monthly total potential evapotranspiration for one climate station. (Climate station data from Western Regional Climate Center or from the CIMIS; Goldstone December 1, 1973, to July 31, 2006; http://www.wrcc.dri.edu/cgi-bin/cliMAIN.pl?ca3498; Daggett July 1, 1948, to December 31, 2010; http://www.wrcc.dri.edu/cgi-bin/cliMAIN.pl?ca2257; Barstow Fire May 1, 1980, to December 31, 2010; http://www.wrcc.dri.edu/cgi-bin/cliMAIN.pl?ca0521; Dunn Siding July 8, 1959, to August 31, 1971; http://www.wrcc.dri.edu/cgi-bin/cliMAIN.pl?ca2570; San Bernardino-Barstow NE January 1, 1997, to May 31, 2011; http://wwwcimis.water.ca.gov/WSNReportCriteria.aspx).

Groundwater Pumping and Water Use

Groundwater development in Bicycle Basin began in 1955 when production well 14N/3E-13K1 (fig. 2) was drilled although pumping did not begin until 1967. Production wells 14N/3E-14H1 and 14N/3E-13M1 were drilled in 1964 and 1965, respectively. Production well 14N/4E-18N1 was drilled in 1983, and well 14N/3E-14P1 was drilled in 1988. Groundwater pumped from Bicycle Basin is transported (by buried pipeline) to Irwin Basin, where it is blended with the water pumped from Irwin and Langford Basins. With the exception of ponded water at a standpipe used to fill water trucks in the southwestern part of the basin, none of the water that is pumped from Bicycle Basin is used in or returned to the basin.

Between January 1967 and December 2010, an average of about 1,050 acre-ft/yr of water was pumped from Bicycle Basin (table 3). Total pumpage during this period was about 46,000 acre-feet (acre-ft). Pumpage records included annual basin pumpage (not by well) for 1967–83, annual pumpage by well for 1984–90 (fig. 6*A*), and monthly pumpage by well for 1990–2010 (fig. 6*B*). Average annual pumping rates were estimated from the number of years for which there were pumpage records from individual wells. Based on this, average annual pumpage was 294, 95, 212, 488, and 751 acre-ft/yr for production wells 14N/3E-13K1, 14N/3E-14H1, 14N/3E-13M1, 14N/4E-18N1, and 14N/3E-14P1, respectively (table 3). Wells 14N/3E-13K1 and 14N/3E-14H1 ceased pumping during 2006 and 1994, respectively; these wells have since been destroyed. Well 14N/3E-13M1 ceased pumping during 2005, after which the well was rehabilitated; pumping resumed in 2009. Annual groundwater pumpage in the basin ranged from about 125 acre-ft in 1977 to 2,145 acre-ft in 1998; pumpage in 2010 was 1,090 acre-ft. Reported average monthly (1991–2010) pumpage in Bicycle Basin ranged from about 65 acre-ft in February to about 165 acre-ft in August (table 4). Average monthly pumpage in the basin for January 1991 to December 2000 ranged from about 40 acre-ft for February to about 180 acre-ft for July (table 4). Average monthly pumpage during January 2001–December 2010 ranged from about 85 acre-ft for February to about 155 acre-ft for September. Differences in average monthly pumpage between 1991–2000 and 2001–10 indicated that pumping management practices changed over time. For 2001–10 compared to 1991–2000, average monthly pumpage increased 4–65 acre-ft during the months of September through May, but decreased by 5–36 acre-ft during the months of June–August. This change in pumpage could be due to an increase in personnel and activities at the facility during the winter months and the extended block leave (break in rotational training) during June and July.

Groundwater Altitudes and Movement

Prior to groundwater development in Bicycle Basin, the groundwater gradient in the basin was relatively flat, with a slight gradient from the recharge sources toward the Bicycle Lake (dry) playa, where there was likely a subsurface outlet near the southeast end. This was inferred from the low recharge rate, no surface expression of discharge (such as a spring), and a water table too low (based on predevelopment water levels described earlier) to allow for discharge from the playa. Natural discharge was inferred at the southeast end, because the predevelopment water levels were higher than the basement only in this location along the basin boundary. Groundwater-level altitudes for the earliest (1955–97) and more recent (2010–11) measurements are shown in figure 7*A* and *B*, respectively; these are altitudes for the shallowest well in multiple-well monitoring sites, the test wells, and the production wells. The water-table altitude was about 2,225 ft above NAVD 88 at the time the first well was drilled in 1955 (Kunkel and Riley, 1959). By 2010, the groundwater-level altitude ranged from about 2,130 ft in the northern part of the basin to 2,170 ft near Bicycle Lake (dry) playa. The interpreted direction of groundwater flow from the fall of 2010 to winter of 2011 was from south-southwest to north-northeast, reflecting groundwater flow toward production wells in the northern part of the basin (fig. 7*B*). Water-level measurements for the period of record, 1955–2015, are presented in appendix 2. These data are in the USGS National Water Information System (NWIS) database and may be accessed at http://waterdata.usgs.gov/ca/nwis/.

Groundwater levels in Bicycle Basin declined in response to pumping, with relatively large declines near areas of larger withdrawals. Hydrographs in figure 8 show groundwater-level changes in selected wells in Bicycle Basin. These hydrographs indicate that water levels in the northeastern part of the basin declined as much as 100 ft in production well 14N/3E-13K1 since the 1960s and as much as 75 ft in production well 14N/4E-18N1 and test well 14N/4E-18N2 since 1990 (fig. 8*A*1). Groundwater levels in production wells 14N/3E-13M1 and 14N/3E-14H1 (fig. 8*A*2) in the northwestern part of the basin declined about 90 ft from the 1960s through the early 1990s, when water levels stabilized as a result of reduced pumpage in these wells; these wells are north of the South Coyote Canyon fault. Likewise, groundwater levels in production well 14N/3E-14P1 and test well 14N/3E-14P2 (fig. 8*A*3) in the western part of the basin, south of the South Coyote Canyon fault, declined about 100 ft since the 1980s. Groundwater levels declined more slowly near the Bicycle Lake playa, with about 40-ft declines in well 14N/3E-24H1 (northeast of Bicycle Lake playa) during 1980–96 and in well 14N/3E-23G1 (northwest of Bicycle Lake playa) during 1996–2010 (fig. 8*A*4).

Since 1993, water levels were measured sporadically in six multiple-well monitoring sites in Bicycle Basin (appendix 2; locations shown on fig. 2). Multiple-well monitoring sites 14N/3E-24Q1–5, 14N/3E-13M2–4, and 14N/3E-23B1–3 have three to five 2-in.-diameter monitoring wells, each with a discrete perforated interval at various depths in the aquifer (table 1).

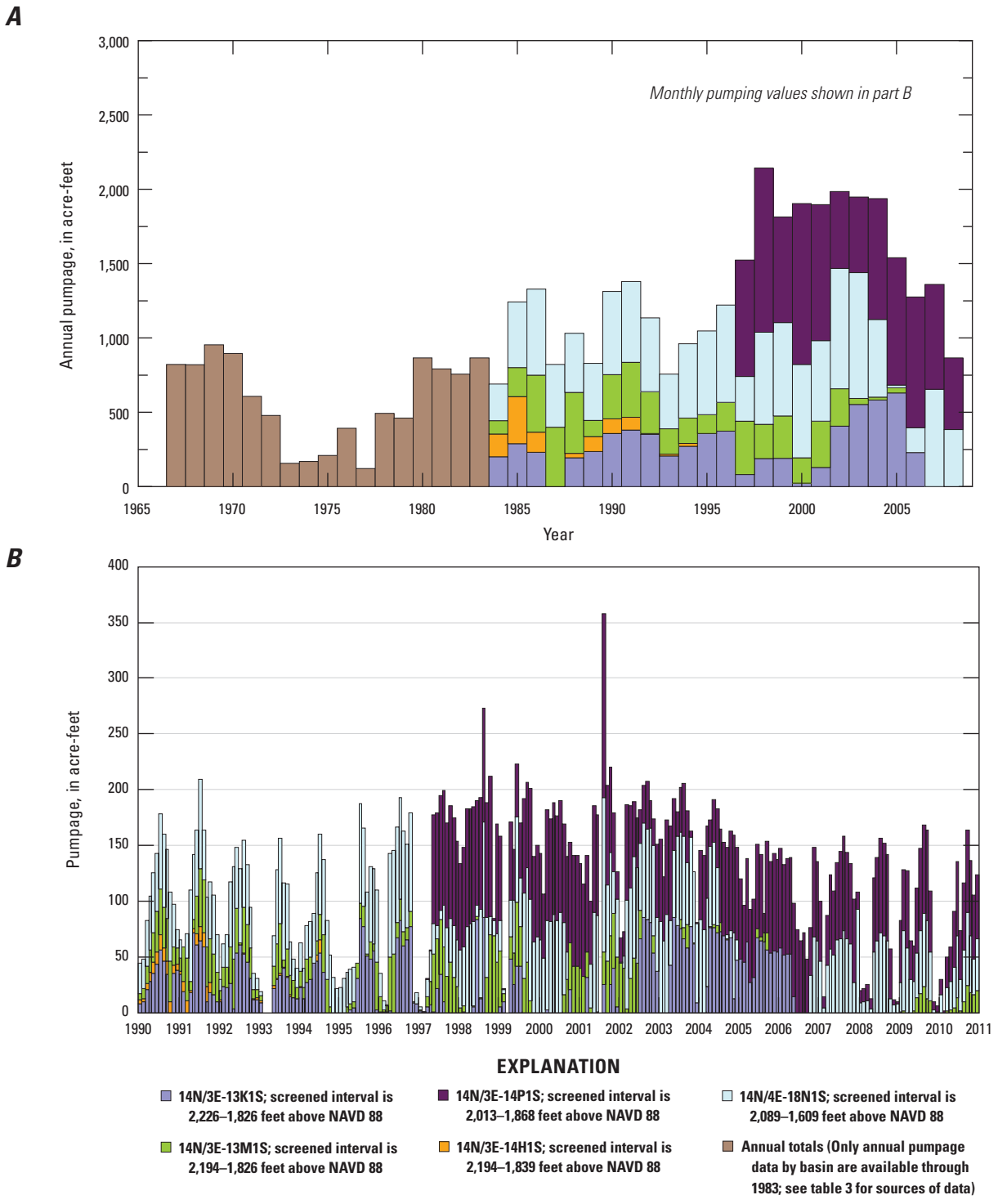

Figure 6. Pumpage by production well, for Bicycle Basin, Fort Irwin National Training Center, California: *A*, annual, 1967 to 2008, and *B*, monthly, 1990 to 2010. Location of wells shown on figure 2.

Table 3. Annual pumpage, in acre-feet, for Bicycle Basin at Fort Irwin National Training Center, California, 1967–2010.

[Location of wells shown on figure 2.]

Year	Annual total	14N/3E-13K1S B-1	14N/3E-14H1S B-2	14N/3E-13M1S B-4	14N/4E-18N1S B-5	14N/3E-14P1S B-6
1967	[1]821	[2]307	[2]252	[2]263	0	0
1968	[1]819	[2]306	[2]251	[2]262	0	0
1969	[1]953	[2]356	[2]292	[2]305	0	0
1970	[1]895	[2]335	[2]274	[2]286	0	0
1971	[1]608	[2]227	[2]186	[2]194	0	0
1972	[1]480	[2]179	[2]147	[2]153	0	0
1973	[1]157	[2]59	[2]48	[2]50	0	0
1974	[1]170	[2]64	[2]52	[2]54	0	0
1975	[1]210	[2]78	[2]64	[2]67	0	0
1976	[1]393	[2]147	[2]120	[2]126	0	0
1977	[1]123	[2]46	[2]38	[2]39	0	0
1978	[1]493	[2]184	[2]151	[2]158	0	0
1979	[1]462	[2]173	[2]141	[2]148	0	0
1980	[1]865	[2]324	[2]265	[2]277	0	0
1981	[1]792	[2]296	[2]243	[2]253	0	0
1982	[1]757	[2]283	[2]232	[2]242	0	0
1983	[1]865	[2]324	[2]265	[2]277	0	0
1984	689	201	153	90	245	0
1985	1,243	289	317	196	441	0
1986	1,329	231	135	384	578	0
1987	822	0	0	400	423	0
1988	1,032	195	29	411	398	0
1989	829	237	101	108	384	0
1990	1,312	357	99	298	558	0
1991	1,380	380	87	368	544	0
1992	1,135	353	4	282	495	0
1993	757	206	12	171	369	0
1994	961	272	19	170	500	0
1995	1,047	358	0	127	563	0
1996	1,222	373	0	194	654	0
1997	1,524	81	0	359	301	783
1998	2,143	188	0	230	621	1,104
1999	1,814	191	0	285	627	711
2000	1,904	24	0	171	627	1,082
2001	1,896	129	0	312	540	915
2002	1,984	407	0	252	808	516
2003	1,948	553	0	41	845	509
2004	1,938	583	0	18	523	813
2005	1,541	631	0	35	18	857
2006	1,275	229	0	0	166	880
2007	1,360	0	0	0	655	705
2008	868	0	0	0	384	484

Table 3. Annual pumpage, in acre-feet, for Bicycle Basin at Fort Irwin National Training Center, California, 1967–2010.—Continued

[Location of wells shown on figure 2.]

Year	Annual total	14N/3E-13K1S B-1	14N/3E-14H1S B-2	14N/3E-13M1S B-4	14N/4E-18N1S B-5	14N/3E-14P1S B-6
2009	1,180	0	0	81	493	607
2010	1,090	0	0	116	424	551
Total pumpage	[4]46,088	6,470	955	5,098	13,184	10,516
Number of years with reported pumpage	44	22	10	24	27	14
Average per year[3]	1,047	294	95	212	488	751

[1]Distribution of pumpage by well was not available from historical data. Only total pumpage had been reported. Data for 1967–71 and 1973–79 were from James M. Montgomery and Associates, 1981; data for 1972 and 1980 were estimated by the U.S. Geological Survey; 1981–83 were from Wilson F. So and Associates, 1989; and 1984–2010 were from U.S. Army, Fort Irwin Directorate of Public Works.

[2]Estimated distribution of pumpage by well based on averaged ratios of well pumpage to total pumpage for three years of recorded pumpage, 1984–86.

[3]Average for each well was estimated based on only the number of years with reported pumpage from 1984 to 2010. Average of total annual pumpage was calculated for 44 years of reported pumpage. Because of rounding of numbers, calculation of total pumpage from averages and years reported may not equal total pumpage.

[4]Total annual pumpage includes total pumpage for 1967–84 that was not available by well.

Table 4. Comparison of minimum, maximum and average monthly pumpage, in acre-feet, for Bicycle Basin, Fort Irwin National Training Center, California, 1991 to 2010.

Month	1991–2010	1991–2000			2001–2010			Difference in average monthly pumpage
	Average	Minimum	Maximum	Average	Minimum	Maximum	Average	
January	82.2	5.3	158.7	57.8	20.0	155.6	100.5	42.7
February	65.4	0.0	148.2	42.1	1.4	141.2	84.6	42.6
March	95.4	0.0	183.2	58.9	25.2	186.3	123.4	64.5
April	109.4	0.0	182.6	100.5	12.5	185.3	111.8	11.3
May	132.3	41.0	188.1	125.2	60.0	192.4	133.9	8.8
June	150.0	44.9	222.6	151.2	74.3	183.0	146.2	-5.0
July	160.8	128.9	209.4	177.2	64.9	201.9	141.6	–35.6
August	163.2	116.8	273.4	172.6	71.4	205.5	153.1	–19.6
September	147.7	83.0	206.8	140.6	48.9	207.5	155.7	15.1
October	137.2	51.7	212.2	134.4	57.2	219.8	138.5	4.0
November	102.7	9.7	174.3	85.5	9.9	179.7	116.0	30.5
December	95.4	18.2	169.0	83.6	6.1	151.3	102.7	19.1

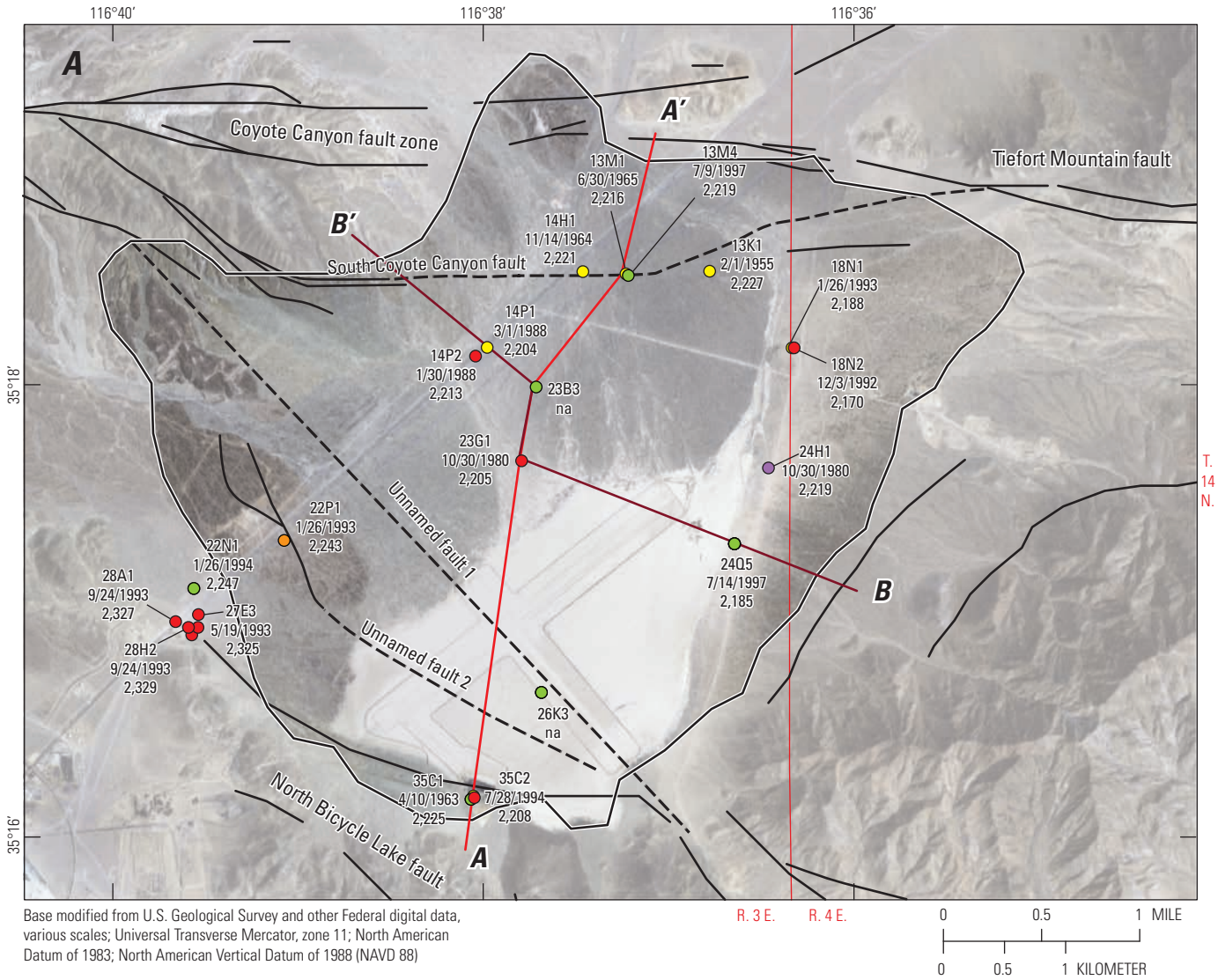

Figure 7. Water levels measured at production wells, test wells, and shallowest wells at multiple-well monitoring sites, Bicycle Basin, Fort Irwin National Training Center, California: *A*, earliest, 1955–97, and *B*, 2010–11.

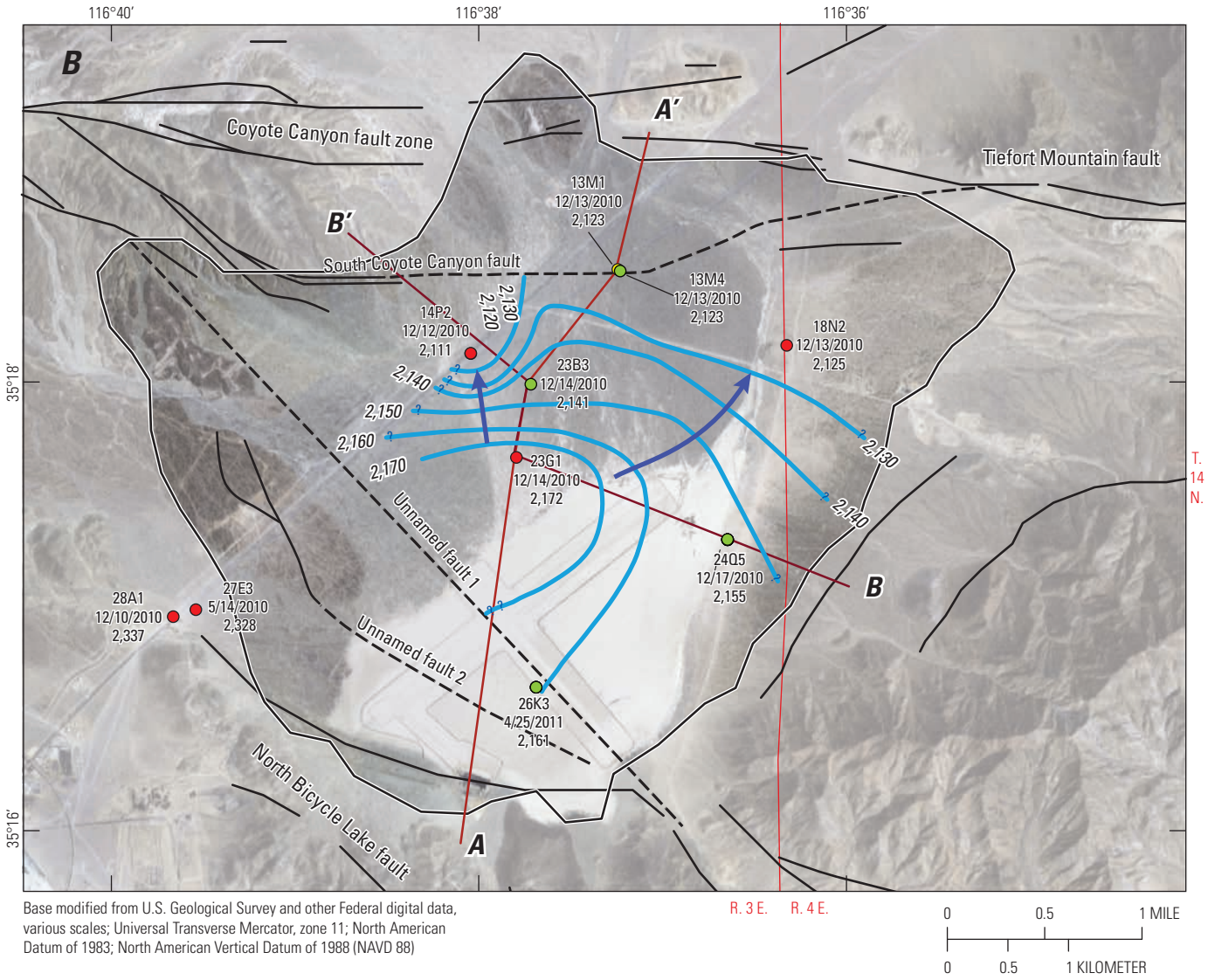

Base modified from U.S. Geological Survey and other Federal digital data, various scales; Universal Transverse Mercator, zone 11; North American Datum of 1983; North American Vertical Datum of 1988 (NAVD 88)

EXPLANATION

- Bicycle groundwater basin
- Section *A–A′*
- Section *B–B′*
- Fault
- Model inferred fault
- Line of equal water level, 2010. Contour interval is 10 feet.
- Township/range
- Direction of groundwater flow

Well type and stacked identifier (see table 1)—top number is the well identifier; middle number is date of earliest measurement (mm/dd/yyyy, mm=month; dd=day; yyyy=year); bottom number is altitude of water table in feet above NAVD 88

14P1 3/1/1988 2,204 — Production

24Q5 7/14/1997 2,185 — Multiple-well monitoring site

14P2 1/30/1988 2,213 — Test well

Figure 7. —Continued

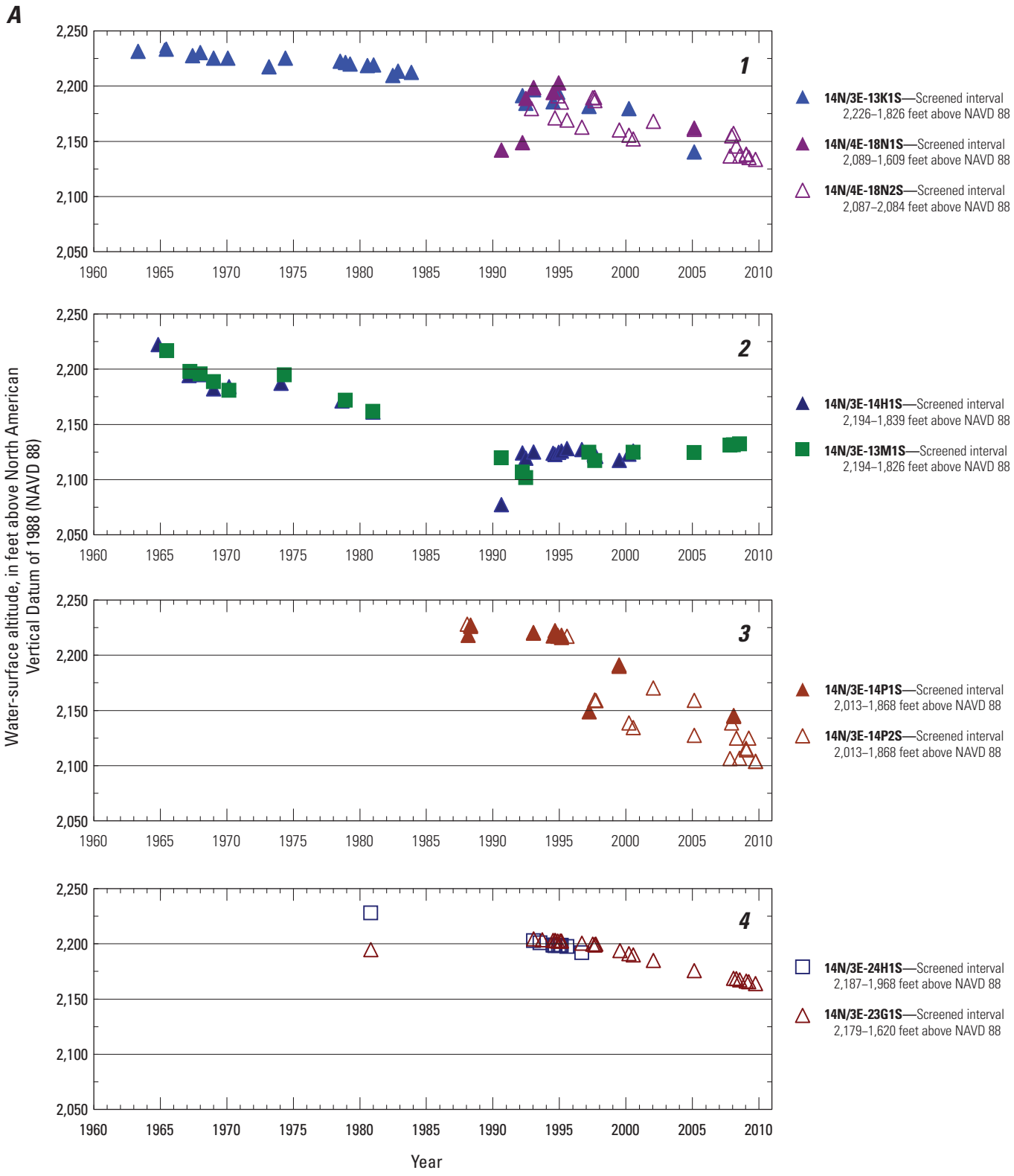

Figure 8. Water-surface altitude in production and monitoring wells in Bicycle Basin, Fort Irwin National Training Center, California: *A*, periodic, 1963–2010, and *B*, continuous, 2007–10.

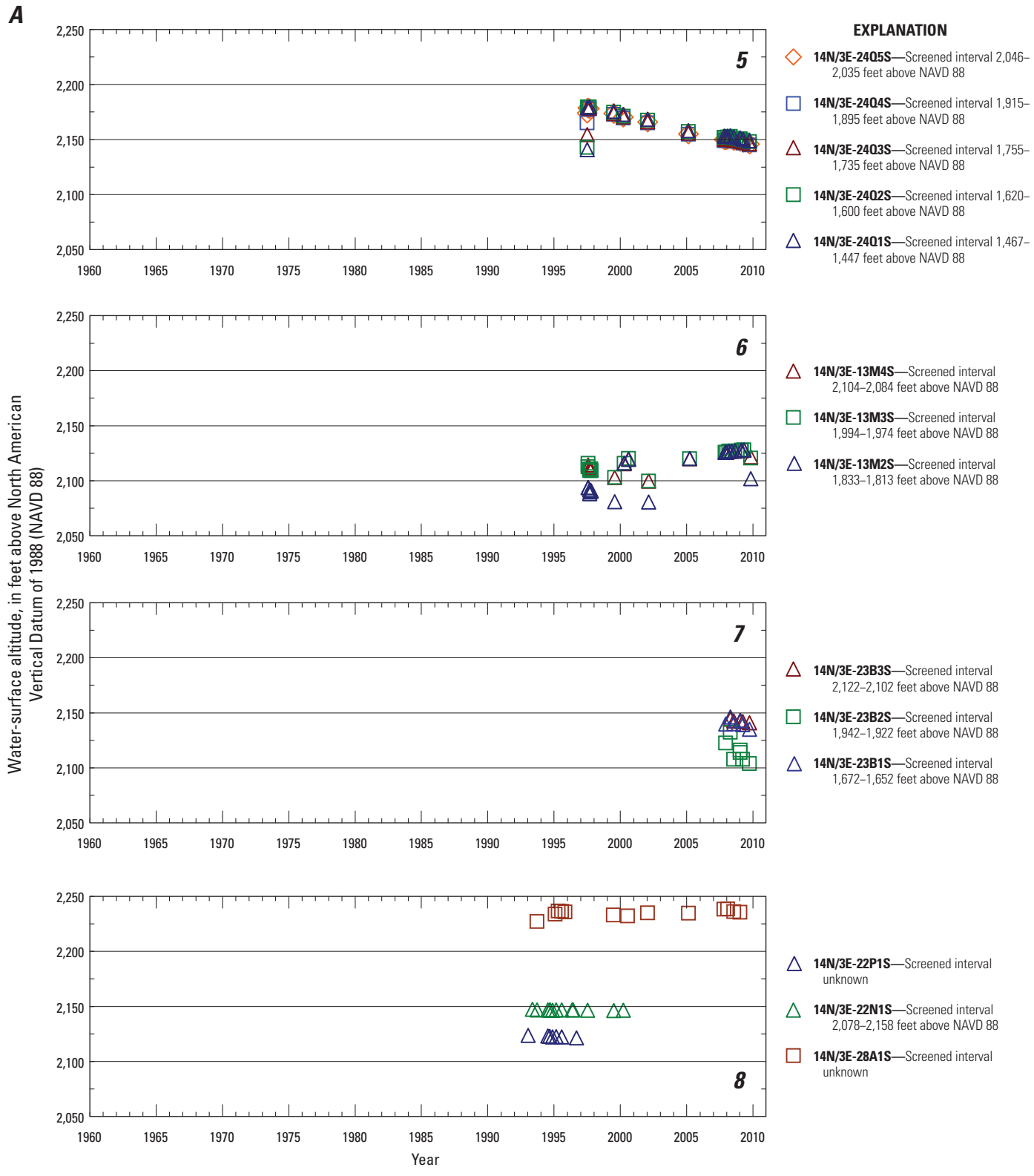

Figure 8. —Continued

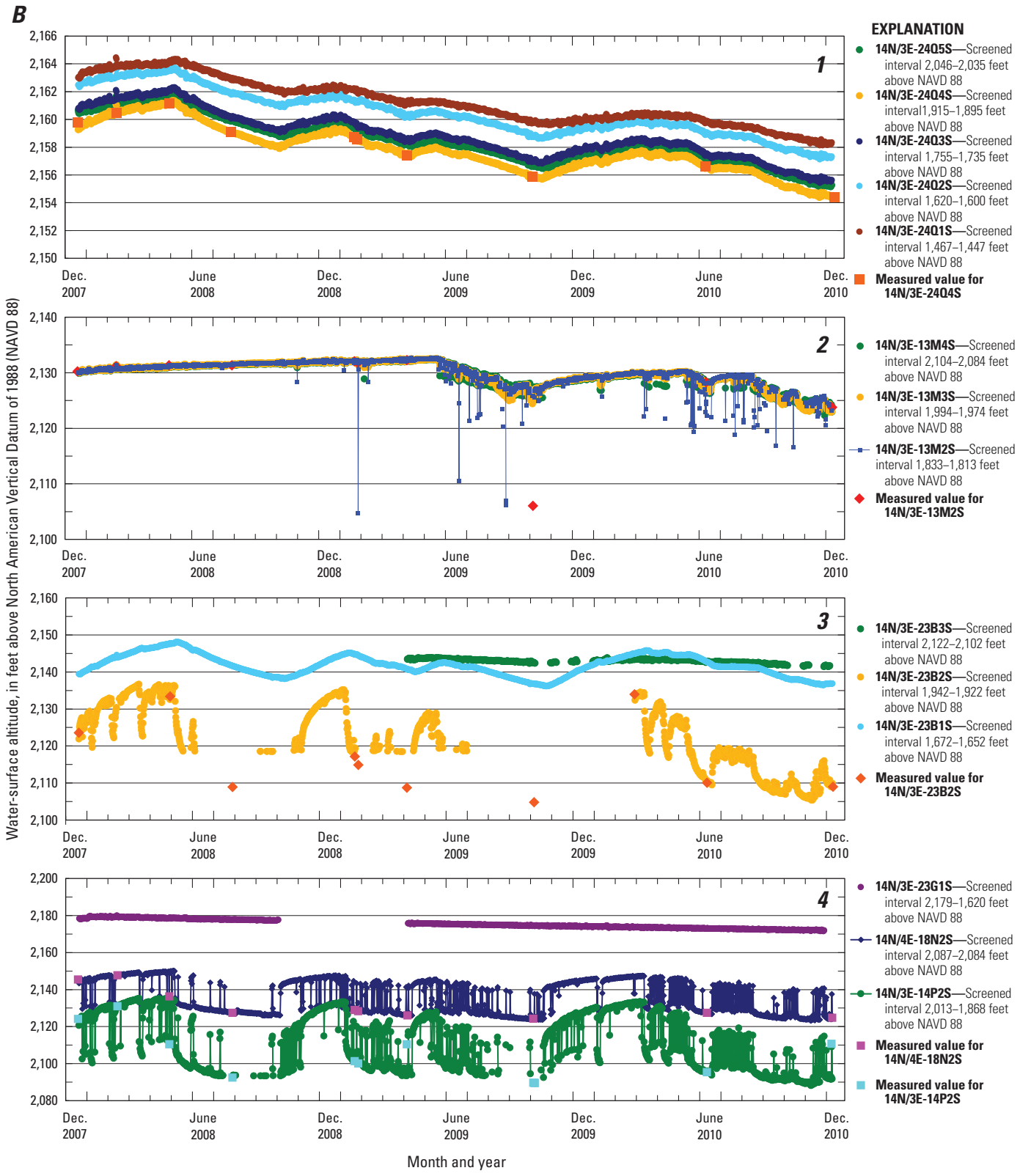

Figure 8. —Continued

Water levels in wells 14N/3E-24Q1–5 (fig. 8*A*5) showed a similar long-term water-level decline as those in test hole 14N/4E-18N2, used as a proxy for water levels in production well 14N/4E-18N1 (fig. 8*A*1). Monitoring well site 14N/3E-24Q1–5 is along the southeastern edge of Bicycle Lake (dry), south of wells 14N/4E-18N1, -18N2 and 14N/3E-24H1, and east of wells 14N/3E-14P1 and -14P2. Wells 14N/3E-24Q1–5, 14N/4E-18N1 and -18N2, are perforated in Quaternary-Tertiary older alluvium, Tertiary younger gravels, and Tertiary older gravels (QToa, Tyg, and Tog). Water levels in wells 14N/3E-24Q1–5 were also similar to, but consistently higher than, water levels in well 14N/3E-24H1, perforated in Quaternary older alluvium (Qoa) and Quaternary-Tertiary older alluvium (QToa). During the late-1990s, water levels in wells 14N/3E-24Q1–5 (fig. 8*A*5) were lower than those in production well 14N/3E-14P1 and nearby test well 14N/3E-14P2 (fig. 8*A*3), to the west, but by 2007–09, water levels in wells 14N/3E-24Q1–5 were higher than water levels in well 14N/3E-14P1 and -14P2, indicating a shift in groundwater-flow directions as a result of pumping in well 14N/3E-14P1. A seasonal trend was also observed in the continuous water-level data (fig. 8*B*1), described later in this section.

Water levels in wells 14N/3E-13M2–4 (fig. 8*A*6), near production well 14N/3E-13M1 in the northern part of the basin, showed long-term trends similar to water levels in the production well (fig. 8*A*2). Water levels in the shallower wells 14N/3E-13M3 and 14N/3E-13M4, perforated in Quaternary-Tertiary older alluvium (QToa), were similar to those in the production well 14N/3E-13M1, perforated in the Quaternary-Tertiary older alluvium and Tertiary younger gravels (QToa and Tyg); whereas, water levels were lower in the deeper well 14N/3E-13M2, perforated in Tertiary younger gravels (Tyg). Occasional steep water-level declines in well 14N/3E-13M2 reflected water levels when production well 14N/3E-13M1 was pumping, indicating less groundwater flow from the Tertiary younger gravels (Tyg) to the production well. These wells also showed a seasonal trend in the continuous water-level data (fig. 8*B*2).

Wells 14N/3E-23B1–3 are in the center of the basin near production well 14N/3E-14P1 and adjacent test well 14N/3E-14P2; water levels in these wells (fig. 8*A*7) showed a similar decline as in test well 14N/3E-14P2, used as a proxy for the production well 14N/3E-14P1 (fig. 8*A*3). Water levels in the middle well, 14N/3E-23B2, perforated in the main production zone, mimicked water levels measured in wells 14N/3E-14P1 and -14P2 (fig. 8*A*3). Declines in water levels in the deep well, 14N/3E-23B1, were damped slightly, indicating less groundwater flow from the lower aquifer and Tertiary units to the production well. Water levels in the shallowest well, 14N/3E-23B3, showed very little seasonal change and declined slightly in response to pumping in well 14N/3E-14P1. At wells 14N/3E-23B1–3, the vertical gradients indicating downward and upward flow toward the production zone were likely a response to nearby pumping in 14N/3E-14P1.

Water levels in well 14N/3E-22P1 (fig. 8*A*8) showed a slight decline from 1993 to 1997, while water levels in wells 14N/3E-22N1 and 14N/3E-28A1, south-southwest of well 14N/3E-22P1, showed minimal or no water-level decline. This indicated that these wells were isolated from pumping in other parts of the basin by faults acting as barriers to groundwater flow or differences in lithology not related to faulting.

Continuous water-level data from multiple-well monitoring sites indicated that the water levels varied with depth in some areas, primarily showing groundwater moving from relatively shallow and deep parts of the aquifer to the zones in between, from which groundwater was withdrawn (figs. 2, 8*B*). Hourly water levels were collected from December 2007 through December 2010. To simplify, continuous water-level data were filtered to show only the noon (12 p.m.) and midnight (12 a.m.) values (figs. 8*B*1–4). Water levels in well 14N/3E-13M4 were lower than those in well 14N/3E-13M3, which were usually higher than water levels in well 14N/3E-13M2 (fig. 8*B*2). These water levels showed slight upward vertical flow between wells 14N/3E-13M4 and 14N/3E-13M3 and downward vertical flow between wells 14N/3E-13M3 and 14N/3E-13M2.

The water-level differences between the shallow wells 14N/3E-24Q5 and 14N/3E-24Q4 (fig. 8*B*1), east of Bicycle Lake, indicated downward vertical flow. Water-level differences among wells 14N/3E-24Q3, 14N/3E-24Q2, and 14N/3E-24Q1 indicated upward vertical flow to the depth perforated by well 14N/3E-24Q4, which had the lowest water-level altitudes of all wells at this site.

In the monitoring wells 14N/3E-23B1–3 (fig. 8*B*3), there were large downward vertical hydraulic gradients between the shallow well 14N/3E-23B3 and the middle well 14N/3E-23B2 and large upward vertical gradients between the deep well 14N/3E-23B1 and the middle well 14N/3E-23B2. The large gaps in data were times when the water levels fell below the position of the recording pressure transducer.

Continuous water-level responses in deep monitoring wells 14N/3E-13M2 and 14N/3E-23B1 that differed from shallower wells (14N/3E-13M3, 14N/3E-13M4, and 14N/3E-23B2, and 14N/3E-23B3, respectively) indicated confined conditions in the lower aquifer at these sites. Supporting evidence for confined conditions included periodic larger drawdowns in 14N/3E-13M2 than in the shallower wells at this site (fig. 8*B*2). In addition, larger drawdowns and temporal responses in 14N/3E-23B1 compared to 14N/3E-23B3 (fig. 8*B*3) indicated that the deep well (14N/3E-23B1) was in at least semi-confined conditions.

Figure 8*B*4 shows continuous water levels for test wells 14N/3E-14P2, 14N/3E-23G1 and 14N/4E-18N2. Well 14N/3E-14P2 is near production well 14N/3E-14P1, northwest of the multiple-well monitoring site 14N/3E-23B1–3 (fig. 2), and is perforated at similar depths as production well 14N/3E-14P1. Water levels in well 14N/3E-14P2 showed seasonal fluctuations, pumping drawdown and rebound that were similar to well 14N/3E-23B2. Test well 14N/3E-23G1 is south of wells 14N/3E-23B1–3. Water levels in well 14N/3E-23G1 represented the long, 560-ft perforated interval. The hydrograph showed no seasonal fluctuations, but did show a decline of about 5 ft over the 2-year period. A video log of 14N/3E-23G1 from February 2015 showed scaling in the well beginning at a depth of about 230 ft and heavy scaling below 530 ft. This information, coupled with the water-level data, suggested that water levels measured in this well were representative of the water table. Test well 14N/4E-18N2 is near production well 14N/4E-18N1, in the northeastern part of the basin. Water levels in well 14N/4E-18N2 showed similar seasonal fluctuations as in wells 14N/3E-14P2 and 14N/3E-23B2. Drawdowns in well 14N/4E-18N2 could be less than in well 14N/3E-14P2 because the perforated interval in the monitoring well 14N/4E-18N2 is shorter and shallower than that in test well 14N/3E-14P2.

Land-Surface Deformation

Land-surface deformation, in the form of an earth fissure and sink-like depressions associated with land subsidence, was present on the Bicycle Lake (dry) playa; the playa is used as an aircraft runway for transporting troops and supplies to the base. Land-surface deformation attributed to groundwater pumping is found in many aquifer systems that, at least in part, are made up of unconsolidated, interbedded, fine- to coarse-grained deposits and have undergone extensive groundwater development (Poland, 1984). Several methods were used as part of this study to evaluate the cause of land-surface deformation in Bicycle Basin. These included Interferometric Synthetic Aperture Radar (InSAR), electromagnetic induction (EM), electrical resistivity tomography (ERT), and geodetic surveys. InSAR images were developed for Bicycle Basin and were used to map the areal extent and amount of vertical land-surface change in the basin. Electromagnetic induction and electrical resistivity data were collected to detect the presence and delineate the depth of earth fissures, macropolygons, and other related features. Geodetic surveys were done to monitor vertical and horizontal land-surface change across the basin, specifically on the playa, where InSAR does not work as well. This section briefly summarizes the InSAR methods used in the land-surface deformation study and presents maps showing the areal extent of the subsidence and time-series data calculated for input in the subsidence model.

InSAR, a satellite-based remote sensing technique, is an effective way to measure vertical changes of land surface and can detect centimeter-level ground-surface displacement over a 62-by-62-mi (100-by-100-km) area with spatial resolution on the order of 295 ft (90 m) or less. This technique has been used to investigate deformation resulting from earthquakes (Massonnet and others, 1993), volcanoes (Massonnet and others, 1995), and land subsidence (Massonnet and others, 1997; Fielding and others, 1998; Galloway and others, 1998; Amelung and others, 1999, Hoffmann and others, 2003; Sneed and Brandt, 2007). Synthetic Aperture Radar (SAR) data from the European Space Agency's (ESA) European Remote Sensing satellites I and II (ERS-1 and ERS-2), and ENVISAT satellite were used to map and measure range (vertical) change. The satellites are side-looking, orbit the Earth at an altitude of approximately 497 mi (800 km), have 35-day repeat cycles, and have effectively the same accuracy. The use of InSAR involved the development and analysis of interferograms that show vertical changes in the ground surface between images. The interferograms had timelines ranging from 4.6 to 36.3 months, using 24 SAR scenes acquired during 1992–2000 by the ERS-1 and ERS-2 satellites, and timelines ranging from 1.1 to 32.1 months, using 13 SAR scenes acquired during 2003–06 by the ENVISAT satellite (table 5).

Figure 9*A* shows the interferogram of land-surface deformation for November 30, 2003, through January 23, 2005, during the period when the earth fissure was first detected. The direction of change—subsidence or uplift—is indicated by the color progression of the fringe toward the center of a deforming feature. The color-fringe progression of red-purple-blue-green-yellow-orange indicates subsidence; the opposite progression indicates uplift.

During 2003–05, subsidence was identified in the area immediately north of Bicycle Lake (dry) playa. The nearest production well was 14N/3E-14P1. The area affected by subsidence was about 2.6 mi^2 and coincided with an area containing substantial clay deposits, as documented in lithology logs for wells 14N/3E-23B1–3, 14N/3E-14P1, 14N/3E-14P2, and 14N/3E-23G1. Subsidence was not detected elsewhere in the basin, where lithology logs for wells 14N/3E-24Q1–5, 14N/3E-13M2–4, 14N/3E-13M1, 14N/3E-13K1, 14N/3E-14H1, 14N/3E-24H1, and 14N/4E-18N1 indicated that clay deposits were less prevalent (fig. 3*A*, *B*; appendix 1).

Subsidence rates during 2003–06 were nearly double those during 1992–2000. Subsidence rates calculated from interferograms spanning 1992–2000 ranged from 0.02–0.1 inches per month, or in./mo (0.62 to 2.6 millimeters per month [mm/mo]) and averaged 0.06 in./mo (1.5 mm/mo; table 5). Subsidence rates calculated from interferograms spanning 2003–06 ranged from 0–0.2 in./mo (0 to 4.36 mm/mo) and averaged 0.1 in./mo (2.2 mm/mo). Furthermore, subsidence rates generally accelerated during 1999–2000 and 2003–06 regardless of seasonal conditions, whereas subsidence rates during 1992–99 were more variable and correlated with seasonal conditions. The increase in subsidence rates after 1999 generally coincided with the start of pumping from well 14N/3E-14P1.

Table 5. Acquisition dates of synthetic aperture radar data, interferogram timelines, and subsidence magnitudes and rates for 72 interferograms analyzed for Bicycle Lake Basin, Fort Irwin National Training Center, California, 1992–2010.

[ERS-1 and ERS-2, European Space Agency's (ESA) European Remote Sensing satellites I and II; ENVISAT, European Space Agency's Environmental Satellite that replaced ERS-1 and ERS-2; in., inch; mm, millimeters; mm/dd/yyyy, month/day/year; —, not applicable]

Interferogram reference number	Acquisition dates		Timeline of data collection (months)	Magnitude[1]		Rate[1]		Seasonal span of interferogram		
	Start (mm/dd/yyyy)	End (mm/dd/yyyy)		(mm)	(in.)	(mm per month)	(in. per month)	Annual/ multi-annual	Winter/spring–summer/fall	Summer/fall–winter/spring
ERS-1 and ERS-2										
1	08/07/1992	08/20/1995	36.3	25	0.98	0.69	0.03	x	—	—
[2]2	11/05/1993	09/25/1995	22.6	30	1.18	1.33	0.05	x	—	—
[2]3	01/08/1996	07/01/1996	5.7	5	0.20	0.87	0.03	—	x	—
[2]4	10/14/1996	07/21/1997	9.2	15	0.59	1.63	0.06	x	—	—
5	09/25/1995	05/27/1996	8.0	10	0.39	1.24	0.05	—	—	x
[2]6	06/16/1997	01/12/1998	6.9	10	0.39	1.45	0.06	—	—	x
7	08/05/1996	04/07/1997	8.0	5	0.20	0.62	0.02	—	—	x
8	08/05/1996	08/10/1998	24.1	30	1.18	1.24	0.05	x	—	—
9	03/03/1997	08/25/1997	5.7	15	0.59	2.61	0.10	—	x	—
10	03/03/1997	03/23/1998	12.6	25	0.98	1.98	0.08	x	—	—
11	04/07/1997	08/25/1997	4.6	10	0.39	2.18	0.09	—	x	—
12	08/25/1997	06/01/1998	9.2	10	0.39	1.09	0.04	—	—	x
[2]13	03/23/1998	08/10/1998	4.6	10	0.39	2.18	0.09	—	x	—
14	03/23/1998	06/21/1999	14.9	25	0.98	1.68	0.07	—	x	—
15	07/06/1998	03/08/1999	8.0	10	0.39	1.24	0.05	—	—	x
[2]16	08/10/1998	06/21/1999	10.3	10	0.39	0.97	0.04	x	—	—
[2]17	07/26/1999	03/27/2000	8.0	20	0.79	2.49	0.10	—	—	x
[2]18	03/27/2000	09/18/2000	5.7	15	0.59	2.61	0.10	—	x	—
ENVISAT										
[2]19	10/26/2003	06/27/2004	8.0	15	0.59	1.87	0.07	—	—	x
20	10/26/2003	11/14/2004	12.6	30	1.18	2.38	0.09	x	—	—
21	10/26/2003	12/19/2004	13.8	30	1.18	2.18	0.09	x	—	—
22	10/26/2003	02/27/2005	16.1	35	1.38	2.18	0.09	—	—	x
23	10/26/2003	04/03/2005	17.2	50	1.97	2.90	0.11	—	—	x
24	10/26/2003	06/12/2005	19.5	50	1.97	2.56	0.10	—	—	x
[3]25	11/30/2003	01/23/2005	13.8	35	1.38	2.54	0.10	—	—	x
26	11/30/2003	09/25/2005	21.8	65	2.56	2.98	0.12	x	—	—
27	05/23/2004	01/23/2005	8.0	10	0.39	1.24	0.05	x	—	—
28	05/23/2004	04/03/2005	10.3	25	0.98	2.42	0.10	x	—	—
29	05/23/2004	07/17/2005	13.8	35	1.38	2.54	0.10	—	x	—
30	05/23/2004	09/25/2005	16.1	45	1.77	2.80	0.11	—	x	—
31	05/23/2004	04/23/2006	23.0	80	3.15	3.49	0.14	x	—	—
32	06/27/2004	11/14/2004	4.6	10	0.39	2.18	0.09	—	—	x
[2]33	06/27/2004	02/27/2005	8.0	25	0.98	3.11	0.12	—	—	x
34	06/27/2004	03/19/2006	20.7	65	2.56	3.15	0.12	—	—	x
35	11/14/2004	12/19/2004	1.1	0	0.00	0.00	0.00	x	—	—
[2]36	04/03/2005	06/12/2005	2.3	10	0.39	4.36	0.17	—	—	x
37	07/17/2005	09/25/2005	2.3	10	0.39	4.36	0.17	x	—	—

Table 5. Acquisition dates of synthetic aperture radar data, interferogram timelines, and subsidence magnitudes and rates for 72 interferograms analyzed for Bicycle Basin, Fort Irwin, California, 1992–2010.—Continued

[ERS-1 and ERS-2, European Space Agency's (ESA) European Remote Sensing satellites I and II; ENVISAT, European Space Agency's Environmental Satellite that replaced ERS-1 and ERS-2; in., inch; mm, millimeters; mm/dd/yyyy, month/day/year; —, not applicable]

Interferogram reference number	Acquisition dates		Timeline of data collection (months)	Magnitude[1]		Rate[1]		Seasonal span of interferogram		
	Start (mm/dd/yyyy)	End (mm/dd/yyyy)		(mm)	(in.)	(mm per month)	(in. per month)	Annual/ multi-annual	Winter/spring–summer/fall	Summer/fall–winter/spring
ENVISAT—Continued										
[2]38	07/17/2005	04/23/2006	9.2	30	1.18	3.27	0.13	—	x	—
39	01/23/2005	09/25/2005	8.0	25	0.98	3.11	0.12	—	x	—
[2]40	02/27/2005	06/12/2005	3.4	10	0.39	2.90	0.11	—	x	—
41	02/27/2005	03/19/2006	12.6	45	1.77	3.56	0.14	x	—	—
42	02/27/2005	11/19/2006	20.7	60	2.36	2.90	0.11	—	x	—
43	02/27/2005	12/24/2006	21.8	65	2.56	2.98	0.12	x	—	—
44	04/03/2005	06/12/2005	2.3	5	0.20	2.18	0.09	x	—	—
45	04/03/2005	10/15/2006	18.4	50	1.97	2.72	0.11	—	x	—
46	06/12/2005	12/24/2006	18.4	60	2.36	3.27	0.13	—	—	x
[2]47	07/17/2005	09/25/2005	2.3	10	0.39	4.36	0.17	x	—	—
48	07/17/2005	04/23/2006	9.2	35	1.38	3.81	0.15	—	—	x
[2]49	09/25/2005	04/23/2006	6.9	30	1.18	4.36	0.17	—	—	x
[2]50	03/19/2006	11/19/2006	8.0	25	0.98	3.11	0.12	—	x	—
51	10/15/2006	01/28/2007	3.4	15	0.59	4.36	0.17	—	—	x
52	10/15/2006	03/04/2007	4.6	15	0.59	3.27	0.13	—	—	x
[2]53	10/15/2006	02/17/2008	16.1	35	1.38	2.18	0.09	—	—	x
54	12/24/2006	01/13/2008	12.6	30	1.18	2.38	0.09	x	—	—
55	12/24/2006	08/30/2009	32.1	75	2.95	2.33	0.09	—	x	—
56	01/28/2007	02/17/2008	12.6	25	0.98	1.98	0.08	x	—	—
57	03/04/2007	02/17/2008	11.5	25	0.98	2.18	0.09	x	—	—
58	08/26/2007	07/26/2009	23.0	50	1.97	2.18	0.09	x	—	—
59	01/13/2008	08/10/2008	6.9	15	0.59	2.18	0.09	—	x	—
60	01/13/2008	05/17/2009	16.1	25	0.98	1.56	0.06	x	—	—
61	02/17/2008	09/14/2008	6.9	20	0.79	2.90	0.11	—	x	—
[2]62	02/17/2008	03/08/2009	12.6	25	0.98	1.98	0.08	x	—	—
63	02/17/2008	04/12/2009	13.8	30	1.18	2.18	0.09	x	—	—
64	08/10/2008	05/17/2009	9.2	15	0.59	1.63	0.06	—	—	x
65	09/14/2008	05/17/2009	8.0	10	0.39	1.24	0.05	—	—	x
66	03/08/2009	05/02/2010	13.8	15	0.59	1.09	0.04	x	—	—
[2]67	03/08/2009	08/15/2010	17.2	20	0.79	1.16	0.05	—	x	—
68	04/12/2009	05/02/2010	12.6	15	0.59	1.19	0.05	x	—	—
69	05/17/2009	05/02/2010	11.5	15	0.59	1.31	0.05	x	—	—
70	05/17/2009	08/15/2010	14.9	25	0.98	1.68	0.07	—	x	—
71	08/30/2009	08/15/2010	11.5	15	0.59	1.31	0.05	x	—	—
72	05/02/2010	08/15/2010	3.4	10	0.39	2.90	0.11	—	x	—

[1]Subsidence magnitudes in this table represent the line-of-sight ground-surface displacement (range change), which constitutes about 92 percent of true vertical change.

[2]Used for the time series generation shown in figure 9*B*.

[3]Shown in figure 9*A*.

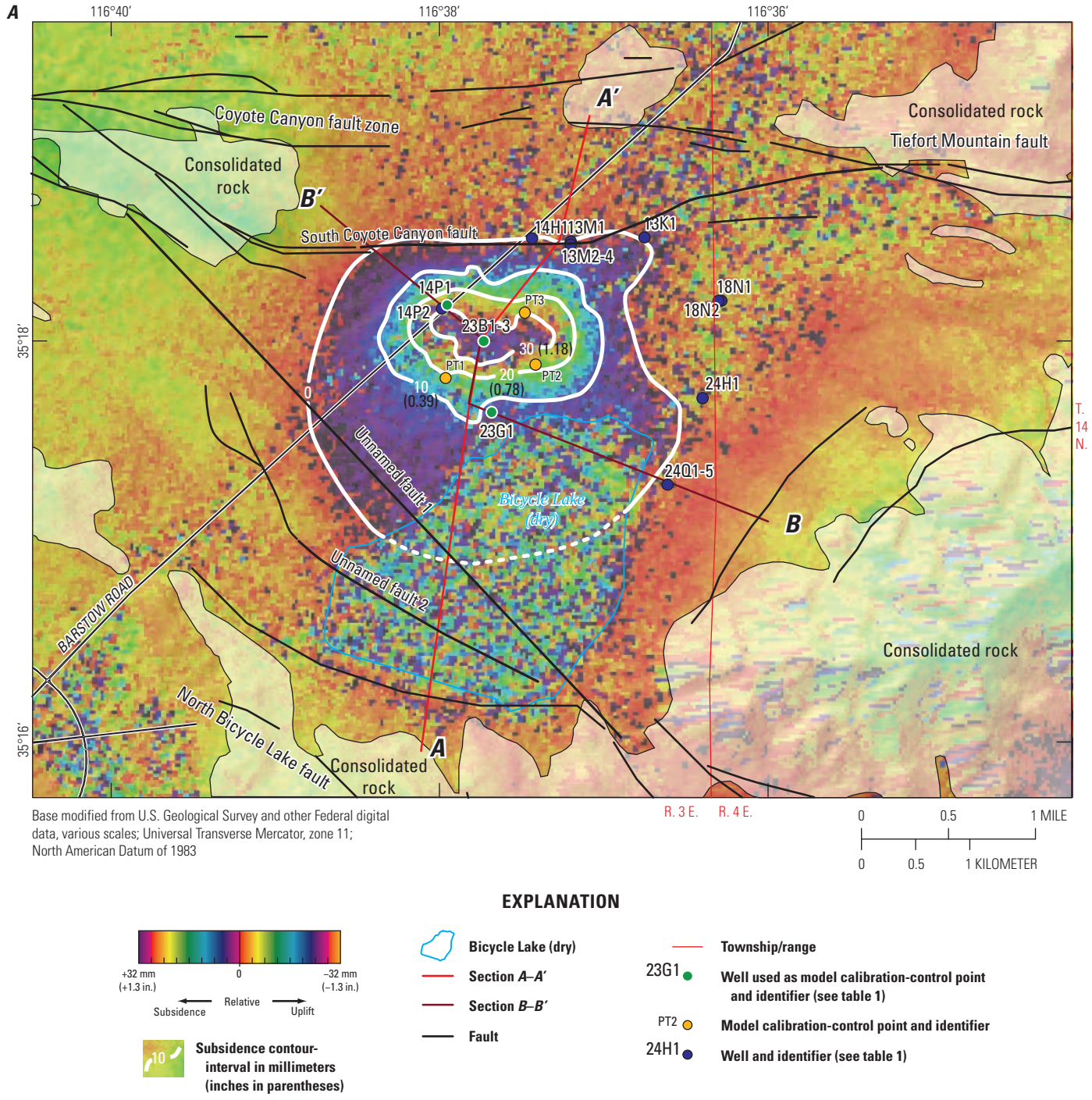

Figure 9. Subsidence in Bicycle Basin, Fort Irwin National Training Center, California: *A*, interferogram showing subsidence contours for November 30, 2003, through January 23, 2005, faults, selected wells, and model calibration points, and *B*, interferogram-derived subsidence time-series data for six selected locations, 1993–2010.

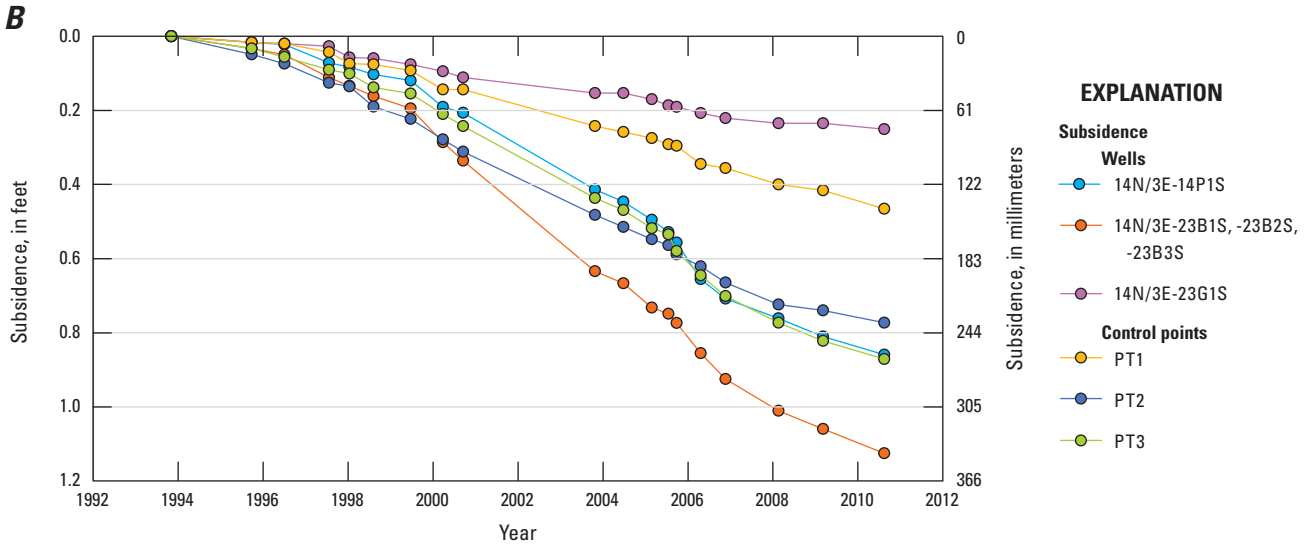

Figure 9. —Continued

The subsidence rates generally were higher during the summer and fall when water levels declined and were lower during the winter and spring when water levels recovered. Time-series data were generated for six selected locations used for model calibration to compute total subsidence for 1993–2010 by 'stacking' interferograms, such that the end date for one interferogram was used as the beginning date for the next interferogram (fig. 9*B*). Where data gaps (2001–03 and 2010–13) or overlaps existed, subsidence rates were used to compute magnitudes for the time interval of the gap or overlap, and the time series was adjusted accordingly. The time-series data were extrapolated from March 2009 to August 2010 using average subsidence rates computed from selected interferograms.

Time-series data constructed for the six locations from 1993 to 2010 indicated that subsidence ranged from about 2.8 in. or 0.2 ft (70 millimeters, mm) at well 14N/3E-23G1 to about 13.8 in. or 1.1 ft (350 mm) at well 14N/3E-23B1–3 (fig. 9*B*). Average subsidence over this 17-yr period ranged from 0.16 inch per year (in./yr), or 0.01 foot per year, ft/yr (4 millimeters per year, mm/yr) to 0.8 in/yr or 0.06 ft/yr (20.6 mm/yr). These subsidence data were used to calibrate the storage properties in the groundwater-flow model.

Geochemistry of Groundwater

Water-quality samples were collected from 30 wells at 20 monitoring sites (appendix 3) in Bicycle Basin during 1993–2011. In addition, one sequential replicate sample was collected from well 14N/3E-26K1 and evaluated to assess the precision of the water-quality data (Kjos and others, 2014). Six of the sites sampled were multiple-well monitoring sites; two sites contained two wells (14N/3E-35C2–3 and -22N1–2), three sites contained three wells (14N/3E-13M2–4, -23B1–3, and -26K1, 3, 4), and one site contained five wells (14N/3E-24Q1–5). Wells 14N/3E-35C3 and 14N/3E-22N2 were dry and not sampled. The remaining 14 wells were monitoring wells, test wells, or production wells.

Sample collection and processing followed the methods described in the USGS National Field Manual (Wilde and others, 1999, 2004). Groundwater samples were analyzed in the field for specific conductance, pH, temperature, and alkalinity. Water samples were analyzed in the laboratory for major ions, selected trace elements, nutrients, ratios of the stable oxygen (O) and hydrogen (H) isotopes, and concentrations of radioactive isotopes of tritium and carbon-14 (^{14}C). Data collected as part of this study were supplemented with historical data for selected wells, from C.F. Hostrup and Associates (1955), Kunkel and Riley (1959), James M. Montgomery and Associates (1981), and Wilson F. So and Associates (1989). Additional nutrient and nitrogen isotope samples were collected and analyzed for wells in the fire-fighting training area. These results, reported in Densmore and Bohlke (2000), were included here.

Groundwater samples for major and minor ions, trace elements, alkalinity, and total dissolved solids analyses included both raw groundwater, and filtered groundwater (Wilde and others, 2004). Filtered samples were filtered using a 0.45-micrometer (µm) capsule filter. The filtered sample was preserved with nitric acid. The ^{14}C samples were analyzed by accelerator mass spectrometry (Beukins, 1992). Major ions, selected trace elements, and nutrient samples were analyzed at the USGS National Water-Quality Laboratory (NWQL) or by laboratories contracted by the NWQL. Stable isotopes were analyzed by the USGS Stable Isotope Laboratory in Reston, Virginia, using methods described by Epstein and Mayeda (1953), Coplen and others (1991), and Coplen (1994).

Carbon-14 was analyzed by Woods Hole Oceanographic Institution, National Ocean Sciences Accelerator Mass Spectrometry Facility (NOSAMS) in Massachusetts, using methods described by Vogel and others (1987), Donahue and others (1990), Gagnon and Jones (1993), and Schneider and others (1994). Tritium was analyzed by the USGS Stable Isotope and Tritium Laboratory in Menlo Park, California, using methods described by Thatcher and others (1977). These data are in the USGS NWIS database and can be accessed at https://waterdata.usgs.gov/ca/nwis.

General Water-Quality Characteristics and Areal Variation

The chemistry of the recharge water and various geochemical reactions, including dissolution, precipitation of minerals in the subsurface, and evapoconcentration, controlled the major-ion chemistry of the groundwater in the Bicycle Basin. To visually characterize differences among major-ion chemistry (water types) in the Bicycle Basin, trilinear diagrams were plotted using a method described by Piper (1945; figs. 10*A*–*C*). To further describe general quality and areal differences, water-quality diagrams were produced using a method suggested by Stiff (1951; fig. 11).

Trilinear diagrams are a graphical representation of the relative contribution of major cations and anions to the total ionic content of the water. A percentage scale shows the cation concentrations on the upper right and lower left sides of the diamond and the anion concentrations on the upper left and lower right sides. The position of a sample on the diagram gives an indication of the chemical character of the water and allows a comparison to be made among different samples.

Trilinear diagrams were prepared from samples collected during 1965–2011 with complete analyses from each well for the northern, central, and southern part of the basin (figs. 10*A*–*C*). The north area (fig. 10*A*) includes five wells that are north of the South Coyote Canyon fault. The central area (fig. 10*B*) includes 14 wells that are between South Coyote Canyon fault and unnamed fault 1. The south area (fig. 10*C*) includes eight wells that are south of unnamed fault 1.

Groundwater in Bicycle Basin varied from sodium-bicarbonate-sulfate ($NaHCO_3$-SO_4)-type water to sodium-bicarbonate-chloride ($NaHCO_3$-Cl)-type water, depending on the sulfate and chloride concentrations, and sodium-chloride (NaCl)-type water. Groundwater from wells in the north area (fig. 10*A*) was $NaHCO_3$-SO_4-type water. Groundwater from wells in the central area (fig. 10*B*) ranged from $NaHCO_3$-SO_4 along the western side of the basin to $NaHCO_3$-Cl, as chloride (Cl) becomes more dominant than sulfate (SO_4), in wells near the playa (perforated in Quaternary-Tertiary older alluvium (QToa) and along the eastern side of the basin (perforated in Tertiary older gravels (Tog). Groundwater from wells in the south area (fig. 10*C*) was generally $NaHCO_3$-SO_4-type water, with the exception of wells 14N/3E-27E1 and 14N/3E-28A1, which are perforated in Tertiary (Tog) deposits. Firefighting training activities in the vicinity of wells 14N/3E-27E1–3, -28A1, and -28H1–2 (fig. 2) impacted groundwater in wells 14N/3E-27E1 and 14N/3E-28A1 by evapoconcentration and leaching of salts from the soils (Densmore and Bohlke, 2000), causing increased nitrate concentrations.

Water-quality diagrams show the general quality differences in the chemical character of the water by location (fig. 11). Similarly shaped diagrams indicate the presence of groundwater with similar major-ion characteristics. The width of the diagrams differs, according to the concentrations of dissolved solids.

Relatively poor groundwater quality with higher total dissolved solids appeared to be associated primarily with water withdrawn from wells perforated in the Quaternary-Tertiary older alluvium, QToa (likely evaporite deposits), and Tertiary older gravels, Tog. Groundwater quality was relatively poor, with total dissolved solids (TDS) ranging from 786 to 1,130 milligrams per liter (mg/L) and NaCl-type waters in six wells: 14N/3E-23B2, 14N/3E-24Q1, 14N/3E-24Q2, 14N/3E-27E1, 14N/3E-28A1, and 14N/4E-18N1 (fig. 11). Groundwater in these wells differed from other wells in that it is enriched in chloride and depleted in bicarbonate (HCO_3). Five of these six wells have the bottom of perforations in the Tertiary older gravels (Tog). Four of these wells, 14N/4E-18N1, 14N/3E-23B2, 14N/3E-24Q1, and 14N/3E-24Q2, are in the central area (fig. 10*B*), and two wells, 14N/3E-27E1 and 14N/3E-28A1, are in the southern area (fig. 10*C*). Well 14N/4E-18N1 is perforated from 300 to 780 ft in Quaternary-Tertiary older alluvium and Tertiary gravels (QToa, Tyg, and Tog) northeast of the playa; however, the water quality was more reflective of the Tertiary older gravels (Tog). Well 14N/3E-23B2 is perforated from 440 to 460 ft in Quaternary-Tertiary older alluvium (QToa) in the area of greatest subsidence, west of the playa; however, the water quality likely was more representative of evaporite deposits, such as the Quaternary-Tertiary older lacustrine deposits (QTol). Wells 14N/3E-24Q1 and 14N/3E-24Q2 are perforated from 878 to 898 ft and from 725 to 745 ft, respectively, in Tertiary older gravels (Tog) on the east side of Bicycle Lake (dry) playa.

The relatively high-salinity (TDS of 1,130 mg/L) water present in well 14N/3E-23B2 likely originated from buried lacustrine or playa (evaporite) deposits. Groundwater quality near playas generally reflected the lateral flow of groundwater and remobilization of buried salts from evaporate deposits. Geophysical surveys of Bicycle Lake (dry) playa showed higher conductivity in the shallow subsurface in the northern part of the Bicycle Lake (dry) playa, and core-sample x-ray diffraction analysis of shallow surficial deposits (Qp) showed that halite (NaCl) was present (Craig Rasmussen, University of Arizona, written commun., 2010). These data indicated that NaCl also would be expected in buried playa deposits.

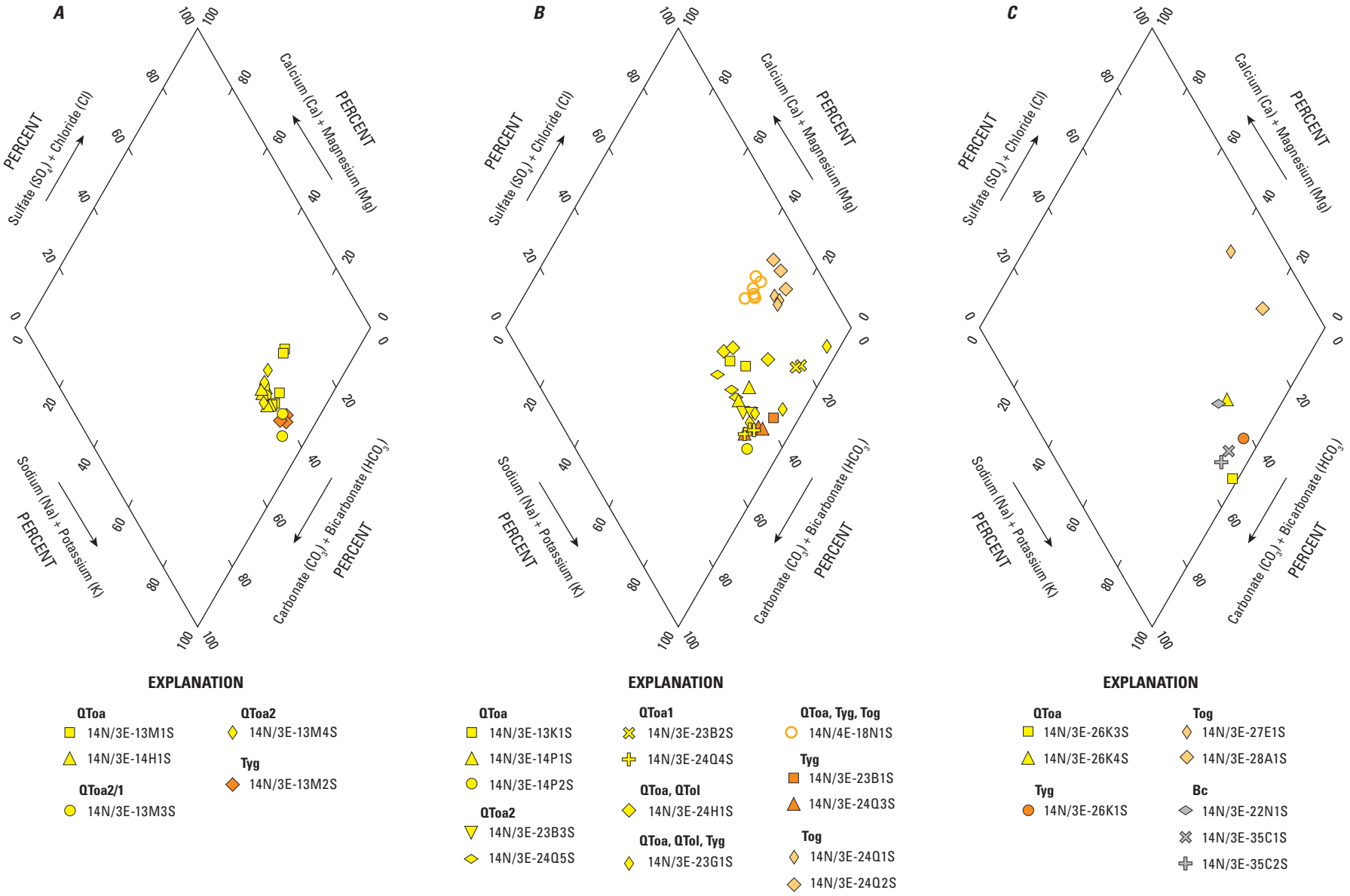

[QToa, Quaternary-Tertiary older alluvium; QTol, Quaternary-Tertiary older lacustrine; Tog, Tertiary older gravels; Tyg, Tertiary younger gravels; Bc, Basement complex]

Figure 10. Water-quality data for selected wells in the following areas in Bicycle Basin, Fort Irwin National Training Center, California: *A*, north, *B*, central, and *C*, south (location of wells shown on figure 2).

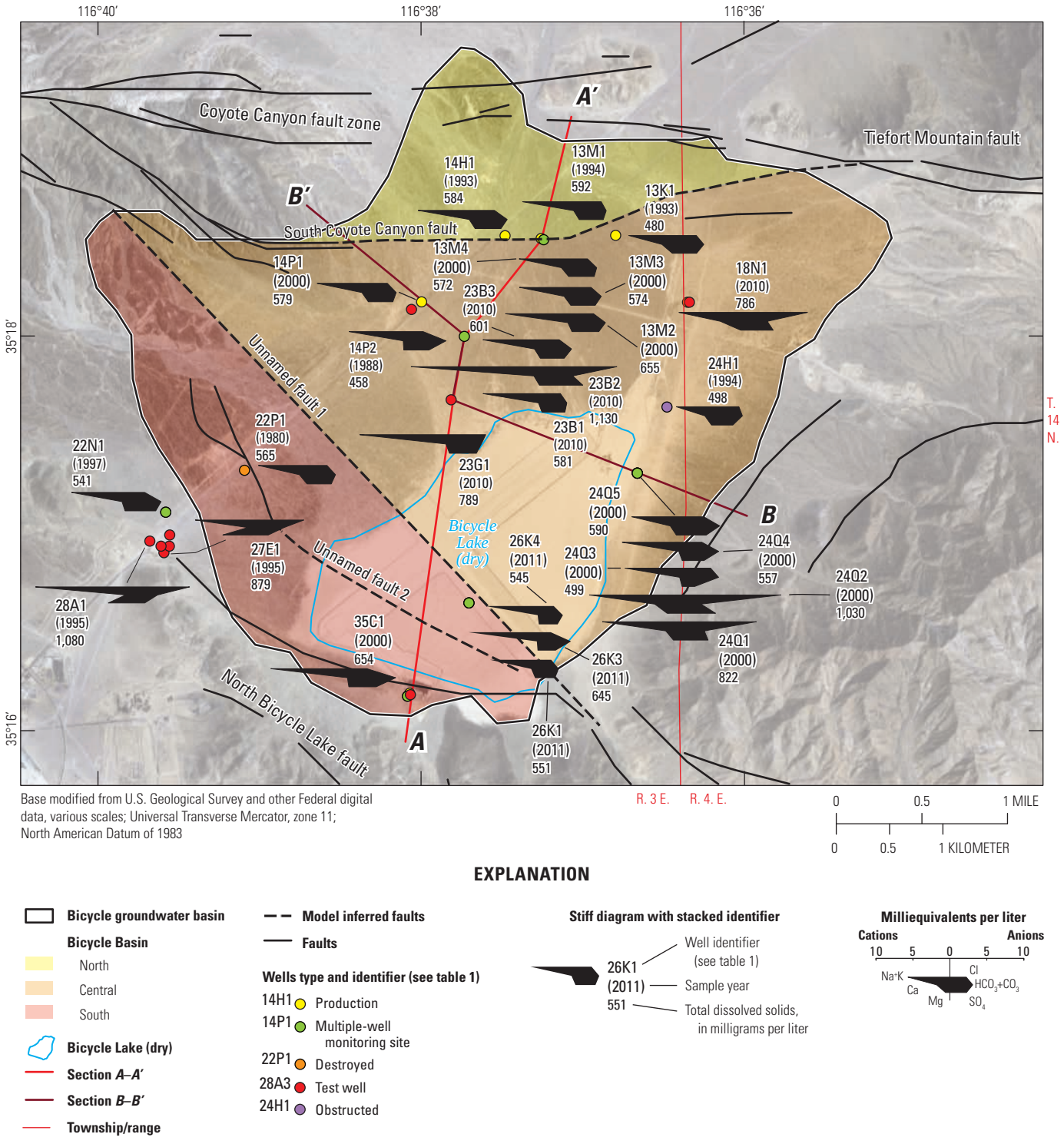

Base modified from U.S. Geological Survey and other Federal digital data, various scales; Universal Transverse Mercator, zone 11; North American Datum of 1983

EXPLANATION

- Bicycle groundwater basin
- Bicycle Basin
  - North
  - Central
  - South
- Bicycle Lake (dry)
- Section *A*–*A*′
- Section *B*–*B*′
- Township/range
- Model inferred faults
- Faults

Wells type and identifier (see table 1)

- 14H1 — Production
- 14P1 — Multiple-well monitoring site
- 22P1 — Destroyed
- 28A3 — Test well
- 24H1 — Obstructed

Stiff diagram with stacked identifier

- 26K1 — Well identifier (see table 1)
- (2011) — Sample year
- 551 — Total dissolved solids, in milligrams per liter

Milliequivalents per liter

Cations: 10 5 0 — Anions: 5 10

Na^+K, Ca, Mg; Cl, HCO_3+CO_3, SO_4

Figure 11. Water-quality diagrams and dissolved-solids concentrations of groundwater from selected wells in Bicycle Basin, Fort Irwin National Training Center, California.

Groundwater contacting evaporite deposits would be expected to have higher salinity and could move laterally from the evaporite deposits toward the production well 14N/3E-14P1, northwest of well 14N/3E-23B2. Well 14N/3E-23B2 is the middle well of a multiple-well monitoring site. Saline water was not present in the shallower (14N/3E-23B3) or deeper (14N/3E-23B1) wells, which are perforated in Quaternary-Tertiary older alluvium and Tertiary younger gravels (QToa and Tyg), respectively.

The relatively high TDS water in wells 14N/3E-24Q1, 14N/3E-24Q2, and 4N/4E-18N1 was enriched in calcium and was primarily from wells perforated in Tertiary older gravels (Tog) at depth (fig. 10*B*). Wells 14N/3E-24Q1 and 14N/3E-24Q2 are the deepest wells in a multiple-well monitoring site. Relatively high TDS water was not in the shallow wells perforated in Quaternary-Tertiary older alluvium (QToa) at this site. The relatively high-salinity water could represent the typical water-quality characteristic of old, deep groundwater in the Tertiary older gravels (Tog), which might move laterally or vertically toward well 14N/4E-18N1, which is north of wells 14N/3E-24Q1 and 14N/3E-24Q2.

The relatively high TDS water in wells 14N/3E-27E1 and 14N/3E-28A1 in the southwestern part of the basin might be influenced partly by firefighting activities, described later, or could reflect old groundwater from the Tertiary older gravels (Tog), similar to that of other wells perforated in Tertiary older gravels (Tog). The perforated intervals of wells 14N/3E-27E1 and 14N/3E-28A1 are unknown; however, these wells could be perforated in Tertiary older gravels (Tog), similar to the deposits exposed nearby at land surface. The source of the increased salinity in wells 14N/3E-27E1 and 14N/3E-28A1 might not be the evaporite deposits encountered in the wells in the central area, however. Nitrogen isotope analyses of soil-leachate and well samples collected to identify source of nitrate (Densmore and Bohlke, 2000) indicated the groundwater near these wells had been affected by firefighting training. Water sprayed on burning material resulted in leaching of nitrates from the soils into the groundwater in this area. It is likely that sodium and chloride also would be leached from the soils in addition to their concentration by evaporation of the sprayed water.

As described in the previous section, groundwater quality varied with depth and from the western side to eastern side of the basin, perhaps primarily reflecting spatial variations in well depth (fig. 11). In general, groundwater in wells 14N/3E-14H1 in the northern area, 14N/3E-13K1, 14N/3E-14P1, 14N/3E-14P2, 14N/3E-23B1, 14N/3E-23B3, and 14N/3E-24Q5, in the central area of Bicycle Basin, perforated at least partly in the Quaternary-Tertiary alluvium (or Tertiary younger gravels, in the case of 14N/3E-23B1), was $NaHCO_3$-SO_4-type water. Groundwater in wells 14N/3E-23G1, 14N/3E-24H1, 14N/3E-24Q3, and 14N/3E-24Q4, near the playa and on the eastern side of the basin, was $NaHCO_3$-Cl-type water, with chloride becoming more prominent than sulfate. Groundwater in well 14N/3E-24Q5 began to shift to $NaHCO_3$-Cl-type water in 2011 as the chloride content increased (appendix 3).

Total dissolved-solids (TDS), chloride (Cl), and nitrite plus nitrate as nitrogen (NO_2 and NO_3 as N) concentrations were used to further describe the areal variation in groundwater from Bicycle Basin. For simplicity, only TDS concentrations for the most recent sample (from 1988 to 2011) from each well are shown in figure 11. Water-quality data collected during 1993–2011 for this study are presented in appendix 3. Because nitrite concentrations in these samples were generally below the detection limit, nitrite plus nitrate (appendix 3) were used as an approximation of nitrate as nitrogen concentrations of groundwater in Bicycle Basin. The TDS concentrations in groundwater in Bicycle Basin ranged from about 458 mg/L TDS in well 14N/3E-14P2 (Wilson F. So and Associates, 1989) to about 2,500 mg/L TDS in well 14N/3E-23G1 (James M. Montgomery and Associates, 1981). The chloride concentrations ranged from 59 mg/L in well 14N/3E-14P1 (Wilson F. So and Associates, 1989) to 1,000 mg/L in well 14N/3E-23G1 (James M. Montgomery and Associates, 1981). The nitrate concentrations ranged from 0.72 mg/L NO_3 as N in well 14N/3E-23G1 (James M. Montgomery and Associates, 1981) to 31 mg/L NO_3 as N in well 14N/3E-28A1 (appendix 3).

The highest TDS and chloride concentrations in groundwater were in a sample collected in 1980 from well 14N/3E-23G1 immediately after the well was drilled and could represent the quality of water influenced by contact with evaporate deposits beneath the playa. These high concentrations were not observed in later samples from this well. During 2010, TDS and chloride concentrations in 14N/3E-23G1 were 789 mg/L and 145 mg/L, respectively. The change in quality could indicate that the well had not been thoroughly developed prior to sampling in 1980 or that portions of the screens in this well have become partially clogged as a result of scaling in the well over time, changing the depth distribution of inflow and water quality in the well. The 1980 concentrations in water from this well might be representative of relatively saline water that was present in the Quaternary-Tertiary older alluvium (QToa), lacustrine (QTol), and Tertiary deposits, opposite the perforations in this well (table 1). Relatively high concentrations of TDS and chloride also were detected in groundwater in well 14N/3E-23B2 during 2010 and, during 2000, in well 14N/3E-24Q2, east of the playa. The high concentrations in groundwater from these wells are of concern because poor-quality water from these areas could migrate toward the production wells as water levels decline, causing water quality to degrade. Except for these wells, groundwater from most wells generally contained less than 700 mg/L TDS and less than 100 mg/L chloride. A secondary maximum contaminant level of 500 mg/L for TDS and 250 mg/L for chloride were established by the U.S. Environmental Protection Agency (2002) for aesthetic purposes of taste.

The highest nitrate concentrations were in groundwater from wells 14N/3E-27E1, -27E2, -27E3, -28A1, and -28H2, in the firefighting training area in the southwestern part of the basin (Densmore and Bohlke, 2000). Although perforated intervals are not known for these wells, wells 14N/3E-28A1 and -28H2 are reportedly shallow, 151 and 164 ft, respectively (table 1). As described previously, water sprayed on burning material resulted in leaching of nitrates from the soils into the groundwater in this area. These groundwater samples were not representative of native groundwater in the basin and are not included further in this discussion. Elevated nitrate as nitrogen concentrations (9.51–11.5 mg/L in the late 1970s) were measured in groundwater from one other well, 14N/3E-35C1. Nitrate as nitrogen concentrations decreased to about 7 mg/L in 2000 (appendix 3). Elevated nitrate as nitrogen concentrations in well 14N/3E-35C1 could have resulted from infiltration of wastewater from the septic system at the airport. These groundwater samples also were not representative of native groundwater and are not included further in this discussion.

Excluding wells 14N/3E-27E1–3, -28A1, -28H2, and -35C1, nitrate concentrations ranged from less than 1 mg/L NO_3 as N in well 14N/3E-23B2 (2010) to 8.7 mg/L NO_3 as N in well 14N/3E-23G1 (1993). The nitrate as nitrogen concentrations of native groundwater in Bicycle Basin, as sampled from wells in areas with no evident sources of contamination, were generally less than 5 mg/L. This concentration was slightly higher than background levels of nitrate (2–3 mg/L) measured in desert environments (Umari and others, 1993) and in Irwin and Langford Basins (Densmore and Londquist, 1997; Voronin and others, 2013). The nitrate as nitrogen concentrations (8.4–8.7 mg/L) were high in groundwater from well 14N/3E-23G1. Well 14N/3E-23G1, west of the playa, has a long screened interval (178–737 ft) that perforates Quaternary-Tertiary older alluvium (QToa) and Quaternary-Tertiary older lacustrine deposits (QTol). The elevated nitrate as nitrogen concentrations may be derived from the fine-grained Quaternary-Tertiary deposits (QTol). Evidence indicates that nitrate concentrations in groundwater from nearby multiple-well monitoring well site 14N/3E-23B1–3 were higher in groundwater from the shallow well (14N/3E-23B3 perforated at the base of QToa and near the top of QTol) than in groundwater from the two deeper wells (14N/3E-23B1–2) perforated below Quaternary-Tertiary older lacustrine deposits (QTol). A primary maximum contaminant level of 10 mg/L for nitrate as nitrogen was established by the U.S. Environmental Protection Agency (2002).

Other constituents of concern in groundwater in desert areas are arsenic (As) and fluoride (F). High concentrations of arsenic and fluoride were present in many desert basins at Ft. Irwin (Densmore and Londquist, 1997; Voronin and others, 2013). These constituents tended to concentrate in fine-grained deposits and generally are associated with basin-fill deposits of alluvial-lacustrine origin, particularly in semi-arid areas, and volcanic deposits (Welch, and others, 1988; García and Borgnino, 2015). Concentrations of arsenic in groundwater in Bicycle Basin ranged from 2 micrograms per liter (µg/L) at well 14N/3E-24Q2, east of the playa, to 103 µg/L at well 14N/3E-23B1, northwest of the playa in the area of greatest subsidence (appendix 3). Concentrations of fluoride ranged from 0.5 mg/L in water from well 14N/4E-18N1, northeast of the playa, to 8.1 mg/L in water from well 14N/3E-23G1, immediately west of the playa (James M. Montgomery and Associates, 1981). The fluoride concentration in water from well 14N/3E-23G1 was 5.74 mg/L in 2010; in water from nearby well 14N/3E-23B2, fluoride was 7.81 mg/L in 2011 (appendix 3). In general, concentrations in groundwater from most wells in Bicycle Basin were greater than 10 µg/L for arsenic, except in wells 14N/3E-22N1, 14N/3E-24H1, 14N/3E-24Q1–3, and 14N/4E-18N1, and less than 4 mg/L for fluoride, except in wells 14N/3E-23B2, 14N/3E-23G1, and 14N/3E-35C1–2. Arsenic and fluoride concentrations remained fairly constant over time in groundwater in the basin, except in shallow wells 14N/3E-24Q3, 4, 5, where arsenic concentrations decreased, and in well 14N/3E-13M4, where fluoride concentration decreased. The primary maximum contaminant level of arsenic in drinking water, initially established at 50 µg/L by the U.S. Environmental Protection Agency (2002), was lowered to 10 µg/L in 2006 (U.S. Environmental Protection Agency, accessed Aug 4, 2010, at http://www.epa.gov/safewater/contaminants/index.html#7). For fluoride, the primary maximum contaminant level of 4 mg/L F has been established as a drinking water guideline for public water systems (U.S. Environmental Protection Agency, 2002).

Source and Age of Groundwater

The stable isotopic ratios of oxygen (oxygen-18/oxygen-16, $\delta^{18}O$) and hydrogen (hydrogen-2,^{2}H, or deuterium/hydrogen-1, δD) were analyzed in groundwater samples to help determine the source and movement of water through the study area. The activity of the radioactive isotopes of hydrogen (hydrogen-3, ^{3}H, or tritium) and carbon (^{14}C) was analyzed in groundwater samples to determine the relative age, or time since recharge, of groundwater in Bicycle Basin. A total of 56 water samples collected from 25 wells were analyzed for $\delta^{18}O$ and δD. Samples from selected wells also were analyzed for ^{3}H and ^{14}C (appendix 3).

Stable Isotopes of Oxygen and Hydrogen

Oxygen-18 (^{18}O) and deuterium (D) are natural stable isotopes of oxygen and hydrogen, respectively. Their isotopic ratios are expressed relative to the standard, known as Vienna Standard Mean Ocean Water (VSMOW), in delta notation (δ) as per mil (parts per thousand) differences (Gonfiantini, 1978). More negative values of $\delta^{18}O$ and δD represent enrichment in the lighter isotopes, ^{16}O and ^{1}H (or depletion in the heavier isotopes, ^{18}O and D); less negative values represent enrichment in the heavier isotopes of oxygen (^{18}O) and hydrogen (D). The ratios of oxygen isotopes (^{18}O:^{16}O) and hydrogen isotopes (D:^{1}H) in groundwater are indicators of the hydrologic history of the groundwater.

The linear relation between $\delta^{18}O$ and δD in natural precipitation throughout the world (Craig, 1961) is referred to as the global meteoric water line (fig. 12). The isotopes of oxygen and hydrogen in ocean water are fractionated as the lighter isotopes ^{16}O and ^{1}H are preferentially transferred during the phase change to vapor during evaporation at the ocean surface. During rainfall, water in the atmosphere is fractionated further, as ^{18}O and D are preferentially condensed in precipitation, leaving the remaining water vapor relatively depleted in the heavier isotopes. Latitude, altitude, and air temperature affect the isotopic composition of atmospheric water. Precipitation from a given storm becomes isotopically lighter (more negative) as the storm moves inland and into higher altitudes with cooler temperatures (Fournier and Thompson, 1980). Water that has undergone evaporation is enriched in heavier isotopes relative to its original composition and generally has values below and to the right of the meteoric water line, with a slope between 3 and 6 (International Atomic Energy Agency, 1981). There is no further change in isotopic composition at the relatively low temperatures of most groundwater systems after recharged water has migrated below the depth of evaporation. Any subsequent differences in the isotopic composition of groundwater along a flow line, therefore, generally reflect only mixing within the aquifer system or concentration by evaporation in a discharge area. The $\delta^{18}O$ and δD composition of groundwater, relative to the meteoric water line and the isotopic composition of water from other sources, can be an indicator of the source of groundwater.

Groundwater that is isotopically lighter than modern-day precipitation could indicate groundwater was recharged under conditions that were cooler than present-day conditions (Smith and others, 2002) or that modern-day precipitation is more variable than the available data indicate. The isotopic compositions of groundwater from the wells and one spring in the Irwin, Langford, and Bicycle Basins plotted to the right or below the meteoric water line and available nearby precipitation data (fig. 12*A*; Friedman and others, 1992; Izbicki, 2004). The isotopic composition of groundwater from wells in Bicycle Basin ranged from about –10.4 to –13.4 per mil $\delta^{18}O$ and –86 to –102 per mil δD (appendix 3). The groundwater isotopic data to the right of the global meteoric water line indicated possible evaporation prior to recharge, partial evaporation during precipitation, or a "local" meteoric water line that differs slightly from the global meteoric water line. Volume-weighted samples of local precipitation at Daggett FAA Airport (Friedman and others, 1992) and averaged desert winter precipitation (Izbicki, 2004), representing modern-day precipitation in the western Mojave Desert, plotted near the global meteoric water line (fig. 12*A*). A volume-weighted sample of local precipitation at Goldstone Echo 2 (Friedman and others, 1992) plotted to the right of the meteoric water line and slightly above and to the right of the groundwater samples (fig. 12*B*). This sample, representing precipitation collected during summer 1985 through winter 1987, was notably different than the weighted average for winter precipitation in the Mojave Desert and could represent "local" meteoric water.

The groundwater from wells in the Bicycle Basin was isotopically lighter than groundwater from wells in Irwin and Langford Basins, plotting to the left of most of the samples from Irwin and Langford Basins. This indicated that the precipitation runoff recharging Bicycle Basin originated at a higher altitude than in the other basins. As it does today, groundwater in Bicycle Basin likely recharged from storm runoff and underflow in the higher elevations of the Granite Mountains, to the north and northwest, and the Goldstone upland area, to the west (fig. 1). As in Irwin and Langford Basins, the isotopic composition of groundwater in Bicycle Basin indicated that groundwater from most wells in Bicycle Basin was recharged during a cooler, wetter period than is characteristic of present-day climatic conditions. Groundwater in Bicycle Basin from wells perforated in the deeper Quaternary-Tertiary deposits and Tertiary deposits (table 1) generally was isotopically lighter (more negative) than groundwater from wells perforated in the shallower Quaternary-Tertiary deposits (figs. 3, 12*B*). Wells 14N/3E-13M1, 14N/3E-13M2, 14N/3E-14H1, 14N/3E-23B1–2, 14N/3E-24H1, 14N/3E-24Q1–3, and 14N/4E-18N1 are fully or partially perforated in deeper Quaternary-Tertiary and Tertiary deposits and had groundwater ranging from about –12.1 to –13.2 per mil $\delta^{18}O$ and –95 to –105 per mil δD (appendix 3). Groundwater from wells perforated in shallower Quaternary-Tertiary deposits ranged from about –11.1 to –12.4 per mil $\delta^{18}O$ and –90 to –95 per mil δD, slightly enriched in $\delta^{18}O$ and δD; this difference indicated groundwater from these wells was recharged from a different source or storm trajectory. In addition, these data indicated that the source of recharge to Bicycle Basin had become more like the source of recharge in Irwin and Langford Basins during the Quaternary. Deeper groundwater was recharged near the end of the last North American glaciations, as described in the following "Tritium and Carbon-14" section, when storms were colder and conditions wetter, resulting in lighter (more negative) isotope ratios than younger postglacial recharge.

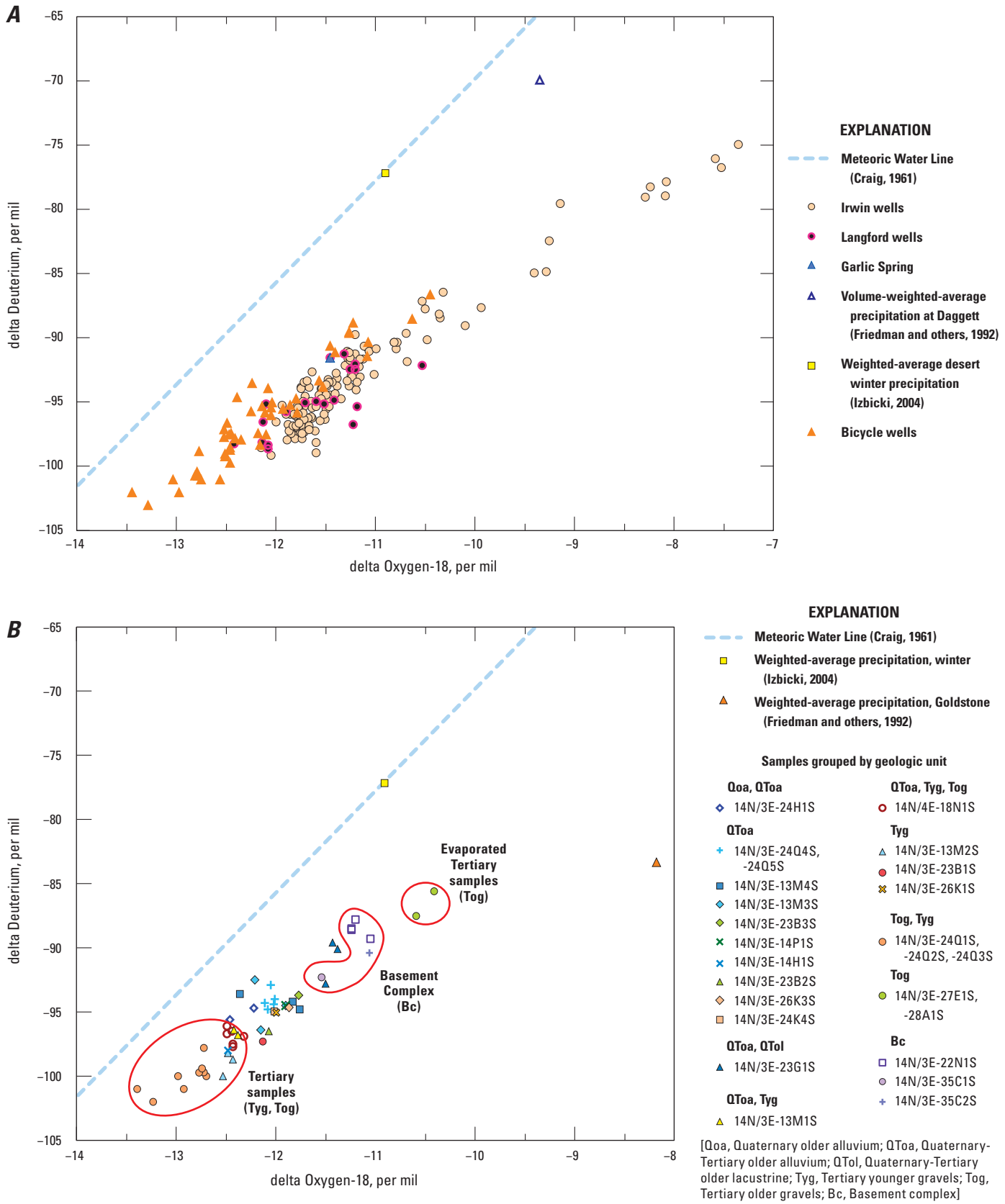

Figure 12. Stable isotopes of groundwater samples from Fort Irwin National Training Center, California, along with reported weighted-average precipitation measurements for *A*, Irwin, Langford, and Bicycle Basins and *B*, for Bicycle Basin by geology.

Tritium and Carbon-14

Tritium (^{3}H) is a natural radioactive isotope of hydrogen that has a half-life of 12.4 years. The concentration of tritium is reported in tritium units (TU; Bartolino and Cole, 2002). Approximately 1,760 pounds (800 kilograms) of tritium was released into the atmosphere from the atmospheric testing of nuclear weapons between 1952 and 1962 (Michel, 1976). As a result, tritium concentrations in precipitation and groundwater recharge increased during that time. Tritium concentrations are not affected by chemical reactions other than radioactive decay, because tritium is part of the water molecule. Therefore, tritium is a tracer of the movement and relative age of water on timescales ranging from recent to about 50 years before present (post 1952). In this report, groundwater that had tritium (^{3}H) concentrations less than a limit of 0.2 TU was interpreted as water recharged prior to 1952, and groundwater that had measurable ^{3}H concentrations was interpreted as water recharged after 1952, or recent recharge.

Carbon-14 is a natural radioactive isotope of carbon that has a half-life of about 5,730 years (Mook, 1980). Carbon-14 data are expressed as percent-modern carbon (pmC) by comparing ^{14}C activities to the specific activity of National Bureau of Standards oxalic acid: 13.56 disintegrations per minute per gram of carbon in the year 1950 equals 100 pmC (Kalin, 2000). Carbon-14 was produced, as was tritium, by the atmospheric testing of nuclear weapons (Mook, 1980). As a result, ^{14}C activities can exceed 100 pmC in areas where groundwater contains tritium. Carbon-14 activities are used to determine the age of a groundwater sample on timescales ranging from recent to more than 20,000 years before present. Carbon-14 is not part of the water molecule, and, therefore, ^{14}C activities can be affected by chemical reactions that remove or add carbon to solution. In addition, ^{14}C activities are affected by mixing younger water that has high ^{14}C activity with older water that has low ^{14}C activity. Carbon-14 ages presented in this report did not account for changes in ^{14}C activity resulting from chemical reactions or mixing and, therefore, were considered uncorrected ages. In general, uncorrected ^{14}C ages are older than the actual age of the associated water. Izbicki and others (1995) estimated that uncorrected ^{14}C ages were as much as 30 percent older than the actual ages of groundwater in the regional aquifer in the Mojave River groundwater basin near Victorville, California (not shown), about 60 mi southwest of the study area. In this report, groundwater that had ^{14}C activities less than 90 pmC was interpreted as being recharged before 1952; groundwater having ^{14}C activities greater than 90 pmC was interpreted as being recharged after 1952 (Izbicki and Michel, 2004).

The lack of ^{3}H in samples from Bicycle Basin indicated that water throughout most of Bicycle Basin was recharged prior to 1952. Measurable concentrations of ^{3}H were present in only one groundwater sample from 20 wells in Bicycle Basin (appendix 3; fig. 13). Well 14N/3E-23B2 had a low, but detectable ^{3}H of 0.22 TU, indicating that some groundwater recharged since the early 1950s could be mixed in with primarily older groundwater.

The uncorrected ^{14}C data indicated the groundwater in these wells had apparent ages of 15,625–39,350 years. Measured ^{14}C activities in samples from Bicycle Basin ranged from about 0.7 to 14.3 pmC. The highest ^{14}C activity (14.3 pmC) was measured in groundwater from well 14N/3E-24H1, along the eastern edge of the basin. The uncorrected ^{14}C data indicated that groundwater in this well was about 15,625 years old. Lower ^{14}C activities (less than 14 pmC) were measured in groundwater from wells throughout the basin.

The low ^{14}C activities and the lack of measurable ^{3}H indicated that Bicycle Basin had not received quantities of recent recharge sufficient to be detected in the groundwater samples collected for this study. Some groundwater recharged since 1952 could be present in shallower parts of the groundwater system than was sampled, but the absence of modern age tracers indicated that modern recharge has not yet reached monitoring and production wells deeper in the system. The age data support that the basin was recharged during a colder and wetter period near the end of the last North American glaciation that ended about 10,000 years ago.

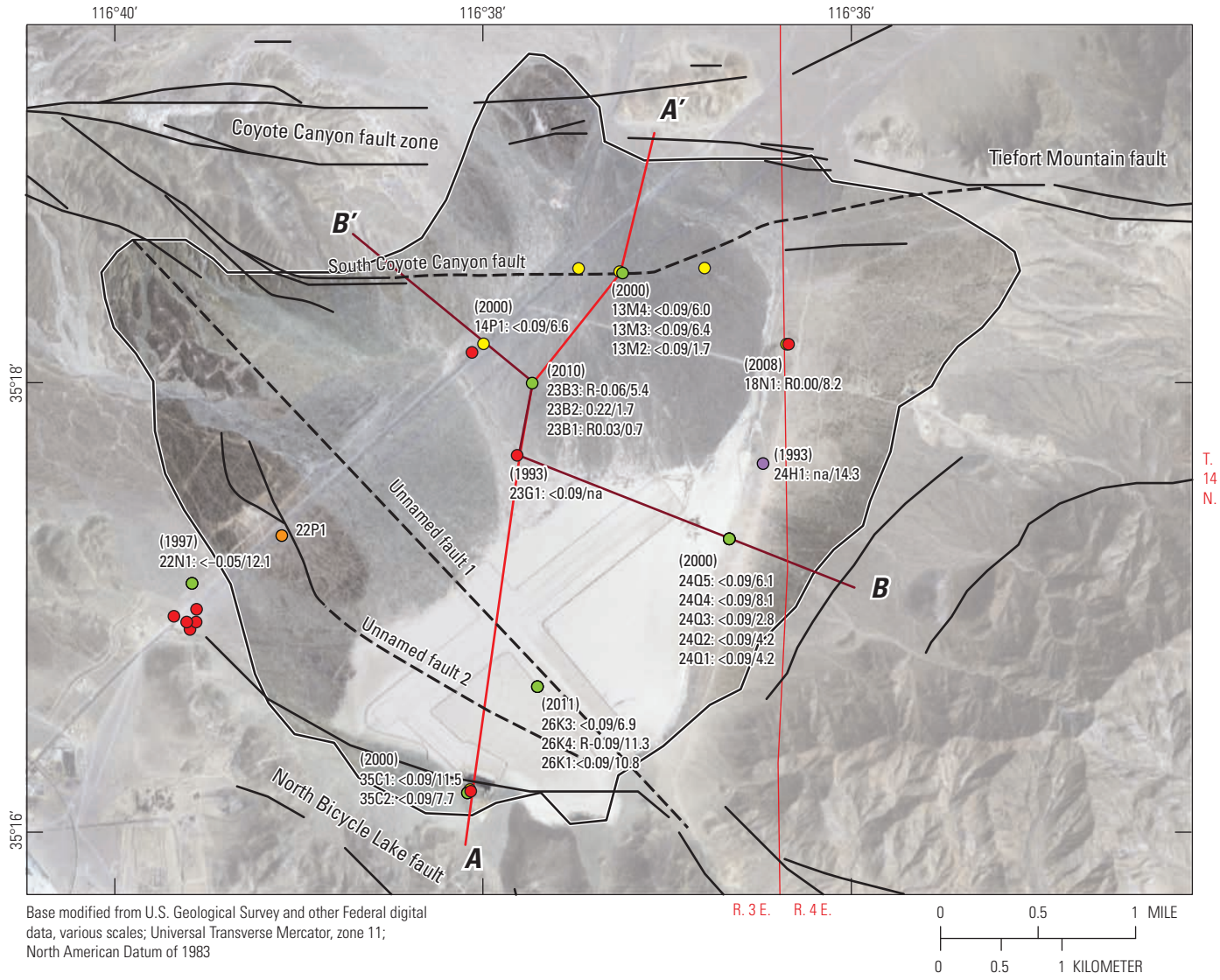

Figure 13. Tritium and carbon-14 activities for groundwater from selected wells, Bicycle Basin, Fort Irwin National Training Center, California.

Groundwater-Flow Model

Groundwater-flow models were developed for the Irwin, Langford, and Bicycle Basins, which supply water to the NTC, to better understand the aquifer systems and the potential effects of groundwater pumping, and for use as tools to help manage groundwater resources at NTC (fig. 14). The groundwater-flow model of the Irwin Basin, which underlies most of the Fort Irwin garrison, originally was described by Densmore (2003) and subsequently was updated by Voronin and others (2014). In addition, a groundwater-flow model was developed for the Langford Basin to the south (Voronin and others, 2013). This report documents the groundwater-flow model for the Bicycle Basin.

The Bicycle Basin model was constructed using MODFLOW-NWT (Niswonger and others, 2011). MODFLOW-NWT is a finite-difference model that simulates groundwater flow in three-dimensional heterogeneous and anisotropic media. The MODFLOW-NWT packages included in model development were the Basic (BAS; Harbaugh, 2005), Upstream Weighting (UPW; Niswonger and others, 2011), Drain (DRN; Harbaugh, 2005), Horizontal-Flow Barrier (HFB6; Hsieh and Freckleton, 1993), Recharge (RCH; Harbaugh, 2005), Multi-Node Well 2 (MNW2; Konikow and others, 2009), and Subsidence and Aquifer-System Compaction package (SUB; Hoffmann and others, 2003) with the Newton formulation (NWT) solver (Niswonger and others, 2011).

Model Discretization

Discretization of the model domain was based on geohydrologic data collected by previous investigators (Densmore, 2003; Voronin and others, 2013) and for this study. To numerically solve for the distribution of hydraulic heads in the aquifer system, it was necessary to discretize the system spatially and temporally. For this study, the model units were feet and days. Annual results are presented in calendar years.

Spatial Discretization

The Bicycle Basin model is discretized spatially using a rectangular grid with uniform grid spacing and is contained within a regional grid with the same grid spacing. The regional grid is large enough to include the Irwin, Langford, and Bicycle Basins, so the models of these basins can be incorporated into one model that can be used to help the NTC manage water resources on a regional basis. The grid-cell size is 500-ft by 500-ft with a total of 49 rows and 63 columns. There are 5,980 active model cells in 8 model layers (figs. 15, 16). The active area of the model varied with depth, with model layer 8 having the least number (537) of active model cells. Model layers 4–8 were not present southwest of unnamed fault 1 because the basement complex is shallow in that part of the basin. The model was divided into parameter zones (figs. 15*A*–*H*) for parameterization of hydraulic properties, which is described in the "Parameter Zonation" section of this report. The hydraulic properties are homogeneous in each model cell.

Land-surface altitudes for each cell in model layer 1 were estimated from a 33-ft (10-m) digital elevation model (DEM; U.S. Geological Survey, 2000; https://nationalmap.gov/elevation.html). The bottom altitudes of the model layers at the production and monitoring wells were determined from lithologic logs and borehole geophysical data. These altitudes were interpolated to the model grid and were flattened near the edges of the basin where the stratigraphic units are steeply dipping, which caused numerical instabilities of the model; consequently, the layer boundaries did not correspond to the stratigraphic boundaries in all parts of the basin. The basement complex altitudes were derived from gravity data (fig. 4) and extrapolated to the model grid to determine the bottom altitude of model layer 8 northeast of unnamed fault 1 and the bottom altitude of model layer 3 southwest of the fault. An altitude of 1,400 ft was assigned to cells of the lowest model layer where the basement complex was at a lower altitude. Because well data were not available at or below this depth, and the general observation was that the alluvial deposits are more consolidated and yield less water at depth, an altitude of 1,400 ft was assumed to be below the active groundwater-flow system.

The vertical layering in the model along cross sections is shown in figures 16*A*–*B*. Locations of these sections are shown in figure 15*A*. The distribution of thickness for each model layer is shown in figures 17*A*–*H*. For model layer 1, the thickness was calculated by subtracting the bottom altitude of the layer from the land surface. For the underlying model layers, the thickness was calculated by subtracting bottom altitudes of the layer from the bottom altitude of the overlying layer. The thickness of each model layer is variable, and the range is given in table 6.

In general, model layers 1–6 represent the upper aquifer, and models layers 7 and 8 represent the lower aquifer. Model layers were mostly flat lying and cut across stratigraphic units, but were delineated to highlight vertical differences in hydraulic properties related to stratigraphic units. The textural variations in stratigraphic units in model layers were reflected in variations in hydraulic properties, described in the "Aquifer System Definitions" section. Model layer 1 generally represents the Quaternary younger alluvium (Qya) and older alluvium (Qoa) and the Quaternary-Tertiary older alluvium (QToa), although the Quaternary playa deposits (Qp) also are represented in model layer 1 in the southern part of the basin (figs. 16*A*–*B*). Model layer 1 is thickest in the eastern part of the basin in parameter zone 1 (fig. 17*A*). Model layer 2 represents the Quaternary-Tertiary older alluvium (QToa), with older clay lacustrine deposits (QTol) present to a limited extent in the southern part of the basin (figs. 16*A*–*B*). Model layer 2 is thickest in the southwestern part of the basin

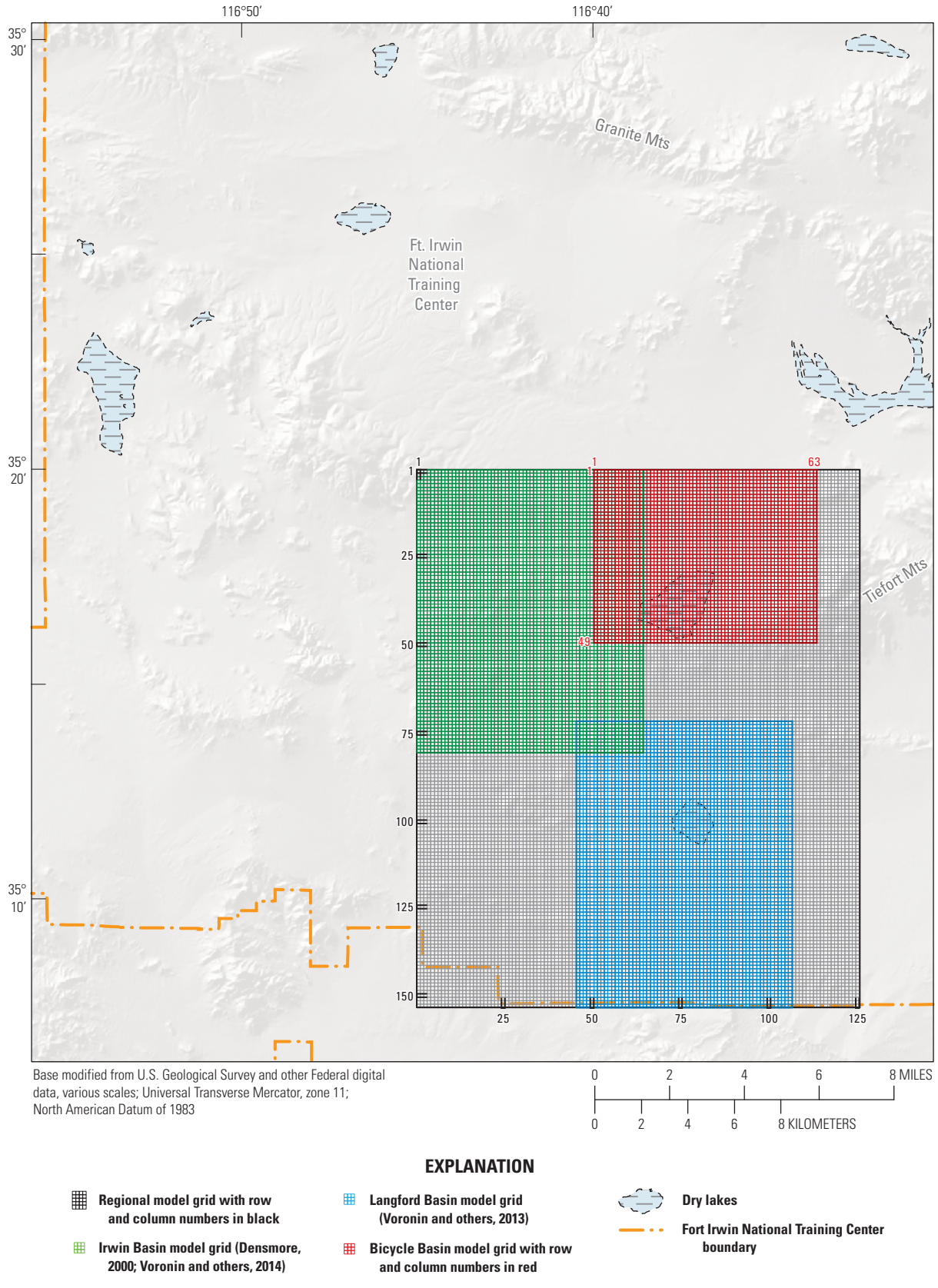

Figure 14. Location of local and regional groundwater-flow model grids, Fort Irwin National Training Center, California.

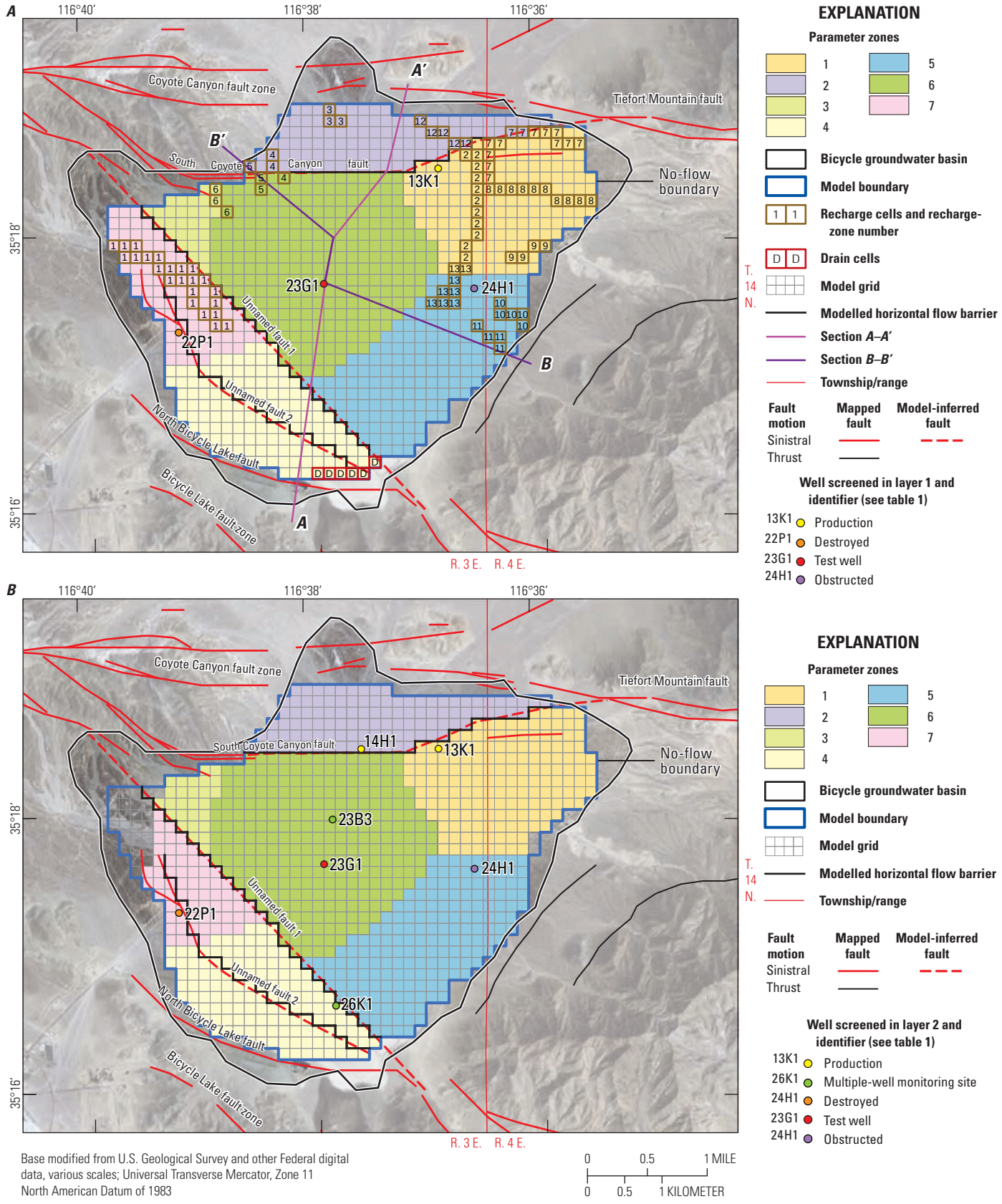

Figure 15. Active model cells, parameter zones, wells perforated in each layer, recharge cells (model layer 1 only), drain cells (model layer 1 only), and modeled faults for Bicycle Basin, Fort Irwin National Training Center, California: *A*, model layer 1; *B*, model layer 2; *C*, model layer 3; *D*, model layer 4; *E*, model layer 5; *F*, model layer 6; *G*, model layer 7; and *H*, model layer 8.

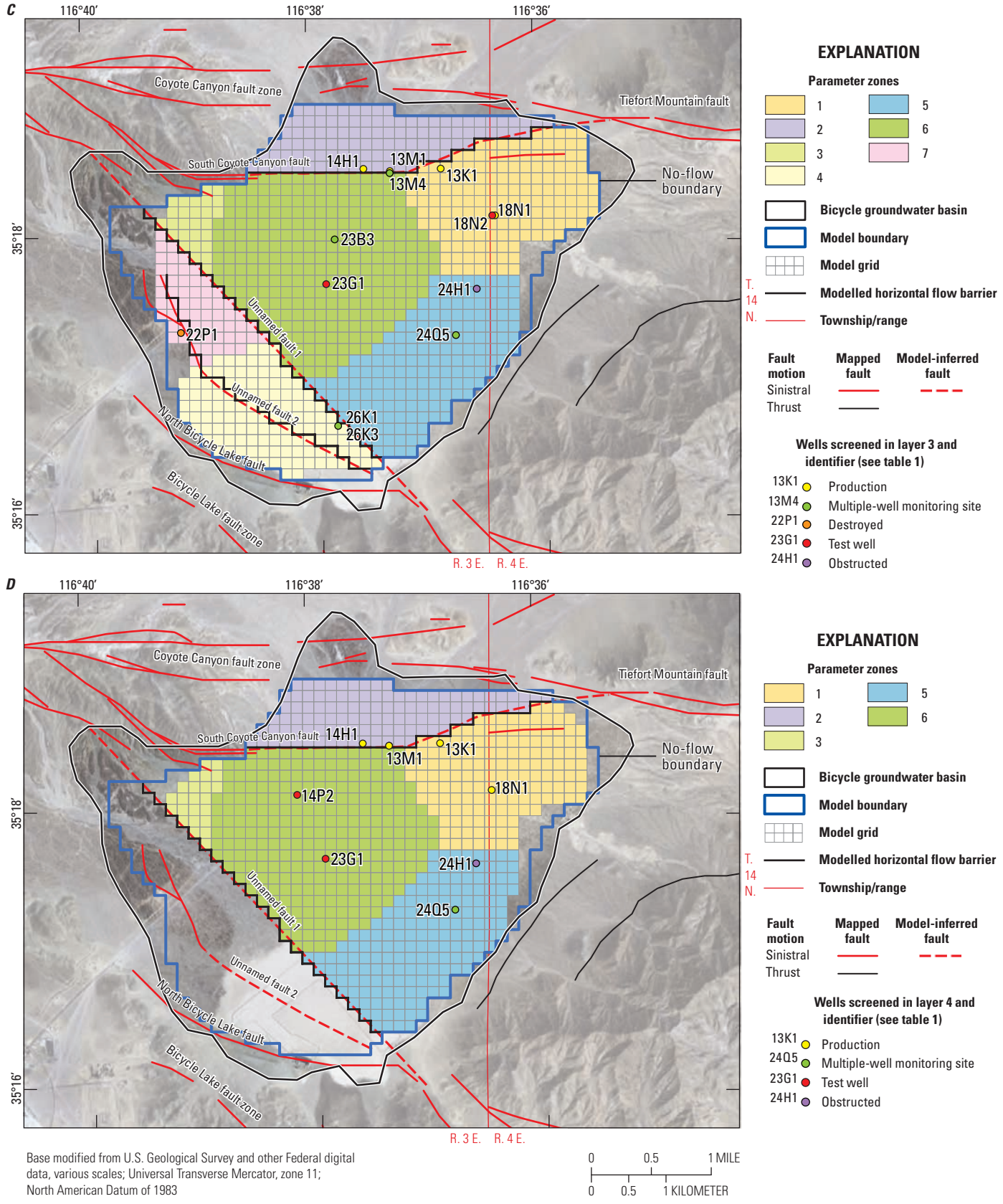

Figure 15. —Continued

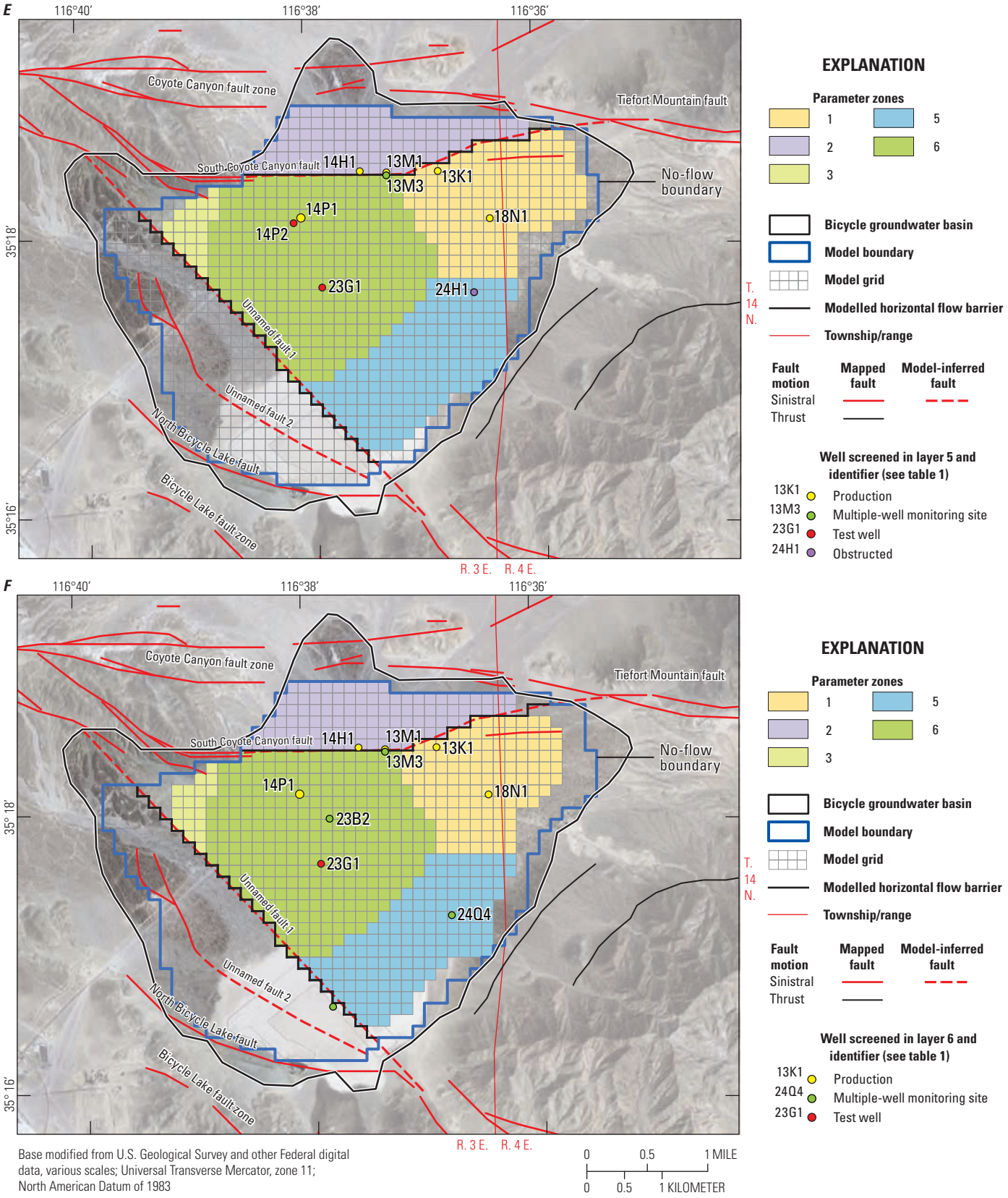

Figure 15. —Continued

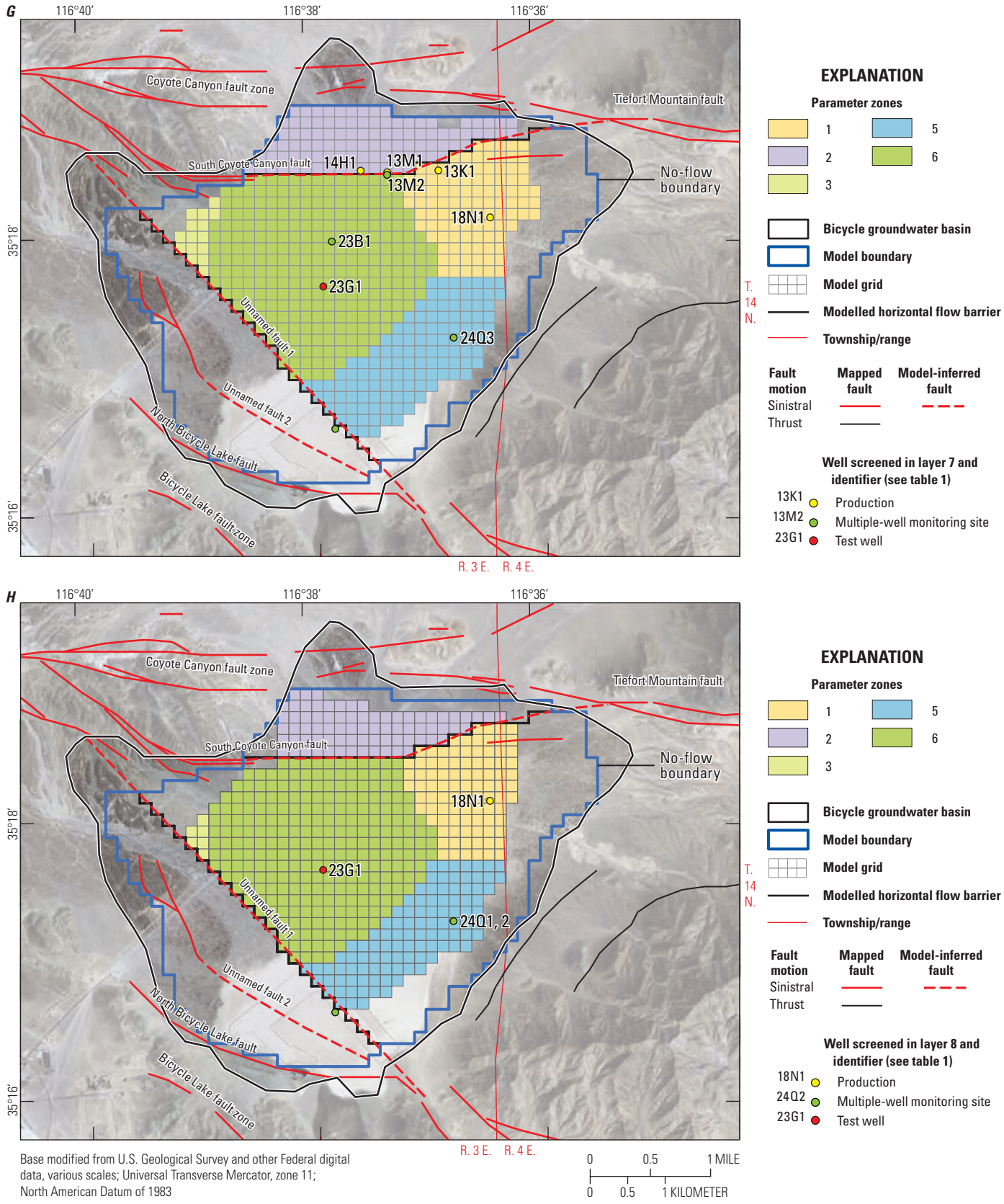

Base modified from U.S. Geological Survey and other Federal digital data, various scales; Universal Transverse Mercator, zone 11; North American Datum of 1983

Figure 15. —Continued

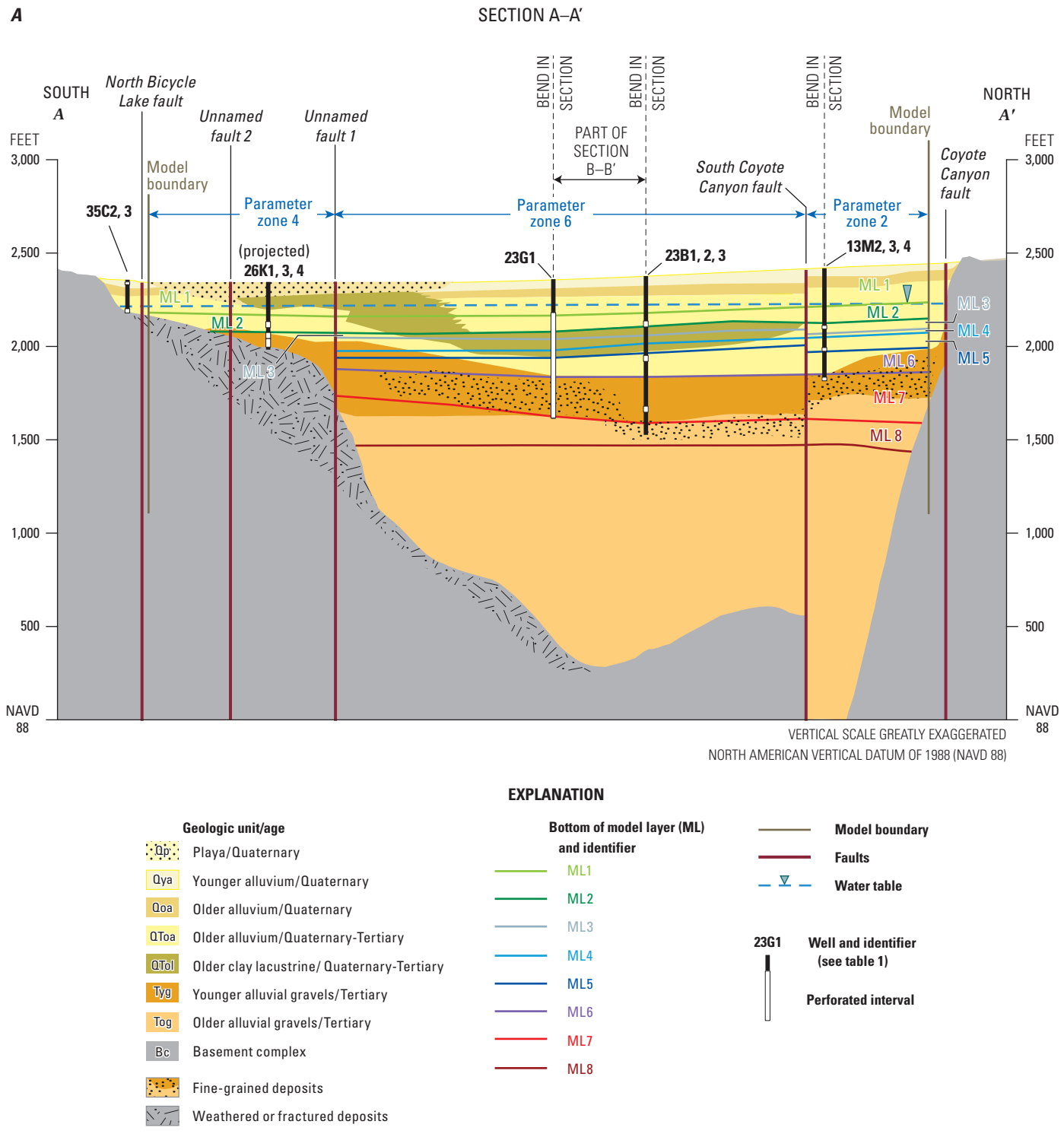

Figure 16. Cross-sectional view across Bicycle Basin, Fort Irwin National Training Center, California, showing generalized geologic sections and model layers along *A*, A–A′ and *B*, B–B′.

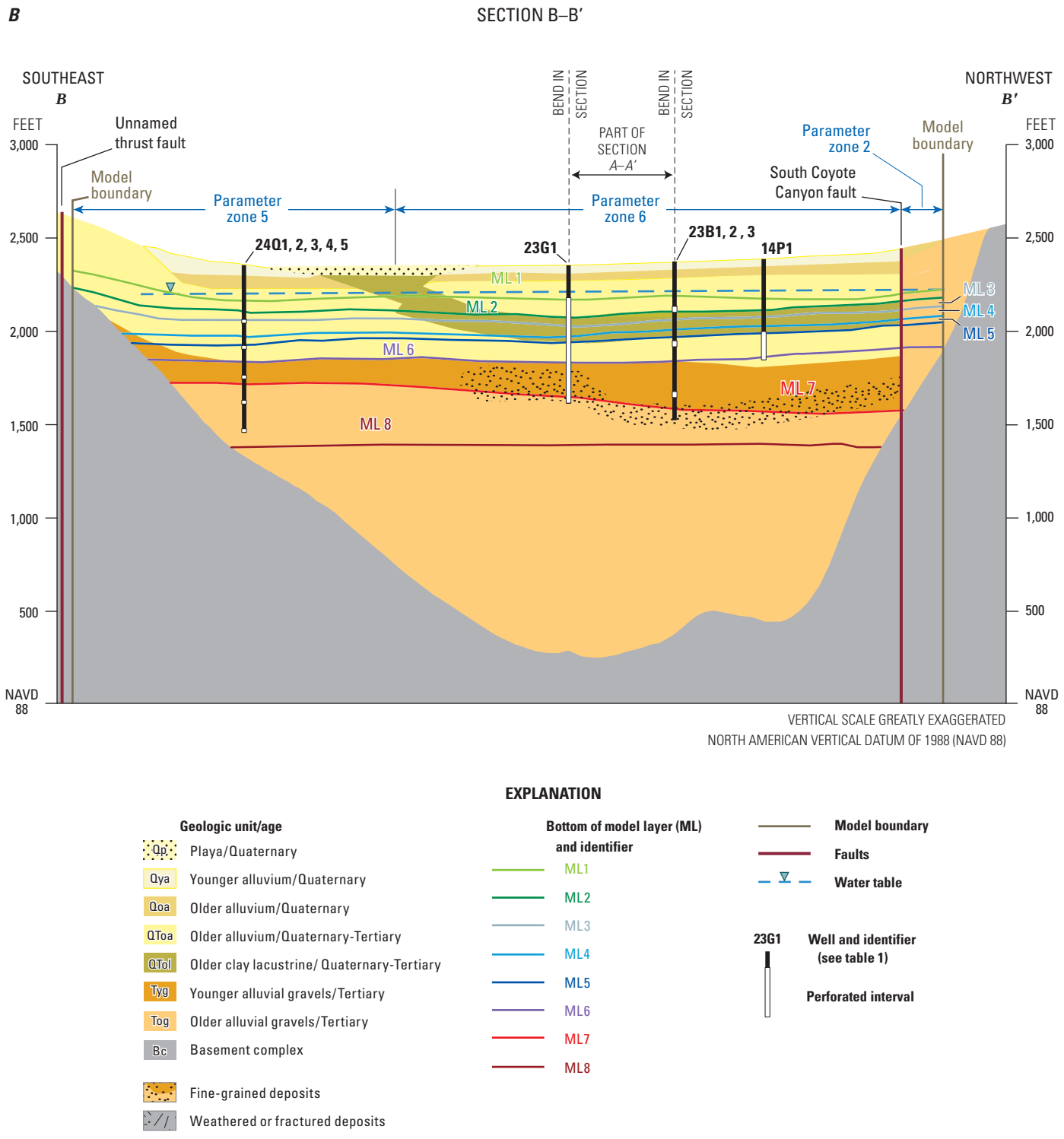

Figure 16. —Continued

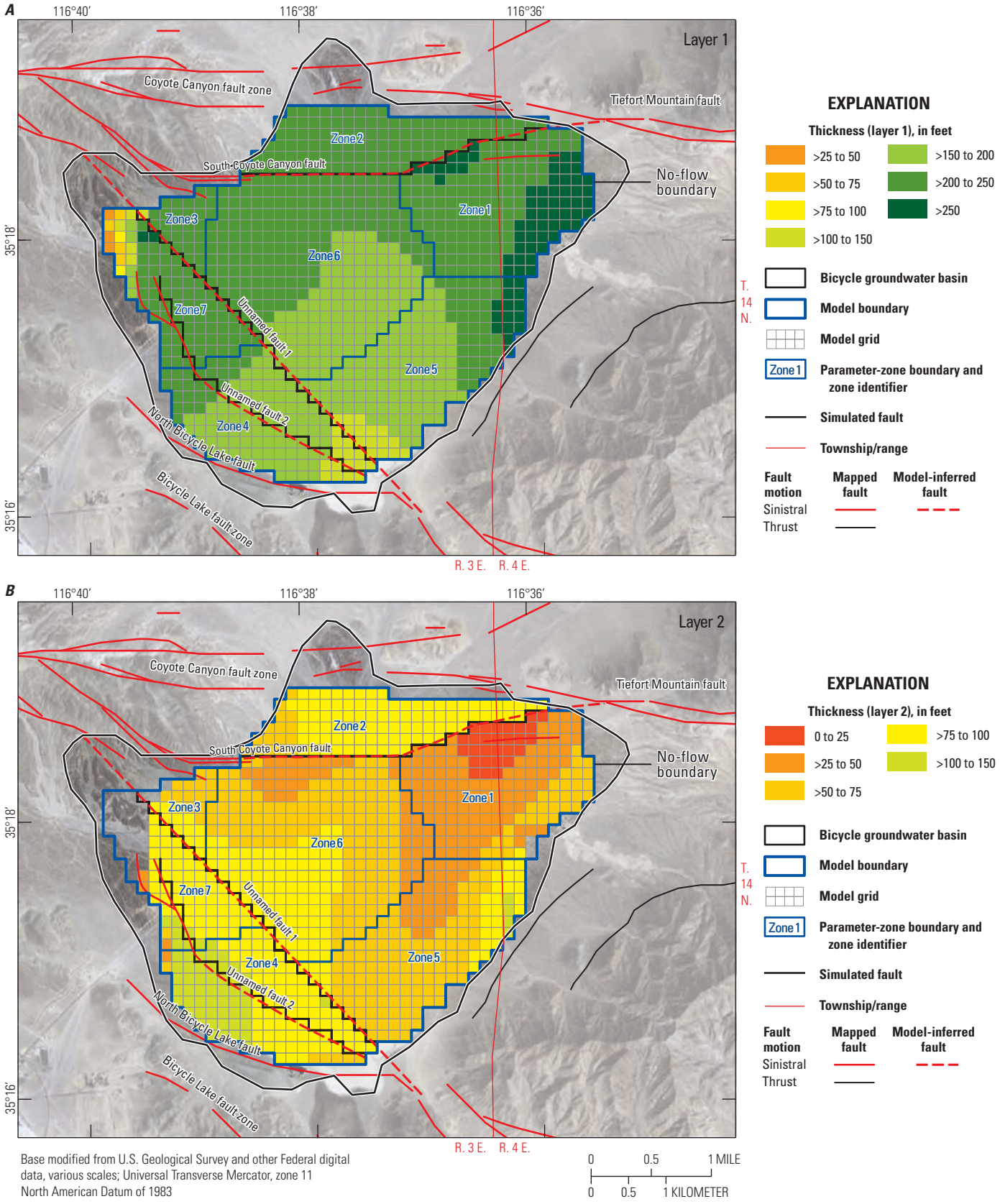

Figure 17. Thickness of model layers in the groundwater-flow model for the Bicycle Basin, Fort Irwin National Training Center, California: *A*, 1; *B*, 2; *C*, 3; *D*, 4; *E*, 5; *F*, 6; *G*, 7; and *H*, 8.

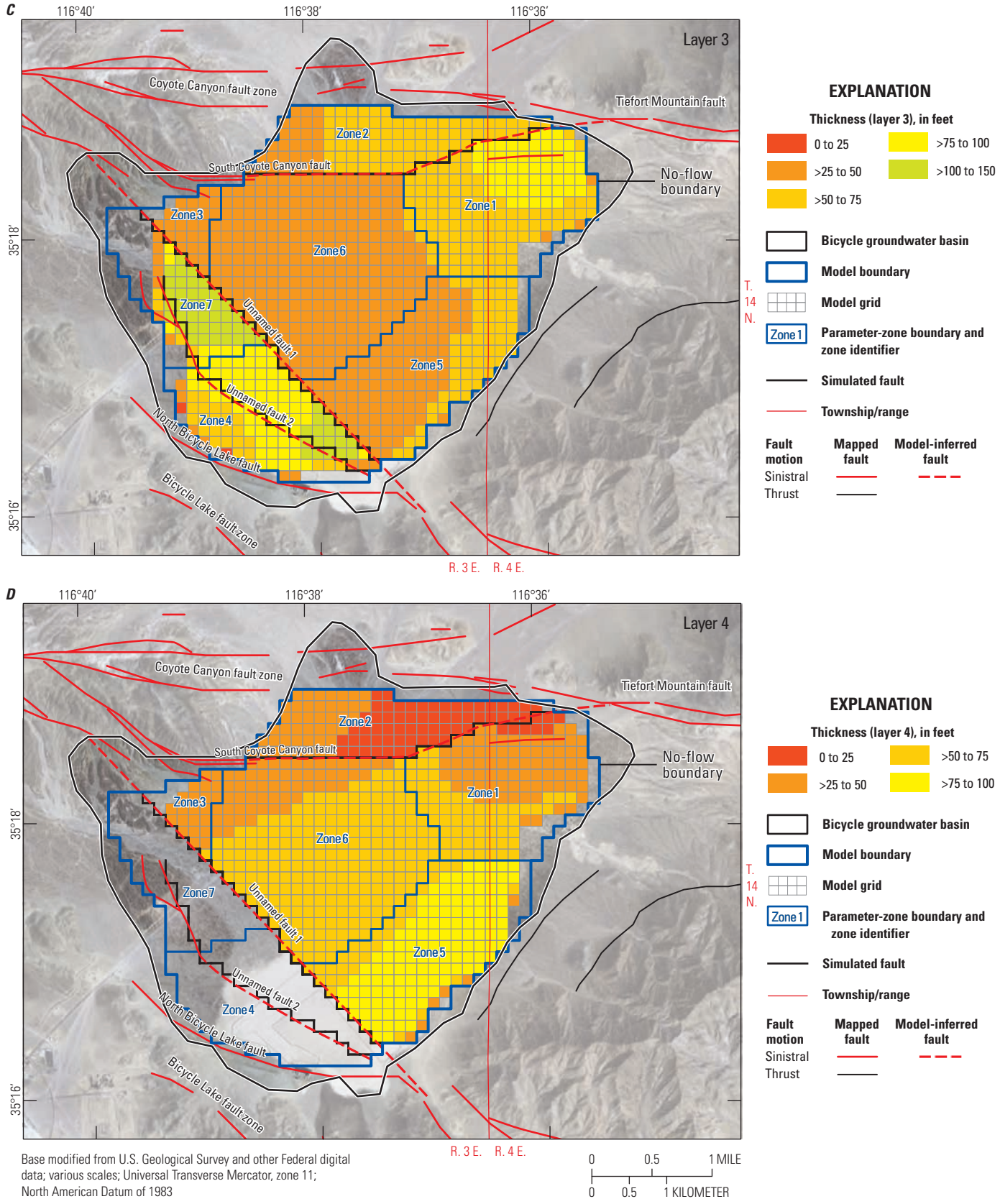

Base modified from U.S. Geological Survey and other Federal digital data; various scales; Universal Transverse Mercator, zone 11; North American Datum of 1983

Figure 17. —Continued

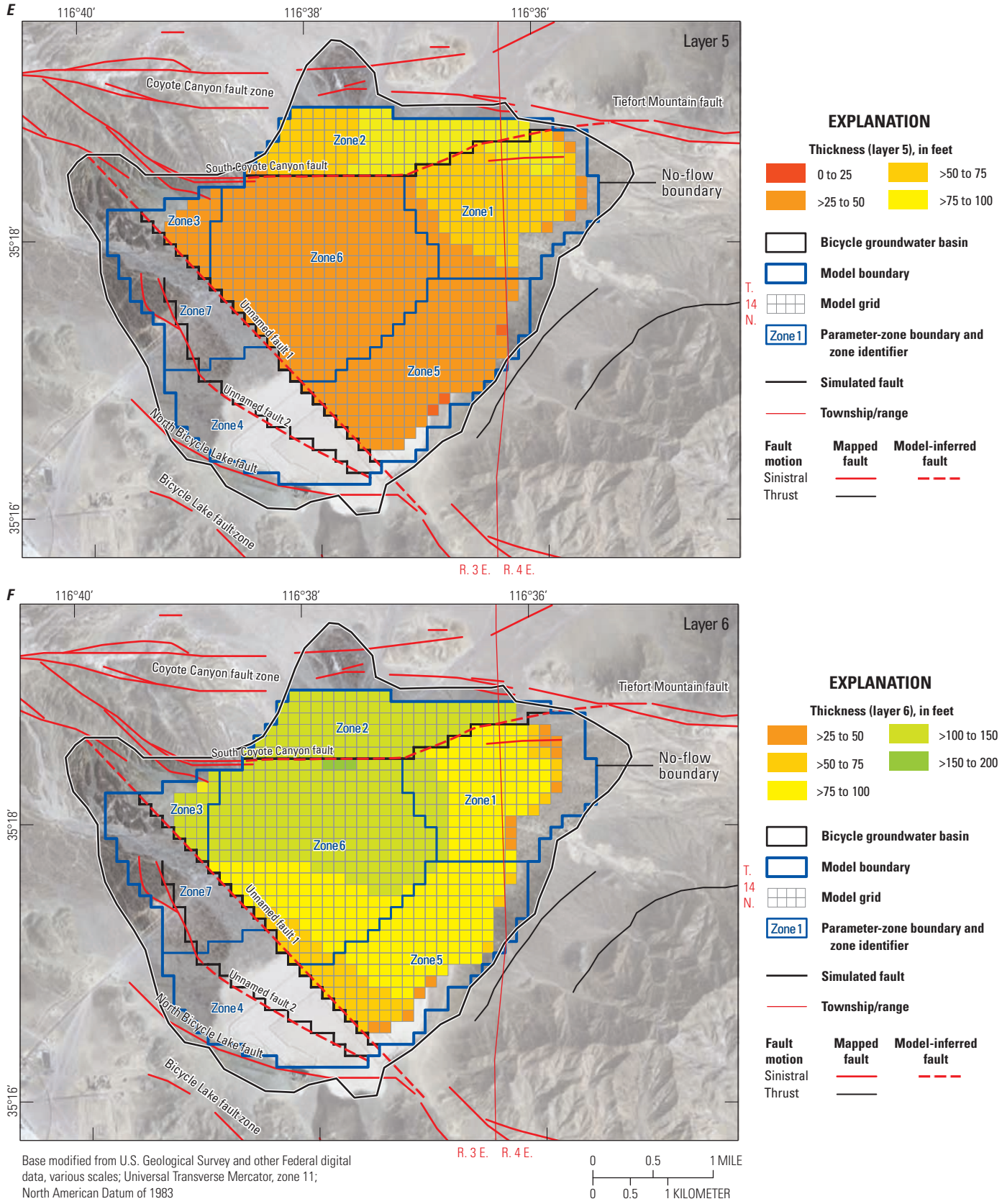

Figure 17. —Continued

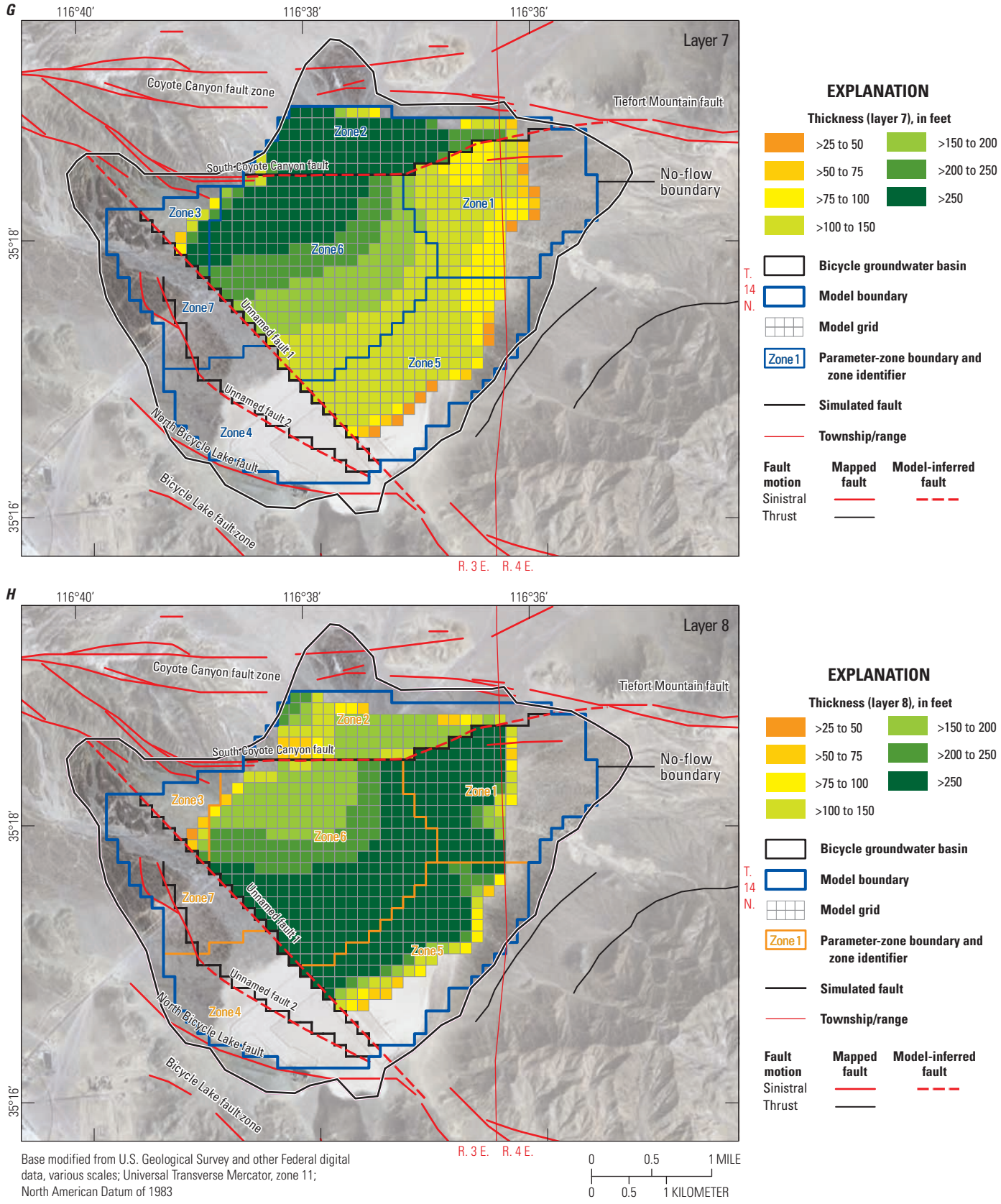

Base modified from U.S. Geological Survey and other Federal digital data, various scales; Universal Transverse Mercator, zone 11; North American Datum of 1983

Figure 17. —Continued

Table 6. Model-layer thickness in the groundwater flow model of Bicycle Basin, Fort Irwin National Training Center, California.

Layer	Thickness (feet)
1	43–275
2	9–105
3	22–111
4	19–88
5	20–83
6	26–153
7	30–338
8	41–551

(fig. 17*B*). Model layers 3–5 represent the Quaternary-Tertiary lacustrine deposits (QTol), primarily in parameter zone 6 where land-surface has subsided, which grade to Quaternary-Tertiary older alluvium (QToa) to the north and Quaternary-Tertiary older alluvium (QToa) and Tertiary younger alluvial gravels (Tyg) to the south. Model layer 3 is thickest southwest of unnamed fault 1 in parameter zones 4 and 7 (fig. 17*C*); model layer 4 is thickest in the southeastern part of the basin in parameter zone 5 (fig. 17*D*); and model layer 5 is thickest north of the South Coyote Canyon fault in parameter zone 2 (fig. 17*E*). Model layer 6 primarily represents the Quaternary-Tertiary older alluvium (QToa), with Tertiary younger gravels (Tyg) present in the southern part of the basin and north of the South Coyote Canyon fault (figs. 16*A–B*). Model layer 6 is thickest in the north and central parts of the basin in parameter zones 1–3 and 6 (fig. 17*F*). Model layers 7 and 8 primarily represent the Tertiary younger and older gravel (Tyg and Tog) units, respectively (figs. 16*A–B*). Model layer 7 is thickest in the northern part of the basin in parameter zones 2, 3, and 6 (fig. 17*G*), and model layer 8 is thickest in the southern part of the basin in parameter zones 5 and 6 and in the eastern part in parameter zone 1 (fig. 17*H*).

Temporal Discretization

For this study, the model simulated steady-state as well as transient conditions. There were 342 stress periods of varying length. The first stress period represented steady-state (predevelopment) conditions before 1967. Because sufficient water-level data were not available from before 1967, the initial conditions for the steady-state stress period were determined from the first water-level measurements in 20 wells described in the "Groundwater Altitudes and Movement" section. The steady-state stress period had one time step. The simulated heads at the end of the steady-state stress period were the initial heads for the transient simulation period. Stress periods 2–18 were 1 year in duration and represented transient conditions for 1967–83. Stress periods 19–342 were each 1 month in duration to represent the variability in pumping for 1984–2010. Each transient stress period had six time steps.

Model Boundaries

The boundaries of the Bicycle Basin groundwater-flow model (fig. 15) were determined by the geohydrologic interpretations discussed in the "Geohydrologic Framework" section of this report and generally coincided with the boundaries of the aquifer system. The top boundary of the model, the water table, was simulated as a free-surface boundary, which is allowed to move vertically in response to changes in inflow, outflow, and storage of water in the aquifer. No-flow boundaries were specified laterally around the modeled domain (fig. 15) to represent contact with low-permeability volcanic and crystalline basement rocks (basement complex) and for the lower boundary (fig. 16) to represent Tertiary older gravels (Tog) deep in the basin and the basement complex south of the unnamed fault 1; these sediments and rocks were assumed to yield little to no water. A no-flow boundary indicates no exchange of water between model cells along the boundary and the area outside the model.

A drain was used along the southern boundary of the basin (fig. 15*A*) to simulate natural groundwater discharge through fractured volcanic material and granitic bedrock southeast of the Bicycle Lake (dry) playa (see "Hydrologic Framework" section). Drain boundary conditions were assigned to six cells in model layer 1 along part of the southern boundary of Bicycle Basin (fig. 15*A*). Discharge through the drain is controlled by the calibrated altitude of the drain relative to the simulated hydraulic head in the aquifer and by the calibrated hydraulic conductance between the aquifer and the drain. These characteristics are discussed in the "Simulation of Natural Recharge and Discharge" section of this report.

Model Input

Input required for this model included hydraulic properties, recharge, discharge, and pumpage. Hydraulic properties included horizontal and vertical hydraulic conductivity for each model parameter zone (fig. 15), specific yield in model layers 1–6, specific storage in model layers 2–8, elastic and inelastic specific storage and preconsolidation heads (necessary to simulate subsidence), and the hydraulic characteristic (associated with faults that act as horizontal flow barriers). Input values for hydraulic conductivity and specific storage are used to calculate transmissivity and storage coefficient values, respectively, in the model. Parameter zones (fig. 15) were defined on the basis of the spatial geometry of the active model domain from interpretations of surface and subsurface geology described earlier in this report. Recharge estimates were based on a subset of the BCM developed by Flint and others (2004). Pumpage data were provided by Fort Irwin personnel (Christopher Woodruff, written commun., 2010). The hydraulic characteristic values were estimated for individual fault segments during model calibration.

Hydraulic Properties

Hydraulic properties assigned to model cells (horizontal and vertical hydraulic conductivity, specific yield, and specific storage) affect the simulated rate at which groundwater moves through an aquifer, the volume of water in storage, and the rate and areal extent of water-level changes caused by groundwater pumping and recharge. Hydraulic properties associated with subsidence (elastic and inelastic specific storage) affect the rates of aquifer deformation, manifested as land subsidence, attributable to dewatering of interbedded fine-grained silts and clays. Horizontal hydraulic conductivity, vertical anisotropy ratio, specific yield, and specific storage were specified in the Upstream-Weighting (UPW package; Niswonger and others, 2011). Elastic and inelastic specific storage and preconsolidation heads were specified in the Subsidence and Aquifer-System Compaction (SUB package; Hoffman and others, 2003). Trial-and-error and automated parameter-estimation methods were both used during the model-calibration process to estimate the final hydraulic properties given in subsequent sections; this process is discussed in the "Model Calibration" section of this report.

Parameter Zonation

Parameter zonation was used because the number and distribution of wells with detailed lithologic and borehole geophysical data to adequately represent complex heterogeneity of the hydraulic properties in the aquifer system were insufficient. Parameter zones (figs. 15*A–H*) were defined on the basis of the horizontal and vertical distribution of stratigraphic units described in the "Geologic Units" section and on horizontal-flow barriers (faults); the resulting zones were used to distribute hydraulic properties to model cells. Parameter zones 1–5 and 7 include parts of the basin beyond the lateral extent of the buried lacustrine deposits (QTol) north and northwest of the Bicycle Lake (dry) playa (fig. 16). In addition, the South Coyote Canyon fault separates parameter zone 2 from the rest of the basin, and parameter zones 4 and 7 are southwest of the unnamed fault 1. The surface expression of the Quaternary older alluvium (Qoa) geologic unit distinguishes parameter zone 7 from parameter zone 4, which includes Quaternary younger alluvium (Qya) and the Bicycle Lake (dry) playa at land surface. Parameter zone 6 was defined by the lateral extent of the Quaternary-Tertiary lacustrine deposits (QTol) geologic unit and land-surface deformation determined from analysis of InSAR images described in the "Land-Surface Deformation" section. Parameter zones 1–3 and 5–6 are in all layers; parameter zones 4 and 7 are only in layers 1–3 (table 7) because the basement complex is shallow in this part of the basin. The hydraulic-property distributions for these parameter zones were input to the UPW package (Niswonger and others, 2011) in MODFLOW-NWT. The UPW package calculates all terms in the numerical formulation of the groundwater-flow equation and is an alternative to the block-centered flow, layer-property flow, and hydrogeologic unit flow packages (Niswonger and others, 2011).

Table 7. Number of hydraulic-parameter zones in model layers 1–8 of the Bicycle Basin groundwater-flow model, Fort Irwin National Training Center, California.

Layer	Number of parameter zones[1]
1	7
2	7
3	7
4	5
5	5
6	5
7	5
8	5
Total	46

[1]Vertical anisotropy ratio (VANI) and specific storage (SS) were not zoned in layer 8.

Hydraulic Conductivity

Initial estimates of horizontal hydraulic conductivity (HK) values for the unconsolidated deposits, based on previous modeling studies (Densmore, 2003; Voronin and others, 2014), aquifer test results, and geologic interpretations for this study or published values for lithologic categories (Bouwer, 1978; Freeze and Cherry, 1979; Fetter, 1994), are summarized for each parameter zone in table 8. These estimates served as starting points for the calibration process. Initial HK values ranged from 0.1 ft/d in model layers 3–5 of parameter zones 3 and 6 to 15 ft/d in model layers 1–6 of parameter zones 1, 2, and 5; model layer 1 in zone 4 and 7; and model layer 6 in zones 3 and 6 (table 8). One HK value was calibrated for each of the parameter zones in each model layer. Final calibrated HK values ranged from 0.04 ft/d for the Quaternary-Tertiary older alluvium (QTol) geologic unit in model layer 5 of parameter zone 6 to 33 ft/d for the predominantly unconsolidated coarse-grained unit represented by model layer 6 of parameter zone 6 (table 8).

The HK values for the upper aquifer (model layers 1–6) estimated from specific-capacity data at selected wells ranged from 3 to 35 ft/d (table 2). The average calibrated HK values for the model layers representing the perforated intervals for these wells ranged from 5.2 to 17 ft/d. The HK value from the specific capacity test for well 14N/4E-18N1 (3 ft/d, in zone 1) reflects, at least partially, the properties of the lower aquifer. The calibrated HK values for layers 7 and 8 (0.63 ft/d and 0.34 ft/d, respectively), which represent the lower aquifer, are considerably less than this value. As mentioned in the "Aquifer System Definitions" section, HK values were determined from slug tests in wells 14N/3E-26K4 (model layer 2) and 14N/3E-26K1 (model layer 3), which are in parameter zone 4. The calibrated HK values for parameter zone 4 (30 ft/d for model layer 2 and 7.0 ft/d for model layer 3) agreed reasonably with the measured data (28 ft/d for 14N/3E-26K4 and 6.78 ft/d for 14N/3E-26K1).

The vertical hydraulic conductivity (VK) for each model layer is computed in the model by dividing the HK values by vertical anisotropy (VANI), where VANI is defined as the ratio of HK to VK. For example, a VANI of 10 means that the HK is 10 times greater than the VK. An initial VANI value of 100 was assumed for all model layers in all parameter zones; however, VANI values typically are unknown and are estimated through model calibration (Anderson and Woessner, 1992). The final VANI values ranged from 2, in model layer 4 of parameter zone 2 and model layer 5 in parameter zone 5, to 22,255, in model layer 1 of parameter zone 6 (table 8). Although these values span a large range, layered heterogeneity frequently can lead to regional anisotropy of 100:1 or greater (Freeze and Cherry, 1979). The final computed values of VK ranged from 2.9×10^{-6} ft/d in model layer 5 of parameter zone 6 to 7.1 ft/d in model layer 4 of parameter zone 3 (table 8).

Vertical conductivity values were determined from analysis of cores from the borehole for wells 14N/3W-23B1–3 (see the "Aquifer System Definitions" section), which is in parameter zone 6 (fig. 15). These values were 9.0×10^{-4} ft/d for the Quaternary-Tertiary lacustrine deposits (QTol; represented by model layers 3–5), 1.0×10^{-2} ft/d for the Tertiary younger gravels (Tyg; represented by model layer 7), and 4.0×10^{-4} ft/d for the Tog (represented by model layer 8). The VK value calculated from the calibrated values for HK and VANI in model layer 3 for parameter zone 6 (8.17×10^{-4} ft/d) was similar to the measured data. The VK values calculated for model layers 7–8 (table 8) were considerably less than the measured data. The discrepancies can be attributed to prioritizing calibration to measured water levels and to observed land-surface deformation rather than to the VK data in parameter zone 6, which are from core samples representing short intervals of a single borehole in heterogeneous sediments.

Specific Yield and Specific Storage

Specific yield (SY) is defined as the volume of water released from storage in an unconfined (water table) aquifer by unit surface area of the aquifer for each unit decline in head (Lohman, 1972). The specific storage (SS) is the volume of water that a unit volume of aquifer releases from storage for a unit decline in hydraulic head in a confined aquifer (Freeze and Cherry, 1979). The SY, which represents gravity drainage following a decline in the water table, is typically orders of magnitude greater than the SS and is the dominant storage parameter volumetrically for each unit thickness of aquifer material.

In MODFLOW-NWT, model-layer types are assigned as convertible or confined. A model layer is converted from confined to unconfined conditions when the hydraulic head in the layer falls below the top of the layer. For this study, model layers 1–6 were convertible, and model layers 7 and 8 were confined. Accordingly, SY and SS were defined for model layers 1–6; one or the other was used, depending on the simulated hydraulic head during each stress period.

During calibration of the transient model, values of SY were estimated for each of the parameter zones in model layers 1–6. Similarly, SS was estimated for each parameter zone in model layers 1–8. An initial SY value of 0.10 was assigned to model layers 1–6 in all zones (table 8). This value has been used for other desert basins (Rewis and others, 2006; Voronin and others, 2013) and is within the range of specific yield estimates from aquifer tests completed for this study

Table 8. Summary of initial and final parameter estimates used in the groundwater-flow model of Bicycle Basin, Fort Irwin National Training Center, California.

[Vertical anisotropy, the ratio of horizontal to vertical hydraulic conductivity; vertical hydraulic conductivity is calculated by HK/VANI. **Abbreviations**: NA, no value; —, not applicable]

Model layers	Parameter zone													
	1		2		3		4		5		6		7	
	Initial	Final	Initial	Final	Initial	Final	Initial	Final	Initial	Final	Initial	Final	Initial	Final
Horizontal hydraulic conductivity (HK), feet per day														
1	15	29	15	1.6	1.0	23	15	7.1	15	32	1.0	3.5	15	0.23
2	15	20	15	2.0	1.0	1.3	10	30	15	9.8	1.0	18	10	0.15
3	15	20	15	6.5	0.10	1.6	1.0	7.0	15	9.2	0.10	0.92	1.0	0.15
4	15	10	15	4.0	0.10	19	NA	NA	15	1.0	0.10	0.06	NA	NA
5	15	8.3	15	14	0.10	3.5	NA	NA	15	3.9	0.10	0.04	NA	NA
6	15	0.81	15	1.7	15	15	NA	NA	15	8.8	15	33	NA	NA
7	10	0.63	10	2.8	10	5.350	NA	NA	10	0.14	10	0.13	NA	NA
8	1.0	0.34	1.0	0.78	1.0	5.2	NA	NA	1.0	0.13	1.0	0.10	NA	NA
Vertical anisotropy (VANI), unitless														
1	100	2,874	100	1,263	100	6.3	100	5,255	100	64	100	22,255	100	3,318
2	100	1,123	100	122	100	39	100	94	100	3.9	100	18	100	1,391
3	100	997	100	83	100	68	100	22	100	33	100	1,123	100	1,411
4	100	28	100	2.0	100	2.61	NA	NA	100	56	100	1,499	NA	NA
5	100	14	100	548	100	26	NA	NA	100	2.0	100	13,806	NA	NA
6	100	57	100	5,914	100	11	NA	NA	100	57	100	10,169	NA	NA
7	100	1,325	100	3,772	100	5,770	NA	NA	100	16,592	100	2,944	NA	NA
8	100	11,730	100	11,730	100	11,730	NA	NA	100	11,730	100	11,730	NA	NA
Vertical hydraulic conductivity (VK), feet per day														
1	0.15	0.01	0.15	1.3E–03	0.01	3.6	0.15	1.4E–03	0.15	0.50	0.01	1.6E–04	0.15	6.9E–05
2	0.15	0.02	0.15	0.02	0.01	0.03	0.10	0.32	0.15	2.5	0.01	0.99	0.10	1.1E–04
3	0.15	0.02	0.15	0.08	1.0E–03	0.02	0.01	0.31	0.15	0.28	1.00E–03	8.2E–04	0.01	1.0E–04
4	0.15	0.37	0.15	2.02	1.0E–03	7.1	NA	NA	0.15	0.02	1.00E–03	3.9E–05	NA	NA
5	0.15	0.60	0.15	0.03	1.0E–03	0.13	NA	NA	0.15	2.0	1.00E–03	2.9E–06	NA	NA
6	0.15	0.01	0.15	3.0E–04	0.15	1.4	NA	NA	0.15	0.15	0.15	3.2E–03	NA	NA
7	0.10	4.8E–04	0.10	7.3E–04	0.10	9.3E–04	NA	NA	0.10	8.2E–06	0.10	4.3E–05	NA	NA
8	0.01	2.9E–05	0.01	6.7E–05	0.01	4.4E–04	NA	NA	0.01	1.1E–05	0.01	8.7E–06	NA	NA

Table 8. Summary of initial and final parameter estimates used in the groundwater-flow model of Bicycle Basin, Fort Irwin National Training Center, California.—Continued

[Vertical anisotropy, the ratio of horizontal to vertical hydraulic conductivity; vertical hydraulic conductivity is calculated by HK/VANI. **Abbreviations**: NA, no value; —, not applicable]

Model layers	Parameter zone													
	1		2		3		4		5		6		7	
	Initial	Final	Initial	Final	Initial	Final	Initial	Final	Initial	Final	Initial	Final	Initial	Final
Specific yield (SY), unitless														
1	0.10	0.12	0.10	0.19	0.10	0.23	0.10	0.12	0.10	0.13	0.10	0.10	0.10	0.02
2	0.10	0.14	0.10	0.19	0.10	0.07	0.10	0.07	0.10	0.12	0.10	0.01	0.10	0.01
3	0.10	0.12	0.10	0.23	0.10	0.07	0.10	0.07	0.10	0.10	0.10	0.01	0.10	0.01
4	0.10	0.23	0.10	0.23	0.10	0.07	0.10	NA	0.10	0.10	0.10	0.01	0.10	NA
5	0.10	0.23	0.10	0.09	0.10	0.07	0.10	NA	0.10	0.10	0.10	0.01	0.10	NA
6	0.10	0.10	0.10	0.05	0.10	0.05	0.10	NA	0.10	0.07	0.10	0.07	0.10	NA
Specific storage (SS), per foot														
1	1.0E–06	1.0E–06	1.0E–06	1.0E–06	1.0E–06	1.0E–06	1.0E–06	1.0E–06	1.0E–06	1.0E–06	1.0E–06	1.0E–06	1.0E–06	1.0E–06
2	1.0E–06	9.0E–07	1.0E–06	8.6E–07	1.0E–06	2.5E–06	1.0E–06	8.7E–07	1.0E–06	2.0E–06	1.0E–06	9.8E–06	1.0E–06	3.9E–06
3	1.0E–06	3.2E–05	1.0E–06	3.9E–06	1.0E–06	8.1E–07	1.0E–06	2.1E–06	1.0E–06	8.6E–07	4.2E–07	4.2E–07	1.0E–06	1.3E–06
4	1.0E–06	3.6E–06	1.0E–06	4.1E–06	1.0E–06	9.0E–07	1.0E–06	NA	1.0E–06	9.0E–07	4.2E–07	4.2E–07	1.0E–06	NA
5	1.0E–06	4.2E–05	1.0E–06	4.9E–05	1.0E–06	1.6E–06	1.0E–06	NA	1.0E–06	8.7E–07	4.2E–07	4.2E–07	1.0E–06	NA
6	1.0E–06	1.3E–05	1.0E–06	7.7E–06	1.0E–06	1.3E–06	1.0E–06	NA	1.0E–06	1.7E–06	1.0E–06	9.7E–07	1.0E–06	NA
7	1.0E–06	1.3E–05	1.0E–06	8.6E–07	1.0E–06	8.4E–07	1.0E–06	NA	1.0E–06	8.3E–07	1.0E–06	9.0E–07	1.0E–06	NA
8	1.0E–06	5.0E–06	1.0E–06	5.0E–06	1.0E–06	5.0E–06	1.0E–06	NA	1.0E–06	5.0E–06	1.0E–06	5.0E–06	1.0E–06	NA

Model layers	Subsidence parameters for parameter zone 6									
	Instantaneous compaction				Delayed compaction					
	Elastic skeletal specific storage (Ske), unitless		Inelastic skeletal specific storage (Skv), unitless		Vertical hydraulic conductivity (Kvi), feet per day		Elastic skeletal specific storage (Sske), per foot		Inelastic skeletal specific storage (Sskv), per foot	
	Initial	Final	Initial	Final	Initial	Final	Initial	Final	Initial	Final
2	—	—	—	—	1.2E–06	1.2E–06	1.8E–05	1.1E–05	1.8E–04	1.6E–04
3	1.8E–05	7.6E–06	1.8E–04	5.4E–05	—	—	—	—	—	—
4	1.8E–05	4.1E–06	1.8E–04	6.7E–05	—	—	—	—	—	—
5	1.8E–05	3.3E–06	1.8E–04	5.4E–05	—	—	—	—	—	—
6	—	—	—	—	1.2E–06	1.2E–06	1.8E–05	8.0E–06	1.8E–04	8.6E–05
7	—	—	—	—	1.2E–06	1.2E–06	1.8E–05	8.5E–06	1.8E–04	8.5E–05

(table 2). Initial SS values for all parameter zones in all layers, except layers 3–5 in parameter zone 6, were 1.0×10^{-6} ft^{-1}. An initial SS value of 4.2×10^{-7} ft^{-1} (the compressibility of water) was used for parameter zone 6 in model layers 3–5, where there is deformation of fine-grained silts and clays; this value was not adjusted during calibration. The final SY values ranged from 0.01 in model layers 2–5 in parameter zone 6 and model layers 2–3 in zone 7 to 0.23 for model layers 4–5 in parameter zone 1, model layers 3–4 in parameter zone 2, and model layer 1 in parameter zone 3 (table 8). The final SS values ranged from 4.20×10^{-7} ft^{-1} in model layer 3–5 of parameter zone 6 to 4.95×10^{-5} ft^{-1} in model layer 5 of parameter zone 2 (table 8).

Elastic and Inelastic Storage

Land subsidence in Bicycle Basin was simulated using the Subsidence and Aquifer-System Compaction (SUB) package (Hoffmann and others, 2003) to allow both for instantaneous and delayed drainage of the fine-grained deposits (interbeds) of model layers 2–7 in parameter zone 6. The confining unit in Bicycle Basin consists primarily of thick, buried lacustrine deposits of the Quaternary-Tertiary lacustrine (QTol) geologic unit. In the Bicycle Basin model, model layers 3–5 represented the Quaternary-Tertiary lacustrine (QTol) confining unit. This unit was divided into three model layers of instantaneous compaction to increase the accuracy of simulated flow and storage changes (Leake and others, 1994). Model layer 2 primarily consists of interbedded sands and gravels of the Quaternary-Tertiary older alluvium (QToa) geologic unit (fig. 16). Model layer 6 consists of the Quaternary-Tertiary older alluvium (QToa) geologic unit and the sand and gravel deposits of the Tertiary younger gravel (Tyg) geologic unit (fig. 16*A*). Model layer 7 consists of the Tertiary younger gravel (Tyg) geologic unit, which grades laterally into fine-grained deposits (fig. 16*B*). Although the deposits in model layers 2, 6, and 7 are primarily coarse-grained, there can be delayed compaction where thin, low-permeability, fine-grained deposits are present.

The thicknesses of the fine-grained interbeds subject to instantaneous and delayed compaction were specified in the SUB package. Estimated storage properties associated with instantaneous compaction of fine-grained deposits include elastic and inelastic skeletal storage coefficient (Ske and Skv, respectively; unitless). Estimated storage properties associated with delayed drainage of fine-grained deposits include elastic and inelastic skeletal specific storage (Sske and Sskv, respectively; per ft). Preconsolidation heads (Hc) are specific for instantaneous and delayed compaction. The simulation of delayed compaction also required the vertical hydraulic conductivity associated with the interbeds (Kvi).

The thickness of the fine-grained deposits in parameter zone 6 was estimated from the borehole geophysical data for monitoring wells 14N/3E-23B1–3 and lithologic logs for wells 14N/3E-14P2 and 14N/3E-23G1 (fig. 2). For the interbeds that compact instantaneously in model layers 3–5, the thickness was interpolated between the wells by using a nearest neighbor method. The thickness distributions for model layers 3–5 are shown in figures 18*A–C*, respectively. The thickness distribution of the interbeds that undergo delayed compaction for model layers 2, 6, and 7 is shown in figure 18*D*. Fine-grained deposits were omitted from model layer 6 in the vicinity of well 14N/3E-23G1 because the lithologic log for that well indicated predominantly coarse-grained deposits at this depth.

Initial estimates for Ske and Skv for instantaneous compaction were 1.8×10^{-5} and 1.8×10^{-4}, respectively, in model layers 3–5 (table 8). These values were adjusted during model calibration, and the final values for Ske ranged from 3.27×10^{-6} in model layer 5 to 7.58×10^{-6} in model layer 3. The final values for Skv ranged from 5.38×10^{-5} in model layer 3 to 6.71×10^{-5} in model layer 4 (table 8). Initial values for Kvi, Sske, and Sskv for delayed compaction were 1.2×10^{-6} ft/d, 1.8×10^{-5} ft$^{-1,}$ and 1.8×10^{-4} ft^{-1}, respectively, in model layers 2, 6, and 7. The Kvi values were insensitive to observations, and the initial values did not change. The Sske and Sskv values were adjusted during model calibration, and the final Sske values ranged from 8.00×10^{-6} ft^{-1} in model layer 6 to 1.08×10^{-5} ft^{-1} in model layer 2; the final Sskv values ranged from 8.46×10^{-5} ft^{-1} in model layer 7 to 1.58×10^{-4} ft^{-1} in model layer 2 (table 8).

Preconsolidation Head

Preconsolidation head, Hc, was defined by Poland (1984) as “the maximum antecedent effective stress to which a deposit has been subjected, and which it can withstand without undergoing additional permanent deformation.” Once the hydraulic head in an interbed falls below the preconsolidation head, permanent inelastic compaction of that interbed occurs. A new Hc is calculated at the end of each transient time step, which is then used in the subsequent time step (Hoffmann and others, 2003). In this study, the Hc value for all layers with fine-grained deposits in parameter zone 6 was assumed to be 2,226 ft, which was similar to the earliest measured water level (well 14N/3E-13K1 in 1955; fig. 7*A*). Simulated water levels declined to the preconsolidation head when pumping began in the mid-1960s; the initial Hc value was not adjusted during model.

Horizontal-Flow Barriers

The Bicycle Basin model used an updated version of the Horizontal Flow Barrier (HFB package (Hsieh and Freckleton, 1993) for use with MODFLOW-NWT; the functionality of the HFB package was unchanged (Niswonger and others, 2011). The HFB package simulates barriers or faults as thin, vertical, low-permeability geologic features situated between pairs of adjacent cells in the model grid that impede the horizontal flow of groundwater (Hsieh and Freckleton, 1993).

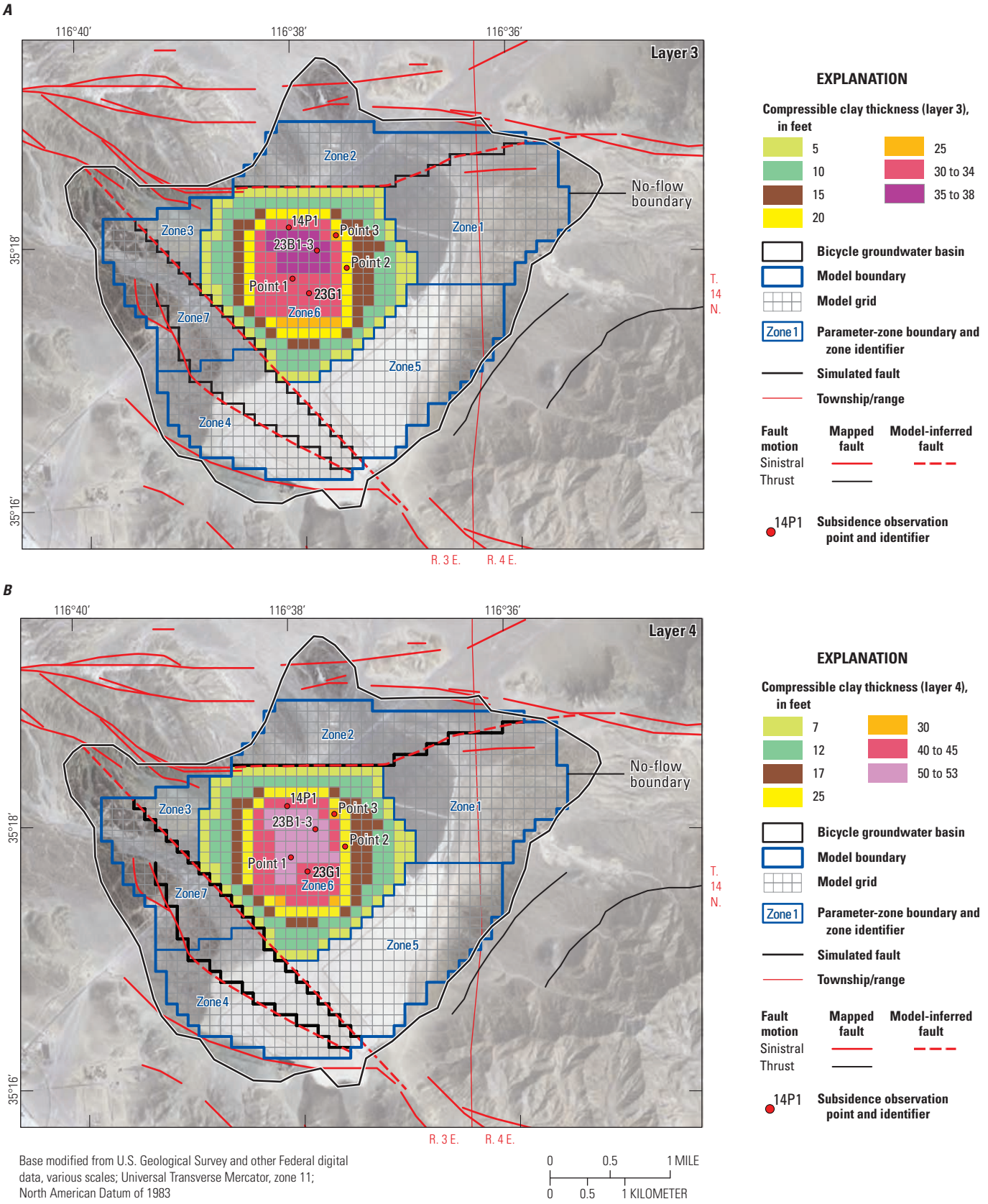

Figure 18. Thickness of fine-grained deposits in parameter zone 6 for the Bicycle Basin groundwater-flow model, Fort Irwin National Training Center, California, for instantaneous compaction in *A*, model layer 3; *B*, model layer 4; and *C*, model layer 5; and delayed compaction in model layers 2, 6, and *D*, 7.

C

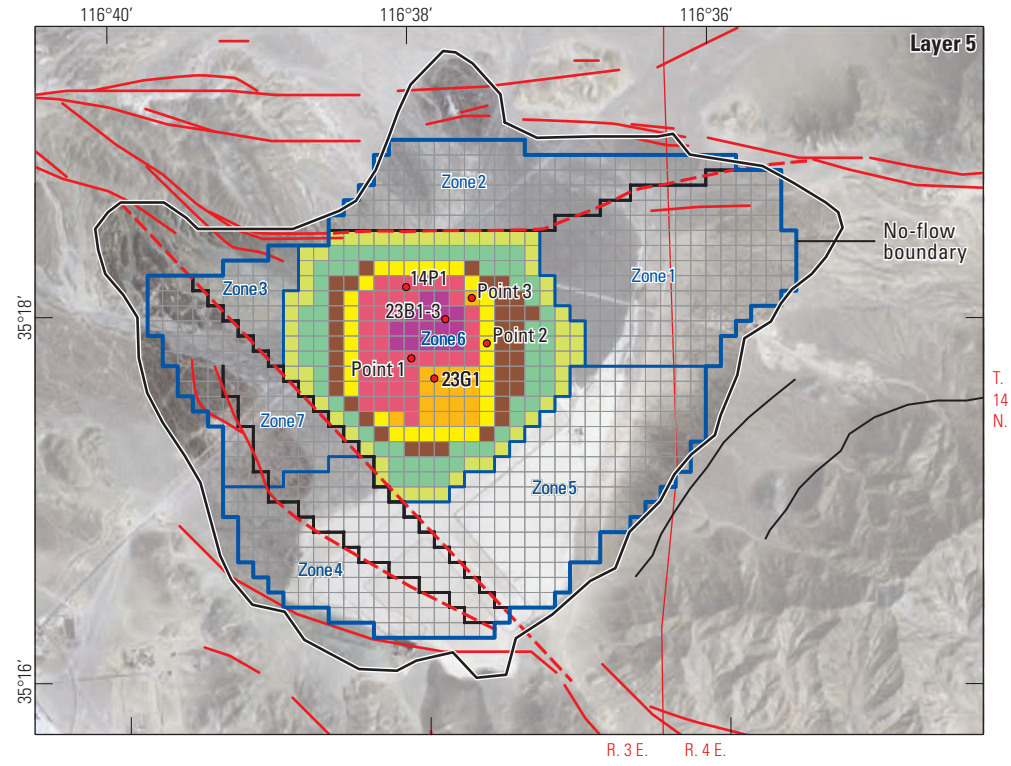

EXPLANATION

Compressible clay thickness (layer 5), in feet

5	25
10	30 to 34
15	35 to 37
20	

- Bicycle groundwater basin
- Model boundary
- Model grid
- Zone 1 — Parameter-zone boundary and zone identifier
- Simulated fault
- Township/range

Fault motion	Mapped fault	Model-inferred fault
Sinistral		
Thrust		

- 14P1 — Subsidence observation point and identifier

D

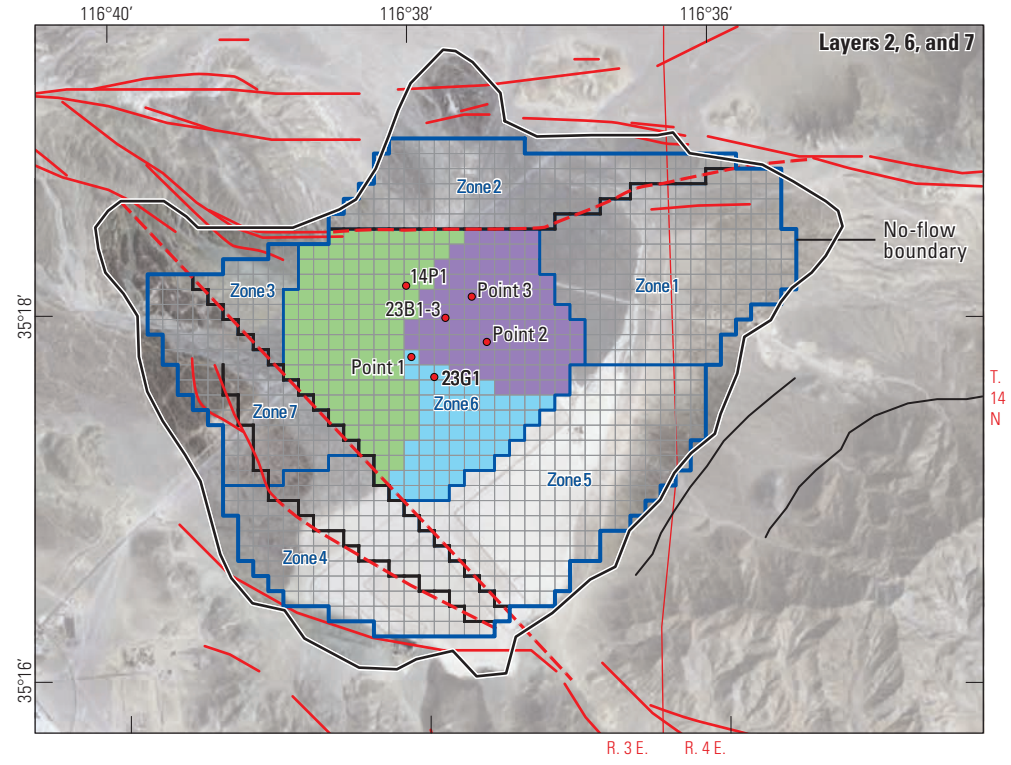

EXPLANATION

Compressible clay thickness (layer 2, 6, and 7), in feet

	Model layer 2	Model layer 6	Model layer 7
	2	0	1
	35	25	55
	36	24	18

- Bicycle groundwater basin
- Model boundary
- Model grid
- Zone 1 — Parameter-zone boundary and zone identifier
- Simulated fault
- Township/range

Fault motion	Mapped fault	Model-inferred fault
Sinistral		
Thrust		

- 14P1 — Subsidence observation point and identifier

Base modified from U.S. Geological Survey and other Federal digital data, various scales; Universal Transverse Mercator, zone 11; North American Datum of 1983

0 0.5 1 MILE
0 0.5 1 KILOMETER

Figure 18. —Continued

Groundwater flow across a simulated barrier is proportional to the hydraulic-head difference between adjacent cells, where the constant of proportionality is the hydraulic characteristic (Hchar, in d^{-1}), which is defined as the hydraulic conductivity of the barrier divided by the distance across the barrier in the flow direction ($Hchar = K_{barrier} / L_{barrier}$).

The simulated faults were the South Coyote Canyon fault and two unnamed faults (fig. 15*A*). The locations and areal extents of faults in the basin were identified from the geologic analysis. During model calibration, it was determined that mapped faults next to and in the southwestern part of the basin needed to be extended (fig. 2) to match water levels better in that area. Additional analysis of the geologic and geophysical data determined that this change was justified. Initially, it was assumed that the faults were not important barriers to groundwater flow, and the Hchar value was set to 1.0 d^{-1} for the horizontal-flow barriers in all layers (table 9). The Hchar values were adjusted in each model layer during model calibration to determine if the unnamed faults impeded lateral groundwater flow. The South Coyote Canyon fault was simulated separately for model layer 1; model layers 2–8 were grouped, because it was determined during model calibration that the fault was similarly restrictive to groundwater flow at these depths. This was supported by the water-level data for wells 14N/3E-13M1 and -14H1, which are north of the South Coyote Canyon fault and are perforated in model layers 2–7. The data indicated that when pumping was reduced or discontinued in these wells, water levels stabilized or rose. Water levels in similarly perforated wells in other parts of the basin, however, continued to decline (fig. 8), indicating little or no hydraulic connection across this fault. The Hchar value for each horizontal-flow barrier was calibrated to match measured drawdown throughout the calibration period. The final values represent the spatial variability of the estimated ability of these faults to restrict groundwater flow. The calibrated Hchar for the South Coyote Canyon fault indicated the fault was a restrictive barrier in model layers 2–8 and somewhat less restrictive in model layer 1. The final Hchar values ranged from 2.58×10^{-7} d^{-1} for the South Coyote Canyon fault in model layers 2–8 to 1.15 d^{-1} for the unnamed fault 1 in model layer 1 (table 9), indicating the faults at most depths were more restrictive to groundwater flow than the initial value indicated. The calibrated Hchar value for unnamed fault 1 indicated the fault was not a restrictive groundwater-flow barrier in model layer 1; the final values for model layers 2 and 3 indicated the fault was somewhat restrictive in these layers (table 9). The calibrated Hchar values for unnamed fault 2 indicated the fault is less restrictive than unnamed fault 1 in model layers 2 and 3 and more restrictive in model layer 1 (table 9).

Table 9. Summary of initial and final hydraulic characteristics for horizontal-flow barriers in the groundwater-flow model of Bicycle Basin, Fort Irwin National Training Center, California.

[Units in 1/day]

	Hydraulic characteristic (Hchar)	
	Initial	**Final**
South Coyote Canyon fault		
Layer 1	1.0	9.5E–03
Layers 2–8	1.0	2.6E–07
Unnamed fault 1		
Layer 1	1.0	1.1E+00
Layer 2	1.0	9.7E–03
Layer 3	1.0	5.0E–03
Unnamed fault 2		
Layer 1	1.0	3.9E–01
Layer 2	1.0	4.4E–01
Layer 3	1.0	8.7E–01

Simulation of Natural Recharge and Discharge

Recharge to the Bicycle basin was simulated using the Recharge (RCH) package. The BCM was used in this study to provide subsurface inflows and runoff along the margins of Bicycle Basin. Total recharge (subsurface inflow and runoff) was initially distributed to 95 cells in 11 recharge zones that represent the normally dry washes in the uppermost active model layers. Recharge zone 2 was subdivided into three separate recharge zones during model calibration, which are labeled 2, 12, and 13 on figure 15*A*. The recharge zones were based on the stream channels and washes that drain to the Bicycle Basin from adjacent watersheds (fig. 19). Subsurface inflow to the Bicycle Basin was simulated by the BCM at the boundary between Bicycle Basin and the surrounding mountain blocks. It was assumed that 100 percent of the calculated subsurface inflow recharged the Bicycle Basin. Runoff from the surrounding watersheds draining into the Bicycle Basin also was simulated by the BCM. It was assumed that 10 percent of the simulated runoff recharged the groundwater system. Izbicki and others (2002) indicated that about 10 percent of ephemeral streamflow in the southern Mojave Desert became recharge; hence, this value was used with the results of the BCM for the Bicycle groundwater basin.

Total recharge was assumed to be constant during the transient simulation period (1967–2010). Results from a study by Bouwer (1980) indicated that seasonal and annual fluctuations in infiltration were attenuated as a function of sediment particle size in the unsaturated zone and vertical distance to the water table. Bouwer (1980) found that downward velocities in the unsaturated zone decreased with decreasing particle size of the materials and that deep percolation virtually reaches a steady, uniform flow at a depth of about 50–100 ft bls. Because the unsaturated zone mostly contains fine-grained sediment and the depth to water in the basin is in excess of 100 ft, a constant recharge rate in each recharge zone was a reasonable assumption. The initial recharge rate for each model cell in a recharge zone ranged from 1.98×10^{-6} ft/d in recharge zone 7 to 2.09×10^{-3} ft/d in recharge zone 2 (table 10). The recharge rates were parameterized and adjusted during model calibration. The final recharge rates for each model cell in a recharge zone ranged from 3.09×10^{-6} ft/d in recharge zone 7 to 2.99×10^{-3} ft/d in recharge zone 2 (table 10). Final recharge rates were higher than initial estimates for the areas recharged by the largest contributing watersheds (recharge zones 1 and 2; fig. 19). Final recharge rates were lower than initial estimates in most areas recharged by the smaller contributing watersheds (table 10).

Table 10. Summary of initial and final groundwater–recharge values for the groundwater-flow model of the Bicycle Basin, Fort Irwin Training Center, California.

[Recharge rates are for each model cell in the recharge zone. See figure 15*A* for location of recharge zones.]

Recharge zone[2]	Recharge[1]		
	Initial (feet/day)	Final (feet/day)	Difference (percent)
1	7.30E–04	9.25E–04	27
2	2.09E–03	2.99E–03	43
3	2.77E–05	1.81E–05	–35
4	2.57E–06	4.62E–06	80
5	2.10E–05	2.70E–05	29
6	8.73E–06	4.11E–06	–53
7	1.98E–06	3.09E–06	56
8	2.10E–04	9.10E–06	–96
9	5.31E–04	4.85E–05	–91
10	4.76E–04	9.31E–05	–80
11	3.85E–04	3.42E–06	–99
12	NA[3]	3.42E–05	NA[3]
13	NA[3]	3.76E–06	NA[3]

[1]Recharge is the sum of infiltration of runoff and watershed underflow.

[2]Recharge zones numbers were based on the upstream watersheds shown in figure 19.

[3]Recharge zones 12 and 13 originally were part of recharge zone 2; both were separated from zone 2 during model calibration.

Groundwater discharge was simulated using the MODFLOW Drain (DRN package (Harbaugh, 2005). Groundwater discharges to the drain cells near the southern boundary (fig. 15*A*) only when the simulated hydraulic head in the aquifer is greater than the drain altitude. Discharge in this part of the basin was inferred because (1) long-term runoff and recharge into the basin was greater than zero, (2) there were no outflows from the basin other than subsurface flow in the southeast, and (3) the estimated predevelopment water level was higher than the estimated bedrock elevation at this point. The initial drain altitude was assumed to be representative of the predevelopment water level in this area because it is the low spot in the basin. The earliest measured water level of 2,216 ft (fig. 7*A*) was assigned as the drain altitude in each of the six drain cells. This water level ranged from 117 to 121 ft bls in these cells. The altitude was adjusted during model calibration, and the final value was 2,211 ft in each drain cell to match water levels better. Flow out of the drain also is controlled by the conductance between the aquifer and the drain. The initial drain conductance, 100 ft^2/d in each drain cell, was adjusted during model calibration so that the simulated recharge equaled the simulated discharge through the drain for the steady-state stress period. The final drain conductance was 4,335 ft^2/d in each drain cell.

Groundwater Pumpage

The MODFLOW Multi-Node Well package, MNW2 (Konikow and others, 2009) with the partial penetration option was used to simulate groundwater pumping from the five production wells in the Bicycle Basin. The MNW2 package simulates wells completed in multiple aquifers and allows vertical groundwater movement through the well bores. The groundwater-pumping rate at an individual well was distributed dynamically to model layers (multi-well nodes) on the basis of the hydraulic conductivity and the saturated length of the perforated interval in each layer. Initially, groundwater pumpage for each production well was distributed to perforated intervals in model layers 1–8, with only the perforated interval of production well 14N/3E-13K1 extending into model layer 1 (fig. 15*A*) and the perforated interval of production well 14N/4E-18N1 extending into layer 8 (fig. 15*H*). Pumpage was redistributed to deeper perforations as the water table declined during the simulation period.

Annual and monthly pumpage compiled and estimated for this study was assigned to the active cell that contained the production well (fig. 15). Pumpage records included annual basin pumpage (not by well) for 1967–83 (table 3), annual pumpage by well for 1984–90 (fig. 6*A*; table 3), and monthly pumpage by well for 1991–2010 (fig. 6*B*). The ratio of average annual pumpage by well to total annual pumpage for the basin for 1984–86 was used to estimate the annual pumpage by well for 1967–83. The average ratio of monthly pumpage by well to total monthly pumpage for the basin for 1991–93 was used to estimate the monthly pumpage by well for 1984–90.

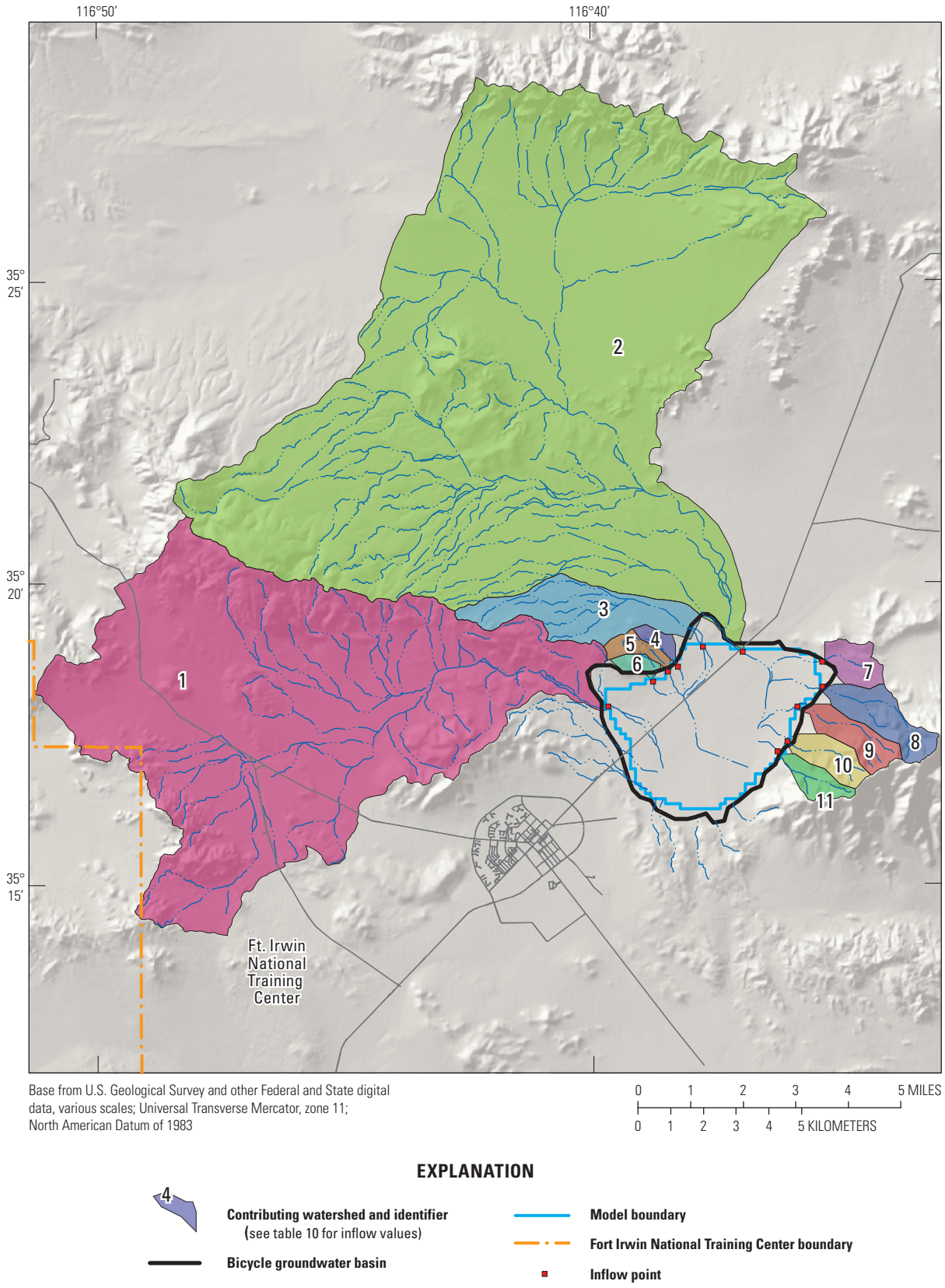

Figure 19. Watersheds that contribute recharge to Bicycle Basin, washes, and groundwater-flow model boundary for the Bicycle Basin groundwater-flow model, Fort Irwin National Training Center, California.

Model Calibration

The Bicycle Basin model was calibrated through a combination of trial-and-error and automated parameter-estimation methods. Hydraulic properties, hydraulic characteristic of faults, recharge rates, and drain properties were modified as part of this process. These parameters were estimated by automated parameter-estimation methods using a nonlinear-regression, parameter-estimation software known as PEST (Doherty, 2010a, b, c), which employs a widely used algorithm known as the Gauss-Marquardt-Levenberg method. This method adjusts initial parameter values so that the weighted sum of the squared differences between the observations and their corresponding model-simulated values (that is, the objective function) is minimized. Each model cell must have values for each physical property (for example, hydraulic conductivity or storativity). For most groundwater models, this can result in a large number of parameters, which can be reduced using parameterization techniques, such as the parameter zonation discussed in the "Parameter Zonation" section of this report. In the Bicycle Basin model, parameterization was used in PEST to characterize the following properties:

- Horizontal hydraulic conductivities for layers 1–8 and vertical anisotropy ratios in layers 1–7 for all parameter zones.
- Specific yield (SY) values for model layers 1 and 2 and specific storage values for model layers 1–8 for all parameter zones (SY values for layers 3–6 initially were calibrated by trial-and-error and subsequently fixed for calibration using PEST; SY values for layers 7–8 were specified, but not adjusted during model calibration because these layers are confined and the values not used).
- Elastic and inelastic skeletal storage properties associated with the fine-grained interbeds in layers 2–7 in parameter zone 6.
- Hydraulic characteristics of horizontal-flow barriers in layers 1–8.
- Recharge rates by recharge cell in all recharge zones.

Pest Observation Groups and Parameter Weights

Four observation groups were defined in PEST: (1) water levels for initial conditions, (2) transient water levels, (3) drawdown, and (4) land-surface deformation. Water-level observations for initial conditions, representing predevelopment conditions, included the first water-level measurements in 21 wells; transient water-level observations included 364 measurements in 23 wells (appendix 2) that represent conditions during periods of groundwater pumping (1967–2010). The 341 drawdown observations were based on the transient water levels and were calculated as the water-level rise or decline after the first water-level observation. The 108 observations of land-surface deformation were determined at 6 locations (fig. 18) by the methods described in the "Land-Surface Deformation" section. In addition, available data about what value a parameter should take (prior information) can be incorporated into the parameter estimation process (Doherty, 2010a). For the Bicycle Basin model, these data included hydrologic conductivity and specific yield values at selected wells (table 2).

Because the number of observations at each site varied and to prevent sites with many observations from dominating the calibration process, sites with fewer observations were given additional weight so that the weights for the individual sites were spatially consistent. The highest weights were given to the land-surface deformation observations, and the lowest weights given to the drawdown and initial-conditions observations. Observation weights varied within the transient water-level and land-surface deformation observation groups. The drawdown and initial-condition observations were given a weight of one. Most water-level observations were given a weight of two; however, higher weights (three or four) were given to observations with shorter periods of record. Data were not available to determine when subsidence began, so the land-surface deformation observations values were assumed to begin at zero. These values were included in the observation data, but given a weight of zero. The other land-surface deformation observations were given a weight 500, with the exception of the observations for well site 14N/3E-23B1–3. Greater weight (2,500) was given to observations for this site because detailed lithology and borehole geophysical data were available to determine the thickness of interbeds (appendix fig. 1–3). These land-surface deformation weights were considerably larger than the water-level weights because there were fewer observations. Weights associated with the prior information (table 2) were 300 for hydraulic conductivity values from aquifer tests in this study, 10 for reported hydraulic conductivity values, and 1 for reported specific yield values.

Hydrograph and Observed Land-Surface Deformation and Simulated Subsidence Comparison

Simulated hydraulic heads were compared directly with measured groundwater levels if the wells were perforated in a single model layer. For wells perforated in multiple model layers, MODFLOW-NWT calculated a composite, simulated-equivalent hydraulic head, which is a function of the simulated hydraulic heads and hydraulic properties of the perforated model layers, by using the hydraulic-head observation (HOB) package (Hill and others, 2000). The model layers representing the perforated intervals for each observation well are given in table 1. Measured water-level data for these wells are given in appendix 2. Measures of model fit included the following:

- Model-fit statistics for residuals (measured value minus simulated value), including the average, median, minimum, maximum, and root-mean-square error (RMSE).
- Plotting measured groundwater levels against simulated hydraulic heads and residuals against simulated hydraulic heads.
- Hydrograph comparison of measured water levels and simulated hydraulic heads for the transient simulation period (1967–2010).
- Graphical comparison of observed land-surface deformation and simulated subsidence for September 1995–August 2010 (observed period of record).

When plotting simulated hydraulic heads or subsidence against measured groundwater levels or observed land-surface deformation, all the points would lie on the one-to-one (1:1) correlation line if the model results matched the measured data perfectly. Similarly, when plotting the residuals against the simulated hydraulic heads, all the points would be at zero residual if the model results matched the data perfectly.

The RMSE for the transient simulation was 11 ft (table 11), indicating an overall good fit of the simulated heads to the measured water levels; the RMSE was small relative to the approximate 100-ft range of observed and simulated head values in the study area (fig. 20). The RMSE for the production and unused wells, typically composite water levels integrating multiple model layers, was 13 ft; the RMSE for the monitoring wells, typically water levels specific to a single layer, was 8.5 ft (table 11). The RMSE was the greatest for well 14N/3E-14P2 in parameter zone 6 (18 ft) and least for production well 14N/3E-13K1 in parameter zone 1 and observation well 14N/3E-24Q2 in parameter zone 5 (3.5 ft).

The RMSE for the land-surface deformation was small (0.071 ft; table 12), indicating a good fit between observed and simulated subsidence, considering the magnitude of observed subsidence was as much as 1.2 ft.

The composite equivalent simulated heads are plotted against the measured water levels in figure 20. Simulated heads plotting above the 1:1 correlation line indicated the model overestimated the measured water levels; conversely, simulated heads plotting below the line indicated the model underestimated the measured water levels. Overall, the measured water levels and simulated heads generally followed a 1:1 correlation line; however, there was a bias for the model to overestimate measured water levels, which is reflected by the greater number of simulated heads plotting above the 1:1 correlation line (figs. 20*A–C*).

The residuals are plotted against the simulated hydraulic heads in figure 20*D*. If residuals are randomly distributed about zero, there is no bias in the simulated values. In general, the plot showed the residuals distributed about zero; however, there were a larger number of residuals less than zero (59 percent) than greater than zero (41 percent), indicating a tendency of the model to overestimate measured water levels.

The observed land-surface deformation is plotted against the simulated subsidence in figure 21*A*. Overall, the values generally followed the 1:1 correlation line, indicating a good fit. The greater number of simulated values above the line, however, indicated the simulated subsidence had a tendency to overestimate observed values (fig. 21*A*). The difference between observed and simulated subsidence indicated that the model underestimated 29 percent of the observed values, whereas 71 percent were overestimated. Uncertainty in the thickness of the clay interbeds used in the model might have contributed to the general overestimation of subsidence. This pattern was evident in the time-series plots of simulated and observed subsidence at observation points (fig. 21*B*). The graphs for all observation points, except point 1 (fig. 9*A*), indicated subsidence was overestimated for most of the simulation. The graph for point 1 indicated subsidence was underestimated for most of the simulation. Temporal patterns of simulated heads and subsidence relative to observations are discussed in the following section.

Simulated Hydrographs and Subsidence Time Series

Simulated heads and measured water levels for wells are shown by parameter zone in figures 22*A–M*. The wells represent temporal variations (water-level trends, seasonal fluctuations, and vertical gradients) as well as spatial coverage. Although the simulated heads approximately matched the measured water levels, there were times when the simulated heads overestimated or underestimated the measured data.

Table 11. Summary of model-fit statistics for differences between measured water levels and simulated heads for the Bicycle Basin groundwater-flow model, Fort Irwin National Training Center, California.

Well name	Range of residuals (feet)				Root mean square error (RMSE) (feet)	Number of measurements
	Average	Median	Minimum	Maximum		
14N/3E-13K1S	–0.72	–0.52	–8.1	5.2	3.5	20
14N/3E-13M1S	–0.53	–0.65	–14	7.4	6.0	15
14N/3E-13M2S	–8.5	–8.3	–25	4.1	12.0	23
14N/3E-13M3S	2.1	1.1	–12	14	6.2	23
14N/3E-13M4	0.66	1.0	–12	5.9	4.3	24
14N/3E-14H1	–8.9	–9.0	–18	4.6	11	21
14N/3E-14P1S	7.6	7.8	–4.4	22	11	9
14N/3E-14P2S	–12	–12	–34	13	18	27
14N/3E-22P1S	20	20	20	21	12	7
14N/3E-23B1S	–5.2	–6.4	–8.9	–1.6	5.7	13
14N/3E-23B2S	–15	–15	–23	–12	16	11
14N/3E-23B3S	–12	–12	–13	–11	12	11
14N/3E-23G1S	8.8	11	–25	18	12	30
14N/3E-24H1S	–16	–17	–18	–11	17	12
14N/3E-24Q1S	1.6	3.5	–5.2	5.3	3.9	17
14N/3E-24Q2S	0.83	2.40	–5.0	4.5	3.5	17
14N/3E-24Q3S	–2.5	–0.12	–14	2.2	5.7	17
14N/3E-24Q4S	–7.3	–5.8	–15	–2.3	8.4	17
14N/3E-24Q5S	–9.8	–6.9	–20	–5.6	11	17
14N/4E-18N1S	6.6	6.8	–3.8	17	9.9	4
14N/4E-18N2S	–8.2	–9.2	–23	17	11	27
Production and unused wells	–2.6	–1.6	–34	22	13	172
Monitoring wells	–4.1	–3.3	–25	14	8.5	190
All data	–3.4	–2.5	–34	22	11	362

[1]Water levels for wells 14N/3E-26K1,3–4 were omitted from this table because there was only one measurement each for the deep and shallow wells.

Table 12. Summary of model-fit statistics for differences between observed land-surface deformation and simulated subsidence for the Bicycle Basin groundwater-flow model, Fort Irwin National Training Center, California.

Well name	Range of residuals (feet)				Root mean square error (RMSE) (feet)	Number of measurements
	Average	Median	Minimum	Maximum		
14N/3E-14P1S	–0.066	–0.083	–0.186	0.072	0.106	18
14N/3E-23G1S	–0.019	–0.022	–0.052	0.008	0.026	18
14N/3E-23B1–3S	–0.013	–0.010	–0.128	0.098	0.072	18
Point 1	0.032	0.030	–0.012	0.095	0.044	18
Point 2	–0.038	–0.043	–0.064	0.007	0.043	18
Point 3	–0.084	–0.101	–0.138	–0.013	0.097	18
All data	0.354	–0.026	–0.186	0.098	0.071	108

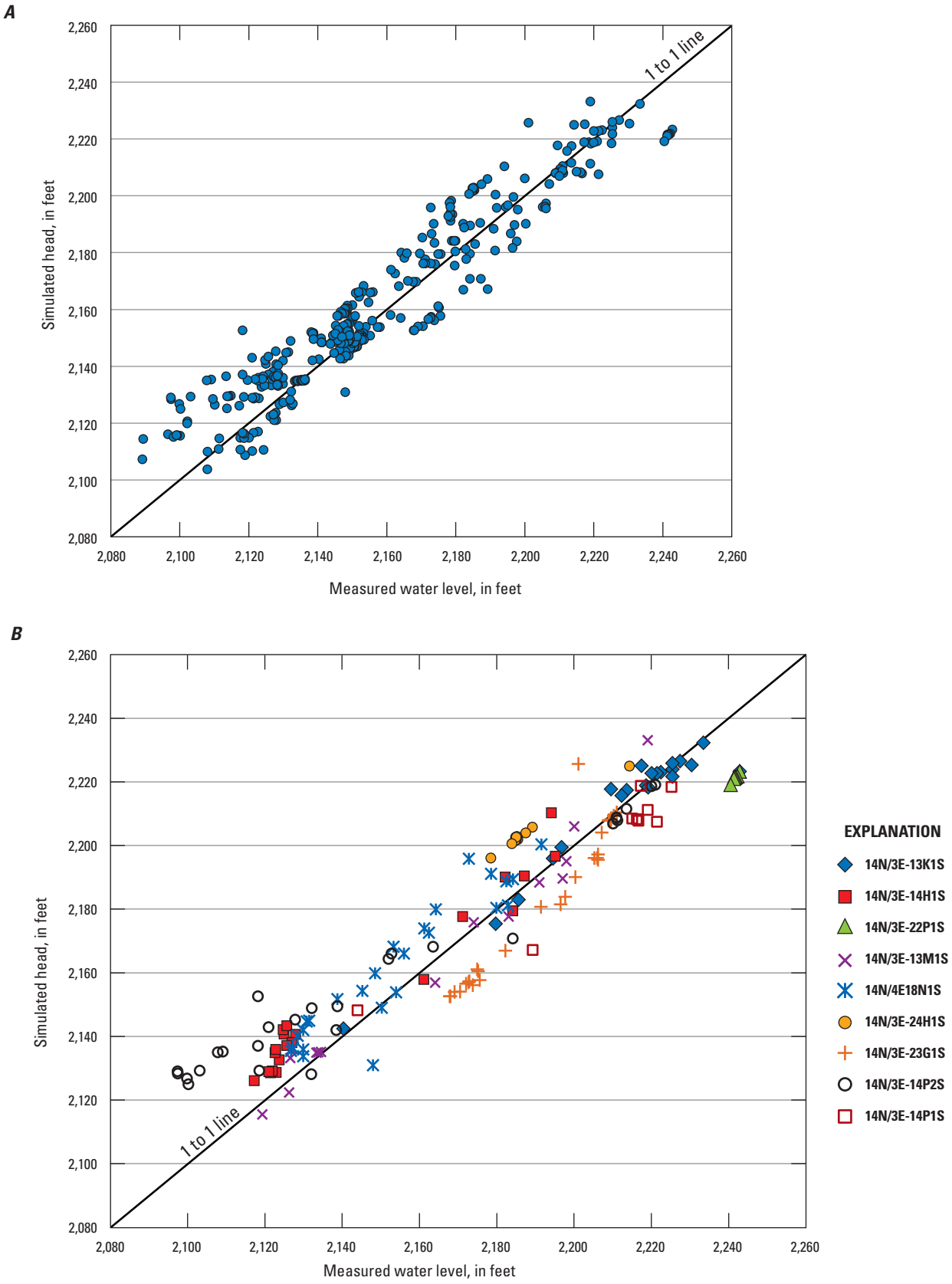

Figure 20. Simulated heads from the Bicycle Basin groundwater-flow model, Fort Irwin National Training Center, California, compared with *A*, measured groundwater levels for all wells; *B*, measured water levels at production wells; *C*, measured water levels at monitoring wells; and *D*, differences between measured water levels and simulated heads (residuals).

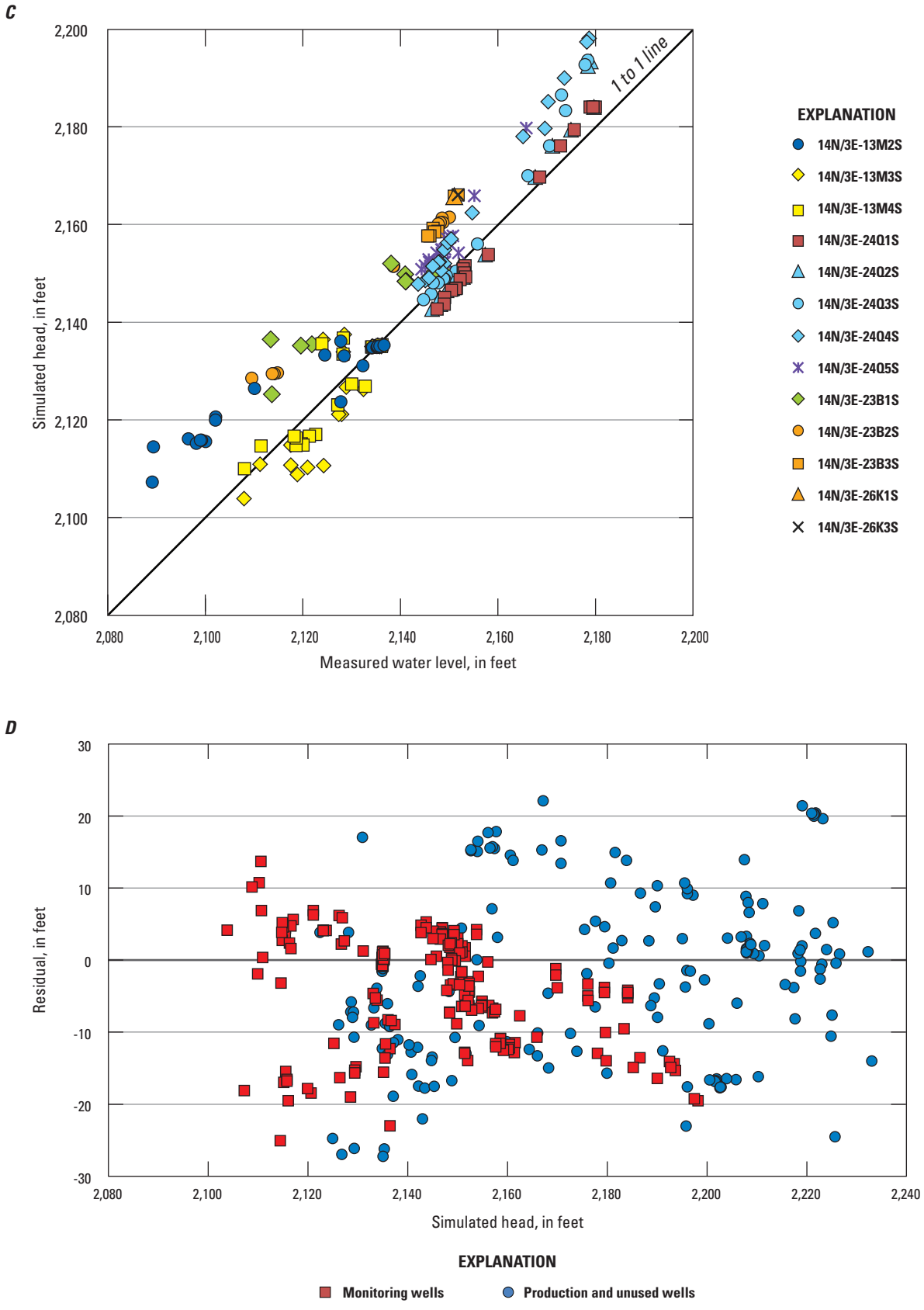

Figure 20. —Continued

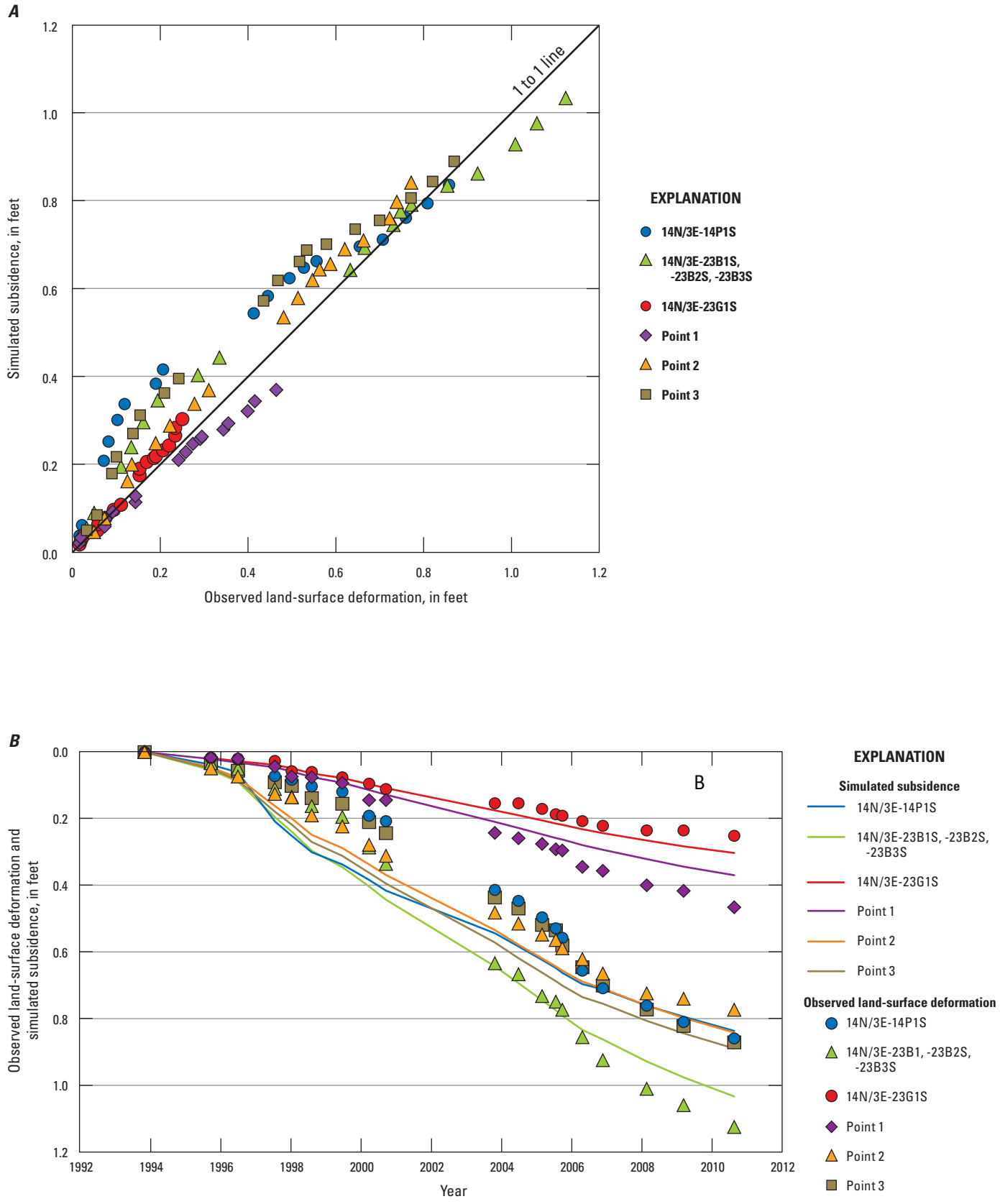

Figure 21. Simulated subsidence from the Bicycle Basin groundwater-flow model, Fort Irwin National Training Center, California, compared with *A*, observed total land-surface deformation and *B*, time series of observed land-surface deformation.

Mismatches between simulated heads and measured water levels can be attributed partly to uncertainty in the estimated distribution of annual basin-wide pumpage among active wells for 1967–83 and the estimated distribution of monthly pumpage from annual values for 1984–90. Estimates of the spatial and temporal distribution of pumpage from limited data could result in excess or insufficient pumpage in some locations, causing overestimation or underestimation, respectively, of measured water levels. The variability in hydraulic properties in parameter zones, which is not reflected in the model, also could contribute to the underestimation or overestimation of the measured water levels.

The simulated heads in all wells from the predevelopment period through 2010 generally matched the trend and seasonal fluctuations of the measured water levels. These results indicated the model reasonably simulated the timing and magnitude of water-level changes in Bicycle Basin. The greatest difference between simulated heads and measured water levels was in well 14N/3E-14H1 in parameter zone 2 (fig. 22*C*) and wells 14N/3E-24H1 (fig. 22*H*) and 14N/3E-24Q1–5 (fig. 22*G*) in parameter zone 5. Although the measured water levels in well 14N/3E-14H1 generally were within the range of fluctuation of the simulated heads, the overall trend in the simulated heads showed smaller declines than the measured water levels for January 1993–July 2000. For well 14N/3E-24H1, simulated heads were consistently about 15 ft higher than measured water levels. Simulated heads were higher than measured water levels in wells 14N/3E-24Q3–5 and 14N/3E-24Q1 for July 1997–January 2002. These discrepancies can be attributed to uncertainties in the earlier estimates of the spatial distribution of pumping. Simulated heads were in good agreement with measured water levels in wells 14N/3E-24Q1 and 14N/3E-24Q2 for March 2005–December 2010. However, the vertical gradient between these wells was not well simulated because both wells are screened only in model layer 8 (table 1).

The differences between simulated heads and measured groundwater levels among model layers indicated that vertical hydraulic gradients fluctuated and even reversed in some parts of the basin as pumpage rates changed seasonally and annually. This reversal of gradients was evident in parameter zone 2, where the direction of vertical flow in wells 14N/3E-13M2–4 varied in the simulated as well as the measured values (table 13). Although the model simulated the hydraulic gradient variability with seasonal pumping reasonably in this zone, the magnitude of the fluctuations differed considerably between the simulated and measured values. In parameter zone 5, the measured vertical water-level differences between wells 14N/3E-24Q5 and 14N/3E-24Q4 indicated a downward direction of flow, which also was simulated by the model. The measured vertical water-level differences between wells 14N/3E-24Q4 and 14N/3E-24Q3 and wells 14N/3E-24Q3 and 14N/3E-24Q2, however, indicated an upward direction of flow, whereas the model simulated a downward direction for wells 14N/3E-24Q4 and 14N/3E-24Q3 and variable direction of flow for wells 14N/3E-24Q3 and 14N/3E-24Q2 (table 13). The simulated magnitudes of vertical head difference also differed considerably from the measured values (table 13). The discrepancies between measured vertical water-level differences and simulated hydraulic head differences in parameter zones 2 and 5 can primarily be attributed to the uncertainty in the distribution of stresses in the basin. In parameter zone 6, the hydraulic gradient between wells 14N/3E-23B3 and 14N/3E-23B2 was simulated by the model. The simulated vertical head differences and direction of flow in parameter zone 6, given for wells 14N/3E-23B1–3 in table 13, mostly agreed with the measured values owing to the explicit simulation of the confining Quaternary-Tertiary lacustrine (QTol) geologic unit by model layers 3–5 in this parameter zone. Model layers 3–5 restricted vertical flow from the shallower layers to model layer 6, where most of the pumping was centered, which allowed the model to simulate the direction of vertical flow and magnitude of the vertical head differences created by the pumping reasonably well.

Simulated subsidence and observed land-surface deformation at wells 14N/3E-14P1 14N/3E-23B1–3, and 14N/3E-23G1 and at points 1–3 in parameter zone 6 (fig. 18) during September 1995–August 2010 are shown in figure 21*B*. Data were not available to determine when subsidence began, so the observed and simulated values begin at zero. It is likely, however, that subsidence began before November 1993 because the decline in water levels began before then. In general, the simulated subsidence corresponded with the observed subsidence. The maximum simulated subsidence ranged from 0.30 ft at well 14N/3E-23G1 to 1.03 ft at well site 14N/3E-23B1–3. At well 14N/3E-23G1, the model simulated the observed data reasonably well. At well site 14N/3E-23B1–3, simulated subsidence was greater than the observed data through 2001 and less than the observed data after 2006 (fig. 21*B*). Between these dates, however, the model simulated measured subsidence reasonably well. At well 14N/3E-14P1, the model overestimated subsidence through October 2006, but simulated observed subsidence reasonably well after that date. Simulated subsidence was greater than observed subsidence at points 2 and 3 and less for point 1 for the period of record (fig. 21*B*).

Mismatches between the observed and simulated values primarily can be attributed to uncertainty in the thickness and lateral heterogeneity of the fine-grained interbeds in model layers 2–7, because detailed lithologic and borehole geophysical data for parameter zone 6 are limited. Uncertainties associated with the interpretation of the interferograms described in the "Land-Surface Deformation" section of this report also can contribute to mismatches between measured and simulated subsidence.

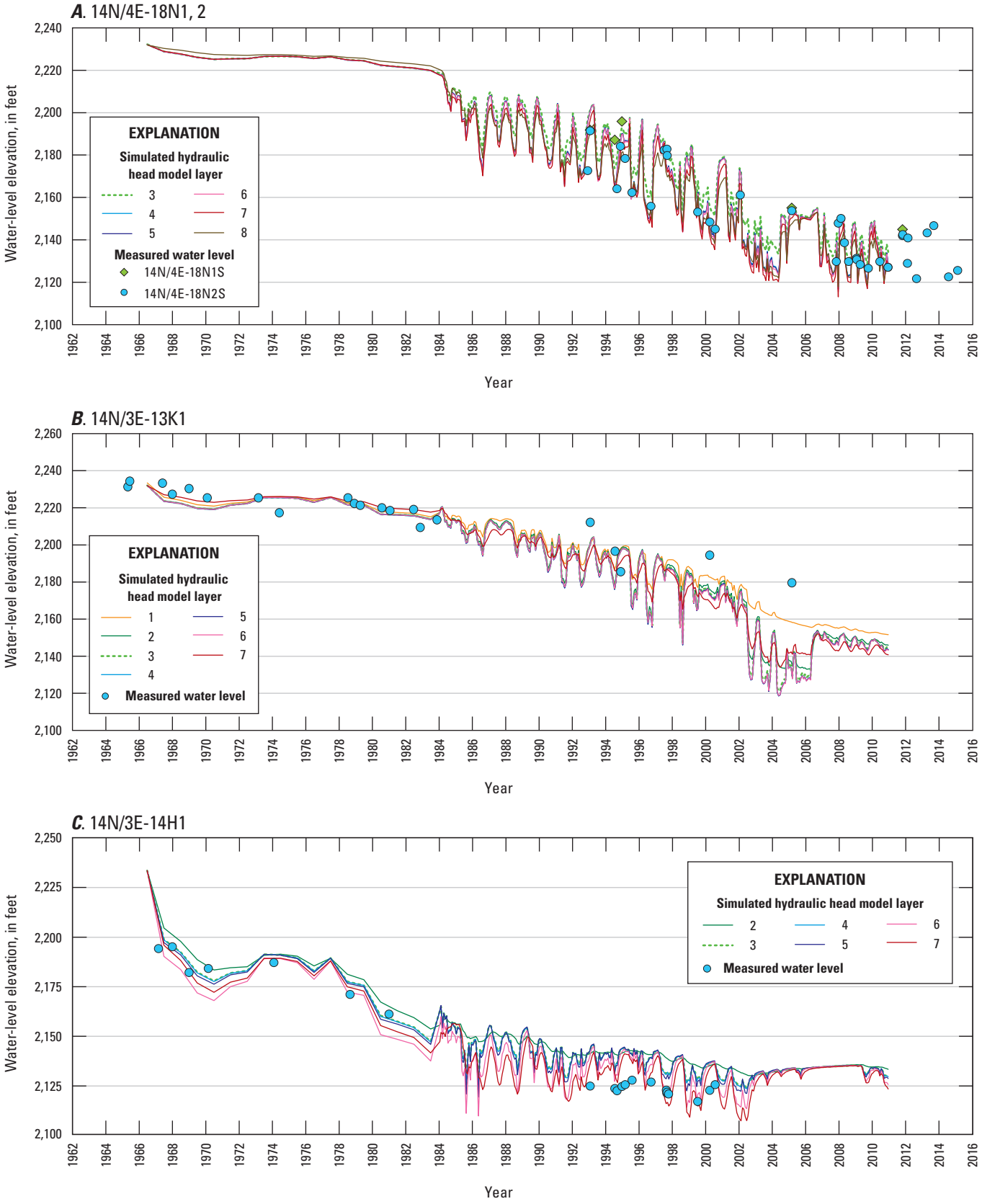

Figure 22. Measured groundwater levels and simulated heads in wells in the Bicycle Basin groundwater-flow model, Fort Irwin National Training Center, California: *A*, 14N/4E-18N1,2; *B*, 14N/3E-13K1; *C*, 14N/3E-14H1; *D*, 14N/3E-13M1; *E*, 14N/3E-13M2–4; *F*, 14N/3E-26K1, 3–4; *G*, 14N/3E-24Q1–5; *H*, 14N/3E-24H1; *I*, 14N/3E-23G1; *J*; 14N/3E-23B1–3; *K*, 14N/3E-14P1; *L*, 14N/3E-14P2; *M*, 14N/3E-22P1.

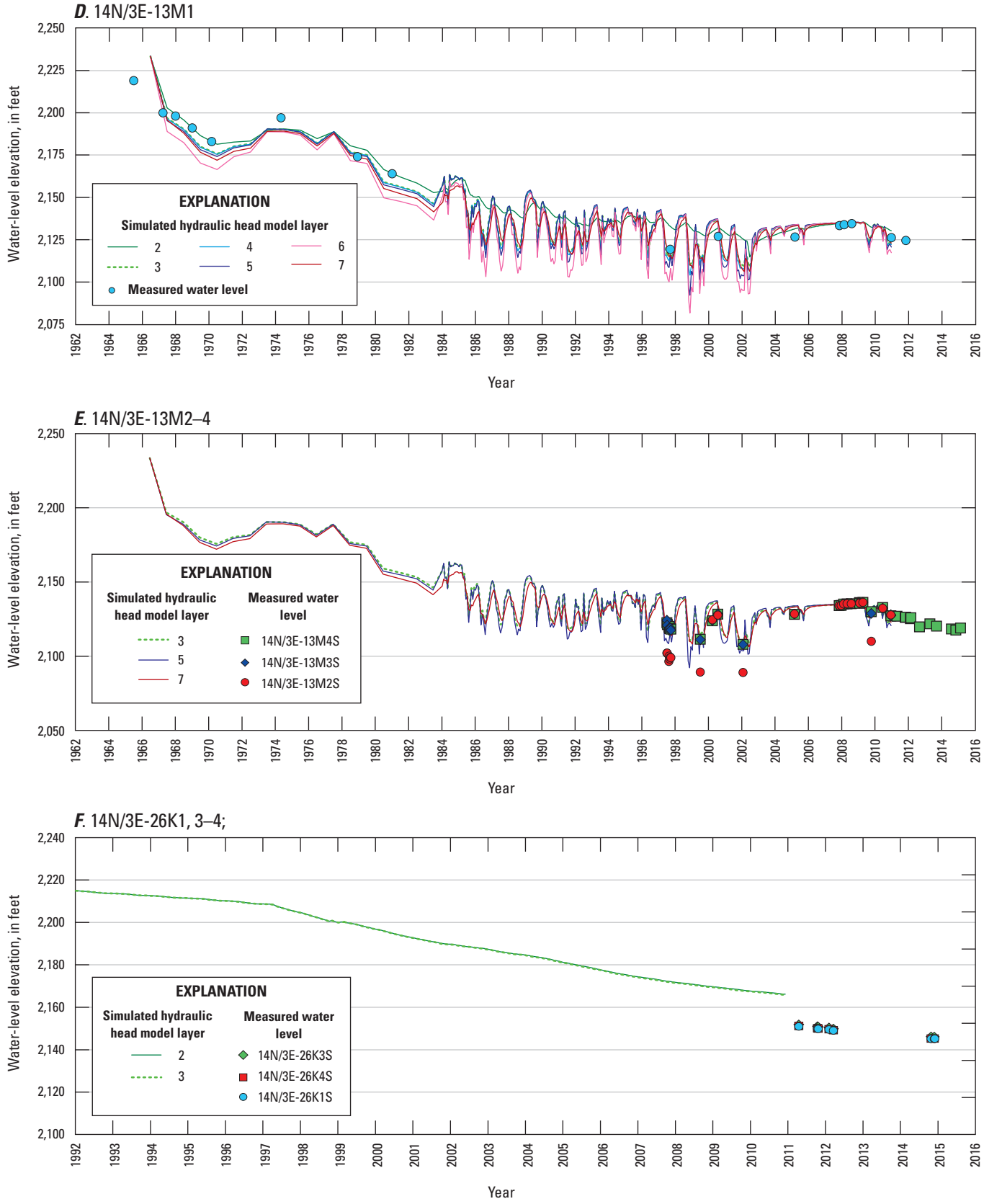

Figure 22. —Continued

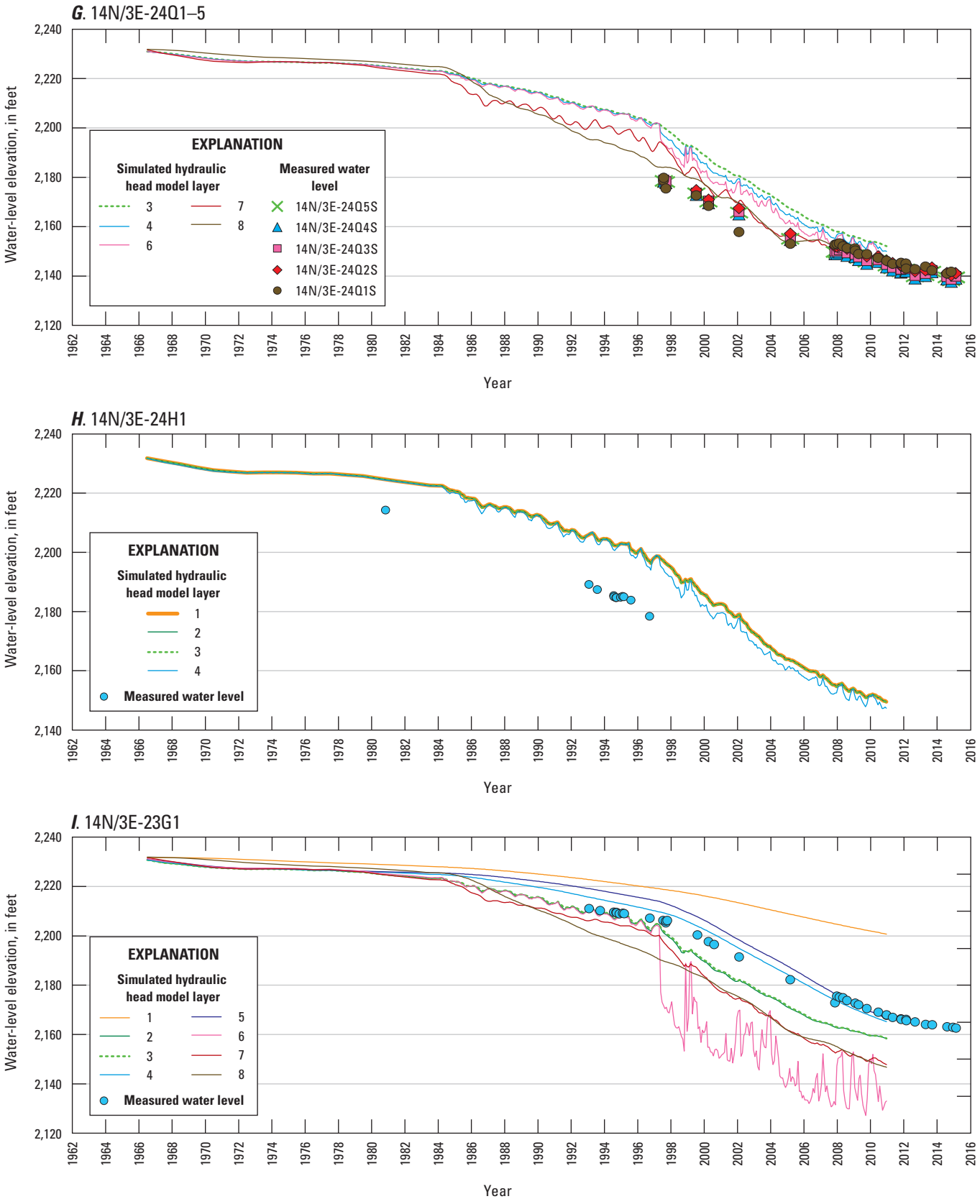

Figure 22. —Continued

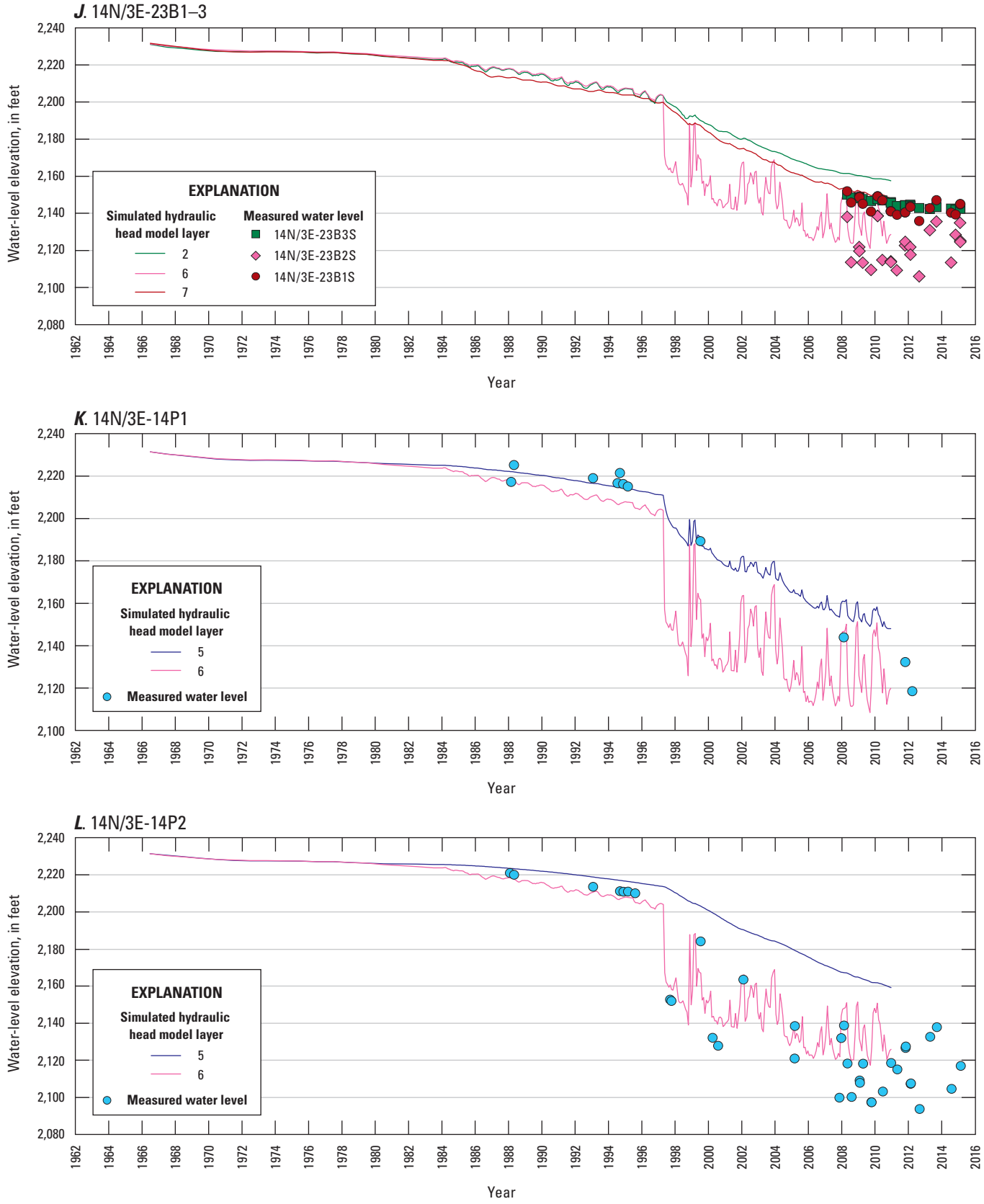

Figure 22. —Continued

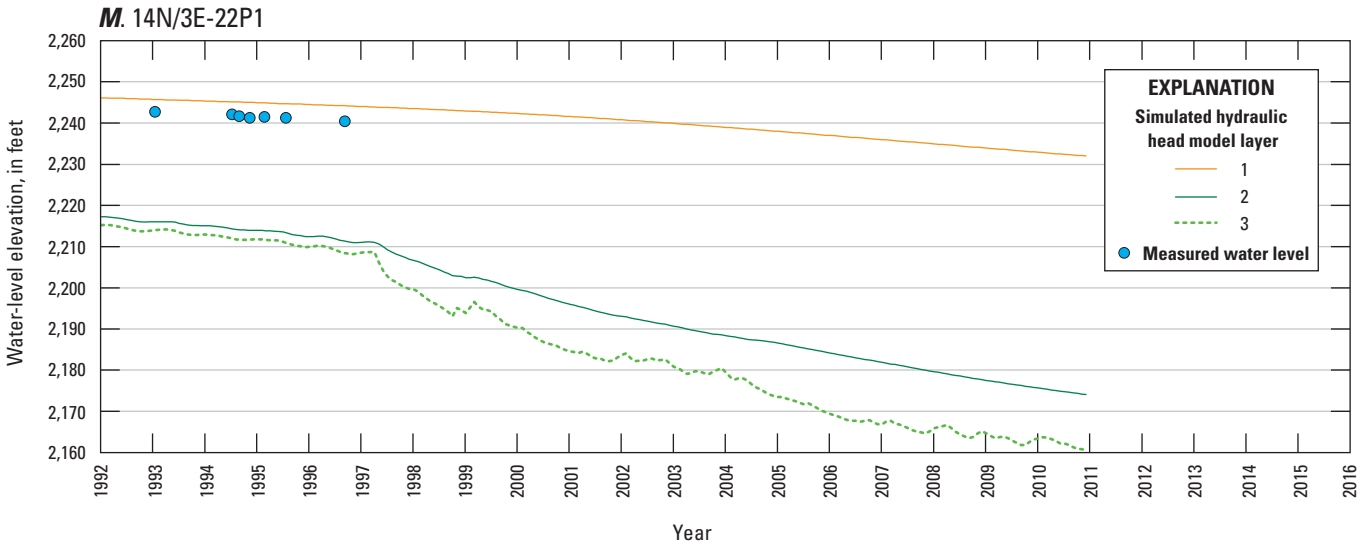

Figure 22. —Continued

Table 13. Summary of average, minimum, and maximum vertical differences in measured water levels and simulated heads, and direction of flow for multiple-well monitoring sites for 1997–2010 in the Bicycle Basin, Fort Irwin National Training Center, California.

[Wells 14N/3E-13M2–4 is in parameter zone 2; 14N/3E-24Q1–5 is in parameter zone 5; and 14N/3E-23B1–3 is in parameter zone 6. See figure 15*A* for location of parameter zones.
Abbreviation: ID, identification]

State well number	Local ID	Model layer intersected by perforated interval of well	Number of data values	Measured				Simulated			
				Average vertical water-level difference (feet)[1,2]	Vertical water-level difference (feet)		Direction of flow	Average vertical head difference (feet)[3]	Vertical head difference (feet)		Direction of flow
					Minimum	Maximum			Minimum	Maximum	
14N/3E-13M4S	BLA2-3	3	22	0.07	–1.6	1.2	Variable	1.6	–0.9	6.5	Variable
14N/3E-13M3S	BLA2-2	5	22	0.07	–1.6	1.2	Variable	1.6	–0.9	6.5	Variable
14N/3E-13M3S	BLA2-2	5	23	8.1	–0.4	22	Variable	–1.5	–32	27	Variable
14N/3E-13M2S	BLA2-1	7	23	8.1	–0.4	22	Variable	–1.5	–32	27	Variable
14N/3E-24Q5S	BLA3-5	3–4	17	0.65	0.3	0.90	Downward	3.1	0.62	5.5	Downward
14N/3E-24Q4S	BLA3-4	6	17	0.65	0.3	0.90	Downward	3.1	0.62	5.5	Downward
14N/3E-24Q4S	BLA3-4	6	17	–1.0	–1.2	–0.60	Upward	3.9	0.25	8.1	Downward
14N/3E-24Q3S	BLA3-3	7	17	–1.0	–1.2	–0.60	Upward	3.9	0.25	8.1	Downward
14N/3E-24Q3S	BLA3-3	7	17	–1.4	–1.9	–0.40	Upward	1.8	–2.8	9	Variable
14N/3E-24Q2S	BLA3-2	8	17	–1.4	–1.9	–0.40	Upward	1.8	–2.8	9	Variable
14N/3E-24Q2S	BLA3-2	8	17	–0.8	–1.7	0.55	Variable	0.0	0.0	0.0	None
14N/3E-24Q1S	BLA3-1	8	17	–0.8	–1.7	0.55	Variable	0.0	0.0	0.0	None
14N/3E-23B3S	BLA4-3	2–3	11	26	9.0	37	Downward	23	7.1	36	Downward
14N/3E-23B2S	BLA4-2	6	11	26	9.0	37	Downward	23	7.1	36	Downward
14N/3E-23B2S	BLA4-2	6	11	–25	–32	–10	Upward	–16	–29	–2.1	Upward
14N/3E-23B1S	BLA4-1	7	11	–25	–32	–10	Upward	–16	–29	–2.1	Upward

[1]The measured vertical water-level differences were calculated from the data given in appendix 2.

[2]The average vertical water-level or head difference is the sum of shallow minus deep divided by the number of data values; a positive value indicates that the shallower value is higher than the deeper value; the converse is true for a negative number.

[3]Simulated heads are calculated at the center of the model cell, which does not necessarily coincide with altitudes of the perforated intervals of the wells.

Model Sensitivity

A sensitivity analysis was performed on the model parameters and stresses to test how robust the parameter values estimated during the calibration process were. The analysis involved keeping all input parameters and tested model stresses constant, except the one being analyzed, and varying that parameter or model stress through a range of values that included the uncertainties in that parameter or stress. Varying a parameter or stress by a small amount causes a large change in the simulation results for a sensitive parameter (more robust); an insensitive parameter causes a small change in the simulation results (less robust). Model sensitivity was evaluated using PEST (Doherty, 2010a).

Calculations presented in this section assume the Bicycle Basin model results varied linearly with changes in parameter value; however, the model sensitivity could be greater because of a non-linear response of the model. For the analysis in this section, all prior information was removed from the objective function. Values for the 144 parameters that were log transformed during calibration with PEST were not transformed for the sensitivity analysis. To determine composite sensitivity values for all observation types, 160 parameters were tested with 834 observations. Multiplying the composite sensitivity by the parameter value provided the relative composite sensitivity (table 14; fig. 23), which allows for comparison of the composite sensitivities of parameters of different magnitudes (Doherty, 2010a). When comparing the sensitivities of different parameter groups, however, consideration should be given to how the adjustment affects the parameter value. For example, adjustment to a sensitive parameter of a specific group can result in an unrealistic value, whereas a similar adjustment to an insensitive parameter of a different group can result in a value that still could be reasonable (Doherty, 2010a; Traum and others, 2014).

Table 14. Parameter names, relative composite sensitivity values, and sensitivity rank in the Bicycle Basin groundwater-flow model, Fort Irwin National Training Center, California.

[Number in recharge parameter name corresponds to recharge zone in figure 15*A*. **Abbreviations**: ft, foot; d, day; ft/day, feet per day, ft²/day, square feet per day; —, not applicable]

Parameter name	Model layer	Parameter zone number	Final parameter value	Relative composite sensitivity	Rank
Horizontal hydraulic conductivity (ft/day)					
hkl1z1	1	1	29	1.07E-01	33
hkl2z1	2	1	20	5.42E-02	48
hkl3z1	3	1	20	2.15E-01	25
hkl4z1	4	1	10	7.90E-02	39
hkl5z1	5	1	8.3	8.02E-02	38
hkl6z1	3	1	0.81	1.15E-01	31
hkl7z1	7	1	0.63	7.42E-02	40
hkl8z1	8	1	0.34	2.30E-01	22
hkl1z2	1	2	1.6	2.42E-01	21
hkl2z2	2	2	2.0	6.07E-02	45
hkl3z2	3	2	6.5	9.14E-02	35
hkl4z2	4	2	4.0	2.12E-02	78
hkl5z2	5	2	14	2.26E-01	23
hkl6z2	3	2	1.7	2.35E-02	75
hkl7z2	7	2	2.8	5.70E-02	46
hkl8z2	8	2	0.78	9.23E-03	92
hkl1z3	1	3	23	5.65E-03	100
hkl2z3	2	3	1.3	7.15E-02	41
hkl3z3	3	3	1.6	3.34E-02	62
hkl4z3	4	3	19	3.55E-03	114
hkl5z3	5	3	3.5	1.15E-02	86

Table 14. Parameter names, relative composite sensitivity values, and sensitivity rank in the Bicycle Basin groundwater-flow model, Fort Irwin National Training Center, California.—Continued

[Number in recharge parameter name corresponds to recharge zone in figure 15*A*. **Abbreviations**: ft, foot; d, day; ft/day, feet per day, ft²/day, square feet per day; —, not applicable]

Parameter name	Model layer	Parameter zone number	Final parameter value	Relative composite sensitivity	Rank
Horizontal hydraulic conductivity (ft/day)—Continued					
hkl6z3	3	3	15	9.99E-03	91
hkl7z3	7	3	5.4	6.48E-02	43
hkl8z3	8	3	5.2	3.85E-03	110
hkl1z4	1	4	7.1	4.36E-01	11
hkl2z4	2	4	30	1.09E-02	87
hkl3z4	3	4	7.0	3.63E-03	113
hkl1z5	1	5	32	1.05E-01	34
hkl2z5	2	5	10	2.50E-02	72
hkl3z5	3	5	9.2	2.05E-02	79
hkl4z5	4	5	1.0	2.72E-01	20
hkl5z5	5	5	3.9	3.97E-02	56
hkl6z5	6	5	8.8	3.11E-01	16
hkl7z5	7	5	0.14	1.03E-02	89
hkl8z5	8	5	0.13	3.49E-02	60
hkl1z6	1	6	3.5	4.16E-01	12
hkl2z6	2	6	18	5.33E-02	49
hkl3z6	3	6	0.92	4.18E-02	54
hkl4z6	4	6	0.06	3.08E-01	17
hkl5z6	5	6	0.04	3.94E-01	14
hkl6z6	6	6	33	5.20E-01	10
hkl7z6	7	6	0.13	2.95E-01	18
hkl8z6	8	6	0.10	3.06E-02	65
hkl1z7	1	7	0.23	3.53E-02	58
hkl2z7	2	7	0.15	1.95E-02	81
hkl3z7	3	7	0.15	7.30E-03	97
Vertical anisotropy ratio (dimensionless)					
vanl1z1	1	1	2,875	8.50E-02	37
vanl2z1	2	1	1,123	2.79E-02	67
vanl3z1	3	1	997	6.36E-02	44
vanl4z1	4	1	27	1.72E-03	136
vanl5z1	5	1	14	1.28E-03	143
vanl6z1	6	1	57	4.23E-02	53
vanl7z1	7	1	1,325	1.74E-02	82
vanl1z2	1	2	1,263	2.26E-01	24
vanl2z2	2	2	122	4.51E-02	50
vanl3z2	3	2	83	1.21E-02	85

Table 14. Parameter names, relative composite sensitivity values, and sensitivity rank in the Bicycle Basin groundwater-flow model, Fort Irwin National Training Center, California.—Continued

[Number in recharge parameter name corresponds to recharge zone in figure 15*A*. **Abbreviations**: ft, foot; d, day; ft/day, feet per day, ft²/day, square feet per day; —, not applicable]

Parameter name	Model layer	Parameter zone number	Final parameter value	Relative composite sensitivity	Rank
Vertical anisotropy ratio (dimensionless)—Continued					
vanl4z2	4	2	2.0	3.66E-03	111
vanl5z2	5	2	548	2.45E-02	74
vanl6z2	6	2	5914	2.47E-02	73
vanl7z2	7	2	3,772	4.17E-03	106
vanl1z3	1	3	6.3	1.73E-03	135
vanl2z3	2	3	39	3.51E-02	59
vanl3z3	3	3	68	3.30E-02	63
vanl4z3	4	3	2.6	1.82E-03	133
vanl5z3	5	3	26	8.41E-03	94
vanl6z3	6	3	11	3.26E-03	119
vanl7z3	7	3	5,770	6.72E-02	42
vanl1z4	1	4	5,255	1.13E-01	32
vanl2z4	2	4	94	3.65E-03	112
vanl3z4	3	4	22	1.69E-03	137
vanl1z5	1	5	64	2.56E-02	71
vanl2z5	2	5	3.9	2.46E-03	129
vanl3z5	3	5	33	7.98E-03	96
vanl4z5	4	5	56	2.77E-01	19
vanl5z5	5	5	2.0	2.52E-03	127
vanl6z5	6	5	57	2.58E-02	70
vanl7z5	7	5	16,592	6.02E-03	98
vanl1z6	1	6	22,255	8.80E-02	36
vanl2z6	2	6	18	3.28E-03	118
vanl3z6	3	6	1,123	1.00E-02	90
vanl4z6	4	6	1,499	1.51E-01	28
vanl5z6	5	6	13,806	1.69E-01	27
vanl6z6	6	6	10,169	3.29E-03	117
vanl7z6	7	6	2,944	1.23E-01	30
vanl1z7	1	7	3,318	4.63E-03	103
vanl2z7	2	7	1,391	2.84E-03	123
vanl3z7	3	7	1,411	2.19E-03	131
Specific yield (dimensionless)					
syl1z1	1	1	0.12	1.35	4
syl1z2	1	2	0.19	2.09E-01	26
syl2z2	2	2	0.19	1.07	5
syl1z3	1	3	0.23	1.39E-01	29

Table 14. Parameter names, relative composite sensitivity values, and sensitivity rank in the Bicycle Basin groundwater-flow model, Fort Irwin National Training Center, California.—Continued

[Number in recharge parameter name corresponds to recharge zone in figure 15*A*. **Abbreviations**: ft, foot; d, day; ft/day, feet per day, ft^2/day, square feet per day; —, not applicable]

Parameter name	Model layer	Parameter zone number	Final parameter value	Relative composite sensitivity	Rank
Specific yield (dimensionless)—Continued					
syl1z4	1	4	0.12	3.75E-01	15
syl1z5	1	5	0.13	1.85	1
syl1z6	1	6	0.10	8.80E-01	7
syl1z7	1	7	1.93E-02	2.68E-02	69
Specific storage (1/ft)					
ssl2z1	2	1	8.99E-07	2.76E-03	124
ssl3z1	3	1	3.21E-05	4.11E-02	55
ssl4z1	4	1	3.56E-06	8.06E-03	95
ssl5z1	5	1	4.23E-05	4.31E-02	52
ssl6z1	3	1	1.28E-05	2.22E-02	76
ssl7z1	7	1	1.33E-05	3.93E-02	57
ssl2z2	2	2	8.65E-07	1.29E-03	142
ssl3z2	3	2	3.86E-06	2.50E-03	128
ssl4z2	4	2	4.06E-06	1.52E-03	138
ssl5z2	5	2	4.95E-05	3.48E-02	61
ssl6z2	3	2	7.72E-06	2.94E-02	66
ssl7z2	7	2	8.55E-07	4.45E-02	51
ssl2z3	2	3	2.53E-06	3.88E-03	109
ssl3z3	3	3	8.07E-07	1.43E-03	141
ssl4z3	4	3	8.99E-07	3.43E-03	116
ssl5z3	5	3	1.59E-06	1.81E-03	134
ssl6z3	3	3	1.27E-06	1.20E-03	144
ssl7z3	7	3	8.43E-07	4.04E-03	108
ssl2z4	2	4	8.71E-07	3.48E-03	115
ssl3z4	3	4	2.07E-06	2.66E-03	125
ssl2z5	2	5	1.97E-06	4.83E-03	102
ssl3z5	3	5	8.58E-07	1.50E-03	139
ssl4z5	4	5	8.95E-07	2.60E-03	126
ssl5z5	5	5	8.66E-07	1.90E-03	132
ssl6z5	3	5	1.71E-06	5.77E-03	99
ssl7z5	7	5	8.28E-07	9.03E-03	93
ssl2z6	2	6	9.78E-06	2.74E-02	68
ssl6z6	6	6	9.65E-07	1.08E-02	88
ssl7z6	7	6	8.99E-07	5.48E-02	47

Table 14. Parameter names, relative composite sensitivity values, and sensitivity rank in the Bicycle Basin groundwater-flow model, Fort Irwin National Training Center, California.—Continued

[Number in recharge parameter name corresponds to recharge zone in figure 15*A*. **Abbreviations**: ft, foot; d, day; ft/day, feet per day, ft²/day, square feet per day; —, not applicable]

Parameter name	Model layer	Parameter zone number	Final parameter value	Relative composite sensitivity	Rank
Specific storage (1/ft)—Continued					
ssl2z7	2	7	3.87E-06	4.06E-03	107
ssl3z7	3	7	1.34E-06	3.03E-03	121
Delayed inelastic skeletal specific storage (1/ft)					
sskv2	2	6	1.58E-04	1.84	2
sskv6	6	6	8.55E-05	1.66	3
sskv7	7	6	8.46E-05	6.99E-01	9
Instantaneous inelastic skeletal specific storage (1/ft)					
skv3	3	6	5.38E-05	8.42E-01	8
skv4	4	6	6.71E-05	9.70E-01	6
skv5	5	6	5.44E-05	4.12E-01	13
Delayed elastic skeletal specific storage (1/ft)					
sske2	2	6	1.08E-05	2.37E-03	130
sske6	6	6	8.00E-06	2.15E-02	77
sske7	7	6	8.46E-06	3.15E-03	120
Instantaneous inelastic skeletal specific storage (1/ft)					
ske3	3	6	7.58E-06	4.30E-03	105
ske4	4	6	4.14E-06	6.22E-04	147
ske5	5	6	3.27E-06	1.44E-03	140
Recharge (ft/day)					
rech1	1	—	9.25E-04	6.57E-05	149
rech2	1	—	2.99E-03	9.84E-04	145
rech3	1	—	1.81E-05	1.89E-08	154
rech4	1	—	4.62E-06	2.69E-09	156
rech5	1	—	2.70E-05	6.97E-08	152
rech6	1	—	4.11E-06	2.38E-09	157
rech7	1	—	3.09E-06	4.75E-09	155
rech8	1	—	9.10E-06	1.43E-09	159
rech9	1	—	4.85E-05	6.63E-08	153
rech10	1	—	9.31E-05	1.79E-07	150
rech11	1	—	3.42E-06	1.23E-09	160
rech12	1	—	3.42E-05	8.53E-08	151
rech13	1	—	3.76E-06	2.18E-09	158
Drain conductance (ft²/day)					
drncond	1	—	4,335	3.10E-02	64
Hydraulic characteristic (1/d)					
coyotecl1	1	—	9.50E-03	2.92E-03	122
coyotecl28	2–8	—	2.58E-07	1.40E-02	83
unnamedl1	1	—	1.15	5.35E-03	101
unnamedl2	2	—	9.75E-03	2.02E-02	80
unnamedl3	3	—	5.02E-03	4.36E-03	105

Table 14. Parameter names, relative composite sensitivity values, and sensitivity rank in the Bicycle Basin groundwater-flow model, Fort Irwin National Training Center, California.—Continued

[Number in recharge parameter name corresponds to recharge zone in figure 15*A*. **Abbreviations**: ft, foot; d, day; ft/day, feet per day, ft²/day, square feet per day; —, not applicable]

Parameter name	Model layer	Parameter zone number	Final parameter value	Relative composite sensitivity	Rank
Hydraulic characteristic (1/d)—Continued					
unnamedl1_1	1	—	0.39	1.22E-02	84
unnamedl2_1	2	—	4.41E-01	2.17E-04	148
unnamedl3_1	3	—	0.87	7.21E-04	146

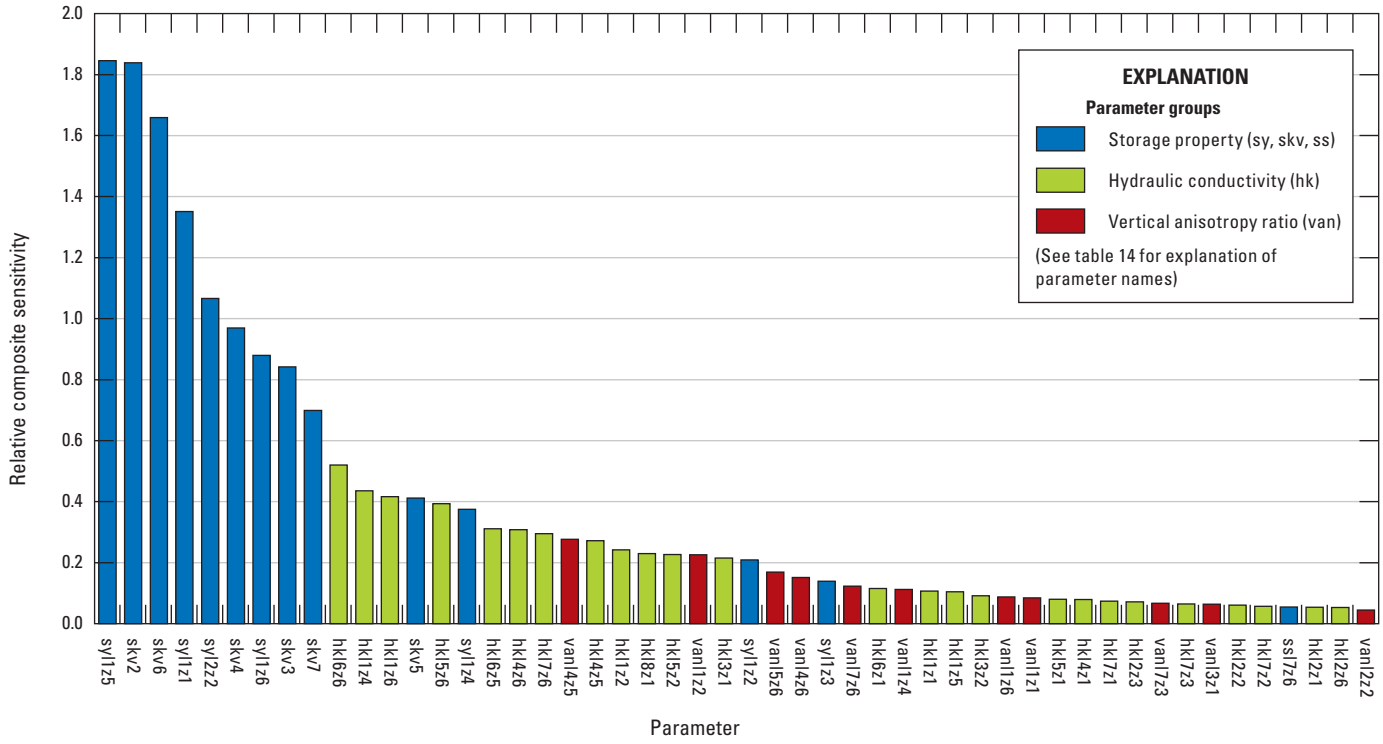

Figure 23. Relative composite sensitivities for the 50 most sensitive parameters for the Bicycle Basin groundwater-flow model, Fort Irwin National Training Center, California.

Figure 23 shows the relative composite sensitivities by parameter group for the most sensitive 50 of the 160 parameters included in the sensitivity analysis, in order of highest to lowest sensitivity. The parameters in table 14 were grouped by hydraulic conductivity, vertical anisotropy, storage properties (specific yield, specific storage, and elastic and inelastic skeletal storage properties), recharge, drain conductance, and hydraulic characteristic of horizontal flow barriers (faults). The parameter names and descriptions also are given in table 14. The parameters within the groups shown in figure 23 include members of five of the groups used in the table: specific yield, specific storage, inelastic skeletal storage, hydraulic conductivity, and vertical anisotropy. Results of the sensitivity analysis indicated the model was most sensitive to storage properties, including specific yield (syl1z5, syl1z1, and sy2z2) and inelastic skeletal storage properties (skv2, skv6, skv4, skv3, and skv7). The next most sensitive parameters included hydraulic conductivity, other storage properties, and vertical anisotropy ratios (table 14; fig. 23). The model was least sensitive to the recharge rates for model cells in the recharge zones, the elastic storage coefficient for model layer 4, and the hydraulic characteristic for the unnamed fault 2 in model layers 2 and 3 (ske4, unnamedl2_1 and unnamedl3_1, respectively, table 14).

Model Results

The Bicycle Basin model was used to simulate distributions of drawdown in all model layers (drawdown in layers 1 and 6 are shown in fig. 24) at the end of the simulation period, the distribution of subsidence (fig. 25), and components of the groundwater budget (table 15). Model layer 1 was chosen to represent the water table, and model layer 6 was chosen to represent the layer with most of the pumpage. Simulated drawdown is the difference between simulated heads at the end of the steady-state period (before 1967) and simulated heads at the end of the transient period (December 2010). Subsidence is the sum of the compaction at the end of the simulation period in each model layer containing fine-grained interbeds (layers 2–7) in parameter zone 6. The simulated groundwater budget is presented for the steady-state, before 1967, and transient simulation periods, 1967–2010.

Simulated Drawdown

The distributions of drawdown in all model layers generally were similar with the larger amount of drawdown north of the South Coyote Canyon fault and smaller amount of drawdown south of the fault. Simulated drawdown in model layer 1 in the Bicycle Basin ranged from no drawdown or increased hydraulic head in the western part of the basin, primarily in zone 7, to more than 100 ft in parameter zone 2 (fig. 24*A*). The absence of drawdown in the western part of the basin (parameter zone 7) was because the recharge rate in recharge zone 1 (fig. 15*A*) was comparatively high and there were no production wells in that part of the basin. Total groundwater pumpage of about 47,000 acre-ft from 1967 through 2010 (table 15) resulted in drawdown of as much as 189 ft in model layer 6 (fig. 24*B*). Simulated drawdown in this model layer ranged from 65 ft in parameter zone 5 to more than 110 ft in the area around production wells 14N/3E-14P1 in parameter zone 6 and in parameter zone 2 (fig. 24*B*). This drawdown resulted in water-quality changes in nearby well 14N/3E-23B2 that are described in the "General Water-Quality Characteristics and Areal Variation" section. Groundwater pumpage from production well 14N/4E-18N1 resulted in simulated drawdown of more than 100 ft in a pumping depression around this well (fig. 24*B*). The drawdowns in model layer 6 were larger than in model layer 1 because model layer 6 intersects the perforations of the five production wells, whereas model layer 1 intersects the perforations of only one production well. Pumping in this well was discontinued in October 1986, allowing the water table to recover to some extent. Drawdown in order of layers 2–5 and 7–8 ranged from 49 to 181 ft, 51 to 181 ft, 59 to 181 ft, 62 to 181 ft, 74 to 192 ft, and 74 to 189 ft, respectively.

Simulated Subsidence

The areal distribution of total simulated subsidence at the end of the simulation period showed that subsidence was greatest in the center of parameter zone 6 and generally decreased toward the parameter-zone boundary (fig. 25). Simulated subsidence in a wedge-shaped area in the vicinity of point 1 and well 14N/3E-23G1 was less than the surrounding areas (fig. 25) because the thickness of the fine-grained interbeds was reduced or omitted in that area of the model, as discussed in the "Elastic and Inelastic Storage" section.

Water Budgets

Groundwater budgets for the steady-state and transient stress periods are given in table 15. The monthly variation and cumulative volumes of selected budget components are shown in figure 26. Between January 1967 and December 2010, about 5,100 acre-ft of water was recharged in the Bicycle Basin, and about 47,000 acre-ft of groundwater was pumped from the basin (table 15; fig. 26*A*, *B*, respectively), resulting in declining water levels throughout the basin (fig. 22) and subsidence in parameter zone 6 (fig. 21*B*). Simulated outflow from the Bicycle Basin, simulated as a drain, decreased from 1967 to 1999 (table 15; fig. 26*C*). Total groundwater-storage depletion (total inflows minus total outflows) was about 42,100 acre-ft (table 15), indicating that about 91 percent of pumpage was from depletion of groundwater storage, about 4.7 percent from reduced outflow from the basin, and about 2.3 percent from net instantaneous and delayed compaction of interbeds (total compaction inflow minus total compaction outflow). Net pumpage (pumpage minus well loss) was used to calculate the percentages. These percentages do not sum to 100 percent because of rounding of numbers. A trend of declining monthly pumpage between August 2005 and June 2007 (fig. 26*B*) reduced the rate of decline in groundwater storage during that period (fig. 26*F*).

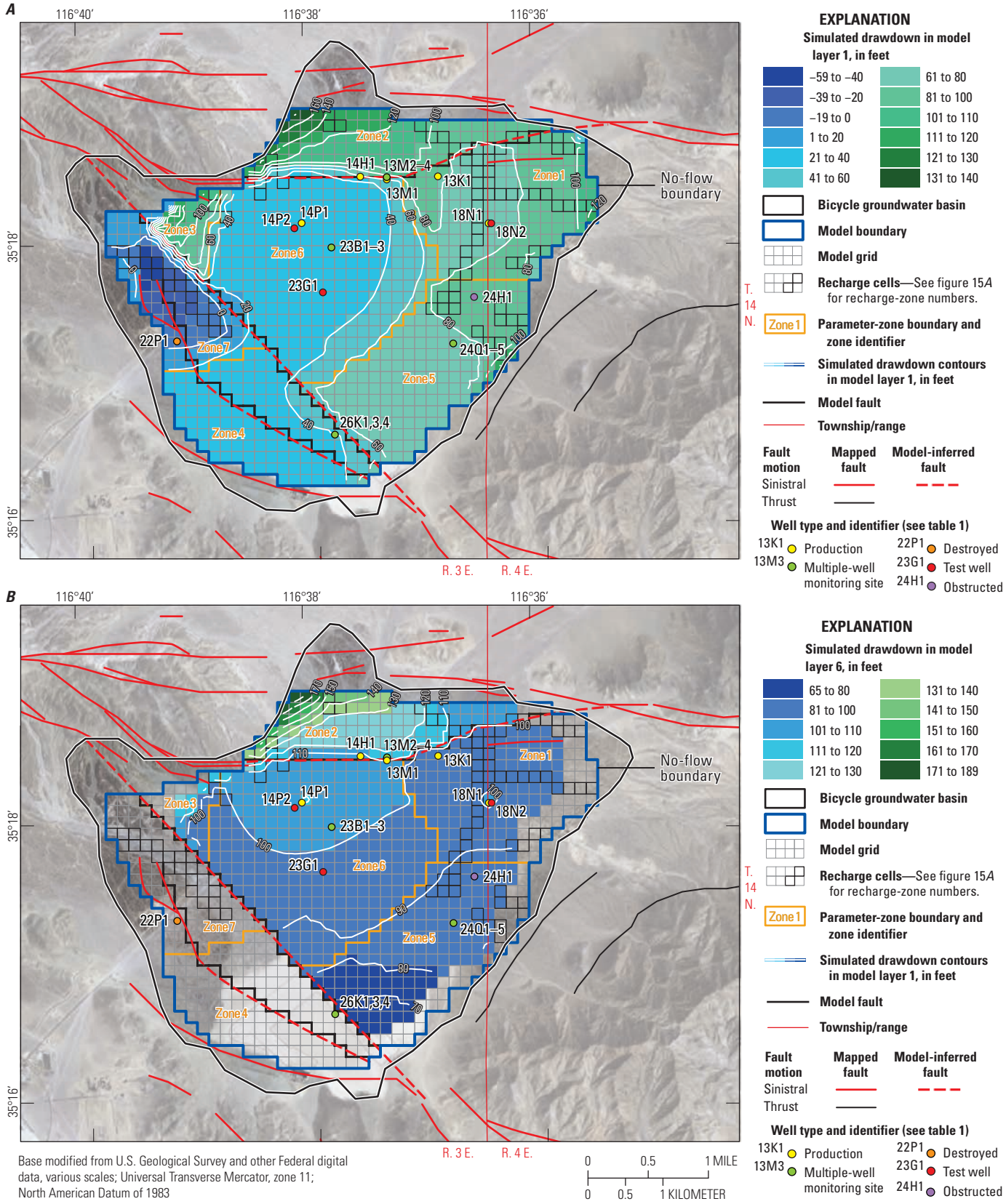

Figure 24. Simulated drawdown from the end of the predevelopment period (before 1967) to the end of the simulation period in December 2010 for the groundwater-flow model of the Bicycle Basin, Fort Irwin National Training Center, California, for *A*, model layer 1 and *B*, model layer 6.

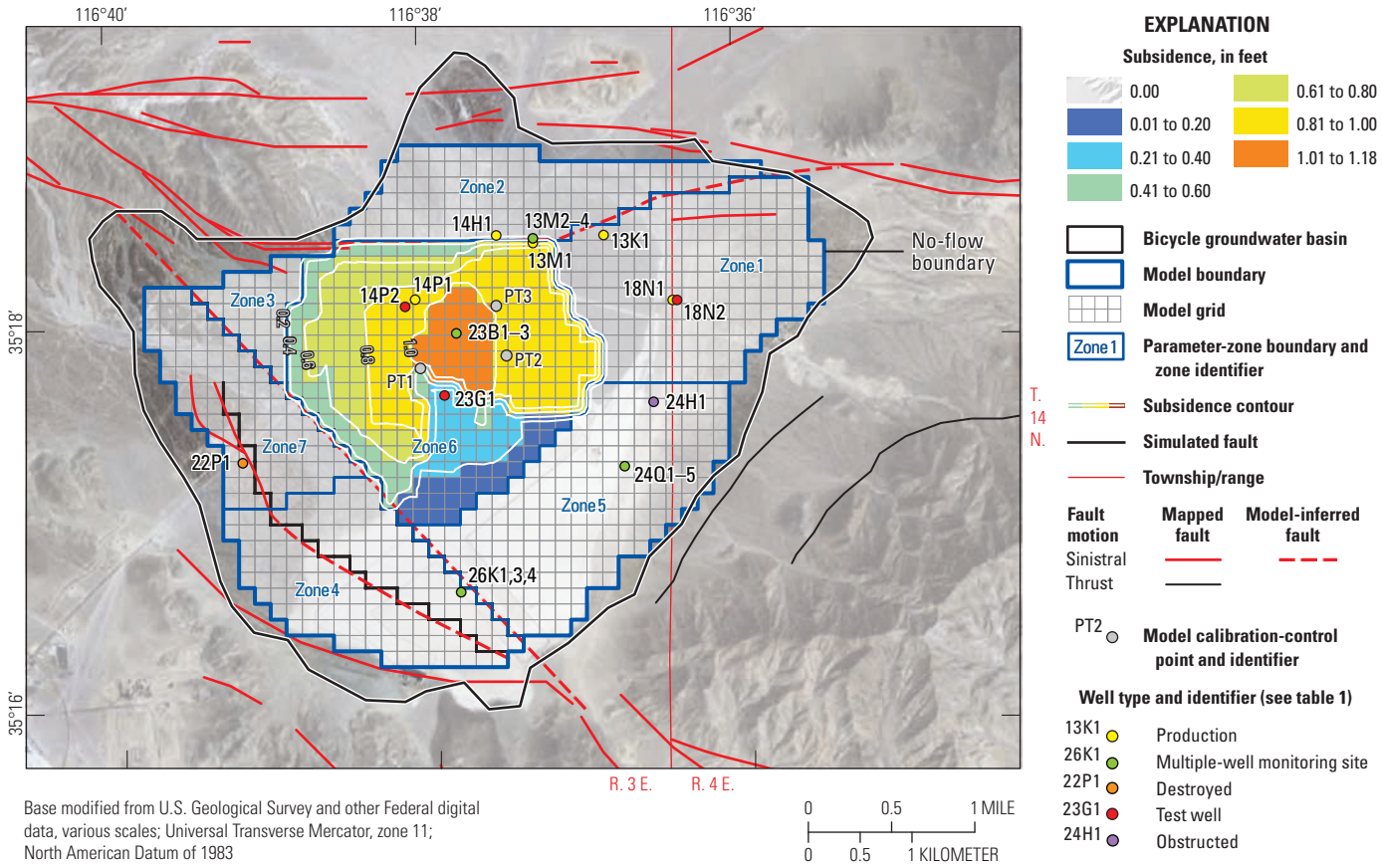

Figure 25. Simulated subsidence at the end of the simulation period in December 2010 for the Bicycle Basin groundwater-flow model, Fort Irwin National Training Center, California.

Table 15. Simulated predevelopment and transient (1967–2010) groundwater budgets for the Bicycle Basin groundwater-flow model, Fort Irwin National Training Center, California.

[Units are in acre-feet]

Year	Recharge	Well loss	Inflows			Outflows					Total inflows minus total outflows
			No-delay interbed storage	Delay interbed storage	Total inflows	Drains	Pumpage	No-delay interbed storage	Delay interbed storage	Total outflows	
Steady state	116	0	0	0	116	116	0	0	0	116	0
1967	116	1.1	0.51	1.1	119	116	823	0	0	939	–820
1968	116	1.2	0.29	0.87	118	114	821	0	0	935	–816
1969	116	1.5	0.41	1.0	119	111	955	0	0	1,066	–947
1970	116	1.5	0.36	0.83	119	107	897	7.4E–06	0	1,004	–886
1971	116	1.2	0.13	0.42	118	104	609	0.02	0.02	713	–595
1972	116	1.0	0.11	0.30	117	101	481	7.1E–03	6.1E–03	581	–464
1973	116	2.0	0.01	0.04	118	98	159	0.08	0.15	257	–139
1974	116	0.5	0.04	0.07	117	96	171	2.2E–04	0.04	266	–150
1975	116	0.5	0.06	0.12	117	94	210	0	4.2E–03	305	–188
1976	116	0.7	0.17	0.37	117	93	394	0	0	487	–370
1977	116	1.4	0.01	0.05	117	92	124	0.06	0.10	216	–99
1978	116	0.8	0.41	0.53	118	91	494	0	0	584	–467
1979	116	0.8	0.49	0.39	118	89	462	1.4E–05	0	552	–434
1980	116	1.4	2.1	0.94	120	88	867	0	0	955	–834
1981	116	1.3	1.7	0.70	120	85	794	8.7E–05	0	878	–759
1982	116	1.3	1.9	0.63	120	82	759	0	0	841	–721
1983	116	1.5	2.5	0.77	121	79	867	0	0	946	–825
1984	116	16	4.4	1.6	138	76	706	0.12	0.20	782	–644
1985	116	3.9	6.8	2.7	129	72	1,247	0.06	0.10	1,318	–1,189
1986	116	23	7.9	3.5	150	66	1,352	0.36	0.69	1,418	–1,268
1987	116	56	3.6	1.5	177	59	878	0.21	0.52	938	–761
1988	116	37	5.9	2.3	162	52	1,070	0.21	0.43	1,123	–961
1989	116	22	5.3	2.3	146	46	852	0.19	0.32	899	–753
1990	116	8.4	8.8	5.5	139	41	1,319	0.12	0.13	1,360	–1,221
1991	116	11	8.9	8.8	145	34	1,391	0.46	0.35	1,426	–1,281
1992	116	21	8.1	11	156	27	1,158	0.45	0.16	1,186	–1,030
1993	116	17	5.8	7.7	147	21	774	0.50	0.30	796	–649
1994	116	20	7.5	12	156	15	979	0.35	0.01	995	–839

Table 15. Simulated predevelopment and transient (1967–2010) groundwater budgets for the Bicycle Basin groundwater-flow model, Fort Irwin National Training Center, California.—Continued

[Units are in acre-feet]

Year	Recharge	Well loss	Inflows			Outflows					Total inflows minus total outflows
			No-delay interbed storage	Delay interbed storage	Total inflows	Drains	Pumpage	No-delay interbed storage	Delay interbed storage	Total outflows	
1995	116	14	9.2	16	155	10	1,061	0.17	0.02	1,072	–917
1996	116	25	11	22	175	7.3	1,247	1.0	0.12	1,256	–1,081
1997	116	36	18	83	252	4.5	1,560	0.25	0.12	1,564	–1,312
1998	116	57	27	82	281	1.7	2,195	0.62	4.7	2,202	–1,920
1999	116	54	18	40	227	0	1,867	0.54	5.7	1,874	–1,647
2000	116	74	23	57	270	0	1,981	0.11	0.4	1,982	–1,711
2001	116	51	20	42	229	0	1,947	0.22	4.8	1,952	–1,723
2002	116	54	17	37	224	0	2,033	0.35	4.9	2,038	–1,814
2003	116	25	18	41	201	0	1,967	0.30	6.3	1,974	–1,773
2004	116	15	21	57	209	0	1,953	0.08	1.8	1,955	–1,746
2005	116	8.8	20	48	192	0	1,546	0.10	1.7	1,548	–1,356
2006	116	18	18	43	195	0	1,288	0.14	2.0	1,291	–1,095
2007	116	30	15	36	197	0	1,390	0.27	5.9	1,396	–1,199
2008	116	24	11	31	182	0	893	0.45	7.1	900	–718
2009	116	28	12	33	189	0	1,208	0.30	6.4	1,214	–1,026
2010	116	22	9.8	26	174	0	1,112	0.12	2.0	1,114	–940
1967–2010 Total	5,104	791	353	761	7,008	2,172	[1]46,857	8.2	58	49,095	–42,087

[1]Net pumpage (pumpage minus well loss) differs from the value in table 3 because of rounding of numbers.

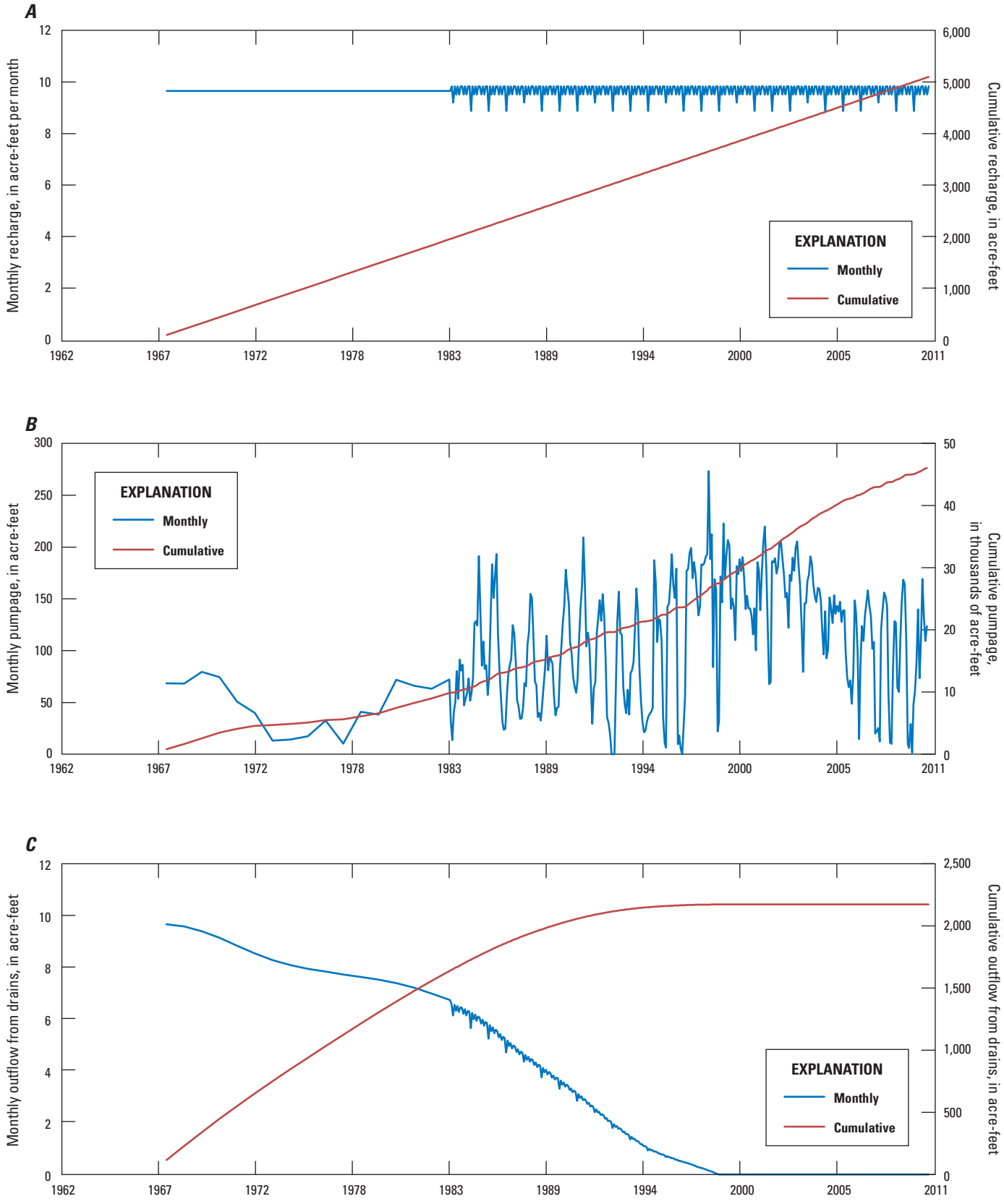

Figure 26. Simulated ground-water budget components for the Bicycle Basin groundwater-flow model, Fort Irwin National Training Center, California: *A*, recharge; *B*, pumpage; *C*, outflow from drains; and changes in *D*, net delayed interbed storage; *E*, net instantaneous interbed storage; and *F*, groundwater storage.

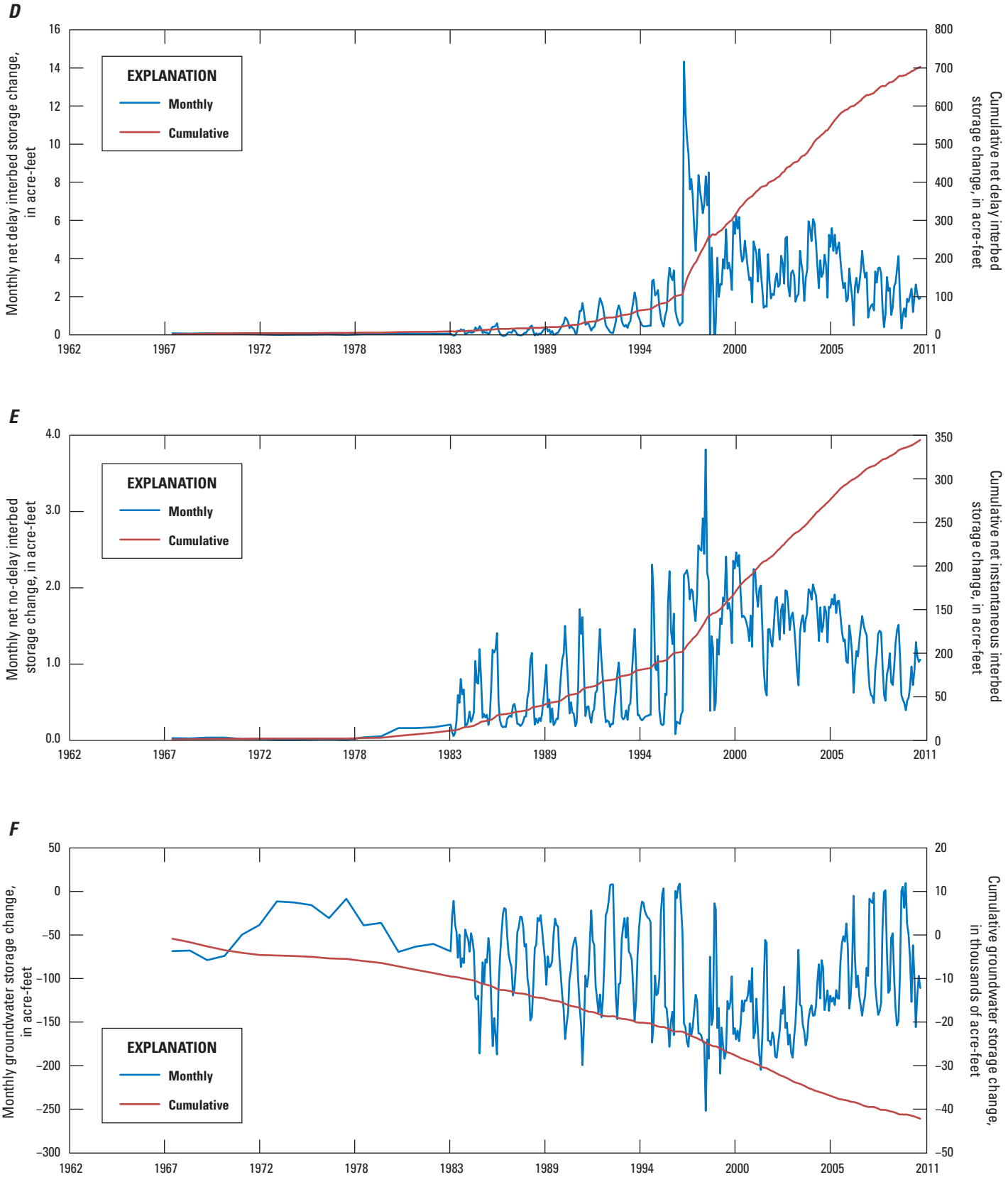

Figure 26. —Continued

Model Limitations

The use of numerical models to simulate hydrologic systems has inherent limitations. Limitations of the modeling software, data, assumptions made during model development, conceptual model error (Bredehoeft, 2005), and model calibration and sensitivity analysis are all factors that constrain the appropriate use of hydrologic models, including the Bicycle Basin model. Differences between simulated and actual hydrologic conditions arise from a number of sources and are known collectively as model error (Walter and Whealan, 2005).

The accuracy and reliability of model results are related to the quality and distribution of available data. In the Bicycle Basin model, uncertainties primarily resulted from limited available spatial and temporal data to characterize aquifers and calibrate for water-level variations and subsidence. For example, hydraulic properties (hydraulic conductivity, vertical anisotropy, specific yield, and specific storage) were estimated and applied over groups of many cells (parameter zones) because of the limited areal distribution of wells with detailed lithologic or borehole geophysical data. Detailed data on the extent, thickness, and hydraulic properties of the fine-grained interbeds needed to simulate subsidence accurately also were limited for the basin. A more complete distribution of multi-completion well sites with detailed lithology and borehole geophysical data would improve the aquifer characterization and the accuracy of simulating water levels as well as subsidence.

Other limitations and assumptions that can contribute to uncertainty in the model include the following:

- Average recharge values were used throughout the simulation period because it was assumed the thick unsaturated zone smoothed the temporal variations in infiltration to long-term-average deep-percolation rates.
- The quantity and distribution of pumpage for 1967–90 were estimated from limited measured pumpage data for that period.
- Recharge and runoff estimated from the BCM, which also has assumptions and limitations, adequately simulated the actual recharge and runoff to the basin.
- The sum of 10 percent of runoff draining into Bicycle Lake Basin and 100 percent of recharge in surrounding watersheds (moving in the subsurface to the study area) estimated by the BCM was a reasonable representation of the quantity of recharge in the basin.
- Vertical changes in land surface estimated from InSAR accurately represented subsidence in the Bicycle Basin.
- InSAR interferogram interpretations to determine land-surface deformation observations used for model calibration were reasonable.

The Bicycle Basin model synthesized the current data and understanding of the Bicycle Basin. The overall fit of the model to measured data (water levels and subsidence) was reasonable. The purpose for developing the Bicycle Basin groundwater-flow model was to provide a tool to help evaluate water-management strategies. When applied carefully, the groundwater-flow model of the Bicycle Basin can be used for simulating groundwater response to changes in stress to the groundwater-flow system. Uncertainty increases as simulated future stresses differ from historical stresses used in model calibration. Water-level and subsidence monitoring during any future management activities allow for recalibration of the model under different stress regimes. The model is most suited for comparison among scenarios rather than for accurately indicating the magnitude of future changes in water levels or subsidence.

Simulated Effects of Runoff Capture and Future Pumpage

The Bicycle Basin groundwater-flow model was used to evaluate changes in groundwater levels and subsidence under five water-management scenarios (table 16). These included capture of runoff into recharge basins (scenario 1) and various amounts and distributions of future pumpage (scenarios 2–5). The simulation period for the runoff-capture scenario was the same as the calibration period (predevelopment through 2010). The pumpage scenarios were extended 50 years from 2011 to 2060 (table 16). To evaluate 2010 pumpage and establish a base case, scenario 2 assumed that 2010 pumping rates continued in the same pumped wells. Pumpage was reduced to zero in well 14N/3E-14P1, and 2010 pumpage continued in the two production wells that were not in the area of subsidence (scenario 5). To evaluate the effect of pumpage changes in the area of subsidence, 2010 pumpage was reduced by 25 percent in well 14N/3E-14P1 and redistributed to the two production wells that were not in the area of subsidence (scenario 3). To evaluate reduced pumpage basin wide, scenario 4 was the same as scenario 3, with an additive reduction in basin-wide pumpage by 3 percent each year through 2020; the resulting 2020 pumpage was used through 2060.

Table 16. Runoff-capture and pumping-management scenarios, 2010–60, for the Bicycle Basin groundwater-flow model, Fort Irwin National Training Center, California.

Scenario	Simulation period	Description
1	predevelopment –2010	Capture of runoff was simulated by adding runoff calculated by the Basin Characterization Model (BCM) that was not included as recharge in the model to specified cells within stream channels.
2	2011–60	Pumpage for active wells in 2010 was repeated for each monthly stress period from 2011 through 2060.
3	2011–60	Pumpage in well 14N/3E-14P1 was reduced by 25 percent with the pumpage distributed to production wells 14N/3E-13M1 and 14N/4E-18N1 according to the percentage of total pumpage for both wells for each month; the adjusted monthly pumpage was repeated for each stress period from 2011 through 2060.
4	2011–60	Same as scenario 3, with the added constraint of the cumulative reduction of annual basin pumpage by 3 percent per year for 2011–20; the resulting pumpage was repeated from 2021 through 2060.
5	2011–60	Same as scenario 2, except pumpage in well 14N/3E-14P1 was reduced to zero.

Scenario 1: Simulated Effects of Captured Runoff

The Bicycle Basin groundwater-flow model was used to evaluate changes in groundwater-level altitudes and subsidence with the addition of runoff capture (scenario 1) not accounted for in the groundwater-flow model. For the groundwater-flow model without runoff capture, it was assumed that 10 percent of the runoff calculated by the BCM contributed to recharge of the groundwater-flow system; the remaining 90 percent was assumed to flow to the Bicycle Lake (dry) playa and evaporate. For scenario 1, the 90 percent of runoff was assumed to be captured for managed aquifer recharge using various approaches, such as diversion to retention basins. Recharge rates for the captured runoff were assigned to one model cell in each recharge zone representing recharge in retention basins in recharge zones 3–11 for the months with runoff. Captured runoff in recharge zones 1 and 2 was distributed to two cells in each zone (fig. 27*A*). Table 17 shows the dates of runoff, the amounts of total runoff, runoff available for capture, and runoff used for capture in the model according to recharge zone in scenario 1. It was assumed that all of the available runoff could be captured for recharge during the simulation period (zero runoff flowing to the playa), except in 2010. Total runoff (the infiltrated runoff and the runoff that flowed to the playa) calculated by the BCM for 2010 was about 59,300 acre-ft; in comparison, the total runoff calculated for 1967–2009 was about 1,480 acre-ft. Given the anomalous runoff for 2010, it was assumed that all of the available runoff for 2010 could be captured only in March, April, October, and November in the recharge zones with runoff (table 17). In addition, it was assumed that all of the available runoff could be captured in recharge zones 4–11 in January and recharge zones 4–9 in February. Available runoff in January, February, and December for recharge zones 1, 2, and 3 and available runoff in December for recharge zones 4–11 was reduced to avoid simulation of unreasonable water levels. In recharge zone 1, where the water-bearing units are thinner and the hydraulic conductivity comparatively low, it was assumed that 0.5 percent of the available runoff could be captured in January and December, and 1 percent in February. In recharge zone 2, which had the largest quantity of runoff, and recharge zone 3, it was assumed that 10 percent of the available runoff could be captured during January, February, and December. In recharge zones 4–11, it was assumed 10 percent of the available December runoff could be captured. The 2010 runoff for recharge zones 1, 2, and 3 in January, February, and December not captured for managed aquifer recharge was assumed to flow to the playa. Although the model was insensitive to changes in recharge (table 14), the runoff for 2010 was more than the long-term average runoff, and all the recharge in Scenario 1 was focused in one or two cells, resulting in a substantial rise in water levels in the vicinity of focused recharge. These runoff-capture assumptions may be idealized and not easily implemented because runoff is highly episodic over long periods; retention basins could be difficult to maintain over these time spans.

Results for scenario 1 are presented as total values of groundwater-budget components in table 18 and as simulated drawdown maps for layers 1 and 6 in figure 27*A*–*D*. The small differences in well losses and pumping can be attributed to numerical computations associated with the multi-node wells. To prevent cells from going dry, pumping was reduced. For the simulation with runoff capture, water levels were higher than without runoff capture, so pumpage was not reduced and well losses increased. A positive value of drawdown indicated simulated heads declined from predevelopment to 2010; a negative value indicated simulated heads increased for the same period. The difference in simulated drawdown (fig. 27*C*, *D*) was calculated by subtracting the values for scenario 1 from the values for the model without runoff capture. The simulated subsidence from 1993 through 2010 with runoff capture and the difference between subsidence for scenario 1 and the model without runoff capture are presented in figures 28*A* and *B*, respectively.

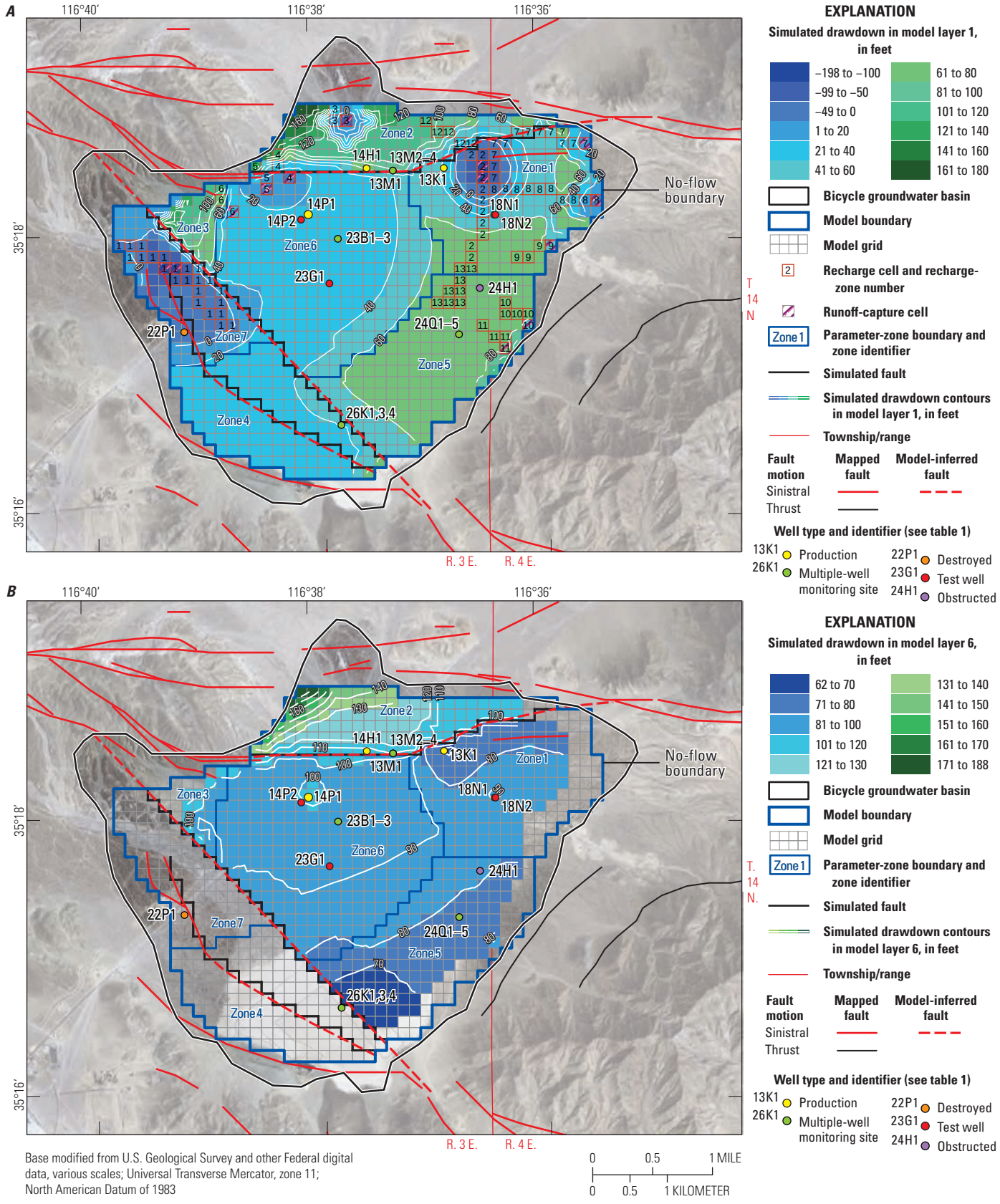

Figure 27. Location of runoff-capture cells for scenario 1 using the Bicycle Basin groundwater-flow model, Fort Irwin National Training Center, California, and *A*, simulated drawdown with runoff capture in December 2010 for model layer 1 and *B*, for model layer 6, and *C*, the difference between simulated drawdown with and without runoff capture for layer 1 and *D*, layer 6.

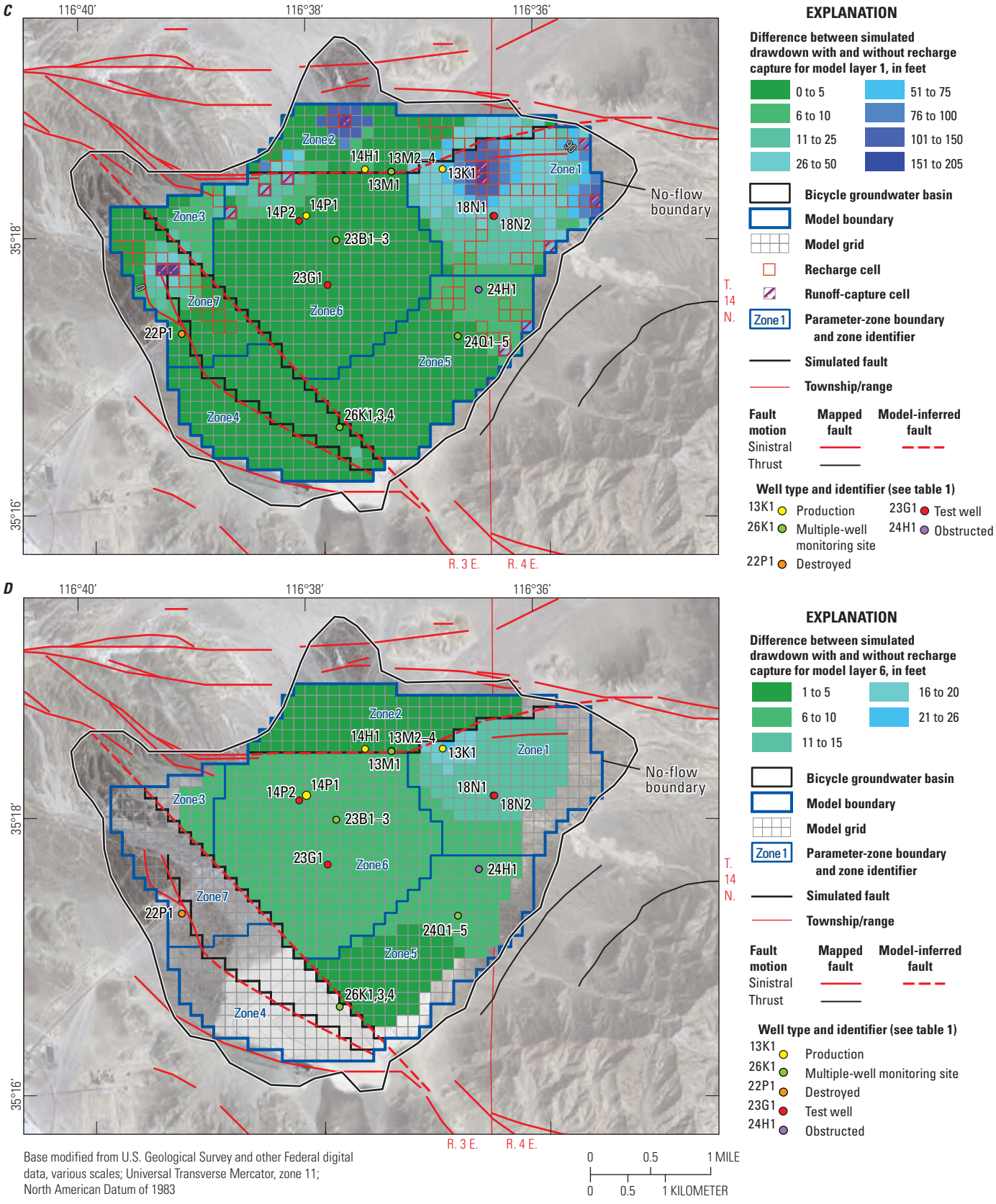

Figure 27. —Continued

Table 17*A*. Estimated total runoff for scenario 1 by the Bicycle Basin groundwater-flow model, Fort Irwin National Training Center, California.

[See figure 27*A* for location of recharge zones. Total runoff is in cubic feet.]

Recharge zone	December 1984	February 1992	January 1993	February 1993	January 1995	February 1998	January 2010	February 2010	March 2010	April 2010	October 2010	November 2010	December 2010
1	1,829	0	92,320	24,867,921	0	0	232,497,534	111,094,662	6,951	169,063	87,145	60,396	424,430,487
2	0	52,700	2,264,451	26,722,792	20,235	0	512,304,361	213,942,272	0	6,192,452	0	0	909,684,767
3	0	0	0	573,380	0	0	23,522,987	10,544,208	0	0	0	0	43,570,944
4	0	0	0	37,098	0	0	2,401,978	1,153,117	0	0	0	0	4,729,451
5	0	0	0	430,422	0	0	2,734,209	1,278,878	0	0	0	0	5,358,361
6	0	0	0	162,705	0	0	2,138,046	955,452	0	0	0	0	4,474,659
7	0	0	0	0	0	0	2,790,666	213,601	0	0	0	0	9,367,200
8	0	0	783,685	2,100,975	81,711	80,090	4,128,139	761,571	0	33,107	0	0	16,221,079
9	0	0	717,446	1,865,797	73,140	73,963	4,046,040	894,463	0	82,253	0	0	13,270,463
10	0	0	425,453	1,408,812	7,490	27,906	1,396,067	0	0	0	0	0	8,628,002
11	0	0	356,947	1,428,736	1,105	4,224	799,672	0	0	0	0	0	6,791,396

Table 17*B*. Estimated runoff available for capture for scenario 1 by the Bicycle Basin groundwater-flow model, Fort Irwin National Training Center, California.

[See figure 27*A* for location of recharge zones. Available runoff in this table is 90 percent of total runoff in table 17*A*. Runoff available for capture in cubic feet.]

Recharge zone	December 1984	February 1992	January 1993	February 1993	January 1995	February 1998	January 2010	February 2010	March 2010	April 2010	October 2010	November 2010	December 2010
1	1,646	0	83,088	22,381,129	0	0	209,247,780	99,985,196	6,256	152,157	78,430	54,357	381,987,439
2	0	47,430	2,038,006	24,050,513	587	0	461,073,925	192,548,045	0	5,573,206	0	0	818,716,290
3	0	0	0	516,042	0	0	21,170,688	9,489,787	0	0	0	0	39,213,850
4	0	0	0	33,388	0	0	2,161,780	1,037,805	0	0	0	0	4,256,506
5	0	0	0	387,380	0	0	2,460,788	1,150,990	0	0	0	0	4,822,525
6	0	0	0	146,435	0	0	1,924,241	859,907	0	0	0	0	4,027,193
7	0	0	0	0	0	0	2,511,600	192,241	0	0	0	0	8,430,480
8	0	0	705,317	1,890,878	73,540	72,081	3,715,325	685,414	0	29,797	0	0	14,598,971
9	0	0	645,701	1,679,218	65,826	66,567	3,641,436	805,017	0	74,028	0	0	11,943,416
10	0	0	382,908	1,267,930	6,741	25,115	1,256,460	0	0	0	0	0	7,765,201
11	0	0	321,252	1,285,862	995	3,801	719,705	0	0	0	0	0	6,112,257

Table 17*C*. Estimated actual runoff rate applied to the runoff-capture model cells for scenario 1 by the Bicycle Basin groundwater-flow model, Fort Irwin National Training Center, California.

[See figure 27*A* for location of recharge zones. Runoff values in this table (in cubic feet) are divided by the number of days in the month and the area of the model cell (250,000 square feet) to obtain the recharge rate for model input in feet per day.]

Recharge zone	December 1984	February 1992	January 1993	February 1993	January 1995	February 1998	January 2010	February 2010	March 2010	April 2010	October 2010	November 2010	December 2010
1	1,646	0	83,088	22,381,129	0	0	[1]1,046,239	[2]999,852	6,256	152,157	78,430	54,357	[1]1,909,937
2	0	47,430	2,038,006	24,050,513	587	0	[3]46,107,392	[3]19,254,804	0	5,573,206	0	0	[3]81,871,628
3	0	0	0	516,042	0	0	[3]2,117,069	[3]948,979	0	0	0	0	[3]3,921,385
4	0	0	0	33,388	0	0	2,161,780	1,037,805	0	0	0	0	[3]425,651
5	0	0	0	387,380	0	0	2,460,788	1,150,990	0	0	0	0	[3]482,252
6	0	0	0	146,435	0	0	1,924,241	859,907	0	0	0	0	[3]402,719
7	0	0	0	0	0	0	2,511,600	192,241	0	0	0	0	[3]843,048
8	0	0	705,317	1,890,878	73,540	72,081	3,715,325	685,414	0	29,797	0	0	[3]1,459,897
9	0	0	645,701	1,679,218	65,826	66,567	3,641,436	805,017	0	74,028	0	0	[3]1,194,342
10	0	0	382,908	1,267,930	6,741	25,115	1,256,460	0	0	0	0	0	[3]776,520
11	0	0	321,252	1,285,862	995	3,801	719,705	0	0	0	0	0	[3]611,226

[1]Runoff values are 0.5 percent of values in table 17*B*.

[2]Runoff values are 1 percent of values in table 17*B*.

[3]Runoff values are 10 percent of values in table 17*B*.

Table 18. Summary of simulated total groundwater budget, in acre-feet, for the Bicycle Basin groundwater-flow model, runoff-capture scenario (scenario 1), and future-pumpage scenarios (scenarios 2–5), Bicycle Basin groundwater-flow model, Fort Irwin National Training Center, California.

[Units are acre-feet; total values are for the end of the simulation period. **Abbreviation**: NA, not applicable]

Simulation period	Recharge	Captured runoff	Well loss	Inflows			Outflows					Storage change (total inflows minus total outflows)
				No-delay interbed storage	Delay interbed storage	Total inflows	Drains	Pumpage	No-delay interbed storage	Delay interbed storage	Total outflows	
Predevelopment through 2010 (historical period)												
Calibrated model—without runoff-capture	5,104	NA	791	353	761	7,008	2,172	46,857	8.2	58	49,095	–42,087
Scenario 1—with runoff-capture	5,104	5,765	986	337	725	12,917	2,185	47,062	9.3	60	49,317	–36,400
2011 through 2060 (projected period)												
Scenario 2—base case	5,796	NA	187	439	1,213	7,635	0	54,628	3.9	135	54,767	–47,132
Scenario 3	5,796	NA	236	419	1,139	7,590	0	54,529	3.2	107	54,639	–47,049
Scenario 4	5,796	NA	183	337	881	7,198	0	41,477	3.6	103	41,584	–34,386
Scenario 5	5,796	NA	199	147	365	6,508	0	27,239	2.4	11	27,252	–20,745

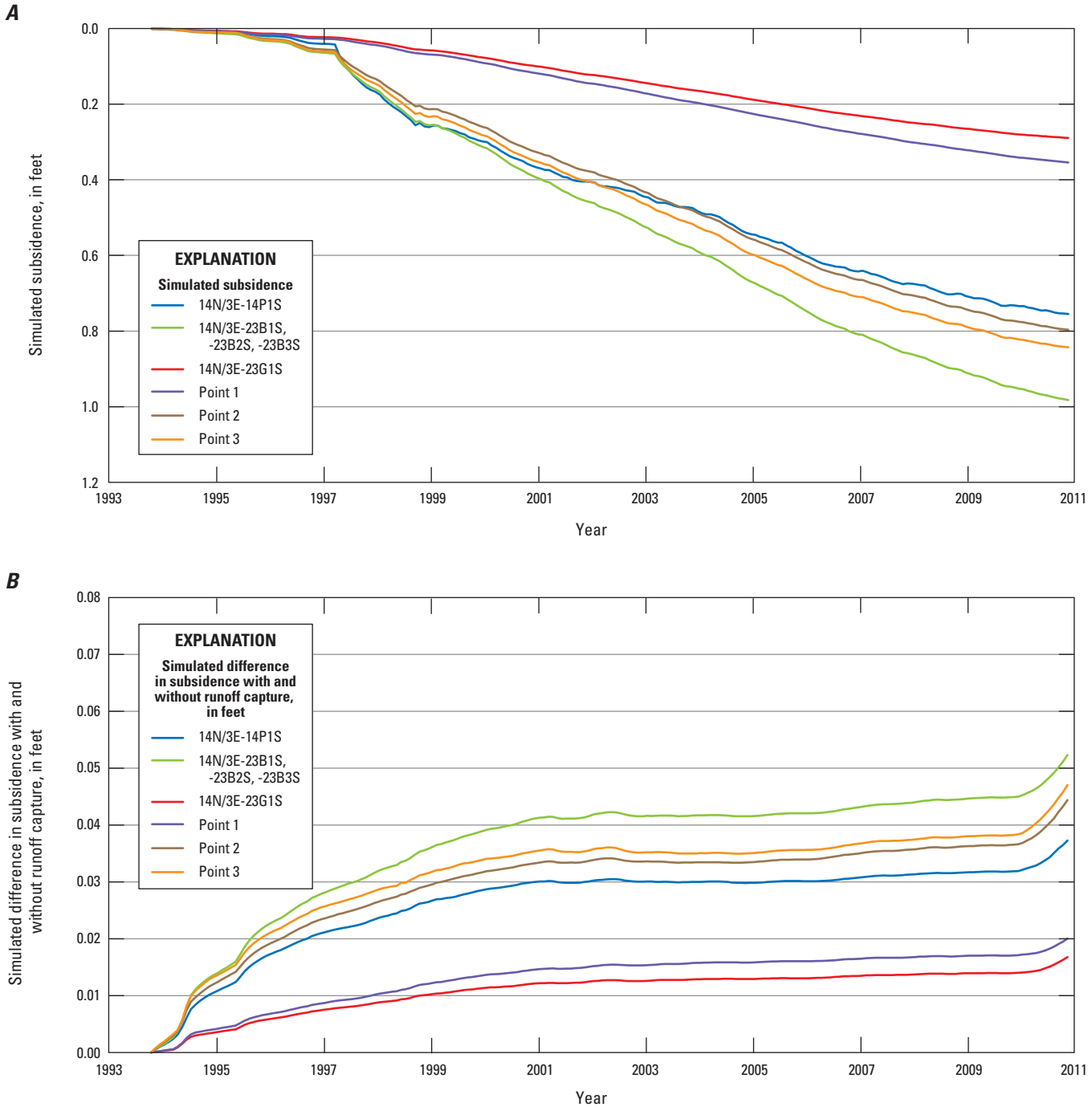

Figure 28. Simulated subsidence from the Bicycle Basin groundwater-flow model, Fort Irwin National Training Center, California, *A*, for the runoff-capture scenario (scenario 1) and *B*, the difference between simulated subsidence with and without runoff capture.

Model results for scenario 1 indicated that total recharge for the simulation period, including natural recharge and runoff capture, was about 10,900 acre-ft; this was more than twice that of the model simulation without runoff capture. The total simulated groundwater-storage depletion was about 36,400 acre-ft, about 5,700 acre-ft less than the model simulation without runoff capture (table 18). Since the recharge of captured runoff did not substantially affect the other water-budget components, this value was similar to the amount of captured runoff.

In general, the distributions of simulated drawdown were similar for the model simulation without runoff capture (figs. 24*A*, *B*) and scenario 1 (figs. 27*A*, *B*); however, there were notable differences in the magnitude of simulated drawdown for both model layers 1 and 6. For example, the negative values of simulated drawdown in model layer 1 in the vicinity of recharge zone 1 for scenario 1 (fig. 27*A*) indicated that the simulated heads were higher in December 2010 than in the predevelopment period. Simulated heads for the model without runoff capture in 2010 also were higher than the predevelopment period; however, the head change was less than in scenario 1. Negative values of drawdown also were simulated in model layer 1 near recharge zone 2 for scenario 1 (fig. 27*A*). In this part of the basin, simulated heads were more than 100 ft higher in December 2010 than in the predevelopment period. In contrast, simulated heads for the model without runoff capture were 80–90 ft lower in December 2010 than in the predevelopment period (fig. 24*A*). The largest differences in simulated drawdown between scenario 1 and the model without runoff capture for model layer 1 were primarily in parameter zone 1; the smallest differences in simulated drawdown were primarily in parameter zones 4–6 (fig. 27*C*).

The simulated runoff-capture scenario resulted in localized increases in water levels from predevelopment to 2010 that partially offset depletion of groundwater due to pumping; the total depletion for this period was reduced by 14 percent, indicating the overall effectiveness of this scenario. Although the distribution of drawdown in model layer 6 for scenario 1 (fig. 27*B*) was similar to that for the model without runoff capture (fig. 24*B*), the magnitude of simulated drawdown was slightly less for scenario 1. For example, in the area around wells 14N/4E-18N1–2 simulated drawdown ranged from 90 to 100 ft for scenario 1; for the model without runoff capture, the simulated drawdown ranged from about 100 to 110 ft (fig. 24*B*). The largest difference in simulated drawdown between scenario 1 and the model without runoff capture was in parameter zone 1; the smallest difference was in the southern part of parameter zone 5 (fig. 27*D*).

Results for the simulated runoff-capture scenario indicated only modest decreases in subsidence compared with the overall magnitude of subsidence. Figure 28*A* shows simulated subsidence for scenario 1, and figure 28*B* shows the difference between scenario 1 and the model without runoff capture. The positive values for the difference in subsidence indicated that subsidence was less in scenario 1 than in the model simulation without runoff capture. Subsidence was mitigated somewhat by runoff capture (fig. 21*B*, 28*A*); the largest decrease in subsidence was about 0.052 ft at monitoring well site 14N/3E-23B1–3; the smallest decrease was about 0.017 ft at 14N/3E-23G1 (fig. 28*B*). The large quantity of runoff in 2010 resulted in a sharp decrease in subsidence beginning in January 2010. The maximum rate of subsidence at monitoring well site 14N/3E-23B1–3 in scenario 1 was 0.98 ft (fig. 28*A*) compared with a value of 1.03 ft for the model simulation without runoff capture (fig. 21*B*); thus, the simulated recharge of captured runoff resulted in a 5 percent decrease in subsidence at this site.

Simulated Effects of Future Pumpage

The groundwater-flow model was extended from 2011 through 2060 and used to simulate the effects of four future pumpage scenarios being considered by the Fort Irwin NTC (Chris Woodruff, Fort Irwin National Training Center, written commun., 2011). Scenario 2 was a base case that continued 2010 conditions for comparison with scenarios 3–5, which had alternate groundwater-pumping conditions (table 16). The groundwater-recharge rate for all the pumpage scenarios was assumed to be the same as in the historical period.

Results of the future pumpage scenarios are presented as drawdown maps for model layer 6 from December 2010 to December 2060 (figs. 29*A*–*D*). Results for model layer 6 are shown because it represents the main aquifer contributing water to production wells in parameter zone 6, where land has subsided. A positive value for drawdown indicated the simulated hydraulic head declined during 2011–60.

Scenario 2

It was assumed for scenario 2 that annual pumpage in 2010 (1,090 acre-ft; table 3) remained constant during 2011–60. The pumpage distribution to wells was based on the pumpage distribution for active production wells in 2010 (14N/3E-13M1, 14N/3E-14P1, and 14N/4E-18N1; table 3). The monthly pumpage values in 2010 for these wells were repeated for monthly stress periods during 2011–60.

Model results for scenario 2 indicated that total pumpage for 2011–60 was about 54,600 acre-ft, and simulated groundwater-storage depletion was about 47,100 (table 18). Simulated drawdown in model layer 6 for 2011–60 ranged from about 46 ft to 135 ft (fig. 29*A*). Simulated drawdown in parameter zone 2 was primarily from pumping in well 14N/3E-13M1, because the South Coyote Canyon fault (fig. 15) is a partial barrier to the effects of pumping in model layer 6 in the rest of the basin. Simulated drawdown was more than 120 ft near well 14N/4E-18N1 in parameter zone 1 and between 120 and 130 ft in parameter zones 3, 5, and 6.

Simulated drawdown near well 14N/4E-18N1 for 2011–60 was greater than for well 14N/3E-14P1 (fig. 29*A*), even though the pumpage for well 14N/3E-14P1 was greater.

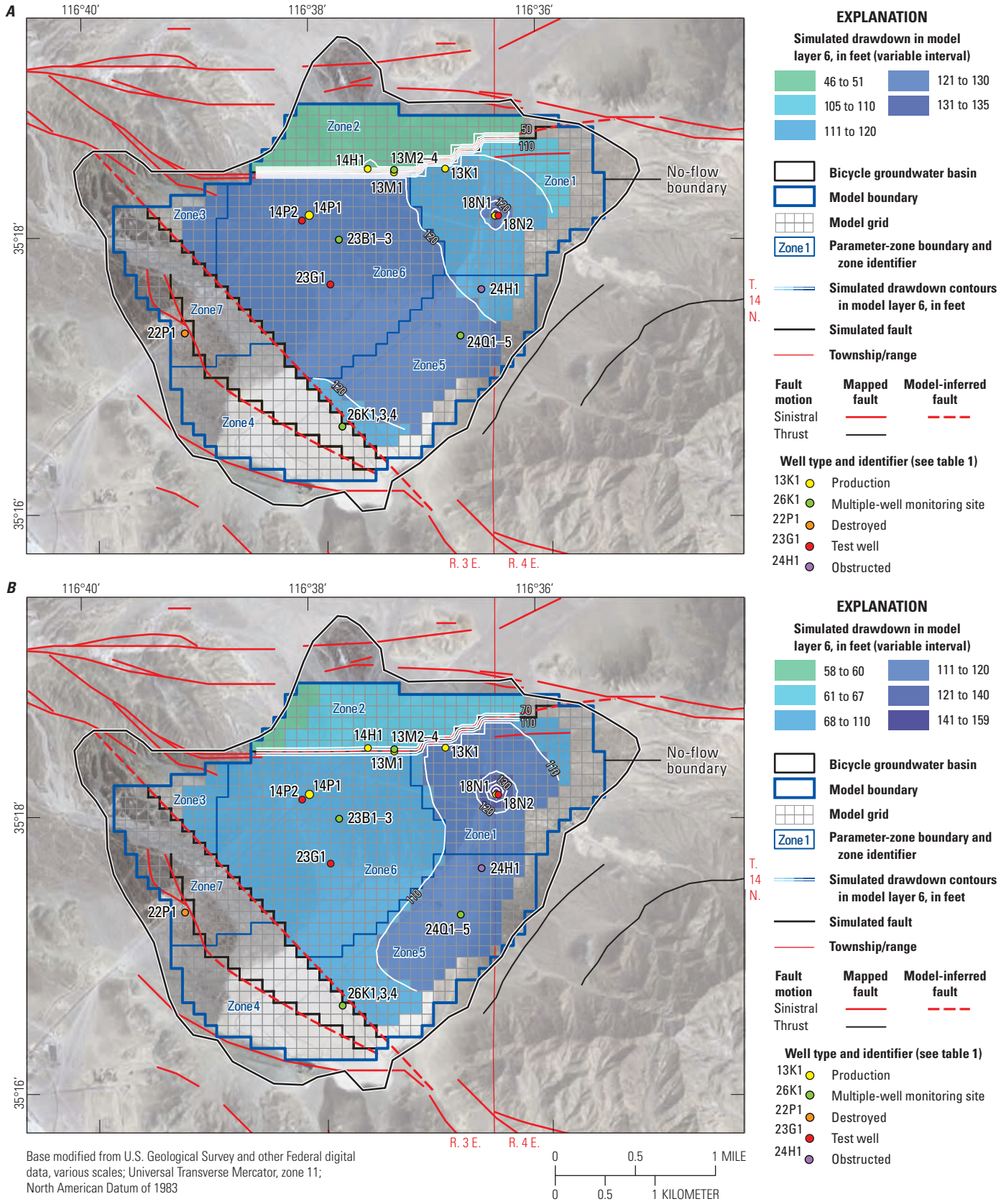

Figure 29. Simulated drawdown in model layer 6 from the end of the historical period in December 2010 to the end of the projected period in December 2060 for the groundwater-flow model of the Bicycle Basin, Fort Irwin National Training Center, California, for *A*, scenario 2; *B*, scenario 3; *C*, scenario 4; and *D*, scenario 5 (see table 16 for description of the scenarios).

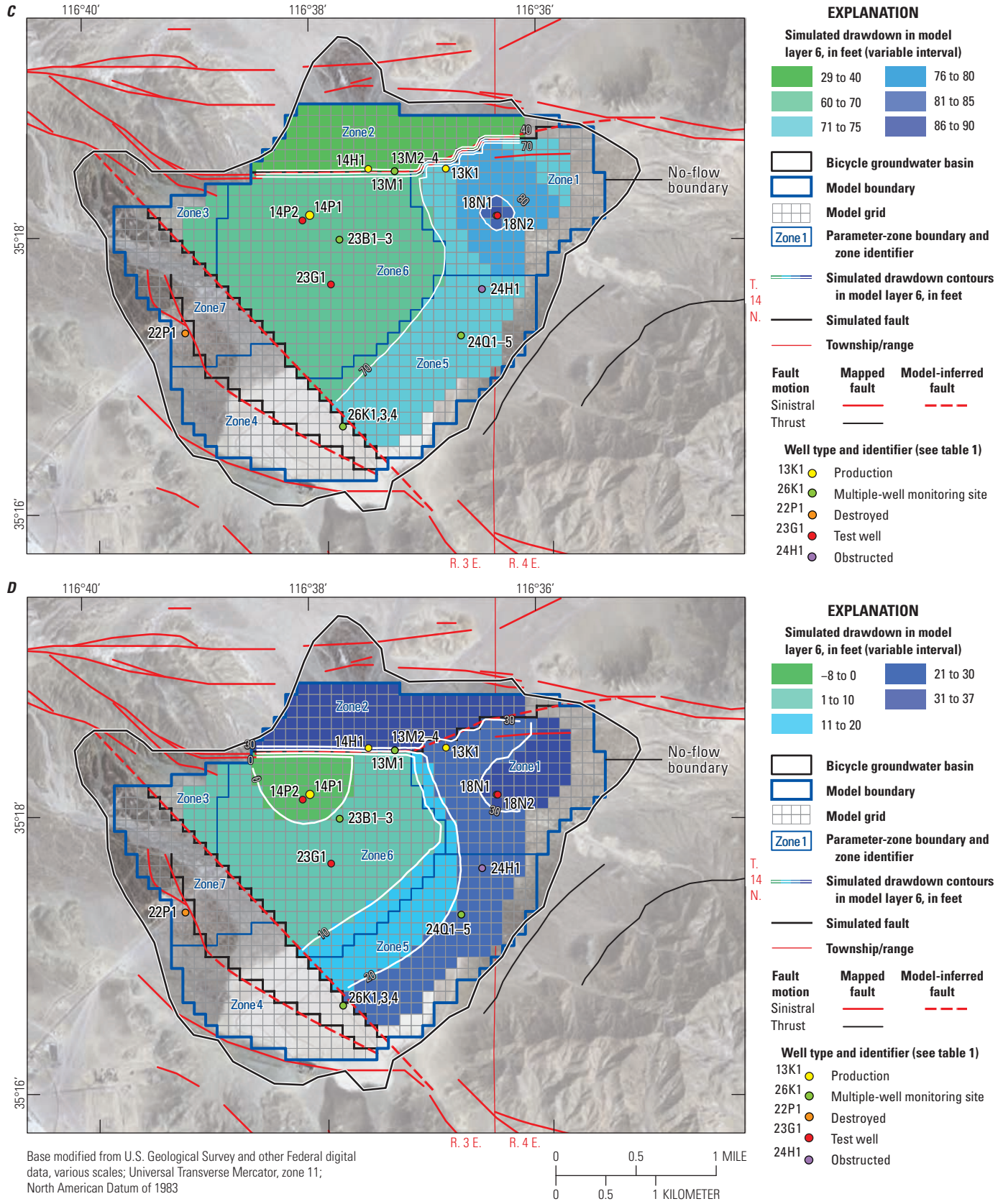

Figure 29. —Continued

This reflects the differences in hydraulic properties in parameter zones 1 and 6, the release of water from storage by compaction of fine-grained interbeds in parameter zone 6, and the distribution of pumpage to the model layers. The high hydraulic conductivity in model layer 6 of parameter zone 6 (33 ft/d) allowed the drawdown to be distributed over a larger area around 14N/3E-14P1; this could influence drawdown near well 14N/4E-18N1 and account for the comparatively high drawdown in the southwestern part of parameter zone 5 (fig. 29*A*).

Continuation of the 2010 pumpage resulted in continued decline in simulated heads through 2060 for the three wells, 14N/4E-18N1, 14N/3E-13M1, and 14N/3E-14P1, shown in figure 30*A–C*, respectively. At well 14N/4E-18N1, the simulated heads in all layers at the end of 2011–60 declined below the bottom elevation of layer 3; layers 1–3 were dewatered near the well. The deeper layers have lower transmissivity values, so the seasonal fluctuations in the simulated heads became more pronounced as the simulated heads declined into these layers (fig. 30*A*).

Simulated heads at well 14N/3E-13M1 indicated that model layer 2 was dewatered early during 2011–60 (fig. 30*B*). Pumpage was substantially less for this well than for wells 14N/4E-18N1 and 14N/3E-14P1, resulting in less drawdown. The seasonal fluctuations were less pronounced than for well 14N/4E-18N1 because of the higher transmissivity values below model layer 2 near well 14N/3E-13M1.

Simulated heads at well 14N/3E-14P1 indicated that model layer 4 was dewatered during 2011–60. The difference in simulated heads between model layers 5 and 6 increased during 2011–60 (fig. 30*C*). The increased vertical gradient from pumpage in model layer 6 could have resulted from release of groundwater by compaction of fine-grained interbeds in model layer 5 and induced lateral flow into parameter zone 6; this also probably helped to damp the seasonal fluctuations in simulated water levels in model layer 6.

Subsidence continued at all observation locations with the projection of 2010 pumpage to 2060 (fig. 31*A*). Total subsidence at the end of 2011–60 ranged from 0.83 ft at well 14N/3E-23G1 to 2.8 ft at monitoring well site 14N/3E-23B1–3. The increase in simulated subsidence since 2010 was smallest at well 14N/3E-23G1 (0.53 ft) and largest at well site 14N/3E-23B1 (1.73 ft). The rate of measured and simulated subsidence began to decrease after 2006, and the simulated rate continued to decrease during 2011–60 (fig. 31*A*). This decrease in the rate of subsidence likely was due to lower annual pumpage during 2007–10 (1,125 acre-ft) compared with the average annual pumpage for the subsidence observation period of 1993–2010 (1,469 acre-ft; table 15).

Scenario 3

Scenario 3 assumed that pumpage for each month in 2010 for well 14N/3E-14P1 was reduced by 25 percent, with the reduced quantity distributed to production wells 14N/3E-13M1 and 14N/4E-18N1. The adjusted pumpage for 2010 was repeated for each stress period during 2011–60. The quantity distributed to production wells 14N/3E-13M1 and 14N/4E-18N1 was based on the percentage of total monthly 2010 pumpage attributed to wells 14N/3E-13M1 and 14N/4E-18N1. The pumpage redistributed from well 14N/3E-14P1 to well 14N/3E-13M1 ranged from 6 percent in July to 35 percent in November, and the pumpage redistributed to 14N/4E-18N1 was 94 percent and 65 percent for July and November, respectively. The pumpage for 2010 for well 14N/3E-14P1 was decreased by an average of about 137 acre-ft, resulting in average annual increased pumpage of about 30 acre-ft for well 14N/3E-13M1 and of about 110 acre-ft for well 14N/4E-18N1.

Model results for scenario 3 indicated that total pumpage for 2011–60 was about 54,500 acre-ft, approximately 99 acre-ft less than the base case. Total pumpage should be the same as the base case; the difference is due to numerical calculations in the MNW2 package. The simulated groundwater-storage depletion was about 47,000 acre-ft, about 80 acre-ft less than the base case (table 18). The distribution of simulated drawdown in model layer 6 for scenario 3 (fig. 29*B*) differed from the base case (fig. 29*A*). Scenario 3 had less drawdown in parameter zones 3, 5, and 6 than the base case, reflecting the reduced pumping in well 14N/3E-14P1. The increase in pumping in wells 14N/3E-13M1 and 14N/4E-18N1 resulted in greater drawdown in parameter zone 2 and in the vicinity of 14N/4E-18N1 (fig. 29*B*).

Adjustment of the 2010 pumpage for 2011–60 resulted in continued decline in simulated heads through 2060 (fig. 32), which generally were similar to the base case (fig. 30). The additional pumpage for 14N/34-18N1, however, resulted in larger seasonal fluctuations for scenario 3 than for the base case (figs. 32*A*, 30*A*, respectively) as layers 1–4 became dewatered and pumpage was redistributed to deeper layers with lower hydraulic conductivity. The additional pumpage for well 14N/4E-18N1 resulted in simulated heads that were as much as 50 ft lower than in the base case at the end of 2060.

The additional pumpage for well 14N/3E-13M1 resulted in greater decline in simulated heads, and seasonal fluctuations were slightly more pronounced during 2011–60 than in the base case (figs. 32*B*, 30*B*, respectively). The simulated heads at the end of this period for scenario 3 were as much as about 20 ft lower than for the base case.

The reduction in pumpage for well 14N/3E-14P1 resulted in less simulated head decline and slightly less pronounced seasonal fluctuations compared with the base case (figs. 32*C*, 30*C*, respectively). The difference in simulated heads between layers 5 and 6 was about 10 ft less than for the base case at the end of 2060; the simulated heads were about 5 ft and 15 ft higher for layers 5 and 6, respectively, in scenario 3 than in the base case.

Subsidence continued at all observation locations with the adjusted 2010 pumpage during 2011–60 (fig. 31*B*).

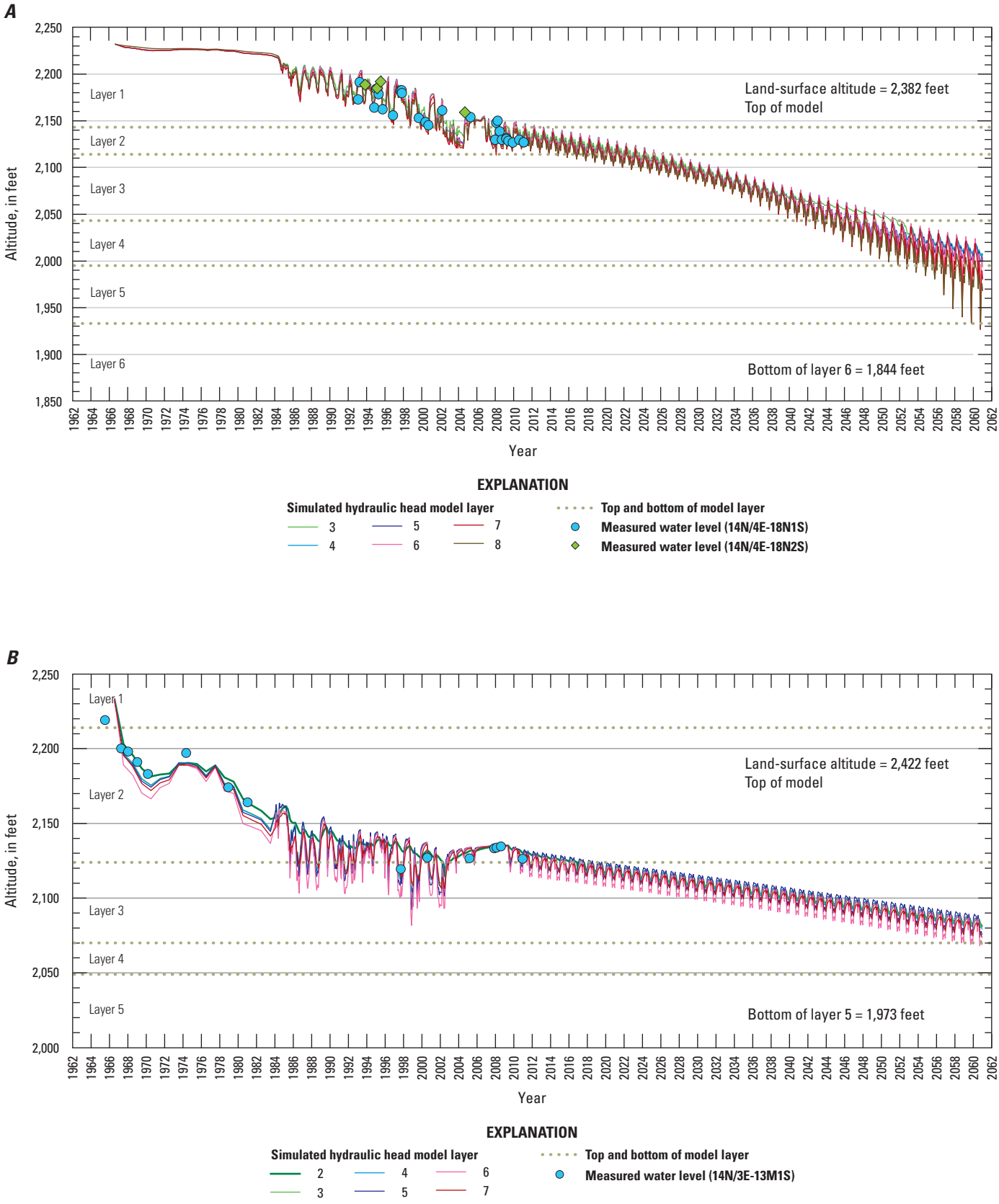

Figure 30. Measured groundwater levels during the historical period and simulated heads for scenario 2 during the historical and projected periods for the Bicycle Basin groundwater-flow model, Fort Irwin National Training Center, California, in wells *A*, 14N/4E-18N1,2; *B*, 14N/3E-13M1; and *C*, 14N/3E-14P1.

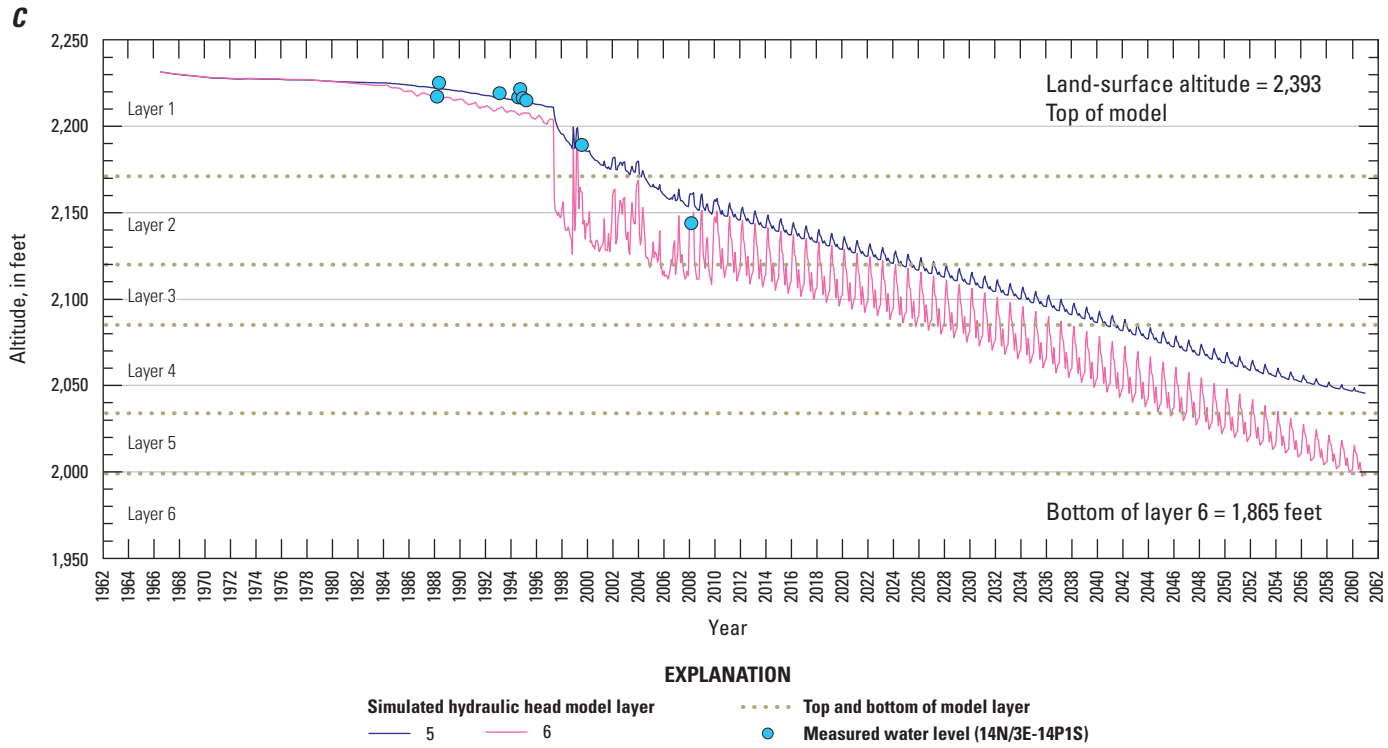

Figure 30. —Continued

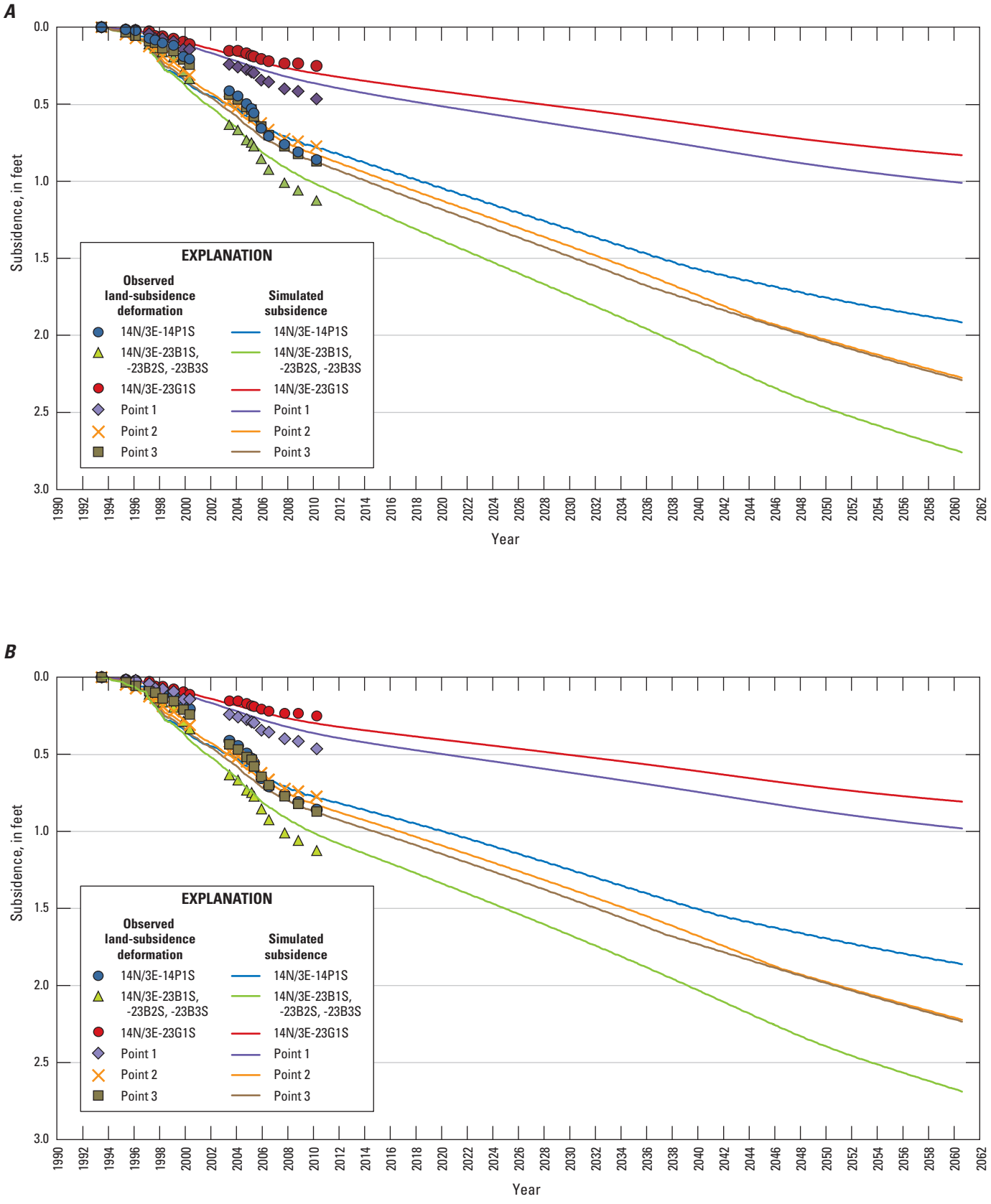

Figure 31. Observed land-surface deformation from 1993 through 2010 and simulated subsidence from 1993 through 2060 for the Bicycle Basin groundwater-flow model, Fort Irwin National Training Center, California, for *A*, scenario 2; *B*, scenario 3; *C*, scenario 4; and *D*, scenario 5.

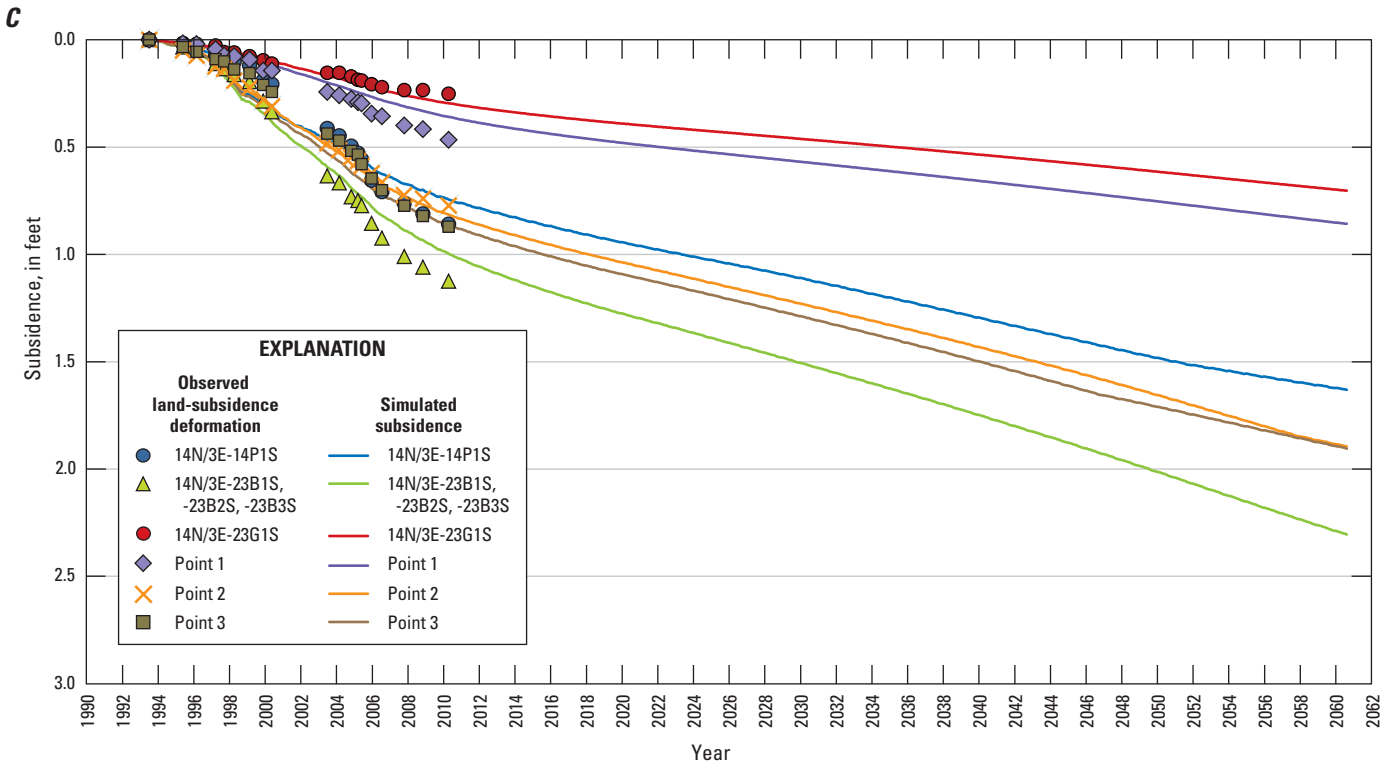

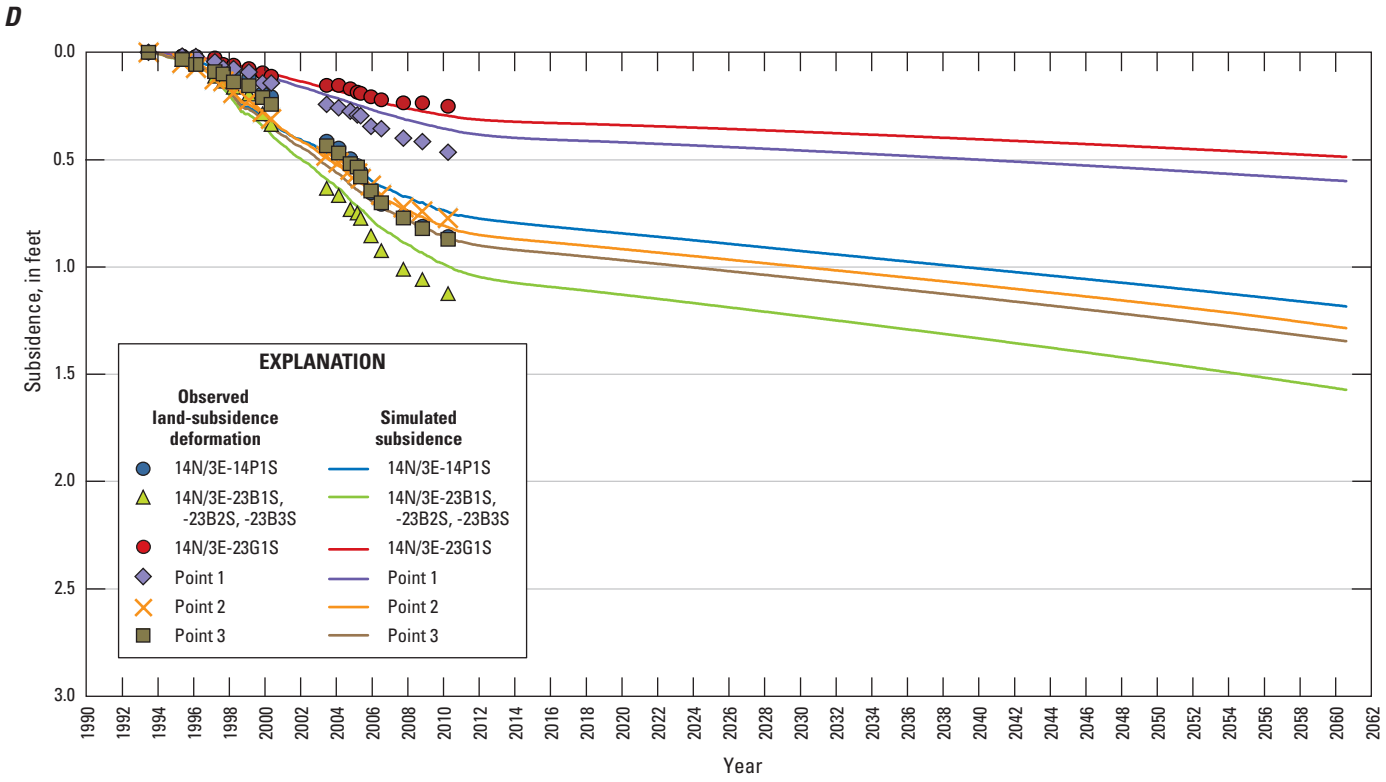

Figure 31. —Continued

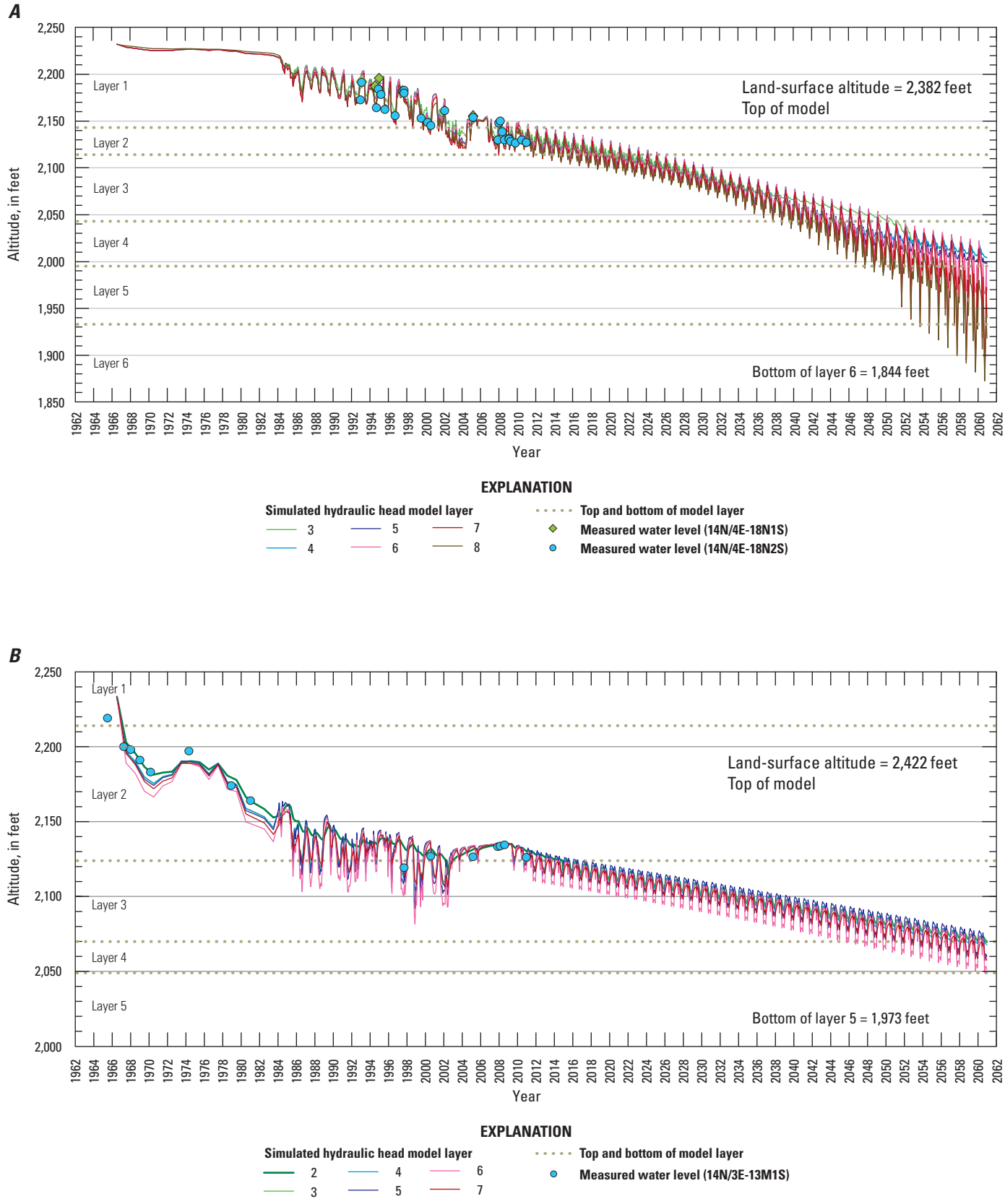

Figure 32. Measured groundwater levels and simulated heads for scenario 3 for the Bicycle Basin groundwater-flow model, Fort Irwin National Training Center, California, in production wells *A*, 14N/4E-18N1,2; *B*, 14N/3E-13M1; and *C*, 14N/3E-14P1.

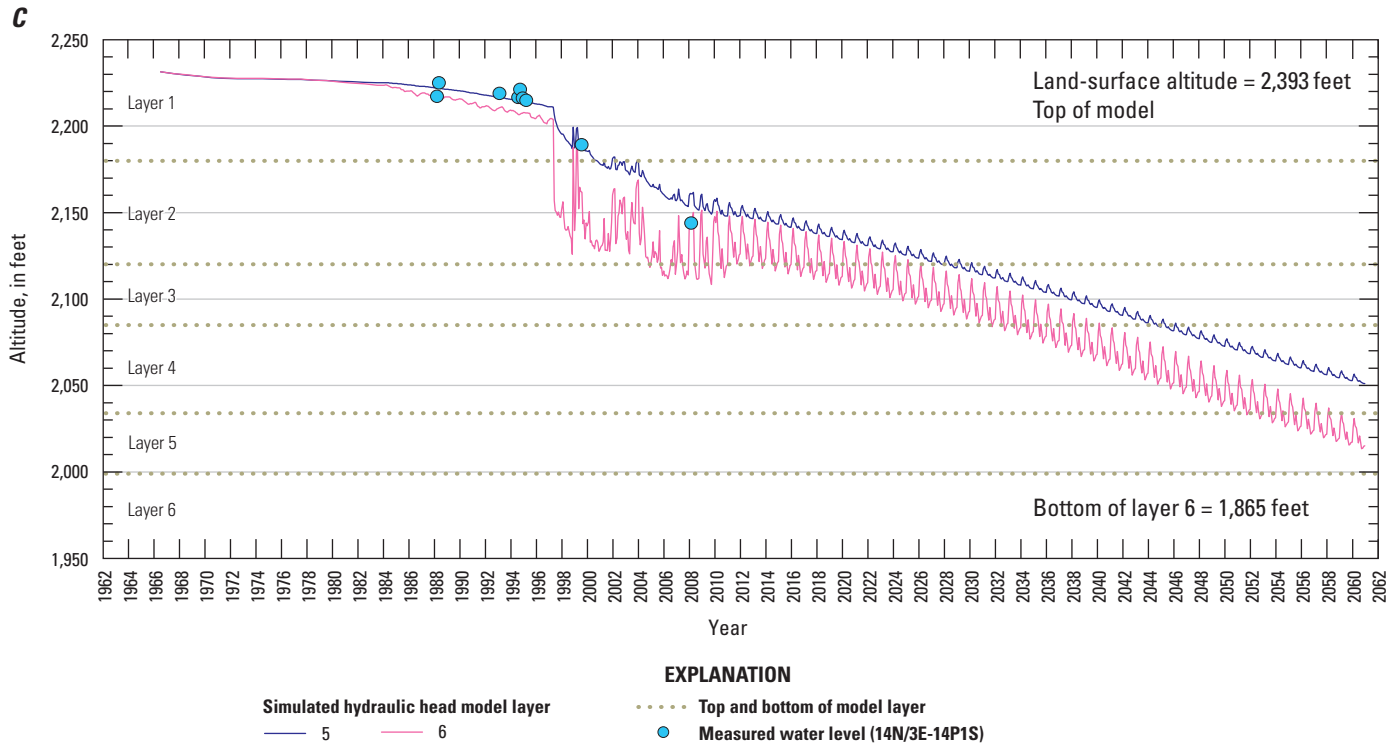

Figure 32. —Continued

Subsidence at the end of this period ranged from 0.81 ft at well 14N/3E-23G1 to 2.69 ft at monitoring well site 14N/3E-23B1–3. Well 14N/3E-23G1 had the smallest increase in subsidence (0.50 ft), and well site 14N/3E-23B1–3 had the largest increase (1.68 ft). The difference in total subsidence at the end of 2060 between the base case and scenario 3 was small, less than or equal to 0.07 ft for all observation points, indicating that changes in pumpage at well 14N/3E-14P1 from this scenario would result in only limited reduction of subsidence.

Scenario 4

Scenario 4 assumed the same adjustments to 2010 pumpage as scenario 3 (25 percent reduced pumpage from well 14N/3E-14P1 redistributed to wells 14N/3E-13M1 and 14N/4E-18N1) with the added constraint of 3 percent per year reduction in total annual pumpage in the basin from 2011 through 2020. The resulting pumpage for 2020 was repeated from 2021 through 2060. The annual pumpage for well 14N/3E-14P1 ranged from 401 acre-ft for 2011 to 304 acre-ft for 2020–60. The annual pumpage for well 14N/4E-18N1 ranged from 517 acre-ft in 2011 to 393 acre-ft for 2021–60. The annual pumpage for well 14N/3E-13M1 ranged from 140 acre-ft in 2011 to 106 acre-ft for 2011–60.

The total pumpage for 2011–60 was about 41,500 acre-ft, or 13,200 acre-ft less than the base case. The simulated groundwater-storage depletion was about 34,400 acre-ft, 12,700 acre-ft less than the base case (table 18). The distribution and magnitude of simulated drawdown in model layer 6 for scenario 4 (fig. 29*C*) was substantially different from the base case (fig. 29*A*) south of the South Coyote Canyon fault (fig. 15). North of the fault, the distribution of drawdown was similar to the base case, but the magnitude was substantially different. The drawdown near well 14N/4E-18N1 was about 40 ft less than for the base case; near well 14N/4E-14P1, drawdown was about 60 ft less than the base case.

The adjusted pumpage for scenario 4 resulted in continued decline in simulated heads during 2011–60 (fig. 33), similar to the base case (fig. 30). In contrast to the base case, however, simulated heads in well 14N/4E-18N1 for scenario 4 were above the bottom of layer 3 for almost all of 2011–60. Although additional pumpage was distributed to well 14N/4E-18N1, the reduction in overall basin-wide pumpage helped to mitigate dewatering of the upper layers, resulting in smaller seasonal fluctuations in well 14N/4E-18N1 (fig. 33*A*) than for the base case (fig. 30*A*). Simulated heads at the end of 2060 in well 14N/4E-18N1 for scenario 4 were as much as about 100 ft higher than for the base case.

The reduction in basin-wide pumpage also helped to mitigate the effects of the additional pumpage for well 14N/4E-13M1; however, the difference in the decline in simulated heads from the base case was less pronounced (figs. 33*B*, 30*B*, respectively). Simulated heads at the end of 2060 in well 14N/4E-13M1 for scenario 4 were about 20 ft higher than for the base case.

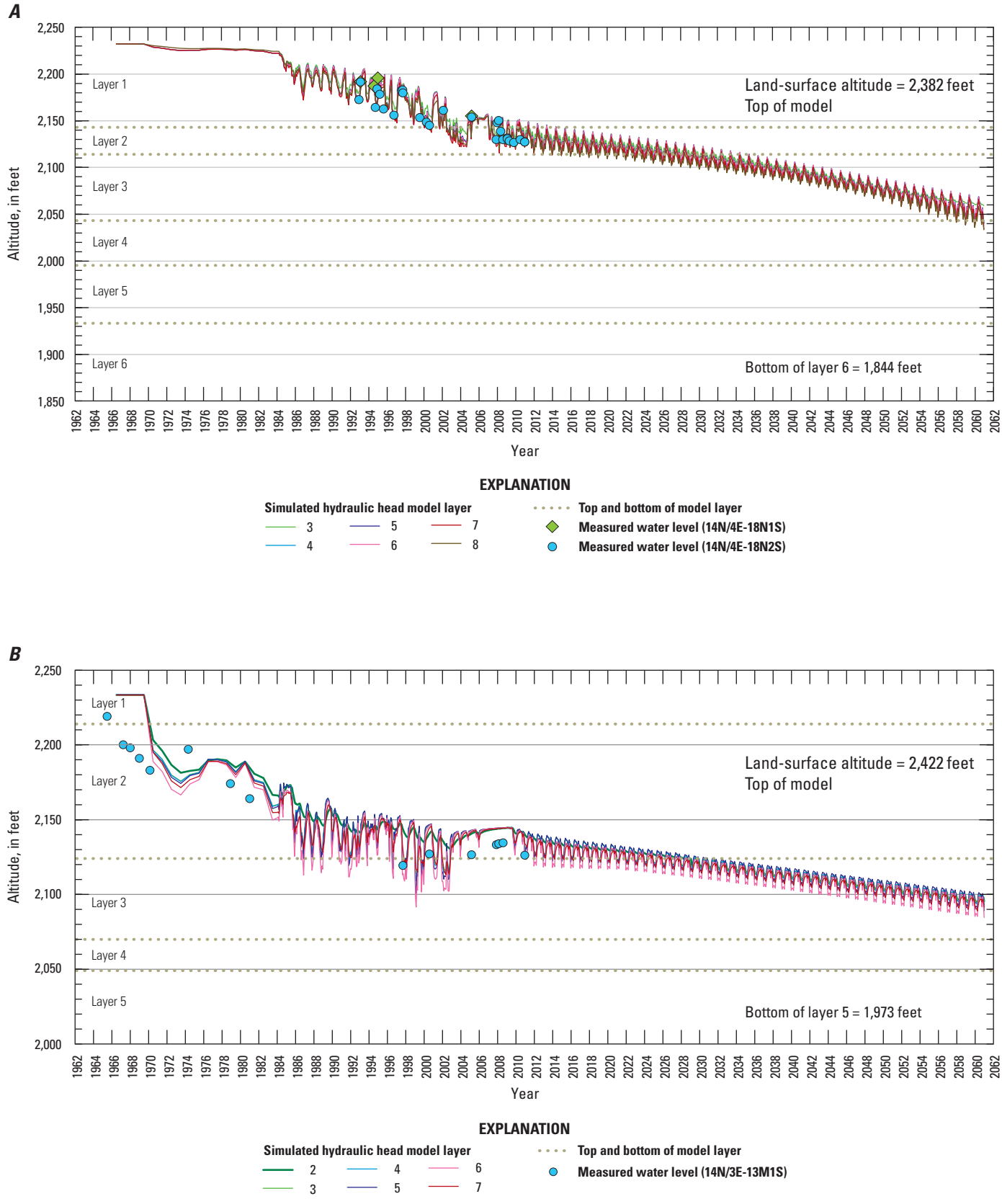

Figure 33. Measured groundwater levels and simulated heads for scenario 4 for the Bicycle Basin groundwater-flow model, Fort Irwin National Training Center, California, in production wells *A*, 14N/4E-18N1, 2; *B*, 14N/3E-13M1; and *C*, 14N/3E-14P1.

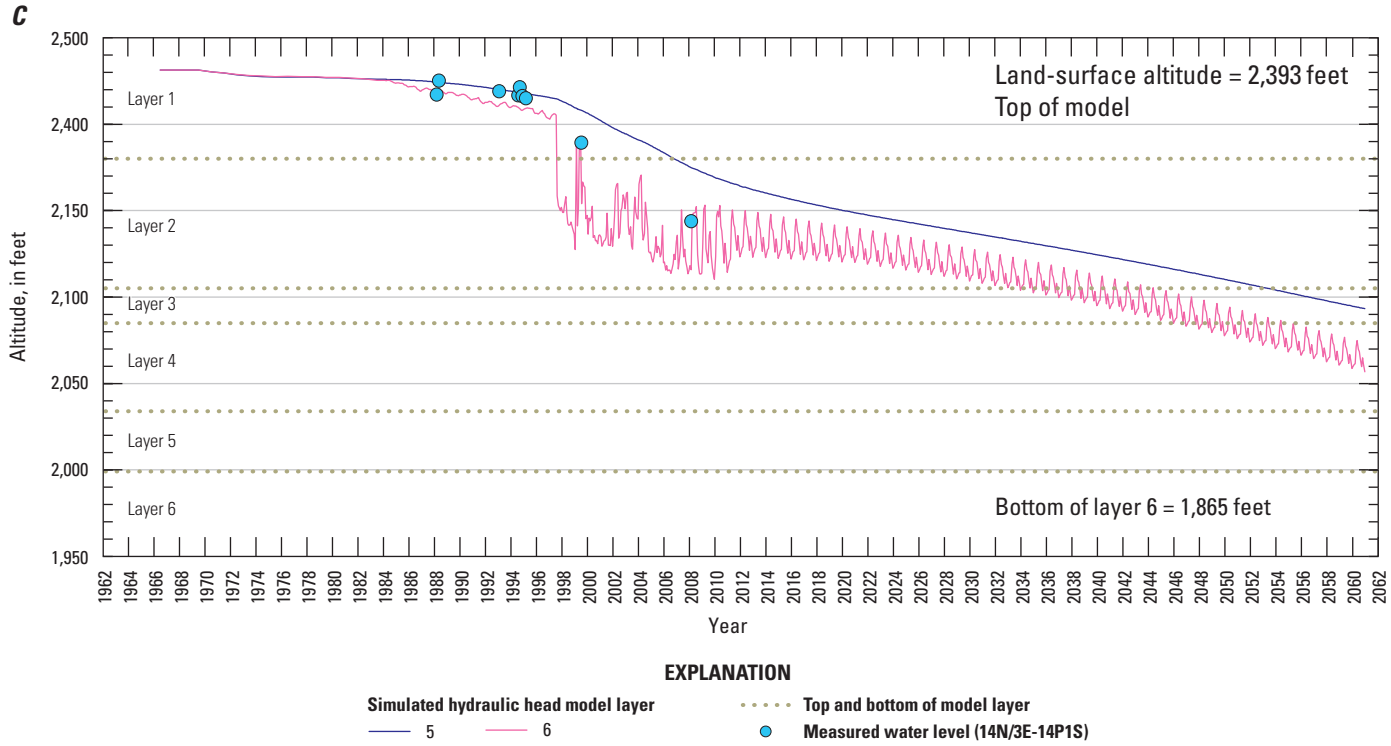

Figure 33. —Continued

The reduction in basin-wide pumpage combined with the reduction in pumpage for well 14N/3E-14P1 during 2011–60 resulted in less overall decline in simulated heads in model layers 5 and 6 (fig. 33*C*) than in the base case (fig. 30*C*). Simulated heads at the end of 2060 in well 14N/3E-14P1 for scenario 4 were about 50 ft higher in model layer 5 and 60 ft higher in model layer 6 than for the base case.

Subsidence continued at all observation locations with the adjusted pumpage for scenario 4 (fig. 31*C*), but at lower rates than in the base case (fig. 31*A*). Subsidence at the end of 2060 ranged from 0.83 ft at well 14N/3E-23G1 to 2.8 ft at monitoring well site 14N/3E-23B1–3. Well 14N/3E-23G1 had the smallest increase in subsidence since December 2010 (0.40 ft), and monitoring well site 14N/3E-23B1–3 had the largest increase (1.29 ft). The total subsidence during 2011–60 was between 0.12 and 0.43 ft less at well 14N/3E-23G1 and well site 14N/3E-23B1–3, respectively, for scenario 4 relative to the base case, indicating that changes in pumpage for this scenario could result in reduction of subsidence.

Scenario 5

Scenario 5 assumed that the distribution of the pumpage to wells 14N/4E-18N1 and 14N/3E-13M1 was the same as in the base case; the 2010 pumpage was constant for these wells during 2011–60. The pumpage for well 14N/3E-14P1 was reduced to zero for this period, resulting in less total pumpage for this scenario than for the base case.

The total pumpage for 2011–60 was about 27,200 acre-ft, about half of the pumpage for the base case (table 18). The simulated groundwater-storage depletion was about 20,700 acre-ft, about 56 percent less than the base case. The distribution and magnitude of simulated drawdown in model layer 6 for scenario 5 (fig. 29*D*) was much different from the base case (fig. 29*A*). The negative values near well 14N/3E-14P1 indicated the simulated heads increased by as much as 8 ft during 2011–60. In the eastern part of parameter zone 1 near 14N/4E-18N1, drawdown was less than 40 ft. In comparison, simulated drawdown near 14N/4E-18N1 for the base case ranged from 110 to 135 ft (fig. 29*A*). The difference in drawdown near well 14N/4E-18N1 between scenario 5 and the base case indicated that pumping in well 14N/3E-14P1 substantially affected simulated heads in this area. In parameter zone 2, simulated drawdown was about 15 ft less than in the base case.

Simulated heads in well 14N/4E-18N1 remained above the bottom of model layer 3 during 2011–60 (fig. 34*A*). The damped seasonal simulated-head fluctuations for this period likely were due to less drawdown and the associated greater overall transmissivity than in the base case. The simulated heads at the end of 2060 in well 14N/4E-18N1 were as much as 120 ft higher in model layer 8 than in the base case.

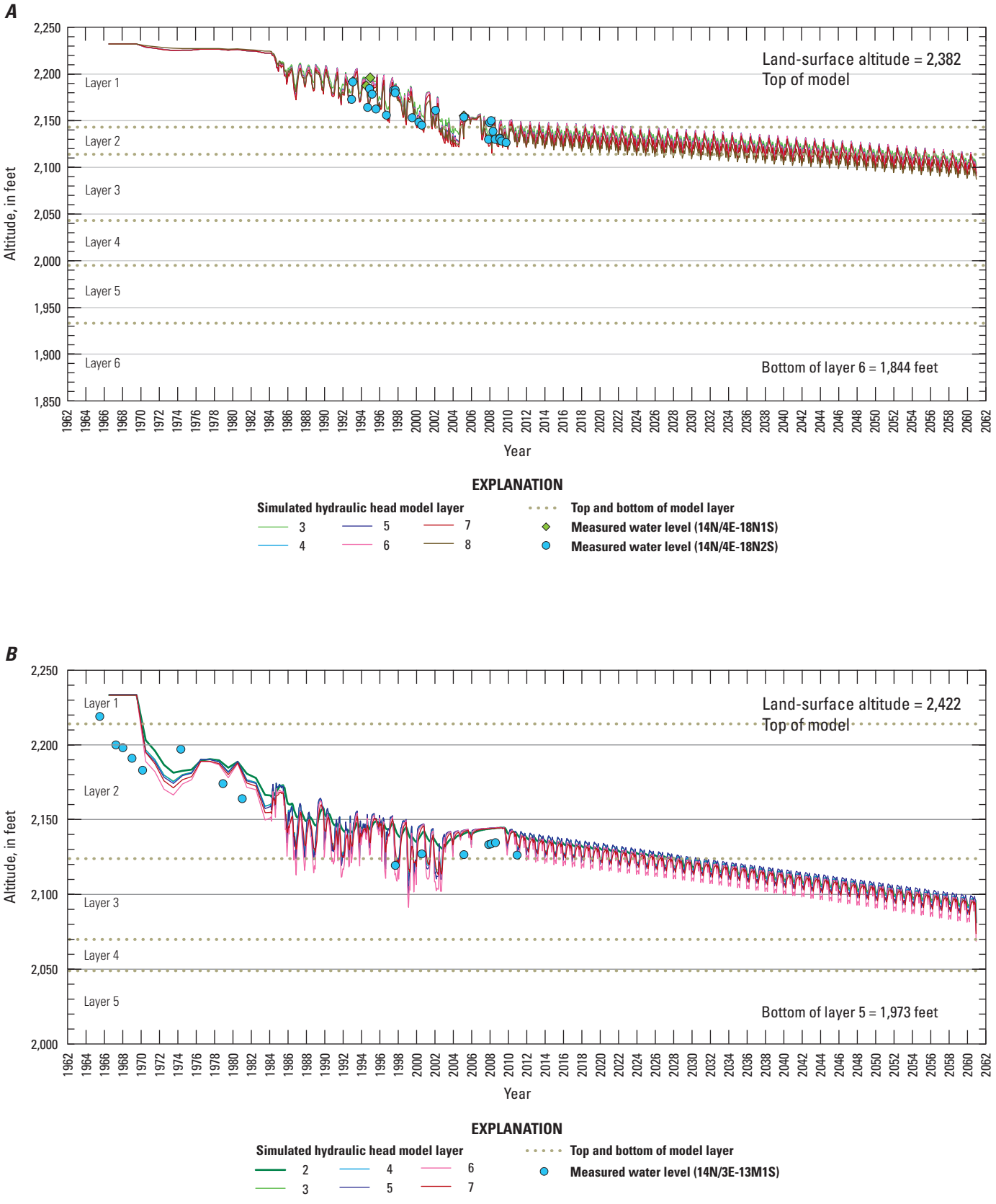

Figure 34. Measured groundwater levels and simulated heads for scenario 5 for the Bicycle Basin groundwater-flow model, Fort Irwin National Training Center, California, in production wells A, 14N/4E-18N1, 2; B, 14N/3E-13M1; and C, 14N/3E-14P1.

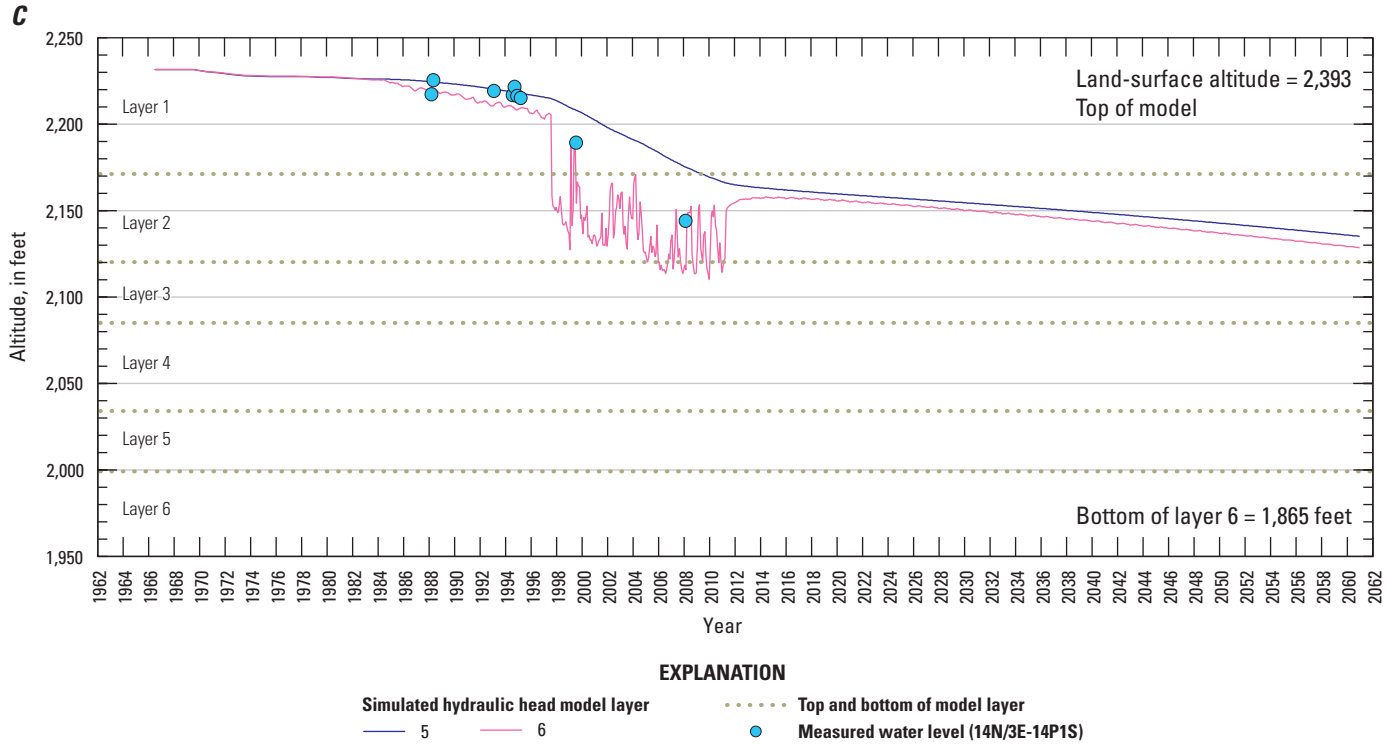

Figure 34. —Continued

The simulated heads in well 14N/3E-13M1 for scenario 5 (fig. 34*B*) were not much different from the base case (fig. 30*B*). The difference in simulated heads between scenario 5 and the base case was less than 6 ft for all model layers, indicating that pumping in well 14N/3E-14P1 had little effect on simulated heads in parameter zone 2. The South Coyote Canyon fault (fig. 15) is a partial barrier to groundwater flow, which somewhat isolates parameter zone 2 from pumping in the rest of the basin.

The absence of pumpage for well 14N/3E-14P1 during 2011–60 allowed simulated heads in model layers 5 and 6 at this well to recover from drawdown caused by the pumping during the historical period (fig. 34*C*). In contrast to the base case, simulated heads in model layers 5 and 6 remained above the bottom of layer 2 during 2011–60. The difference in simulated heads between layers 5 and 6 was reduced by about 40 ft (fig. 34*C*). The simulated heads at the end of 2060 in well 14N/3E-14P1 were about 90 ft and about 130 ft higher in model layers 5 and 6, respectively, than the base case.

Subsidence continued during 2011–60 at all observation locations in the absence of pumping in well 14N/3E-14P1 (fig. 31*D*), but at a much slower rate than in the base case (fig. 31*A*). At the end of 2060, subsidence ranged from 0.49 ft at 14N/3E-23G1 to 1.57 ft at monitoring well site 14N/3E-23B1–3. Well 14N/3E-23G1 was the site of the smallest increase in subsidence (0.19 ft) since December 2010, and the largest increase (0.56 ft) was at monitoring well site 14N/3E-23B1–3. The simulated subsidence during 2011–60 ranged from about 0.19 to about 1.16 ft less at well 14N/3E-23G1 and at well site 14N/3E-23B1–3, respectively, than in the base case, indicating that the discontinuation of pumpage at well 14N/3E-14P1 could substantially reduce subsidence.

Overall, continued declines in the water table dewatered the more productive upper layers of the aquifer, causing more pumpage to be withdrawn from deeper, lower yielding layers and resulting in increasing declines in the water table and greater vertical gradients in the future. The declines of the water table to the perforated intervals of wells could increase maintenance costs and alter the quality of water discharged from the wells. Water-management scenario 1 indicated that additional managed recharge resulted in a modest decrease (4–5 percent) in the rate of subsidence compared with historical conditions without managed recharge. The reduction of pumpage in the area of subsidence and redistribution of the amount of the reduction to wells in other parts of the basin (scenario 3) resulted in modest decreases (5–6 percent) in the rate of subsidence compared with continuation of historical pumping levels. Including a basin-wide reduction of pumpage of 3 percent annually for 10 years—a 24 percent total decrease in pumpage—along with the point-specific reduction and redistribution of pumpage (scenario 4) is predicted to produce a comparable decrease in additional subsidence (22–26 percent); however, a targeted decrease in pumpage for one well in the area of greatest subsidence (scenario 5) showed a predicted decrease in additional subsidence that was proportionally greater (62–68 percent) than the percent change in pumpage.

Summary and Conclusions

Bicycle Basin is within the boundary of the Fort Irwin National Training Center (NTC), which is about 130 miles (mi) northeast of Los Angeles in the Mojave Desert region of southern California. The NTC covers an area of about 1,177 square miles (mi^2) that contains several surface-water drainage basins including Irwin, Bicycle, and Langford Basins. Bicycle Basin (groundwater basin) covers an area of about 10.5 mi^2 that lies in the southeastern part of the much larger Bicycle Drainage Basin, an area of about 140 mi^2. Bicycle Basin, typical of desert basins in the Mojave Desert, is a closed basin with a relatively flat floor surrounded by generally rugged mountains or low-lying hills. No perennial streams are present in the basin, but several washes flow for several days after large storms. The climate of Bicycle Basin, typical of the Mojave Desert region, is characterized by low precipitation; hot summers; and cool winters, during which most precipitation falls, except for the occasional isolated thunderstorms during the summer months.

Bicycle Basin is filled with as much as 2,300 feet (ft) of Tertiary sedimentary deposits, Quaternary older alluvium and clay, and Quaternary younger alluvium. These deposits are unconsolidated at and near land surface and become moderately to well consolidated with increasing depth and also have diminishing permeability and water quality with increasing depth. These deposits are surrounded and underlain by a bedrock complex consisting of pre-Tertiary granitic, metamorphic and volcanic rocks that is assumed to be non-water-bearing because of the low permeability and limited water-storage characteristics of these rocks. The groundwater system in Bicycle Basin consists of two aquifers, referred to in this report as the upper aquifer and lower aquifer. The upper aquifer is composed of the younger and older Quaternary alluvium and clay. The lower aquifer is composed of younger and older Tertiary sedimentary deposits. Several faults mapped in the bedrock hills around Bicycle Basin, and splays off these faults, were projected into the basin using geophysical and gravity surveys and water-level measurements collected for this study. These splays act as partial barriers to groundwater flow through the basin fill.

Natural recharge in Bicycle Basin is from infiltration and underflow of precipitation and storm runoff along washes that drain watersheds surrounding the basin. During the period prior to development of groundwater resources of the basin, a similar quantity groundwater was thought to naturally discharge from the basin as groundwater underflow through fractured volcanic material and granitic bedrock southeast of the Bicycle Lake (dry) playa. Since groundwater development, the decline in groundwater levels is likely to have caused this natural discharge to cease.

The first well in Bicycle Basin was drilled in 1955. Groundwater export to Irwin Basin began in 1967. Annual groundwater pumpage ranged from a low of about 125 acre feet per year (acre-ft/yr) in 1977 to a high of about 2,145 acre-ft/yr in 1998; pumpage in 2010 was 1,090 acre feet (acre-ft). Groundwater pumping in Bicycle Basin from 1967 through 2010 resulted in water-level declines of as much as 100 ft; about 46,000 acre-ft of water was pumped from the basin and transported to the Irwin Basin. During 1967–2010, groundwater pumping was substantially greater than the recharge of 5,400 acre-ft of underflow from adjacent watersheds and washes. Water quality of the groundwater pumped from some wells in the basin declined as well.

Groundwater levels in Bicycle Basin have declined in response to increased pumpage, with relatively larger declines near areas of larger withdrawals. Continuous water-level data from multiple-well monitoring sites indicated that the water level (or hydraulic head) varied with depth in some areas, primarily showing groundwater moving from relatively shallower and deeper parts of the aquifer to the middle zones from which groundwater was withdrawn.

During 2003–05, an earth fissure and sink-like depressions formed on Bicycle Lake (dry) playa, which is used as an aircraft runway for transporting troops and supplies to the base. Interferograms were used to identify areas affected, measure the amount of vertical displacement, and map the extent of subsidence in the basin. The area affected by subsidence was about 2.6 mi^2 that coincided with an area containing substantial clay deposits. The amount of vertical change was about 0.2–1.1 ft from 1993 to 2010. During 2003–06, subsidence rates were nearly double those of 1992–2000. Subsidence was the result of dewatering of the interbedded fine-grained materials due to groundwater pumping in the basin.

The chemistry of the recharge water and various geochemical reactions, including dissolution, precipitation of minerals in the subsurface, and evapoconcentration, controlled the major-ion chemistry of the groundwater in the Bicycle Basin. Water-quality samples from wells in Bicycle Basin indicated that groundwater types varied from sodium-bicarbonate-sulfate ($NaHCO_3$-SO_4) type water and sodium-bicarbonate-chloride ($NaHCO_3$-Cl) type water, depending on the sulfate and chloride concentration, to sodium-chloride (NaCl) type water. Relatively poor groundwater quality, with higher total dissolved solids, primarily appeared to be associated with water withdrawn from wells perforated in Tertiary older alluvium. As groundwater levels in shallower aquifer zones were drawn down by continued pumping, deeper groundwater, such as from the Tertiary older alluvium, supplied more of the groundwater to wells, and this water was poorer quality than that of the shallower aquifer zones. Groundwater quality beneath playas generally results from lateral inflow from groundwater and remobilization of buried salts from evaporite deposits. High concentrations of total dissolved solids and chloride in some samples indicated that saline water could move laterally from the evaporite or playa deposits toward pumping depressions. Concentrations above the primary maximum contaminant level of arsenic and fluoride were measured in groundwater samples from wells in the area of greatest subsidence.

The stable isotopic concentration of oxygen-18 and deuterium/hydrogen-1, $\delta^{18}O$ and δD, of water from sampled wells was isotopically lighter than that of available nearby modern-day precipitation, indicating most of the groundwater in the basin was recharged during a cooler and wetter period than present-day conditions. Samples for stable isotopes, $\delta^{18}O$ and δD, indicated the source of groundwater was infiltration of storm runoff and underflow from the Granite Mountains to the north and the Goldstone upland area to the west. Groundwater from wells perforated in the Tertiary deposits generally was isotopically lighter than groundwater from wells perforated in the Quaternary, indicating that changes in climatic conditions, possibly including changes in storm trajectories, could have affected groundwater recharge rates and source areas in the past.

Nearly all groundwater samples from wells in Bicycle Basin contained no measurable concentrations of tritium (^{3}H), indicating that water in most of the basin was recharged prior to 1952. Uncorrected ^{14}C data indicated the groundwater in these wells had apparent ages of 15,625–39,350 years. These data indicated that the small amounts of recent recharge (since about 1950) have not yet reached the depths of the well perforations sampled in the Bicycle Basin.

A groundwater-flow model was developed to better understand the aquifer system and to assess the long-term availability of groundwater in the basin. The aquifer system was discretized vertically in eight model layers representing the different geologic units making up two aquifers. Boundary conditions, altitudes of the model-layer bottoms, distributions of hydraulic properties, and rates of recharge and discharge were determined using existing and newly collected geohydrologic data or were estimated if data were unavailable.

The Bicycle Basin groundwater-flow model was calibrated by trial and error with an automated process of minimizing the differences between measured data and simulated output. Initial estimates of hydraulic properties, recharge and discharge, were modified to improve the matches between simulated hydraulic heads and measured water levels and between simulated subsidence and observed land-surface deformation. Although simulated heads generally matched measured water levels well, there were periods for which the model overestimated or underestimated measured water levels. Mismatches between simulated heads and measured water levels can be attributed to uncertainty in the estimated distribution of annual basin-wide pumpage to active wells for 1967–83, the estimated distribution of monthly pumpage from annual values for 1984–90, and the local variability in hydraulic properties that were not reflected in the model. In general, the simulated subsidence compared well with the observed land-surface deformation.

Simulated drawdown in model layer 1 in the Bicycle Basin ranged from no drawdown in the northwestern part of the basin to more than 100 ft north of the South Coyote Canyon fault and in the northeastern part of the basin. Total groundwater pumpage of about 47,000 acre-ft from 1967 through 2010 resulted in drawdown of as much as 189 ft in model layer 6. The drawdowns in model layer 6 were larger than in model layer 1 because model layer 6 intersects the perforations of the five production wells, whereas model layer 1 only intersects the perforations of one production well.

Total groundwater-storage depletion (total inflows minus total outflows) was about 42,100 acre-ft. This indicates that about 91 percent of pumpage was supplied by depletion of groundwater storage, about 4.7 percent from reduced outflow from the basin, and about 2.3 percent from net instantaneous and delayed storage depletion.

The Bicycle Basin groundwater-flow model was used to simulate the effects of five water-management scenarios to assess long-term availability of groundwater relative to mitigation of declining water levels and continued subsidence in Bicycle Basin. These scenarios included capture of runoff that was not already accounted for in the model (scenario 1) and four future-pumpage scenarios (scenarios 2–5). The period for scenario 1 was the same as the groundwater-flow model without runoff capture, predevelopment through 2010. The calibrated model was extended from 2011 through 2060 for scenarios 2–5.

Scenario 1 assumed that the 90 percent of runoff calculated by the Basin Characterization Model (BCM) not used for recharge in the groundwater-flow model was captured from drainage basins which had runoff during the simulation period, except for 2010. In 2010, the captured runoff was reduced for January, February, and December because of the large quantity of runoff simulated by the BCM model for these months. Model results indicated simulated groundwater-storage depletion was about 14 percent less than the model without runoff capture. All of the additional recharge thus effectively acted to reduce storage depletion. The distribution of simulated drawdown with captured runoff generally was similar to that without runoff capture; however, there were notable differences in the magnitude of simulated drawdown for model layers 1 and 6 in both simulations. For example, the simulated drawdown in model layer 1 near recharge zone 1 for scenario 1 indicated that the simulated heads were higher in December 2010 than before the onset of groundwater development; simulated heads without runoff capture also were higher, but the head change was much less than in scenario 1. In model layer 6, in the eastern part of the basin near recharge zone 2, simulated heads were more than 100 ft higher in December 2010 than before the onset of development. In contrast, simulated heads without runoff capture were 80–90 ft less in December 2010 than before the onset of development. The simulated runoff capture resulted in only modest decreases in subsidence compared with the magnitude of subsidence without runoff capture.

Scenario 2 assumed the monthly pumpage for 2010 continued for each stress period in the projected period; this scenario was considered the base case for comparison with the other future pumpage scenarios. Total pumpage for scenario 2 was about 54,600 acre-ft, and the simulated groundwater-storage depletion was about 47,100 for the projected period. Simulated drawdown in model layer 6 north of the South Coyote Canyon fault for 2011–60 ranged from 46–51 ft to more than 120 ft in parameter zones 5 and 6 and near well 14N/4E-18N1. The difference between simulated drawdown in model layer 6 in parameter zone 2 and the rest of the basin indicated that the South Coyote Canyon fault effectively isolated parameter zone 2 from pumping in the rest of the basin. The largest simulated drawdown was near well 14N/4E-18N1, even though well 14N/3E-14P1 had larger pumpage, reflecting the differences in hydraulic properties in parameter zones 1 and 6, the release of water from storage by compaction of fine-grained interbeds in parameter zone 6, and the distribution of pumpage to the model layers. Subsidence continued at all observation locations; total subsidence ranged from 0.83 ft at 14N/3E-23G1 to 2.8 ft at well site 14N/3E-23B1–3.

Scenario 3 assumed that pumpage for well 14N/3E-14P1 was reduced by 25 percent, and the amount of the reduction was distributed to wells 14N/3E-13M1 and 14N/4E-18N1. Model results for scenario 3 indicated that simulated groundwater-storage was depleted only about 80 acre-ft less than it was in the base case. The distribution of simulated drawdown in model layer 6 for scenario 3 indicated less drawdown in parameter zones 3, 5, and 6 than in the base case, reflecting the reduced pumping in well 14N/3E-14P1. The increased pumping in wells 14N/3E-13M1 and 14N/4E-18N1 resulted in greater drawdown in parameter zone 2 and near 14N/4E-18N1. The overall decline in simulated heads through 2060 was similar to the base case; however, the monthly fluctuations in well 14N/4E-18N1 were larger than in the base case because, as shallow layers became dewatered, the pumpage was redistributed to deeper layers, which were less permeable. The difference in subsidence at the end of 2060 between scenario 3 and the base case was small (less than 0.07 ft) for all observation locations.

Scenario 4 was similar to scenario 3, but with the added constraint that basin-wide pumpage was reduced by 3 percent per year during 2011–20; pumpage for 2020 was assumed to be constant during 2021–60. Total pumpage for scenario 4 was about 13,200 acre-ft less than in the base case; simulated groundwater-storage depletion was about 12,700 acre-ft less than in the base case. The distribution and magnitude of simulated drawdown in layer 6 for scenario 4 was substantially different from the base case south of the South Coyote Canyon fault. North of the fault, the distribution of drawdown was similar to the base case, but the magnitude was substantially different. The drawdown near well 14N/4E-18N1 was about 40 ft less than for the base case; near well 14N/4E-14P1, drawdown was about 60 ft less than for the base case. The simulated hydraulic heads generally declined in the three production wells for scenario 4, however, the reduction in basin-wide pumpage helped to mitigate dewatering of the upper layers, and the seasonal fluctuations were smaller than in the base case. The simulated subsidence at the end of 2060 ranged from about 0.12 to 0.43 ft less than in the base case.

Scenario 5 was the same as scenario 2, except that the pumpage for well 14N/3E-14P1 was reduced to zero. The total pumpage was about half the pumpage as that of the base case. Simulated groundwater-storage depletion was about 56 percent less than in the base case. The distribution and magnitude of simulated drawdown in model layer 6 for scenario 5 was substantially different from the base case. Simulated heads increased as much as 8 ft near well 14N/3E-14P1 during 2011–60 compared with 100–135 ft of drawdown in the same area for the base case. In the eastern part of the basin near well 14N/4E-18N1, drawdown was as much as 100 ft less than in the base case, indicating that pumping in well 14N/3E-14P1 substantially affected simulated heads in this area. Simulated heads generally declined through 2060, but the amount of decline in the three production wells was substantially less than in the base case. Subsidence continued for the projected period at all observation locations, but at a slower rate than in the base case. The simulated subsidence at the end of 2060 ranged from about 0.19 to 1.16 ft less than in the base case, indicating that the discontinuation of pumpage for well 14N/3E-14P1 would result in a substantial reduction of subsidence.

Overall, continued declines in the water table dewatered the more productive upper layers of the aquifer, causing more pumpage to be withdrawn from deeper, lower yielding layers and resulting in faster declines in the water table and greater vertical gradients in the future. Declines of the water table to the perforated intervals of wells could increase maintenance costs and alter the quality of water discharged from the wells. Water-management scenario 1 indicated that additional managed recharge resulted in a modest decrease (4–5 percent) in the rate of subsidence compared with historical conditions without managed recharge. The reduction of pumpage in the area of subsidence and redistribution of the amount of the reduction to wells in other parts of the basin (scenario 3) resulted in modest decreases (5–6 percent) in the rate of subsidence compared with the continuation of historical pumping levels. Including a basin-wide reduction of pumpage (cumulatively, a 24 percent decrease) along with targeted point-specific reduction and redistribution of pumpage (scenario 4), however, or discontinuing pumping in the area of greatest subsidence (scenario 5) demonstrated that subsidence could be reduced substantially (22–26 percent for scenario 4 and 62–68 percent for scenario 5) compared with subsidence simulated for continuing historical pumping levels.

References Cited

Amelung, F., Galloway, D.L., Bell, J.W., Zebker, H.A., and Laczniak, R.J., 1999, Sensing the ups and downs of Las Vegas—InSAR reveals structural control of land subsidence and aquifer-system deformation: Geology, v. 27, no. 6, p. 483–486.

Anderson, M.P., and Woessner, W.W., 1992, Applied groundwater modeling—Simulation of flow and advective transport: San Diego, Calif., Academic Press Inc., 381 p.

Bartolino, J.R., and Cole, J.C., 2002, Ground-water resources of the Middle Rio Grande Basin: U.S. Geological Survey Circular 1222, 132 p., https://pubs.er.usgs.gov/publication/cir1222.

Beukins, R.P., 1992, Radiocarbon accelerator mass spectrometry—Background, precision, and accuracy, *in* Taylor, R.E., Long, A., and Kra, R.S., eds., Radiocarbon after four decades: New York, N.Y., Springer-Verlag, p. 230–239.

Bouwer, H., 1978, Groundwater Hydrology: McGraw-Hall, Inc., New York, 480 p.

Bouwer, H., 1980, Deep percolation and groundwater management, *in* Proceedings of the Deep Percolation Symposium, May 1–2, 1980, Scottsdale, Arizona: Phoenix, Arizona Department of Water Resources Report 1, p. 13–19.

Bredehoeft, J., 2005, The conceptualization model problem—Surprise: Hydrogeology Journal, v. 13, no. 1, p. 37–46.

Burgess, M.K., and Bedrosian, P.A., 2014, Time-domain electromagnetic surveys at Fort Irwin, San Bernardino County, California, 2010–12, chap. F *in* Buesch, D.C., ed., Geology and geophysics applied to groundwater hydrology at Fort Irwin, California: U.S. Geological Survey Open-File Report 2013–1024, 64 p., https://doi.org/10.3133/ofr20131024F.

California Interagency Watershed Mapping Committee, 2004, The California interagency watershed map of 1999 (updated May 2004): California Department of Fish and Game, http://www.atlas.ca.gov/download.html#/casil/inlandWaters.

California Irrigation Management Information System, 2009, Barstow NE—station 134, 1992–2013: California Department of Water Resources, accessed February 17, 2009, at http://wwwcimis.water.ca.gov/cimis/ [replaced by Newberry Springs II—station 234, 2015–16, accessed June 26, 2016].

C.F. Hostrup and Associates, 1955, Water resources survey, Camp Irwin, California: Consultant report prepared in March 1955 for Corps of Engineers, U.S. Army, Office of the District Engineer, Los Angeles, California, 109 p.

Coplen, T.B., 1994, Reporting of stable hydrogen, carbon, and oxygen isotopic abundances: Pure and Applied Chemistry, v. 66, no. 2, p. 273–276, https://doi.org/10.1351/pac199466020273.

Coplen, T.B., Wildman, J.D., and Chen, J., 1991, Improvements in the gaseous hydrogen-water equilibrium technique for hydrogen isotope ratio analysis: Analytical Chemistry, v. 63, no. 9, p. 910–912, https://doi.org/10.1021/ac00009a014.

Craig, H,, 1961, Isotopic variation in meteoric waters: Science, v. 133, no. 3465, p. 1702–1703, https://doi.org/10.1126/science.133.3465.1702.

Daly, C., Gibson, W.P., Doggett, M.K., Smith, J.I., Taylor, G.H., 2004, Up-to-date monthly climate maps for the conterminous United States, *in* 14th AMS Conference on Applied Climatology, 84th AMS Annual Meeting, Seattle, Washington, January 13–16, 2004, Proceedings [Combined]: American Meteorological Society, Paper P5.1, 8 p., accessed in 2004 at http://www.prism.oregonstate.edu/pub/prism/docs/appclim04-uptodate_monthly_climate_maps-daly.pdf, available at http://prism.nacse.org/.

Densmore, J.N., 2003, Simulation of ground-water-flow in the Irwin Basin aquifer system, Fort Irwin Training Center, California: U.S. Geological Survey Water-Resources Investigations Report 2002–4264, 69 p., https://pubs.er.usgs.gov/publication/wri024264.

Densmore, J.N., and Bohlke, J.K., 2000, Use of nitrogen isotopes to determine nitrate contamination in two desert basins in California: International Association of Hydrological Sciences (IAHS) Interdisciplinary Perspective on Drinking Water Risk Assessment and Management Proceedings, Santiago Chile, September 1998, p. 63–73.

Densmore, J.N., and Londquist, C.J., 1997, Ground-water hydrology and water quality of Irwin Basin at Fort Irwin National Training Center, California: U.S. Geological Survey Water-Resources Investigations Report 97–4092, 159 p., https://pubs.er.usgs.gov/publication/wri974092.

Doherty, J,, 2010a, PEST, model-independent parameter estimation—User manual (5th ed., with slight additions): Brisbane, Australia, Watermark Numerical Computing.

Doherty, J., 2010b, Addendum to the PEST manual: Brisbane, Australia, Watermark Numerical Computing.

Doherty, J., 2010c, BeoPEST for Windows: Brisbane, Australia, Watermark Numerical Computing.

Donahue, D.J., Linick, T.W., and Jull, A.J.T., 1990, Isotope-ratio and background corrections for accelerator mass spectrometry radiocarbon measurements: Radiocarbon, v. 32, book 2, p. 135–142.

EarthInfo, Inc., 1995, National Climatic Data Center summary of the day—West 1994: Boulder, Colo., EarthInfo, Inc., CD-ROM.

EarthInfo, Inc., 2000, EarthInfo CD2 reference manual—for all EarthInfo CD-ROM databases: Boulder, Colo., EarthInfo, Inc.

Epstein, S., and Mayeda, T.K., 1953, Variation of O^{18} content of water from natural sources: Geochimica et Cosmochimica Acta, v. 4, no. 5, p. 213–224, https://doi.org/10.1016/0016-7037(53)90051-9.

Fetter, C.W., 1994, Applied Hydrogeology (3rd ed.): New York, Macmillan College Publishing, Inc., 616 p.

Fielding, E.J., Blom, R.G., and Goldstein, R.M., 1998, Rapid subsidence over oil fields measured by SAR interferometry: Geophysical Research Letters, v. 25, no. 17, p. 3215–3218, https://doi.org/10.1029/98GL52260.

Fitterman, D.V., and Labson, V.F., 2005, Electromagnetic induction methods for environmental problems, chap. 10 *in* Butler, D.K., ed., Near-surface geophysics: Society of Exploration—Geophysicists, Investigations in Geophysics, no. 13, p. 301–355, http://dx.doi.org/10.1190/1.9781560801719.ch10.

Flint, A.L., and Flint, L.E., 2007a, Application of the basin characterization model to estimate in-place recharge and runoff potential in the basin and range carbonate-rock aquifer system, White Pine County, Nevada, and adjacent areas in Nevada and Utah: U.S. Geological Survey Scientific Investigations Report 2007–5099, 21 p., https://pubs.er.usgs.gov/publication/sir20075099.

Flint, L.E., and Flint, A.L., 2007b, Regional analysis of ground-water recharge, chap. B *in* Stonestrom, D.A., Constantz, J., Ferré, T.P.A., and Leake, S.A., eds., Ground-water recharge in the arid and semiarid southwestern United States: U.S. Geological Survey Professional Paper 1703–B, p. 29–60, https://pubs.er.usgs.gov/publication/pp1703B.

Flint, A.L., Flint, L.E., Hevesi, J.A., and Blainey, J.B., 2004, Fundamental concepts of recharge in the Desert Southwest—A regional modeling perspective, *in* Hogan, J.F., Phillips, F.M., and Scanlon, B.R., eds., Groundwater recharge in a desert environment—The southwestern United States: Washington D.C., American Geophysical Union, Water Science and Application, Series 9, p. 159–184, https://ca.water.usgs.gov/pubs/FLint_recharge-concepts-modeling_2004.pdf.

Fournier, R.O., and Thompson, J.M., 1980, The recharge area for the Coso, California, geothermal system deduced from δD and $\delta^{18}O$ in thermal and nonthermal waters in the region: U.S. Geological Survey Open-File Report 80–454, 27 p., https://pubs.er.usgs.gov/publication/ofr80454.

Freeze, R.A., and Cherry, J.A., 1979, Groundwater: Englewood Cliffs, N.J., Prentice Hall, 604 p.

Friedman, I., Smith, G.I., Gleason, J.D., Warden, A., and Harris, J.M., 1992, Stable isotope composition of waters in southeastern California—1. Modern precipitation: Journal of Geophysical Research, v. 97, no. D5, p. 5795–5812, https://doi.org/10.1029/92JD00184.

Gagnon, A.R., and Jones, G.A., 1993, AMS-graphite target production methods at the Woods Hole Oceanographic Institution during 1986–1991: Radiocarbon, v. 35, no. 2, p. 301–310, https://doi.org/10.1017/S0033822200064985.

Galloway, D.L., Hudnut, K.W., Ingebritsen, S.E., Phillips, S.P., Peltzer, G., Rogez, F., and Rosen, P.A., 1998, Detection of aquifer system compaction and land subsidence using interferometric synthetic aperture radar, Antelope Valley, Mojave Desert, California: Water Resources Research, v. 34, no. 10 p. 2573–2585, https://doi.org/10.1029/98WR01285.

García, M.G., and Borgnino, L., 2015, Fluoride in the context of the environment, chap. 1 *in* Preedy, V.R., ed., Fluorine–Chemistry, analysis, function and effects: Washington D.C., Royal Society of Chemistry, p. 3–21, https://doi.org/10.1039/9781782628507-00003.

Gonfiantini, R., 1978, Standards for stable isotope measurements in natural compounds: Nature, v. 271, p. 534–536, https://doi.org/10.1038/271534a0.

Harbaugh, A.W., 2005, MODFLOW-2005, The U.S. Geological Survey modular groundwater model—The groundwater flow process: U.S. Geological Survey Techniques and Methods 6–A16, variously p., https://pubs.er.usgs.gov/publication/tm6A16.

Hill, M.C., Banta, E.R., Harbaugh, A.W., and Anderman, E.R., 2000, MODFLOW-2000, the U.S. Geological Survey modular ground-water model—User guide to the observation, sensitivity, and parameter-estimation process and three post-processing programs: U.S. Geological Survey Open-File Report 2000–184, 209 p., https://pubs.er.usgs.gov/publication/ofr00184.

Hoffmann, J., Leake, S.A., Galloway, D.L., and Wilson, A.M., 2003, MODFLOW-2000 ground-water model—User guide to the subsidence and aquifer-system compaction (SUB) package: U.S. Geological Survey Open-File Report 2003–233, 44 p., https://pubs.er.usgs.gov/publication/ofr03233.

Hsieh, P.A., and Freckleton, J.R., 1993, Documentation of a computer program to simulate horizontal-flow barriers using the U.S. Geological Survey's modular three-dimensional finite-difference ground-water flow model: U.S. Geological Survey Open-File Report 92–477, 32 p., https://pubs.er.usgs.gov/publication/ofr92477.

International Atomic Energy Agency, 1981, Stable isotope hydrology—Deuterium and oxygen-18 in the water cycle: Vienna, Austria, IAEA Technical Reports Series No. 210, 339 p., http://www-naweb.iaea.org/napc/ih/documents/IAEA%20Monographs/TRS%20210%20Stable%20Isotope%20Hydrology1981.pdf.

Izbicki, J.A., 2004, Source and movement of ground water in the western part of the Mojave Desert, Southern California, USA: U.S. Geological Survey Water-Resources Investigations Report 2003–4313, 36 p., https://pubs.er.usgs.gov/publication/wri034313.

Izbicki, J.A., and Michel, R.L., 2004, Movement and age of ground water in the western part of the Mojave Desert, southern California, USA: U.S. Geological Survey Water-Resources Investigations Report 2003–4314, 42 p., https://pubs.er.usgs.gov/publication/wri034314.

Izbicki, J.A., Martin, P.M., and Michel, R.L., 1995, Source, movement, and age of groundwater in the upper part of the Mojave River Basin, California, USA, *in* Adar, E.M., and Leibundgut, C., eds., Proceedings of the 1994 Interantional Symposium on Application of tracers in arid zone hydrology: International Association of Hydrological Sciences, no. 232, p. 43–56.

Izbicki, J.A., Radyk, J., and Michel, R.L., 2002, Movement of water through the thick unsaturated zone underlying Oro Grande and Sheep Creek washes in the western Mojave Desert, USA: Hydrogeology Journal, v. 10, no. 3, p. 409–427, https://link.springer.com/article/10.1007/s10040-002-0194-8.

Jachens, R.C., and Langenheim, V.E., 2014, Gravity survey and interpretation of Fort Irwin and vicinity, Mojave Desert, California, chap. H *in* Buesch, D.C., ed., Geology and geophysics applied to groundwater hydrology at Fort Irwin, California: U.S. Geological Survey Open-File Report 2013–1024, 11 p., https://doi.org/10.3133/ofr20131024H.

James M. Montgomery and Associates, 1981, Water supply investigation, Fort Irwin, San Bernardino County, California—Phase II, Final report on ground water basin development and management: Consultant's report prepared for and in the files of the U.S. Army Corps of Engineers, Sacramento District, variously paged.

Kalin, R.M., 2000, Radiocarbon dating of groundwater systems, *in* Cook, P.G., and Herczeg, A.L., eds., Environmental tracers in subsurface hydrology: Boston, Mass., Kluwer Academic Publishers, p. 111–144, https://doi.org/10.1007/978-1-4615-4557-6_4.

Kjos, A.R., Densmore, J.N., Nawikas, J.M., and Brown, A.A., 2014, Construction, water-level, and water-quality data for multiple-well monitoring sites and test wells, Fort Irwin National Training Center, San Bernardino County, California, 2009–12: U.S. Geological Survey Data Series 788, 139 p., https://doi.org/10.3133/ds788.

Konikow, L.F., Hornberger, G.Z., Halford, K.J., and Hanson, R.T., 2009, Revised multi-node well (MNW2) package for MODFLOW ground-water flow model: U.S. Geological Survey Techniques and Methods 6–A30, 67 p., https://pubs.er.usgs.gov/publication/tm6A30.

Kunkel, F,, and Riley, F.S., 1959, Geologic reconnaissance and test-well drilling, Camp Irwin, California: U.S. Geological Survey Water Supply Paper 1460–F, p. 233–271, https://pubs.er.usgs.gov/publication/wsp1460F.

Leake, S.A., Leahy, P.P., and Navoy, A.S., 1994, Documentation of a computer program to simulate transient leakage from confining units using the modular finite-difference ground-water flow model: U.S. Geological Survey Open-File Report 94–59, 70 p., https://pubs.er.usgs.gov/publication/ofr9459.

Lohman, S.W., 1972, Ground-water hydraulics: U.S. Geological Survey Professional Paper 708, 70 p., https://pubs.er.usgs.gov/publication/pp708.

Massonnet, D., Rossi, M., Carmona, C., Adragna, F., Peltzer, G., Feigl, K., and Rabaute, T., 1993, The displacement field of the Landers earthquake mapped by radar interferometry: Nature, v. 364, p. 138–142, https://www.nature.com/nature/journal/v364/n6433/abs/364138a0.html.

Massonnet, D., Briole, P., and Arnaud, A., 1995, Deflation of Mount Etna monitored by space-borne radar interferometry: Nature, v. 375, p. 567–570, https://www.nature.com/nature/journal/v375/n6532/abs/375567a0.html.

Massonnet, D., Holzer, T., and Vadon, H., 1997, Land subsidence caused by the East Mesa geothermal field, California, observed using SAR interferometry: Geophysical Research Letters, v. 24, no. 8, p. 901–904, http://onlinelibrary.wiley.com/doi/10.1029/97GL00817/pdf.

Mendenhall, W.C., 1909, Some desert watering places in southeastern California and southwestern Nevada: U.S. Geological Survey Water Supply Paper 224, 98 p., https://pubs.er.usgs.gov/publication/wsp224.

Michel, R.L., 1976, Tritium inventories of the world oceans and their implications: Nature, v. 263, p. 103–106, https://www.nature.com/articles/263103a0.

Miller, D.M., and Yount, J.C., 2002, Late Cenozoic tectonic evolution of the north-central Mojave Desert inferred from fault history and physiographic evolution of the Fort Irwin area, California, *in* Glazner, A.F., Walker, J.D., and Bartley, J.M., eds., Geologic evolution of the Mojave Desert and southwestern basin and range: Boulder, Colo., Geological Society of America Memoirs, v. 195, p. 173–197.

Miller, D.M., Yount, J.C., Schermer, E.R., and Felger, T.J., 1994, Preliminary assessment of the recency of faulting at southwestern Fort Irwin, north-central Mojave Desert, California: San Bernardino County Museum Association Special Publications, 94–1, p. 41–52.

Miller, D.M., Menges, C.M., and Lidke, D.J., 2014, Generalized surficial geologic map of the Fort Irwin area, San Bernardino County, California, chap. B *of* Buesch, D.C., ed., Geology and geophysics applied to groundwater hydrology at Fort Irwin, California: U.S. Geological Survey Open-File Report 2013–1024, 11 p., https://doi.org/10.3133/ofr20131024B.

Mook, W.G., 1980, The dissolution-exchange model for dating of groundwater with ^{14}C, *in* Fritz, Peter, and Fontes, J.C., eds., Handbook of Environmental Isotopes Geochemistry: Amsterdam, Netherlands, Elsevier, v. 1, p. 50–74.

Morin, R.L., 2000, Basement structure beneath Langford Well Lake Basin, Fort Irwin, California, based on inversion of gravity data: U.S. Geological Survey Open-File Report 2000–518, 13 p., https://pubs.er.usgs.gov/publication/ofr00518.

Munsell Color, 1975, Munsell soil color charts: Baltimore, Md., Munsell Color, Macbeth Division of Kollmorgen Corporation, 27 p.

National Oceanic and Atmospheric Administration, 1994, Annual summary, California, 1994: Asheville, N.C., Climatological Data, v. 98, no. 13. accessed 1999, at http://www.ncdc.noaa.gov/IPS/cd/cd.html.

National Oceanic and Atmospheric Administration, 2010, Annual summary, California, 2010: Asheville, N.C., Climatological Data, v. 114, no. 13, accessed November 26, 2014, at http://www.ncdc.noaa.gov/IPS/cd/cd.html.

National Oceanic and Atmospheric Administration, 2014, Annual summary, California, 2014: Asheville, N.C., Climatological Data, v. 118, no. 13, accessed November 26, 2014, at http://www.ncdc.noaa.gov/IPS/cd/cd.html.

Niswonger, R.G., Panday, S., and Ibaraki, M., 2011, MODFLOW-NWT, A Newton formulation for MODFLOW-2005: U.S. Geological Survey Techniques and Methods 6–A37, 32 p., https://pubs.er.usgs.gov/publication/tm6A37.

Piper, A.M., 1945, A graphic procedure in the geochemical interpretation of water-analyses: American Geophysical Union Transactions, 25th Annual Meeting, p. 914–928, https://doi.org/10.1029/TR025i006p00914.

Poland, J.F., ed., 1984, Guidebook to studies of land subsidence due to ground-water withdrawal, v. 40 of UNESCO Studies and Reports in Hydrology: Paris, France, United Nations Educational, Scientific and Cultural Organization, 305 p.

Rewis, D.L., Christensen, A.H., Matti, J.C., Hevesi, J.A., Nishikawa, T., and Martin, P., 2006, Geology, ground-water hydrology, geochemistry, and ground-water simulation of the Beaumont and Banning storage units, San Gorgonio Pass area, Riverside County, California: U.S. Geological Survey Scientific Investigations Report 2006–5026, 191 p., https://pubs.er.usgs.gov/publication/sir20065026.

Schermer, E.R., Luyendyk, B.P., and Cisowski, S., 1996, Late Cenozoic structure and tectonics of the northern Mojave Desert: Tectonics, v. 15, no. 5, p. 905–932, https://doi.org/10.1029/96TC00131.

Schneider, R.J., Jones, G.A., McNichol, A.P., von Reden, K.F., Elder, K.L., Huang, K., and Kessel, E.D., 1994, Methods for data screening, flagging, and error analysis at the National Ocean Sciences AMS Facility: Nuclear instruments and methods in physics research, section B—Beam interactions with materials and atoms, v. 92, no. 1–4, p. 172–175, https://doi.org/10.1016/0168-583X(94)96000-3.

Smith, G.I., Friedman, I., Veronda, G., and Johnson, C.A., 2002, Stable isotope compositions of waters in the Great Basin, United States—3. Comparison of groundwaters with modern precipitation: Journal of Geophysical Research—Atmospheres, v. 107, no. D19, https://doi.org/10.1029/2001JD000567.

Sneed, M., and Brandt, J.T., 2007, Detection and measurement of land subsidence using global positioning system surveying and interferometric synthetic aperture radar, Coachella Valley, California, 1996–2005: U.S. Geological Survey Scientific Investigations Report 2007–5251 v. 2.0, 31 p., https://pubs.er.usgs.gov/publication/sir20075251.

Stiff, H.A., Jr., 1951, The interpretation of chemical water analysis by means of patterns: Journal of Petroleum Technology, v. 3, no. 10, p. 15–17, https://doi.org/10.2118/951376-G.

Thatcher, L.L., Janzer, V.J., and Edwards, K.W., 1977, Methods for determination of radioactive substances in water and fluvial sediments: U.S. Geological Survey Techniques of Water-Resources Investigations, book 5, chap. A5, 95 p., https://pubs.er.usgs.gov/publication/twri05A5.

Thomasson, H.G., Jr., Olmsted, F.H., and LeRoux, E.F., 1960, Geology, water resources, and usable ground-water storage capacity of part of Solano County, California: U.S. Geological Survey Water Supply Paper 1464, 693 p., https://pubs.er.usgs.gov/publication/wsp1464.

Traum, J.A., Phillips, S.P., Bennett, G.L., Zamora, C., and Metzger, L.F., 2014, Documentation of a groundwater flow model (SJRRPGW) for the San Joaquin River restoration program study area, California: U.S. Geological Survey Scientific Investigations Report 2014–5148, 151 p., https://doi.org/10.3133/sir20145148.

Umari, M.J., Martin, P.M., Schroeder, R.A., Duell, F.W., and Fay, R.G., 1993, Potential for ground-water contamination from movement of wastewater through the unsaturated zone, upper Mojave River Basin, California: U.S. Geological Survey Water-Resources Investigations Report 93–4137, 117 p., https://pubs.usgs.gov/wri/1993/4137/report.pdf.

U.S. Environmental Protection Agency, 2002, Drinking water standards: accessed September 3, 2002, at http://www.epa.gov/safewater/standards.html.

U.S. Geological Survey, 2000, National Elevation Dataset (NED) 1/3 arc-second: U.S. Geological Survey, The National Map, 1x1-degree tile n36w117, accessed January 10, 2001, at https://nationalmap.gov/elevation.html.

Vogel, J.S., Nelson, D.E., and Southon, J.R., 1987, ^{14}C background levels in an accelerator mass spectrometry system: Radiocarbon, v. 29, no. 3, p. 323–333, https://doi.org/10.1017/S0033822200043733.

Voronin, L.M., Densmore, J.N., Martin, P., Brush, C.F., Carlson, C.S., and Miller, D.M., 2013, Geohydrology, geochemistry, and groundwater simulation (1992–2011) and analysis of potential water-supply managment options, 2010–60, of the Langford Basin, California: U.S. Geological Survey Scientific Investigations Report 2013–5101, 86 p., https://pubs.er.usgs.gov/publication/sir20135101.

Voronin, L.M., Densmore, J.N., and Martin, P., 2014, Analysis of potential water-supply management options, 2010–60, and documentation of revisions to the model of the Irwin Basin aquifer system, Fort Irwin National Training Center, California: U.S. Geological Survey Scientific Investigations Report 2014–5081, 34 p., https://doi.org/10.3133/sir20145081.

Walter, D.A., and Whealan, A.T, 2005, Simulated water sources and effects of pumping on surface and ground water, Sagamore and Monomoy flow lenses, Cape Cod, Massachusetts: U.S. Geological Survey Scientific Investigations Report 2004–5181, 85 p., https://pubs.er.usgs.gov/publication/sir20045181.

Welch, A.H., Lico, M.S., and Hughes, J.L., 1988, Arsenic in ground water of the western United States: Groundwater, v. 26, no. 3, p. 333–347, https://doi.org/10.1111/j.1745-6584.1988.tb00397.x.

Western Regional Climate Center (WRCC-DRI), 2009, Period of record monthly climate summary: Desert Research Institute web pages accessed February 17, 2009, at https://wrcc.dri.edu/cgi-bin/cliMAIN.pl?ca3498.

Wilde, F.D., Radtke, D.B., Gibs, J., and Iwatsubo, R.T., eds., 1999, Collection of water samples: U.S. Geological Survey Techniques for Water-Resources Investigations, book 9, chap. A4.3, 91 p., accessed July 15, 2010, at http://pubs.water.usgs.gov/twri9A4.3.

Wilde, F.D., Radtke, D.B., Gibs, J., and Iwatsubo, R.T., 2004, Processing of water samples: U.S. Geological Survey Techniques of Water-Resources Investigations, book 9, chap. A5, accessed July 15, 2010, at http://pubs.water.usgs.gov/twri9A5/.

Wilson F. So and Associates, Inc., 1989, U.S. Army National Training Center at Fort Irwin, California, water basin development plan, final report: Consultant's report prepared for and in the files of the Commander of the National Training Center at Fort Irwin, 85 p.

Yount, J.C., Schermer, E.R., Felger, T.J., Miller, D.M., and Stephens, K.A., 1994, Preliminary geologic map of Fort Irwin Basin, north-central Mojave Desert, California: U.S. Geological Survey Open-File Report 94–173, 27 p., https://pubs.er.usgs.gov/publication/ofr94173.

Appendix 1. Borehole Data for Selected Wells in Bicycle Basin at Fort Irwin National Training Center, California, 1993–2011

The U.S. Geological Survey (USGS) drilled 6 multiple-well monitoring sites containing 18 wells in Bicycle Basin. Lithologic logs were based on observations recorded during drilling and analysis of drill cuttings collected from the borehole following methods described by Kjos and others (2014) compiled for each well.

Similar lithologic units, determined from the detailed lithologic logs (tables 1–1 to 1–6), were grouped to facilitate compilation of generalized lithologic columns (figs. 1–1 through 1–6). Depths of contacts between lithologic units were determined using borehole geophysical logs.

Table 1–1. Lithologic log from sieve samples for multiple-well monitoring site BLA2 (14N/3E-13M2–4), Bicycle Basin, Fort Irwin National Training Center, California.

[ft, feet]

Depth (ft)		Description
From	To	
0	20	No sample collected
20	40	Sand, fine to very loose and some gravel, granules to pebbles with rock fragments, poorly sorted; subrounded to subangular; moderate yellowish brown (10 YR 5/4) to dark yellowish brown (10 YR 4/2); some mica and mafic minerals.
40	60	Sand, fine to very coarse with granules, pebbles, and rock fragments; poorly sorted; subrounded to angular; moderate yellowish brown (10 YR 5/4) to dark yellowish brown (10 YR 4/2).
60	80	Sand, very fine to coarse with occasional rock fragments, some silt; subrounded to subangular; poorly sorted; moderate yellowish brown (10 YR 5/4) to dark yellowish brown (10 YR 4/2).
80	100	Sand, fine to very coarse with some granules and rock fragments; poorly sorted; subrounded (rock fragments are mostly angular); moderate yellowish brown (10 YR 5/4) to dark yellowish brown (10 YR 4/2).
100	130	Sand, very fine to very coarse with small pebbles, some rock fragments; poorly sorted; subrounded to subangular (rock fragments are angular); moderate yellowish brown (10 YR 5/4) to dark yellowish brown (10 YR 4/2).
130	140	Sand, very fine to coarse with silt and occasional rock fragments; poorly sorted; subrounded; olive gray (5 Y 3/2); abundance of mica and mafic minerals.
140	160	Silt with small amount of fine sand; occasional rock fragments; moderately well sorted; rock fragments are subrounded; light olive gray (5 Y 5/2); abundance of mafic minerals and mica.
160	180	Silt with small amount of very fine sand; occasional subrounded rock fragments; well sorted; olive gray (5 Y 3/2); abundance of mafic minerals and mica.
180	200	Ground-up rock fragments (mostly granitic) medium to very coarse grained, some fragments gravel-sized; grayish olive (10 Y 4/2).
200	220	Ground-up granitic rock, fine to medium ground; moderately well sorted; olive gray (5 Y 3/2); abundance of mafic minerals and mica.
220	240	Ground-up granitic rock, fine to coarse grained; moderately well sorted; occasional granule-size fragments; angular; olive gray (5 Y 3/2); abundance of mafic minerals and mica.
240	265	Ground-up granitic rock, fine to coarse, occasional granule size; poorly sorted; subangular to angular; olive gray (5 Y 3/2); abundance of mafic minerals and mica.

Table 1–2. Lithologic log from sieve samples for multiple-well monitoring site BA1 (14N/3E-22N1–2), Bicycle Basin, Fort Irwin National Training Center, California.

[ft, feet]

Depth (ft)		Description
From	To	
0	20	No sample collected
20	40	Sand, fine to very loose and some gravel, granules to pebbles with rock fragments, poorly sorted; subrounded to subangular; moderate yellowish brown (10 YR 5/4) to dark yellowish brown (10 YR 4/2); some mica and mafic minerals.
40	60	Sand, fine to very coarse with granules, pebbles, and rock fragments; poorly sorted; subrounded to angular; moderate yellowish brown (10 YR 5/4) to dark yellowish brown (10 YR 4/2).
60	80	Sand, very fine to coarse with occasional rock fragments, some silt; subrounded to subangular; poorly sorted; moderate yellowish brown (10 YR 5/4) to dark yellowish brown (10 YR 4/2).
80	100	Sand, fine to very coarse with some granules and rock fragments; poorly sorted; subrounded (rock fragments are mostly angular); moderate yellowish brown (10 YR 5/4) to dark yellowish brown (10 YR 4/2).
100	130	Sand, very fine to very coarse with small pebbles, some rock fragments; poorly sorted; subrounded to subangular (rock fragments are angular); moderate yellowish brown (10 YR 5/4) to dark yellowish brown (10 YR 4/2).
130	140	Sand, very fine to coarse with silt and occasional rock fragments; poorly sorted; subrounded; olive gray (5 Y 3/2); abundance of mica and mafic minerals.
140	160	Silt with small amount of fine sand; occasional rock fragments; moderately well sorted; rock fragments are subrounded; light olive gray (5 Y 5/2); abundance of mafic minerals and mica.
160	180	Silt with small amount of very fine sand; occasional subrounded rock fragments; well sorted; olive gray (5 Y 3/2); abundance of mafic minerals and mica.
180	200	Ground-up rock fragments (mostly granitic) medium to very coarse grained, some fragments gravel-sized; grayish olive (10 Y 4/2).
200	220	Ground-up granitic rock, fine to medium ground; moderately well sorted; olive gray (5 Y 3/2); abundance of mafic minerals and mica.
220	240	Ground-up granitic rock, fine to coarse grained; moderately well sorted; occasional granule-size fragments; angular; olive gray (5 Y 3/2); abundance of mafic minerals and mica.
240	265	Ground-up granitic rock, fine to coarse, occasional granule size; poorly sorted; subangular to angular; olive gray (5 Y 3/2); abundance of mafic minerals and mica.

Table 1–3*A*. Lithologic log from sieve samples for multiple well monitoring site BLA4 (14N/3E-23B1–3), Bicycle Basin, Fort Irwin National Training Center, California.

[Altitude of land surface, approximately 2,377 feet (ft). Drilled by U.S. Geological Survey December 8–12, 2007. Total depth drilled 865 ft. Screened intervals: 710–730, 440–460, 260–280 ft.]

Depth (ft)		Description
From	To	
0	20	Sand (S); very fine to medium sand; well sorted; subangular; brown (10YR 5/3).
20	40	Slightly gravelly sand ((g)S); fine to very coarse sand with granules to small pebbles; poorly sorted; subrounded to subangular; yellowish brown (10YR 5/4).
40	60	Slightly gravelly sand ((g)S); fine to very coarse sand with granules to small pebbles; poorly sorted; subrounded to subangular; yellowish brown (10YR 5/4).
60	80	Gravelly sand (gS); very fine to medium sand and granules to medium pebbles; poorly sorted; subrounded to subangular; yellowish brown (10YR 5/4).
80	100	Gravelly sand (gS); very fine to coarse sand and granules to small pebbles; poorly sorted; subangular; yellowish brown (10YR 5/4).
100	120	Sand (S); very fine to coarse sand; moderately to poorly sorted; subrounded; yellowish brown (10YR 5/4).
120	140	Gravelly sand (gS); very fine to very coarse sand and granules to small pebbles; poorly sorted; subrounded to subangular; yellowish brown (10YR 5/4).
140	160	Silty sand (zS); very fine to coarse sand and silt; moderately to poorly sorted; rounded to subrounded; brown (10YR 5/3).
160	180	Clay (C); clay; very well sorted; brown (10YR 5/3).
180	200	Silty sand (zS); very fine to coarse sand and silt; moderately to poorly sorted; rounded to subrounded; brown (10YR 5/3).
200	220	Silty sand (zS); very fine to coarse sand and silt; moderately to poorly sorted; rounded to subrounded; brown (10YR 5/3).
220	240	Clayey sand (cS); very fine to coarse sand and clay; moderately to poorly sorted; rounded to subrounded; brown (10YR 5/3).
240	260	Clay (C); clay; very well sorted; yellowish brown (10YR 5/4).
260	280	Gravelly sand (gS); fine to very coarse sand and granules to medium pebbles; poorly sorted; subrounded to subangular; dark yellowish brown (10YR 4/4).
280	300	Slightly gravelly clay ((g)M); clay with minor granules; poorly sorted; yellowish brown (10YR 5/4).
300	320	Sand (S); fine to coarse sand; well sorted; subrounded; yellowish brown (10YR 5/4).
320	340	Clayey sand (cS); fine to coarse sand and clay; moderately to poorly sorted; rounded to subrounded; yellowish brown (10YR 5/4).
340	360	Clayey silt (M); silt and clay; well sorted; yellowish brown (10YR 5/4).
360	380	Clayey silt (M); silt and clay; well sorted; yellowish brown (10YR 5/4).
380	400	Sandy clayey silt (sM); silt, clay and medium to coarse sand; moderately to poorly sorted; yellowish brown (10YR 5/4).
400	420	Sandy clay (sC); clay with medium to coarse sand; moderately to poorly sorted; yellowish brown (10YR 5/4).
420	440	Silty sand (zS); very fine to coarse sand and silt; moderately to poorly sorted; subangular to subrounded; yellowish brown (10YR 5/4).
440	460	Silty sand (zS); very fine to coarse sand and silt; moderately to poorly sorted; subangular to subrounded; yellowish brown (10YR 5/4).
460	480	Silty sand (zS); very fine to coarse sand and silt; moderately to poorly sorted; subangular to subrounded; yellowish brown (10YR 5/4).
480	500	Silty sand (zS); very fine to coarse sand and silt; moderately to poorly sorted; subangular to subrounded; yellowish brown (10YR 5/4).
500	520	Clayey silty sand (mS); very fine to medium sand and silt and clay; moderately sorted; rounded to subrounded; brown (10YR 5/3).
520	540	Slightly gravelly sand ((g)S); fine to coarse sand and minor granules; moderately to poorly sorted; subangular to subrounded; brown (10YR 5/3).
540	560	Silty sand (zS); very fine to coarse sand and silt; moderately to poorly sorted; subrounded; yellowish brown (10YR 5/4).
560	580	Gravelly sand (gS); fine to coarse sand and granules; moderately to poorly sorted; subangular to subrounded; yellowish brown (10YR 5/4).

Table 1–3*A*. Lithologic log from sieve samples for multiple well monitoring site BLA4 (14N/3E-23B1–3), Bicycle Basin, Fort Irwin National Training Center, California.—Continued

[Altitude of land surface, approximately 2,377 feet (ft). Drilled by U.S. Geological Survey December 8–12, 2007. Total depth drilled 865 ft. Screened intervals: 710–730, 440–460, 260–280 ft.]

Depth (ft)		Description
From	To	
580	600	Silty sand (zS); fine to coarse sand and silt; moderately to poorly sorted; subangular to subrounded; yellowish brown (10YR 5/4).
600	620	Sandy clay (sC); clay and fine to coarse sand; moderately to poorly sorted; yellowish brown (10YR 5/4).
620	640	Sand (S); fine to medium sand; well sorted; subangular to subrounded; yellowish brown (10YR 5/4).
640	660	Sandy clay (sC); clay and fine to coarse sand; moderately to poorly sorted; yellowish brown (10YR 5/4).
660	680	Sandy clay (sC); clay and fine to coarse sand; moderately to poorly sorted; yellowish brown (10YR 5/4).
680	700	Sandy clay (sC); clay and fine to medium sand; well to moderately sorted; rounded to subrounded; brown (10YR 5/3).
700	720	Silty sand (zS); fine to coarse sand and silt; moderately to poorly sorted; subrounded to subangular; brown (10YR 5/3).
720	740	Gravelly silty sand (gmS); very fine to coarse sand and silt and granules; poorly sorted; subrounded to subangular; brown (10YR 5/3).
740	760	Gravelly silty sand (gmS); very fine to coarse sand and silt and granules; poorly sorted; subrounded to subangular; brown (10YR 5/3).
760	780	Gravelly silty sand (gmS); very fine to coarse sand and silt and granules; poorly sorted; subrounded to subangular; brown (10YR 5/3).
780	800	Silty sand (zS); very fine to coarse sand and silt; poorly sorted; subrounded; brown (10YR 5/3).
800	820	Sandy clay (sC); clay and fine to very coarse sand; poorly sorted; brown (10YR 5/3).
820	840	Sandy clay (sC); clay and very fine to fine sand; well sorted; brown (10YR 5/3).
840	860	Sandy clay (sC); clay and very fine to fine sand; well sorted; brown (10YR 5/3).

Table 1–3*B*. Lithologic log from shaker samples for multiple well monitoring site BLA4 (14N/3E-23B1–3), Bicycle Basin, Fort Irwin National Training Center, California.

[ft, feet]

Depth (ft)	Description
10	Gravelly sand (gS); coarse to very coarse sand and granules; well sorted; subrounded to subangular; assorted colors.
20	Gravelly sand (gS); coarse to very coarse sand and granules; well sorted; subrounded to subangular; assorted colors.
30	Gravelly silty sand (gmS); coarse to very coarse sand, silt and granules; moderately sorted; subrounded to subangular; assorted colors.
40	Gravelly silty sand (gmS); coarse to very coarse sand, silt and granules; moderately sorted; subrounded to subangular; assorted colors.
50	Gravelly silty sand (gmS); coarse to very coarse sand, silt and granules; moderately sorted; subrounded to subangular; assorted colors.
60	Gravelly silty sand (gmS); coarse to very coarse sand, silt and granules; moderately sorted; subrounded to subangular; assorted colors.
70	Sandy gravel (sG); granules and very coarse sand; well sorted; subrounded to subangular; dark yellowish brown (10YR 4/4).
80	Gravelly sand (gS); very fine and very coarse sand and granules; well sorted; subrounded to subangular; light yellowish brown (10YR 6/4).
90	Gravelly sand (gS); very fine and very coarse sand and granules; well sorted; subrounded to subangular; light yellowish brown (10YR 6/4).
100	Gravelly silty sand (gmS); coarse to very coarse sand, silt and granules; moderately sorted; subrounded to subangular; yellowish brown (10YR 5/4).
110	Sand (S); very fine to very coarse sand; poorly sorted; subrounded to subangular; light yellowish brown (10YR 6/4).
120	Gravelly clay (gM); clay with granules; well sorted; yellowish brown (10YR 5/4).

Table 1–3*B*. Lithologic log from shaker samples for multiple well monitoring site BLA4 (14N/3E-23B1–3), Bicycle Basin, Fort Irwin National Training Center, California.—Continued

[ft, feet]

Depth (ft)	Description
130	Gravelly clayey sand (gmS); medium to very coarse sand, clay and granules; moderately sorted; subrounded to subangular; yellowish brown (10YR 5/4).
140	Gravelly silty sand (gmS); medium to very coarse sand, silt and granules to small pebbles; poorly sorted; subrounded to subangular; yellowish brown (10YR 5/4).
150	Silty sand (zS); very fine to coarse sand and silt; poorly sorted; subrounded to subangular; pale brown (10YR 6/3).
160	Sandy clay (sC); clay and very coarse sand; moderately sorted; yellowish brown (10YR 5/4).
170	Clay (C); clay; very well sorted; yellowish brown (10YR 5/4).
180	Sandy clay (sC); clay and coarse sand; moderately sorted; yellowish brown (10YR 5/4).
190	Gravelly silty sand (gmS); very fine to coarse sand, silt and granules to medium pebbles; very poorly sorted; subrounded to subangular; yellowish brown (10YR 5/4) .
200	Sandy clay (sC); clay and coarse to very coarse sand; moderately sorted; yellowish brown (10YR 5/4).
210	Gravelly silty sand (gmS); medium to very coarse sand, silt and granules; moderately sorted; subrounded to subangular; yellowish brown (10YR 5/4).
220	Sandy clay (sC); clay and coarse to very coarse sand; moderately sorted; yellowish brown (10YR 5/4).
230	Clay (C); clay; very well sorted; yellowish brown (10YR 5/4).
240	Sandy clay (sC); clay and coarse sand; moderately sorted; yellowish brown (10YR 5/4).
250	Clay (C); clay; very well sorted; yellowish brown (10YR 5/4).
260	Sandy clay (sC); clay and coarse sand; moderately sorted; yellowish brown (10YR 5/4).
270	Silty sand (zS); very fine to very coarse sand and silt; very poorly sorted; subrounded to subangular; yellowish brown (10YR 5/4).
280	Silty sand (zS); very fine to very coarse sand and silt; very poorly sorted; subrounded to subangular; yellowish brown (10YR 5/4).
290	Clay (C); clay; very well sorted; yellowish brown (10YR 5/4).
300	Sandy clay (sC); clay and coarse to very coarse sand; moderately sorted; yellowish brown (10YR 5/4).
310	Sandy clay (sC); clay and coarse to very coarse sand; moderately sorted; yellowish brown (10YR 5/4).
315 core shoe	Sandy clay (sC); clay and coarse sand; moderately sorted; yellowish brown (10YR 5/4).
320	Clay (C); clay; very well sorted; yellowish brown (10YR 5/4).
330	Gravelly silty sand (gmS); very fine to very coarse sand, silt and granules to small pebbles; very poorly sorted; subrounded to subangular; yellowish brown (10YR 5/4).
340	Gravelly clayey sand (gmS); coarse to very coarse sand, clay and granules to small pebbles; moderately to poorly sorted; subrounded to subangular; yellowish brown (10YR 5/4).
350	Gravelly clayey sand (gmS); coarse to very coarse sand, clay and granules to small pebbles; moderately to poorly sorted; subrounded to subangular; yellowish brown (10YR 5/4).
360	Clay (C); clay; very well sorted; yellowish brown (10YR 5/4).
370	Sandy clay (sC); clay and coarse sand; moderately sorted; yellowish brown (10YR 5/4).
380	Sandy clay (sC); clay and coarse sand; moderately sorted; yellowish brown (10YR 5/4).
390	Sandy clay (sC); clay and coarse sand; moderately sorted; yellowish brown (10YR 5/4).
400	Clay (C); clay; very well sorted; yellowish brown (10YR 5/4).
410	Sandy clay (sC); clay and coarse sand; moderately sorted; yellowish brown (10YR 5/4).
420	No sample collected.
430	Sandy clay (sC); clay and coarse sand; moderately sorted; yellowish brown (10YR 5/4).
440	Sandy clay (sC); clay and coarse sand; moderately sorted; yellowish brown (10YR 5/4).
450	Sandy clay (sC); clay and coarse sand; moderately sorted; yellowish brown (10YR 5/4).
460	Sandy clay (sC); clay and coarse sand; moderately sorted; yellowish brown (10YR 5/4).

Table 1–3*B*. Lithologic log from shaker samples for multiple well monitoring site BLA4 (14N/3E-23B1–3), Bicycle Basin, Fort Irwin National Training Center, California.—Continued

[ft, feet]

Depth (ft)	Description
470	Sandy clay (sC); clay and coarse sand; moderately sorted; yellowish brown (10YR 5/4).
480	Sandy clay (sC); clay and coarse sand; moderately sorted; yellowish brown (10YR 5/4).
490	Sandy silt (sZ); silt and coarse sand; moderately sorted; yellowish brown (10YR 5/4).
500	Sandy silt (sZ); silt and coarse sand; moderately sorted; yellowish brown (10YR 5/4).
510	Sandy silt (sZ); silt and coarse sand; moderately sorted; yellowish brown (10YR 5/4).
520	Silt (Z); silt; very well sorted; yellowish brown (10YR 5/4).
530	Sandy silt (sZ); silt and coarse sand; moderately sorted; yellowish brown (10YR 5/4).
540	Silty sand (zS); very fine sand to coarse sand and silt; poorly sorted; subrounded to subangular; yellowish brown (10YR 5/4).
550	Clay (C); clay; very well sorted; yellowish brown (10YR 5/4).
560	Sandy clay (sC); clay and coarse sand; moderately sorted; yellowish brown (10YR 5/4).
570	Sandy clay (sC); clay and coarse sand; moderately sorted; yellowish brown (10YR 5/4).
580	Sandy clay (sC); clay and coarse sand; moderately sorted; yellowish brown (10YR 5/4).
590	Sandy clay (sC); clay and coarse sand; moderately sorted; yellowish brown (10YR 5/4).
600	Sandy silt (sZ); silt and very fine to coarse sand; moderately to poorly sorted; yellowish brown (10YR 5/4).
610	Sandy clay (sC); clay and coarse sand; moderately sorted; yellowish brown (10YR 5/4).
620	Sandy clay (sC); clay and coarse sand; moderately sorted; yellowish brown (10YR 5/4).
630	Sandy clay (sC); clay and coarse sand; moderately sorted; yellowish brown (10YR 5/4).
640	Sandy clay (sC); clay and coarse sand; moderately sorted; yellowish brown (10YR 5/4).
650	Sandy clay (sC); clay and coarse sand; moderately sorted; yellowish brown (10YR 5/4).
660	Sandy clay (sC); clay and coarse sand; moderately sorted; yellowish brown (10YR 5/4).
Core	
670	Silt (Z); silt; very well sorted; yellowish brown (10YR 5/4).
680	Sandy clay (sC); clay and coarse sand; moderately sorted; yellowish brown (10YR 5/4).
690	Sandy clay (sC); clay and coarse sand; moderately sorted; yellowish brown (10YR 5/4).
700	Sandy clay (sC); clay and coarse sand; moderately sorted; yellowish brown (10YR 5/4).
710	Sandy clay (sC); clay and coarse sand; moderately sorted; yellowish brown (10YR 5/4).
720	Sandy clay (sC); clay and coarse sand; moderately sorted; yellowish brown (10YR 5/4).
730	Sandy clay (sC); clay and coarse sand; moderately sorted; yellowish brown (10YR 5/4).
740	Sandy clay (sC); clay and coarse sand; moderately sorted; yellowish brown (10YR 5/4).
750	Sandy clay (sC); clay and coarse sand; moderately sorted; yellowish brown (10YR 5/4).
760	Sandy clay (sC); clay and coarse sand; moderately sorted; yellowish brown (10YR 5/4).
770	Sandy clay (sC); clay and coarse sand; moderately sorted; yellowish brown (10YR 5/4).
780	Sandy clay (sC); clay and coarse sand; moderately sorted; yellowish brown (10YR 5/4).
790	Sandy clay (sC); clay and coarse sand; moderately sorted; yellowish brown (10YR 5/4).
800	Sandy clay (sC); clay and coarse sand; moderately sorted; yellowish brown (10YR 5/4).
810	Sandy clay (sC); clay and coarse sand; moderately sorted; yellowish brown (10YR 5/4).
820	Sandy clay (sC); clay and coarse sand; moderately sorted; yellowish brown (10YR 5/4).
830	Sandy clay (sC); clay and coarse sand; moderately sorted; yellowish brown (10YR 5/4).
840	Sandy clay (sC); clay and coarse sand; moderately sorted; yellowish brown (10YR 5/4).
850	Sandy clay (sC); clay and coarse sand; moderately sorted; yellowish brown (10YR 5/4).
860	Sandy clay (sC); clay and coarse sand; moderately sorted; yellowish brown (10YR 5/4).

Table 1–4. Lithologic log from sieve samples for multiple-well monitoring site BLA3 (14N/3E-24Q1–5), Bicycle Basin, Fort Irwin National Training Center, California.

[ft, feet]

Depth (ft)		Description
From	To	
0	20	Sand, some gravel, some clay, sand is poorly sorted, very fine to very coarse, gravel size granule to medium pebble; angular to subrounded; yellowish brown (10 YR 5/4).
20	40	Sand, some gravel, sand is very fine to very coarse, gravel size granule to large pebble; poorly sorted; angular to subrounded; yellowish brown (10 YR 5/4).
40	60	Sand, minor gravel, sand is skewed towards fine; gravel size granule to medium pebble; well sorted; angular to subrounded; yellowish brown (10 YR 5/6).
60	80	Gravelly sand, sand is very fine to very coarse; gravel size granule to large pebble; very poorly sorted; angular to subrounded; yellowish brown (10 YR 5/6).
80	100	Sand, minor gravel, trace clay, trace silt, sand is very fine to very coarse; gravel size granule to large pebble; poorly sorted; skewed towards fine angular to subrounded; yellowish brown (10 YR 5/4).
100	120	Gravelly sand, very fine to very coarse; granules to large cobbles; poorly sorted; angular to subrounded; yellowish brown (10 YR 5/6).
120	140	Sand granules, some clay, some gravel, very fine to very coarse sand; granules to large pebbles; poorly sorted; angular to subrounded; yellowish brown (10 YR 5/6).
140	160	Clayey sand, some gravel, very fine to very coarse; granules to large cobbles; poorly sorted; angular to subrounded; yellowish brown (10 YR 5/6).
160	180	Sandy gravel, granules to large cobbles, very fine to very coarse; poorly sorted; angular to subrounded; yellowish brown (10 YR 5/6).
180	200	Clayey sandy gravel, granules to large cobbles, very fine to very coarse; very poorly sorted; angular to subrounded; yellowish brown (10 YR 5/6).
200	220	Gravelly sand, some clay, granules to boulders, very fine to coarse sand; poorly sorted; angular to subrounded; yellowish brown (10 YR 5/6).
220	240	Gravelly sand, minor clay, granules to boulders, very fine to very coarse sand; moderately sorted; angular to subrounded; yellowish brown (10 YR 5/6).
240	260	Gravelly sand, some clay, very fine to very coarse; granules to cobbles; poorly sorted; angular to subrounded; yellowish brown (10 YR 5/4).
260	280	Gravelly sand, trace clay, very fine to very coarse; granules to cobbles; poorly sorted; angular to subrounded; yellowish brown (10 YR 5/6).
280	300	Gravelly sand, minor clay, very fine to very coarse sand; granules to cobbles; moderately sorted; angular to subrounded; yellowish brown (10 YR 5/6).
300	320	Gravelly sand, very fine to very coarse; granules to large pebbles; angular rock chips; moderately sorted; angular to subrounded; yellowish brown (10 YR 5/6).
320	340	Sand, some gravel, very fine to very coarse sand; granules to angular rock chips indicating broken pebbles and cobbles; poorly sorted; angular to subrounded; yellowish brown (10 YR 5/6).
340	360	Sand, some gravel, minor clay, very fine to very coarse; granules to pebbles; poorly sorted; angular to subrounded; yellowish brown (10 YR 5/4).
360	380	Sand, some gravel, very fine to very coarse; granules to small cobbles; moderately sorted; angular to subrounded; light yellowish brown (10 YR 6/4).
380	400	Gravelly sand, some clay, some silt, trace clay, very fine to very coarse; granules to cobbles; moderately sorted; angular chips from bit action to subrounded sand grains; light yellowish brown (10 YR 6/4).
400	420	Gravelly sand, very fine to very coarse; granules to cobbles; moderately sorted; skewed towards coarse; angular to subrounded; yellowish brown (10 YR 5/6).
420	440	Sand, some clay, some gravel, very fine to very coarse; granules to cobbles; moderately sorted; skewed towards fine; angular to subrounded; yellowish brown (10 YR 5/4).
440	460	Gravelly sand, minor clay, very fine to very coarse; granules to large cobbles; poorly sorted; angular to subrounded; yellowish brown (10 YR 5/6).

Table 1–4. Lithologic log from sieve samples for multiple-well monitoring site BLA3 (14N/3E-24Q1–5), Bicycle Basin, Fort Irwin National Training Center, California.—Continued

[ft, feet]

Depth (ft)		Description
From	To	
460	480	Gravelly sand, minor gravel, fine to very coarse; granules to large cobbles; well sorted; angular to rounded; yellowish brown (10 YR 5/6).
480	500	Clayey sand, some gravel, very fine to very coarse; granules to large cobbles; well sorted; angular to subrounded; yellowish brown (10 YR 5/6).
500	520	Silty sand, some clay, minor gravel, very fine to very coarse; granules; very well sorted; angular to subrounded; yellowish brown (10 YR 5/6).
520	540	Sand, very fine to very coarse; moderately sorted; angular to subrounded; yellowish brown (10 YR 5/6).
540	560	Sand, very fine to very coarse; poorly sorted; angular to subrounded; yellowish brown (10 YR 5/6).
560	580	Clayey sand, trace gravel, granules very fine to very coarse; well sorted; angular to subrounded; yellowish brown (10 YR 5/6).
580	600	Sand, some clay, some gravel, very fine to very coarse, granules to small cobbles; poorly sorted; angular to subrounded; yellowish brown (10 YR 5/6).
600	620	Clayey sand, very fine to very coarse; well sorted; angular to subrounded; yellowish brown (10 YR 4/2).
620	640	Sand, some silt, very fine to very coarse; moderately sorted; angular to subrounded; yellowish brown (10 YR 5/6).
640	660	Sand, very fine to very coarse; well sorted; angular to subrounded; yellowish brown (10 YR 5/6).
660	680	Sand, very fine to very coarse; moderately sorted, skewed toward medium; angular to subrounded; yellowish brown (10 YR 5/6).
680	700	Sand, minor clay, very fine to very coarse; poorly sorted; angular to subrounded; yellowish brown (10 YR 5/6).
700	720	Gravelly sand, very fine to very coarse; poorly sorted; angular to subrounded; yellowish brown (10 YR 5/6).
720	740	Gravelly sand, very fine to very coarse, granules to boulders; poorly sorted; angular to subrounded; pale brown (10 YR 6/3).
740	760	Gravelly sand, very fine to very coarse, granules to boulders; moderately sorted; skewed toward coarse; light olive gray (5 Y 5/2).
760	780	Gravelly sand, very fine to very coarse sand, granules to cobbles, increase in sand content; moderately sorted; angular to subrounded; light brown (5 YR 5/6).
780	800	Gravelly sand, very fine to very coarse, granules to boulders; poorly sorted; angular to subrounded; pale brown (10 YR 6/3).
800	820	Gravelly sand, very fine to very coarse sand, granules to cobbles; moderately sorted, skewed; angular to subrounded; light yellowish brown (10 YR 6/4).
820	840	Gravelly sand, very fine to very coarse, granules to cobbles; poorly sorted; angular to subrounded; light yellowish brown (10 YR 6/4).
840	860	Gravelly sand, very fine to very coarse, granules to cobbles; poorly sorted; angular to subrounded; light yellowish brown (10 YR 6/4).
860	880	Gravelly sand, very fine to very coarse, granules to boulders; poorly sorted; angular to subrounded; light yellowish brown (10 YR 6/4).
880	900	Gravelly sand, very fine to very coarse, granules to boulders; poorly sorted; angular to subrounded; light yellowish brown (10 YR 6/4).

Table 1–5*A*. Lithologic log from sieve samples and for multiple-well monitoring site BLA5 (14N/3E-26K1–4), Bicycle Basin, Fort Irwin National Training Center, California.

[Previously published in Kjos and others, 2014. Altitude of land surface, approximately 2,345 feet (ft). Drilled by U.S. Geological Survey using mud-rotary drilling method, March 19, 2011. Total depth drilled, 370 ft. Screened intervals, 320–340, 190–210, and 190–210 ft. Washed—sample was washed to remove fine grained material and drilling mud.]

Depth (ft)	Description
5 1C shoe	Clay (C); clay with trace very fine to fine sand; well sorted; brown (7.5YR 5/4); calcareous.
10 2C shoe	Clay (C); clay with trace very fine to fine sand; well sorted; brown (7.5YR 4/4); calcareous.
15 3C shoe	Clay (C); clay with trace very fine to fine sand; well sorted; brown (7.5YR 5/4); calcareous.
20 4C shoe	Clay (C); clay with trace very fine to fine sand; well sorted; brown (7.5YR 5/4); calcareous.
25 5C shoe	Clay (C); clay with trace very fine to fine sand; well sorted; brown (7.5YR 5/4); calcareous.
26.5 6C shoe	Clay (C); clay with trace very fine to fine sand; well sorted; brown (7.5YR 5/4); calcareous.
30 7C shoe	Clay (C); clay with trace very fine to fine sand; well sorted; brown (7.5YR 5/4); calcareous.
35 8C shoe	Clay (C); clay with trace very fine to fine sand; well sorted; brown (7.5YR 5/4); calcareous.
40 9C shoe	Clay (C); clay with trace very fine to fine sand; well sorted; brown (7.5YR 4/4); calcareous.
45 10C shoe	Clay (C); clay with trace very fine to fine sand; well sorted; brown (7.5YR 5/4).
50 11C shoe	Clay (C); clay with trace very fine to fine sand; well sorted; yellowish brown (10YR 5/4); extremely calcareous.
55 12C shoe	Sandy silt (sZ); silt with very fine to fine sand; well sorted; brown (7.5YR 5/4); slightly calcareous.
60 13C shoe	Silt (Z); silt with trace very fine to fine sand and trace large pebbles; moderately to well sorted; brown (7.5Y 5/4); calcareous.
70	Sandy clayey silt (sM); silt with clay, very fine to medium sand, and trace granules; moderately sorted; yellowish brown (10YR 5/4); calcareous.
80	Clay (C); clay with trace very fine to fine sand; well sorted; yellowish brown (10YR 5/6); calcareous.
90	Clay (C); clay with trace very fine to fine sand; well sorted; dark yellowish brown (10YR 4/4).
100	Clay (C); clay with trace very fine to fine sand; well sorted; yellowish brown (10YR 5/4).
110	Clay (C); clay with trace very fine to medium sand; well sorted; yellowish brown (10YR 5/4); calcareous.
120	Clay (C); clay with trace very fine to medium sand; well sorted; yellowish brown (10YR 5/4); calcareous.
130	Clay (C); clay with trace very fine to medium sand; well sorted; brown (7.5YR 4/4); slightly calcareous.
140	Silty clay (M); clay with silt and trace very fine to medium sand; moderately to well sorted; brown (7.5YR 4/4).
150	Clayey sandy silt (sM); silt with very fine to medium sand and clay; moderately sorted; yellowish brown (10YR 5/4); calcareous.
160	Clay (C); clay with trace very fine to fine sand; well sorted; yellowish brown (10YR 5/4).
170	Gravelly clayey silty sand (gmS); medium to very coarse sand with silt, clay, and granules; poorly sorted; angular to subangular; dark yellowish brown (10YR 4/4); slightly calcareous.
180	Gravelly clayey silty sand (gmS); medium to very coarse sand with silt, clay, and granules to small pebbles; very poorly sorted; angular to subangular; dark yellowish brown (10YR 4/4).
190	Gravelly clayey silty sand (gmS); medium to very coarse sand with silt, clay, and granules; very poorly sorted; angular to subangular; yellowish brown (10YR 5/4).

Table 1–5*A*. Lithologic log from sieve samples and for multiple-well monitoring site BLA5 (14N/3E-26K1–4), Bicycle Basin, Fort Irwin National Training Center, California.—Continued

[Previously published in Kjos and others, 2014. Altitude of land surface, approximately 2,345 feet (ft). Drilled by U.S. Geological Survey using mud-rotary drilling method, March 19, 2011. Total depth drilled, 370 ft. Screened intervals, 320–340, 190–210, and 190–210 ft. Washed—sample was washed to remove fine grained material and drilling mud.]

Depth (ft)	Description
200	Sandy silty clay (sM); clay with silt and fine sand with trace coarse sand; moderately sorted; dark yellowish brown (10YR 4/4); slightly calcareous.
210	Sandy silty clay (sM); clay with silt and fine to coarse sand; moderately to poorly sorted; yellowish brown (10YR 5/4).
220	Gravelly clayey silty sand (gmS); medium to very coarse sand with silt, clay, and granules with trace small to medium pebbles; very poorly sorted; angular to subangular; yellowish brown (10YR 5/4).
230	Silty sandy gravel (msG); granules to medium pebbles with coarse to very coarse sand and silt; moderately to poorly sorted; angular to subangular; dark yellowish brown (10YR 4/4); slightly calcareous.
240	Silty sandy gravel (msG); granules to medium pebbles with silt and coarse to very coarse sand; moderately to poorly sorted; angular to subangular; dark yellowish brown (10YR 4/4); slightly calcareous.
250	Silty sandy gravel (msG); granules to medium pebbles with coarse to very coarse sand and silt; moderately to poorly sorted; angular to subangular; dark yellowish brown (10YR 4/4); slightly micaceous.
260	Silty clayey gravelly sand (gmS); medium to very coarse sand with granules to small pebbles, clay and silt; very poorly sorted; angular to subangular; brown (10YR 4/3).
270	Clayey gravelly sand (gmS); medium to very coarse sand with granules to small pebbles and clay; moderately to poorly sorted; angular to subangular; light olive brown (2.5Y 5/3); calcareous.
280	Silty clayey gravelly sand (gmS); medium to very coarse sand with granules, clay, and silt; very poorly sorted; angular to subangular; olive (5Y 4/3); slightly calcareous.
290	Silty clayey gravelly sand (gmS); medium to very coarse sand with granules, clay, and silt; very poorly sorted; angular to subangular; olive (5Y 4/3); slightly calcareous.
300	Sandy gravelly clayey silt (gM); silt with clay, granules, medium to very coarse sand, and trace small pebbles; very poorly sorted; light olive brown (2.5Y 5/4); calcareous; slightly micaceous.
310	Silty gravelly clayey sand (gmS); medium to very coarse sand with clay, granules, and silt; very poorly sorted; angular to subangular; light olive brown (2.5Y 5/4); slightly calcareous; slightly micaceous.
310 Washed	Gravelly sand (gS); coarse to very coarse sand with granules to small pebbles; well to moderately sorted; very angular to angular; yellowish brown (10YR 5/4); abundant microcrystalline quartz.
320	Sandy clayey silt (sM); silt with clay and medium to very coarse sand; poorly sorted; olive (5Y 5/3); slightly calcareous.
330	Silty clayey sand (mS); medium to very coarse sand with silt, clay, and trace granules to small pebbles; poorly sorted; angular to subangular; olive (5Y 4/3).
340	Silty gravelly sand (gmS); medium to very coarse sand with granules to small pebbles and silt; poorly sorted; angular to subangular; olive brown (2.5Y 4/3); slightly micaceous.
350	Silty gravelly sand (gmS); medium to very coarse sand with granules to small pebbles and silt; poorly sorted; angular to subrounded; olive brown (2.5Y 4/4); micaceous.
360	gravelly sand (gmS); coarse to very coarse sand with granules to small pebbles and silt; poorly sorted; angular to subangular; olive brown (2.5Y 4/4); calcareous; micaceous.
370	Gravelly sand (gS); coarse to very coarse sand with granules to small pebbles and trace silt; moderately to poorly sorted; angular to subangular; light olive brown (2.5Y 5/3); abundant quartz.
370 Washed	Gravelly sand (gS); coarse to very coarse sand with granules to small pebbles; well to moderately sorted; very angular to subangular; yellowish brown (10YR 5/4); slightly calcareous; abundant microcrystalline quartz.

Table 1–5*B*. Lithologic log from shaker samples for multiple-well monitoring site BLA5 (14N/3E-26K1–4), Bicycle Basin, Fort Irwin National Training Center, California.

[Previously published in Kjos and others, 2014. Altitude of land surface, approximately 2,345 feet (ft). Drilled by U.S. Geological Survey using mud-rotary drilling method, March 19, 2011. Total depth drilled, 370 ft. Screened intervals, 320–340, 190–210, and 190–210 ft.]

Depth (ft)		Description
From	To	
0	60	No sample collected; cored interval.
60	80	Clay (C); clay with trace very fine to medium sand; well to moderately sorted; brown (7.5YR 5/4); calcareous.
80	100	Clay (C); clay with trace very fine to medium sand; well to moderately sorted; brown (7.5YR 5/3); calcareous.
100	120	Clay (C); clay with trace very fine to medium sand; well to moderately sorted; brown (7.5YR 5/3); slightly calcareous.
120	140	Clay (C); clay with trace very fine to medium sand; well to moderately sorted; brown (7.5YR 5/4); slightly calcareous.
140	160	Clay (C); clay with trace very fine to medium sand; well to moderately sorted; brown (7.5YR 5/3); calcareous.
160	180	Silty sand (zS); very fine to medium sand with silt; well to moderately sorted; angular to subangular; dark yellowish brown (10YR 4/4); calcareous.
180	200	Slightly gravelly silty sand ((g)mS); fine to coarse sand with silt and granules to small pebbles; poorly sorted; angular to subangular; dark yellowish brown (10YR 4/4); slightly calcareous.
200	220	Clayey silty sand (mS); fine to coarse sand with silt and clay; moderately to poorly sorted; angular to subangular; dark yellowish brown (10YR 4/4); slightly calcareous.
220	240	Silty sand (zS); fine to coarse sand with silt; well to moderately sorted; angular to subangular; brown (10YR 4/3); slightly calcareous.
240	260	Slightly gravelly silty sand ((g)mS); medium to very coarse sand with silt and granules to small pebbles; moderately to poorly sorted; subangular to subrounded; brown (10YR 4/3); calcareous.
260	280	Sand (S); medium to very coarse sand with trace granules, silt and trace fine sand; moderately to poorly sorted; subangular to subrounded; dark grayish brown (2.5Y 4/2); slightly calcareous; micaceous.
280	300	Silty sand (zS); medium to very coarse sand with silt, trace granules and trace fine sand; poorly sorted; subangular to subrounded; very dark grayish brown (2.5Y 3/2); micaceous.
300	320	Silty sand (zS); fine to coarse sand with silt and trace granules to small pebbles; moderately to poorly sorted; subangular to subrounded; very dark grayish brown (2.5Y 3/2); micaceous.
320	340	Silty sand (zS); fine to coarse sand with silt and trace very coarse sand; moderately to poorly sorted; subangular to subrounded; very dark grayish brown (2.5Y 3/2); calcareous; micaceous.
340	360	Slightly gravelly silty sand ((g)mS); medium to very coarse sand with silt and granules to medium pebbles; moderately to poorly sorted; angular to subangular; olive brown (2.5Y 4/3); calcareous; micaceous.
360	370	Slightly gravelly silty sand ((g)mS); medium to very coarse sand with silt and granules to small pebbles; moderately to poorly sorted; angular to subangular; olive brown (2.5Y 4/3).

Table 1–6. Lithologic log of sieve samples log for multiple-well monitoring site BLA1 (14N/3E-35C2–3), Bicycle Basin, Fort Irwin National Training Center, California.

[ft, feet]

Depth (ft)		Description
From	To	
0	20	Sand, fine to coarse with granules and pebbles; poorly sorted; subangular to subrounded; moderate yellowish brown (10 YR 5/4).
20	40	Gravel, granules to pebbles with sand, fine to coarse; poorly sorted; angular to subrounded; moderate yellowish brown (10 YR 5/4).
40	60	Sand, fine to coarse with granules and pebbles; poorly sorted; subrounded ; mafic minerals, mica; dark yellowish brown (10 YR 4/2).
60	105	Gravel, granules to pebbles, with sand, fine to coarse; pootly sorted; angular to subrounded; mafic minerals; dark yellowish brown (10 YR 4/2).
105	120	Clay with sand, fine and medium; abundant mica; olive gray (5 Y 3/2).
120	140	Clay with fine sand, granules and pebbles; abundant mica; olive gray (5 Y 3/2).
140	175	Clay with sand, fine to medium, granules, and pebbles; abundant mica; olive gray (5 Y 3/2).
175	198	Fractured granitic bedrock, angular fragments; biotite, hornblend, feldspar, quartz.
198	200	Diorite with calcified fracture.

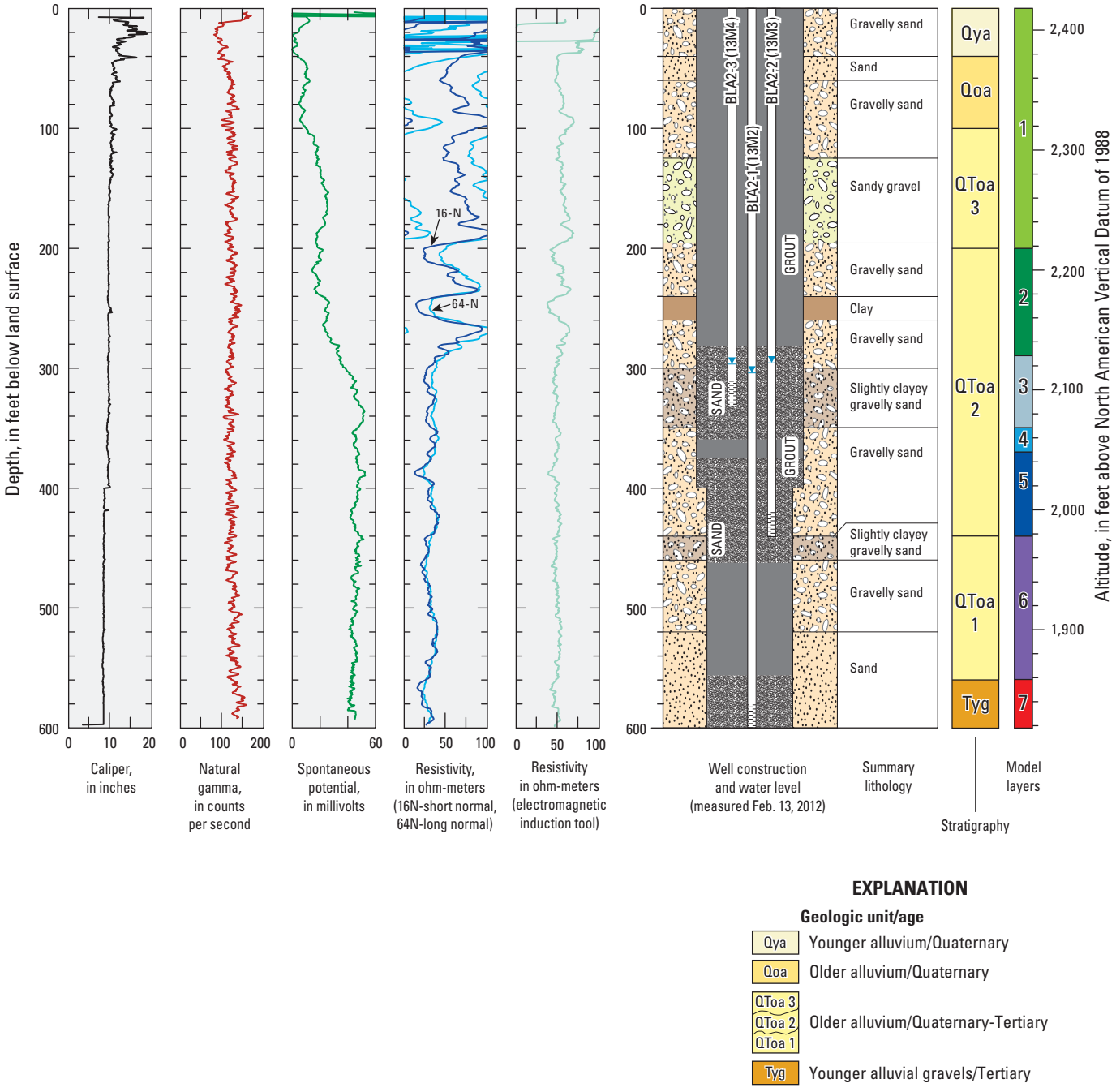

EXPLANATION

Geologic unit/age

Qya	Younger alluvium/Quaternary
Qoa	Older alluvium/Quaternary
QToa 3, QToa 2, QToa 1	Older alluvium/Quaternary-Tertiary
Tyg	Younger alluvial gravels/Tertiary

Figure 1–1. Stratigraphic columnar sections showing a geophysical log, well-construction diagram, and stratigraphic column for borehole of monitoring site BLA2 (14N/3E-13M2–4), drilled in Bicycle Basin, Fort Irwin National Training Center, California.

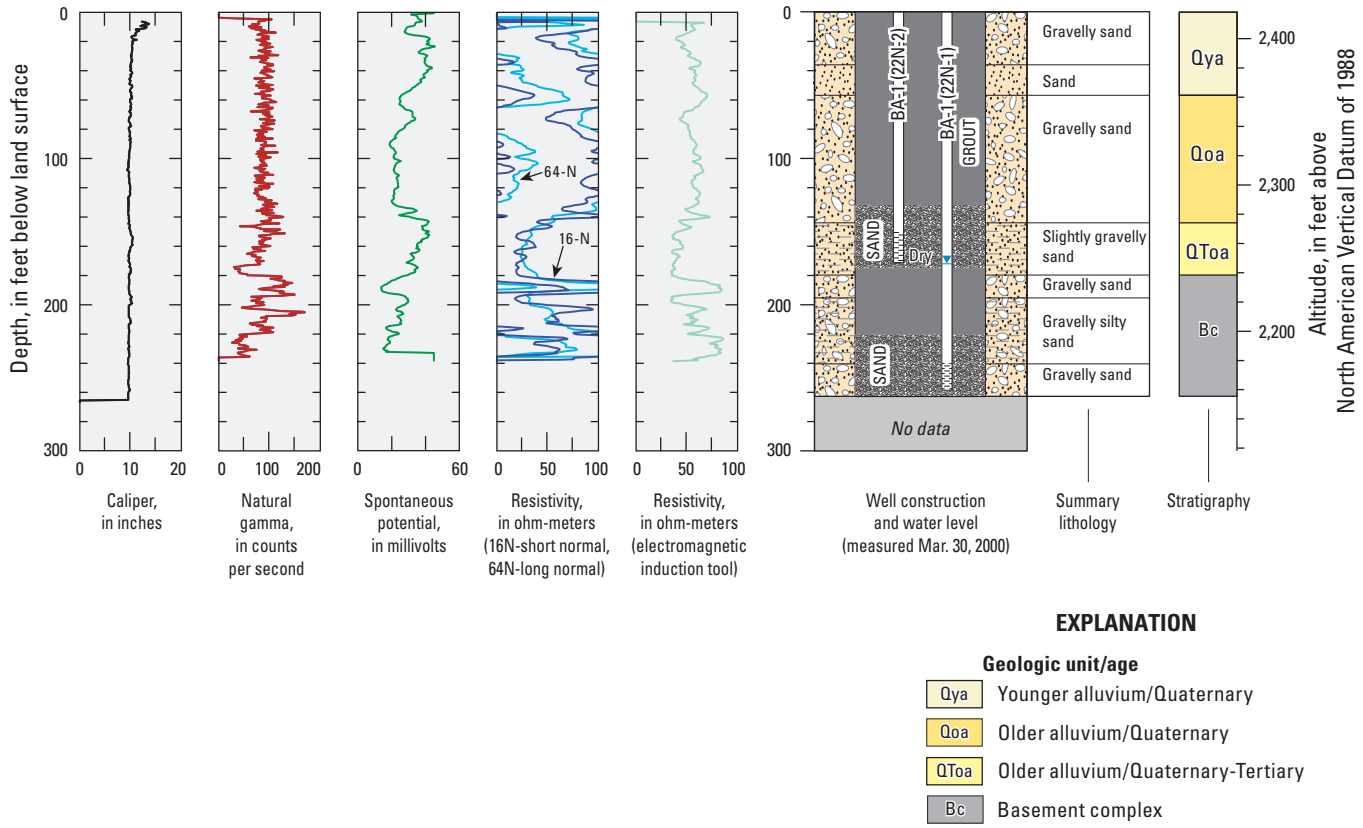

Figure 1–2. Stratigraphic columnar sections showing a geophysical log, well-construction diagram, and stratigraphic column for borehole of monitoring site BA1 (14N/3E-22N1–2), drilled in Bicycle Basin, Fort Irwin National Training Center, California.

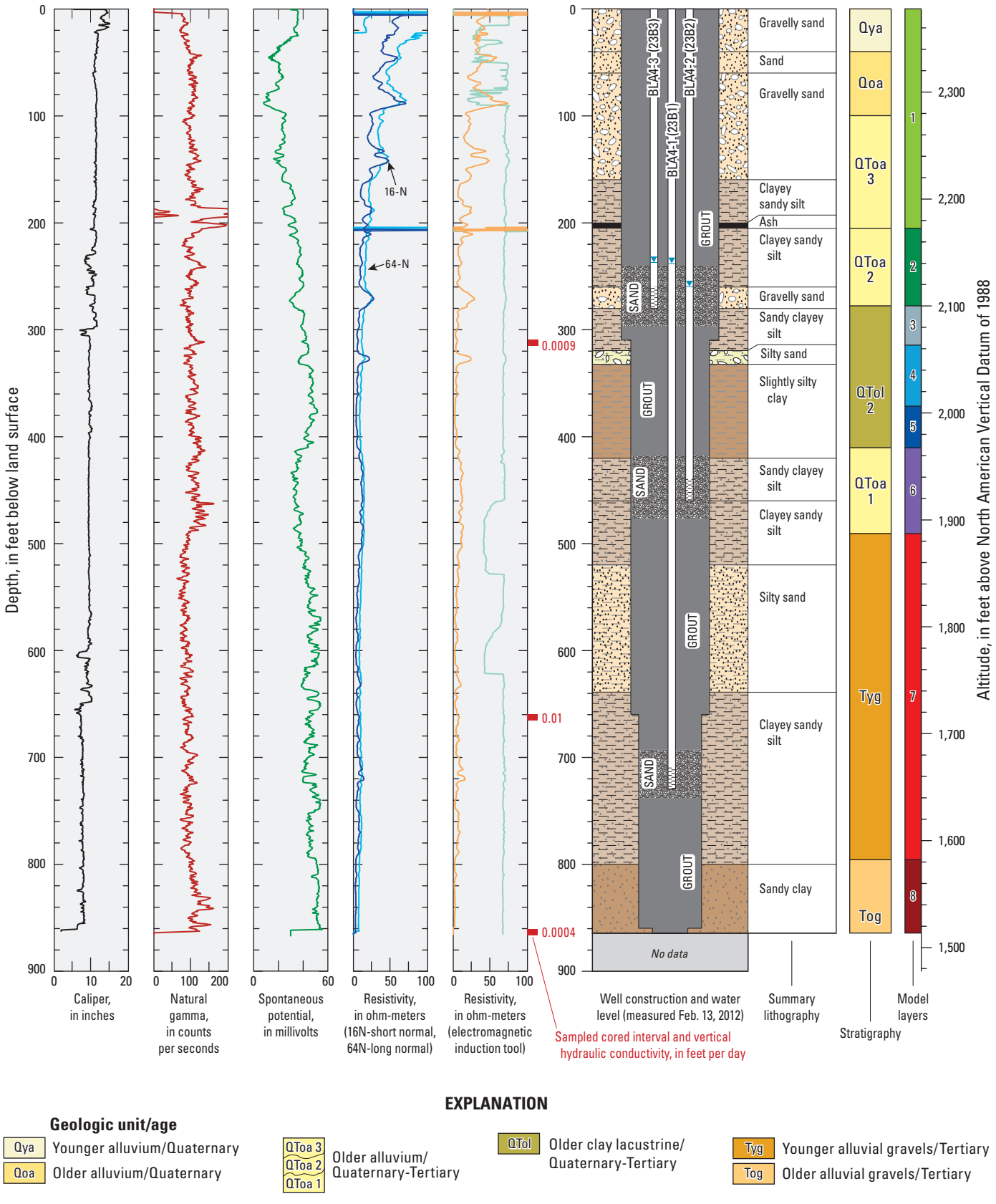

Figure 1–3. Stratigraphic columnar sections showing a geophysical log, well-construction diagram, and stratigraphic column for borehole of monitoring site BLA4 (14N/3E-23B1–3), drilled in Bicycle Basin, Fort Irwin National Training Center, California.

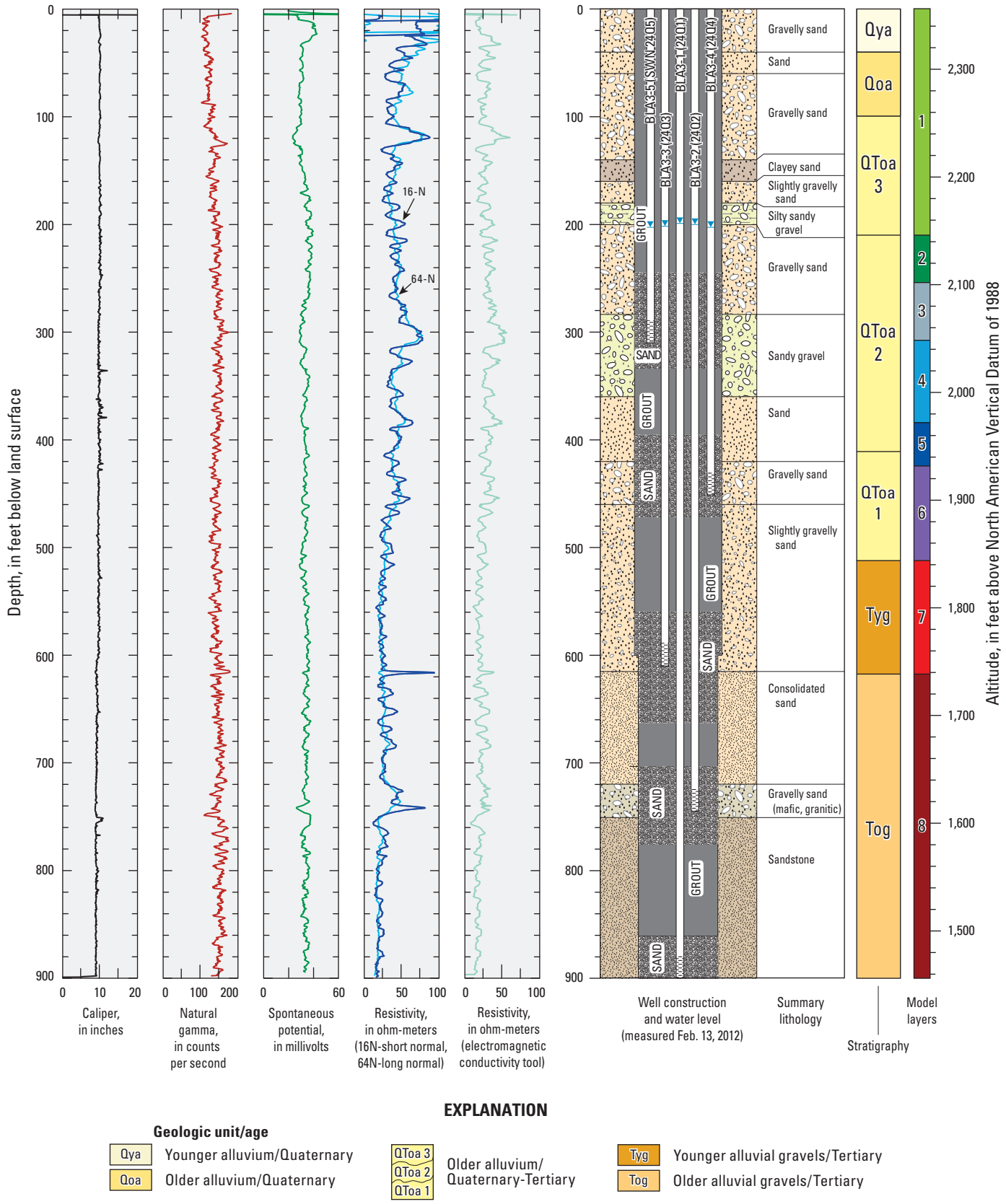

Figure 1–4. Stratigraphic columnar sections showing a geophysical log, well-construction diagram, and stratigraphic column for borehole of monitoring site BLA3 (14N/3E-24Q1–5), drilled in Bicycle Basin, Fort Irwin National Training Center, California.

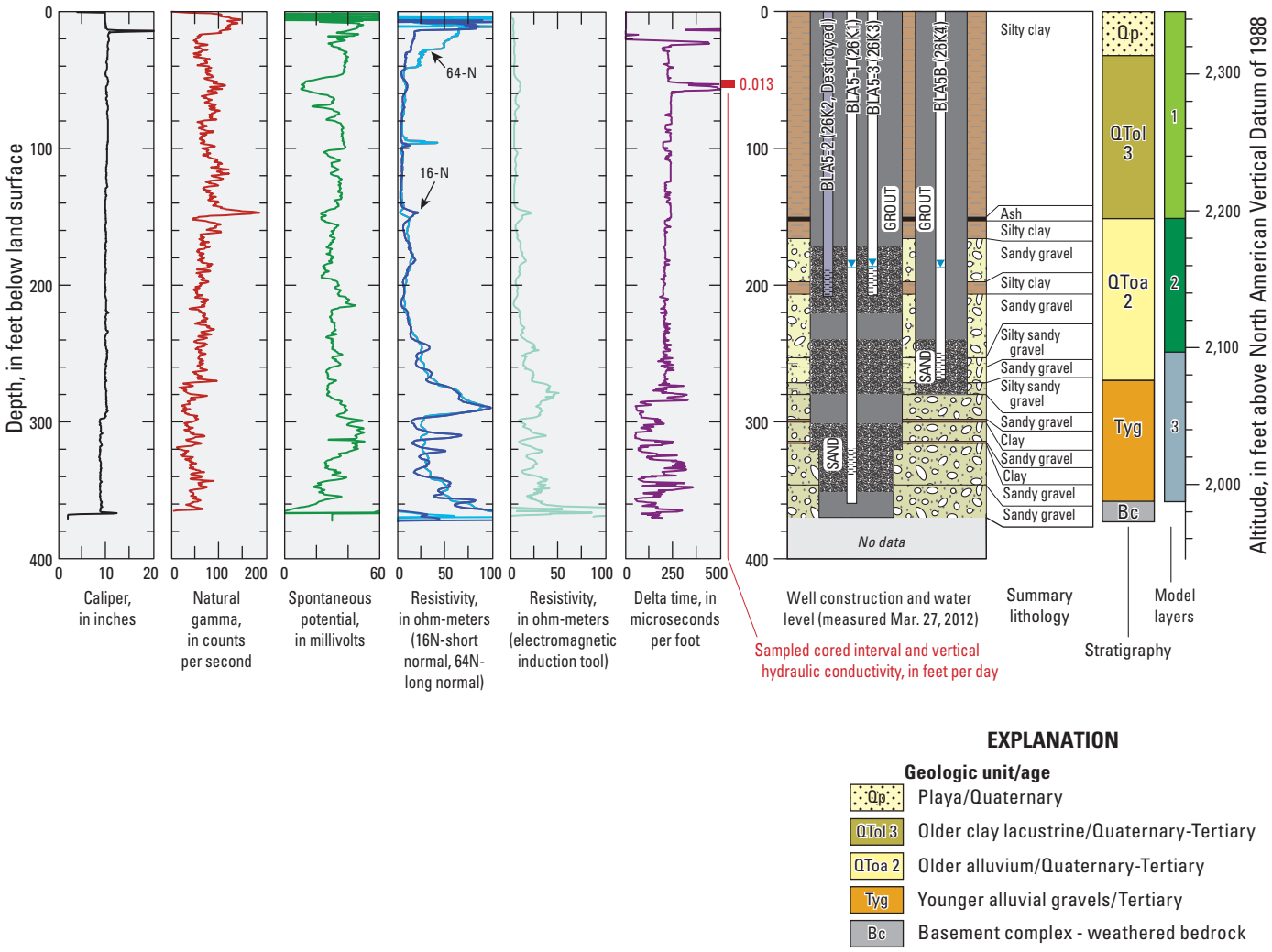

Figure 1–5. Stratigraphic columnar sections showing a geophysical log, well-construction diagram, and stratigraphic column for borehole of monitoring site BLA5 (14N/3E-26K1–4), drilled in Bicycle Basin, Fort Irwin National Training Center, California (modified from Kjos and others, 2014).

Geophysical logs were made at each borehole immediately after completion of drilling using methods described by Kjos and others (2014). The logs of the uncased boreholes, which were filled with drilling mud, included 16- and 64-inch normal resistivity, lateral (6-foot) or, for newer wells, electromagnetic (EM) induction resistivity, spontaneous potential (SP), natural gamma, and caliper logs (figs. 1–1 through 1–6). These logs provide information about the character of the formations and the presence and quality of groundwater. Data from the geophysical logs were used in conjunction with the lithologic logs to determine the placement of piezometers in multiple-well monitoring sites. Additionally, these data from wells, in conjunction with water-quality data, were used to estimate the depths of contacts between stratigraphic units on the basis of the depth at which there are shifts in the geophysical logs as summarized here.

Resistivity devices measure the evident resistivity of a volume of rock under the direct application of an electric current (Keys and MacCary, 1971). Resistivity logs are used to determine formation resistivity. Resistivity generally is correlated to grain size. Low resistivity generally indicates the presence of fine-grained deposits, such as silt, fine sand, and shale; high resistivity indicates the presence of coarse-grained materials, such as coarse sand and gravel.

The SP devices measure voltage differences between the borehole fluid and the surrounding rock (Keys and MacCary, 1971). The SP logs mainly are used for correlating geologic units, determining bed thickness, and differentiating nonporous and porous beds. The SP logs generally have a baseline corresponding to impermeable beds, such as clay or shale. Where formation water is less resistive than the drilling mud (more saline), deflections to the left of the baseline correspond to permeable strata; the opposite is true where formation water is more resistive than the drilling mud.

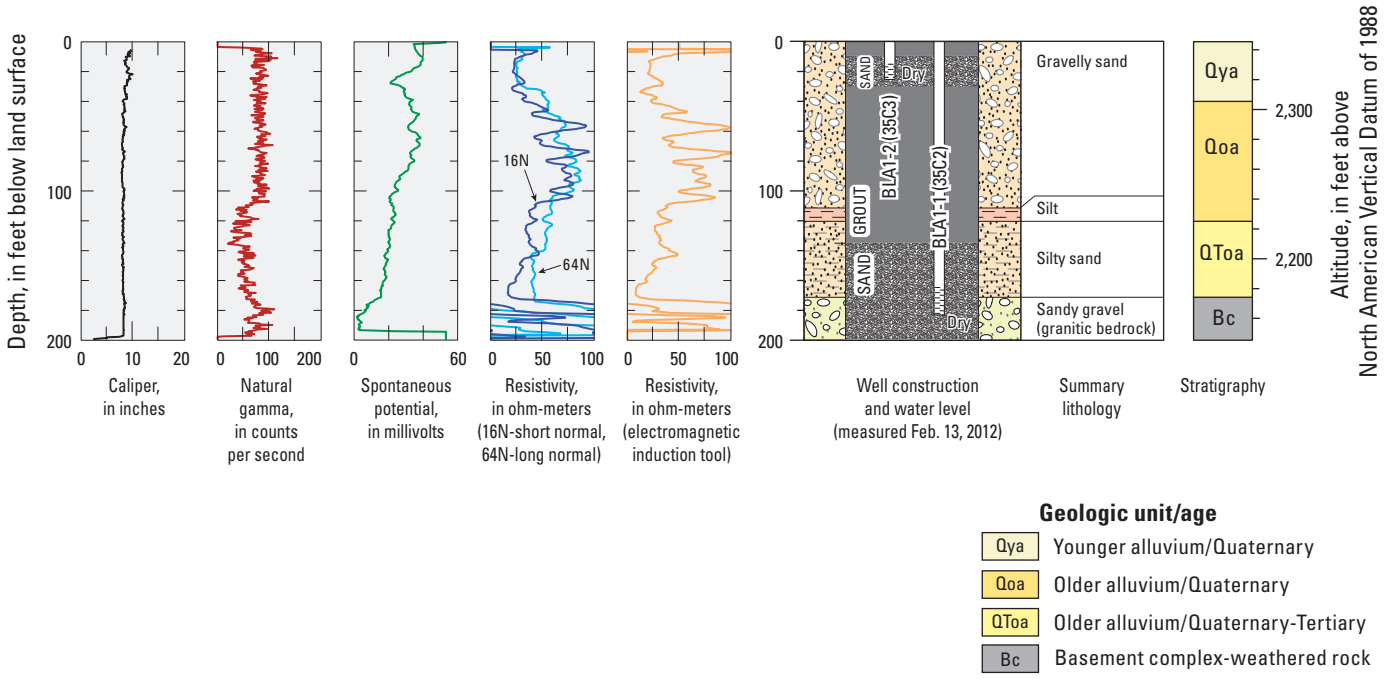

Figure 1–6. Stratigraphic columnar sections showing a geophysical log, well-construction diagram, and stratigraphic column for borehole of monitoring site BLA1 (14N/3E-35C2–3), drilled in Bicycle Basin, Fort Irwin National Training Center, California.

Natural gamma logs measure the intensities of gamma-ray emissions resulting from the natural decay of potassium-40 and of the daughter products of uranium and thorium. Gamma logs primarily are used as indicators of lithology and for geologic correlation. Higher intensity gamma rays generally are emitted by clay and feldspar-rich gravel and granite (Driscoll, 1986). At Fort Irwin, an increase in gamma intensity generally is interpreted as corresponding to an increase in granitic materials in the deposits.

References Cited

Driscoll, F.G., 1986, Groundwater and wells: St. Paul, Minn., Johnson Division, p. 168–200.

Keys, W.S., and MacCary, L.M., 1971, Application of borehole geophysics to water-resources investigations: U.S. Geological Survey Techniques of Water-Resources Investigations Report, book 2, chap. E1, 126 p., https://pubs.er.usgs.gov/publication/twri02E1.

Kjos, A.R., Densmore, J.N., Nawikas, J.M., and Brown, A.A., 2014, Construction, water-level, and water-quality data for multiple-well monitoring sites and test wells, Fort Irwin National Training Center, San Bernardino County, California, 2009–12: U.S. Geological Survey Data Series 788, 139 p., https://doi.org/10.3133/ds788.

Appendix 2. Water-Level Data for Selected Wells in Bicycle Basin, Fort Irwin National Training Center, California, 1955–2015

Table 2–1. Water-level data for selected wells in Bicycle Basin, Fort Irwin National Training Center, California, 1955–2015.

[State well number: See well-numbering system in text. Site identification (ID) is the latitude, longitude, and sequence number of the site.
Abbreviations: mm/dd/yyyy, month/day/year; NAVD 88, North American Vertical Datum of 1988]

Site ID	State well number	Date (mm/dd/yyyy)	Water-surface altitude, feet above NAVD 88	Depth to water, feet below land surface	Land-surface altitude, feet above NAVD 88
			Local ID: B-1		
351830116364501	14N/3E-13K1S	02/01/1955	2,226.80	170.90	2,397.7
351830116364501	14N/3E-13K1S	05/01/1963	2,222.70	175.00	2,397.7
351830116364501	14N/3E-13K1S	05/01/1965	2,225.70	172.00	2,397.7
351830116364501	14N/3E-13K1S	06/14/1965	2,224.70	173.00	2,397.7
351830116364501	14N/3E-13K1S	06/01/1967	2,218.70	179.00	2,397.7
351830116364501	14N/3E-13K1S	01/01/1968	2,221.70	176.00	2,397.7
351830116364501	14N/3E-13K1S	01/01/1969	2,216.70	181.00	2,397.7
351830116364501	14N/3E-13K1S	02/01/1970	2,216.70	181.00	2,397.7
351830116364501	14N/3E-13K1S	03/01/1973	2,208.70	189.00	2,397.7
351830116364501	14N/3E-13K1S	06/01/1974	2,216.70	181.00	2,397.7
351830116364501	14N/3E-13K1S	07/13/1978	2,213.70	184.00	2,397.7
351830116364501	14N/3E-13K1S	12/01/1978	2,212.70	185.00	2,397.7
351830116364501	14N/3E-13K1S	04/10/1979	2,211.30	186.39	2,397.7
351830116364501	14N/3E-13K1S	07/29/1980	2,209.90	187.83	2,397.7
351830116364501	14N/3E-13K1S	01/20/1981	2,210.40	187.25	2,397.7
351830116364501	14N/3E-13K1S	06/24/1982	2,200.80	196.89	2,397.7
351830116364501	14N/3E-13K1S	11/16/1982	2,204.90	192.83	2,397.7
351830116364501	14N/3E-13K1S	11/15/1983	2,203.60	194.14	2,397.7
351830116364501	14N/3E-13K1S	01/26/1993	2,188.00	209.69	2,397.7
351830116364501	14N/3E-13K1S	07/21/1994	2,176.90	220.80	2,397.7
351830116364501	14N/3E-13K1S	11/22/1994	2,185.80	211.87	2,397.7
351830116364501	14N/3E-13K1S	03/30/2000	2,171.00	226.72	2,397.7
351830116364501	14N/3E-13K1S	03/02/2005	2,131.60	266.12	2,397.7
			Local ID: B-4		
351829116371201	14N/3E-13M1S	06/30/1965	2,215.80	203.00	2,418.8
351829116371201	14N/3E-13M1S	04/01/1967	2,196.80	222.00	2,418.8
351829116371201	14N/3E-13M1S	01/01/1968	2,194.80	224.00	2,418.8
351829116371201	14N/3E-13M1S	01/01/1969	2,187.80	231.00	2,418.8
351829116371201	14N/3E-13M1S	03/01/1970	2,179.80	239.00	2,418.8
351829116371201	14N/3E-13M1S	05/01/1974	2,193.80	225.00	2,418.8
351829116371201	14N/3E-13M1S	12/01/1978	2,170.80	248.00	2,418.8
351829116371201	14N/3E-13M1S	01/01/1981	2,160.80	258.00	2,418.8
351829116371201	14N/3E-13M1S	09/07/1997	2,116.10	302.69	2,418.8
351829116371201	14N/3E-13M1S	07/28/2000	2,123.80	295.01	2,418.8
351829116371201	14N/3E-13M1S	03/01/2005	2,123.30	295.46	2,418.8

Table 2–1. Water-level data for selected wells in Bicycle Basin, Fort Irwin National Training Center, California, 1955–2015. —Continued

[State well number: See well-numbering system in text. Site identification (ID) is the latitude, longitude, and sequence number of the site.
Abbreviations: mm/dd/yyyy, month/day/year; NAVD 88, North American Vertical Datum of 1988]

Site ID	State well number	Date (mm/dd/yyyy)	Water-surface altitude, feet above NAVD 88	Depth to water, feet below land surface	Land-surface altitude, feet above NAVD 88
Local ID: BLA2-1					
351829116371201	14N/3E-13M1S	11/06/2007	2,130.10	288.73	2,418.8
351829116371201	14N/3E-13M1S	02/14/2008	2,130.60	288.23	2,418.8
351829116371201	14N/3E-13M1S	07/29/2008	2,131.30	287.50	2,418.8
351829116371201	14N/3E-13M1S	12/13/2010	2,123.00	295.77	2,418.8
351829116371201	14N/3E-13M1S	10/27/2011	2,121.30	297.51	2,418.8
351828116371201	14N/3E-13M2S	07/09/1997	2,098.10	319.89	2,418.0
351828116371201	14N/3E-13M2S	07/14/1997	2,098.10	319.95	2,418.0
351828116371201	14N/3E-13M2S	08/19/1997	2,092.50	325.50	2,418.0
351828116371201	14N/3E-13M2S	08/25/1997	2,096.00	321.97	2,418.0
351828116371201	14N/3E-13M2S	09/03/1997	2,094.10	323.86	2,418.0
351828116371201	14N/3E-13M2S	09/23/1997	2,095.20	322.79	2,418.0
351828116371201	14N/3E-13M2S	10/02/1997	2,095.00	323.02	2,418.0
351828116371201	14N/3E-13M2S	07/09/1999	2,085.30	332.67	2,418.0
351828116371201	14N/3E-13M2S	03/30/2000	2,120.50	297.52	2,418.0
351828116371201	14N/3E-13M2S	07/28/2000	2,123.70	294.26	2,418.0
351828116371201	14N/3E-13M2S	01/30/2002	2,085.10	332.86	2,418.0
351828116371201	14N/3E-13M2S	03/01/2005	2,124.40	293.58	2,418.0
351828116371201	14N/3E-13M2S	11/06/2007	2,130.10	287.90	2,418.0
351828116371201	14N/3E-13M2S	12/19/2007	2,130.20	287.75	2,418.0
351828116371201	14N/3E-13M2S	02/13/2008	2,131.20	286.82	2,418.0
351828116371201	14N/3E-13M2S	04/29/2008	2,131.30	286.67	2,418.0
351828116371201	14N/3E-13M2S	07/29/2008	2,131.30	286.66	2,418.0
351828116371201	14N/3E-13M2S	01/22/2009	2,132.10	285.92	2,418.0
351828116371201	14N/3E-13M2S	01/27/2009	2,131.80	286.25	2,418.0
351828116371201	14N/3E-13M2S	04/08/2009	2,132.30	285.73	2,418.0
351828116371201	14N/3E-13M2S	10/07/2009	2,106.10	311.94	2,418.0
351828116371201	14N/3E-13M2S	06/14/2010	2,128.30	289.72	2,418.0
351828116371201	14N/3E-13M2S	12/13/2010	2,123.80	294.23	2,418.0
351828116371201	14N/3E-13M2S	04/28/2011	2,122.90	295.05	2,418.0
351828116371201	14N/3E-13M2S	10/24/2011	2,122.40	295.55	2,418.0
351828116371201	14N/3E-13M2S	10/30/2011	2,122.60	295.37	2,418.0
351828116371201	14N/3E-13M2S	02/13/2012	2,114.30	303.73	2,418.0
351828116371201	14N/3E-13M2S	02/21/2012	2,121.30	296.72	2,418.0
351828116371201	14N/3E-13M2S	08/30/2012	2,114.20	303.84	2,418.0
351828116371201	14N/3E-13M2S	04/17/2013	2,118.20	299.79	2,418.0
351828116371201	14N/3E-13M2S	09/10/2013	2,103.40	314.55	2,418.0
351828116371201	14N/3E-13M2S	08/01/2014	2,101.50	316.51	2,418.0
351828116371201	14N/3E-13M2S	11/06/2014	2,114.20	303.83	2,418.0
351828116371201	14N/3E-13M2S	02/18/2015	2,108.30	309.66	2,418.0
351828116371201	14N/3E-13M2S	05/20/2015	2,118.40	299.64	2,418.0

Table 2–1. Water-level data for selected wells in Bicycle Basin, Fort Irwin National Training Center, California, 1955–2015. —Continued

[State well number: See well-numbering system in text. Site identification (ID) is the latitude, longitude, and sequence number of the site.
Abbreviations: mm/dd/yyyy, month/day/year; NAVD 88, North American Vertical Datum of 1988]

Site ID	State well number	Date (mm/dd/yyyy)	Water-surface altitude, feet above NAVD 88	Depth to water, feet below land surface	Land-surface altitude, feet above NAVD 88
Local ID: BLA2-2					
351828116371202	14N/3E-13M3S	07/09/1997	2,120.20	297.77	2,418.0
351828116371202	14N/3E-13M3S	07/14/1997	2,116.90	301.07	2,418.0
351828116371202	14N/3E-13M3S	08/25/1997	2,114.80	303.15	2,418.0
351828116371202	14N/3E-13M3S	09/03/1997	2,113.50	304.49	2,418.0
351828116371202	14N/3E-13M3S	09/23/1997	2,115.00	303.03	2,418.0
351828116371202	14N/3E-13M3S	10/02/1997	2,113.50	304.48	2,418.0
351828116371202	14N/3E-13M3S	07/09/1999	2,107.20	310.78	2,418.0
351828116371202	14N/3E-13M3S	03/30/2000	2,120.10	297.88	2,418.0
351828116371202	14N/3E-13M3S	07/28/2000	2,124.50	293.53	2,418.0
351828116371202	14N/3E-13M3S	01/30/2002	2,103.90	314.07	2,418.0
351828116371202	14N/3E-13M3S	03/01/2005	2,124.30	293.71	2,418.0
351828116371202	14N/3E-13M3S	11/06/2007	2,130.10	287.90	2,418.0
351828116371202	14N/3E-13M3S	12/19/2007	2,130.20	287.76	2,418.0
351828116371202	14N/3E-13M3S	02/13/2008	2,131.10	286.86	2,418.0
351828116371202	14N/3E-13M3S	04/29/2008	2,131.30	286.69	2,418.0
351828116371202	14N/3E-13M3S	07/29/2008	2,131.30	286.67	2,418.0
351828116371202	14N/3E-13M3S	01/22/2009	2,132.10	285.92	2,418.0
351828116371202	14N/3E-13M3S	01/27/2009	2,131.70	286.30	2,418.0
351828116371202	14N/3E-13M3S	04/08/2009	2,132.20	285.75	2,418.0
351828116371202	14N/3E-13M3S	10/07/2009	2,124.90	293.13	2,418.0
351828116371202	14N/3E-13M3S	06/14/2010	2,128.40	289.62	2,418.0
351828116371202	14N/3E-13M3S	12/13/2010	2,123.90	294.08	2,418.0
351828116371202	14N/3E-13M3S	12/13/2010	2,123.30	294.69	2,418.0
351828116371202	14N/3E-13M3S	04/28/2011	2,122.80	295.16	2,418.0
351828116371202	14N/3E-13M3S	10/24/2011	2,122.20	295.76	2,418.0
351828116371202	14N/3E-13M3S	10/30/2011	2,122.50	295.54	2,418.0
351828116371202	14N/3E-13M3S	02/13/2012	2,122.30	295.65	2,418.0
351828116371202	14N/3E-13M3S	02/21/2012	2,121.60	296.41	2,418.0
351828116371202	14N/3E-13M3S	08/30/2012	2,115.20	302.75	2,418.0
351828116371202	14N/3E-13M3S	04/17/2013	2,118.00	300.02	2,418.0
351828116371202	14N/3E-13M3S	09/10/2013	2,115.90	302.08	2,418.0
351828116371202	14N/3E-13M3S	08/12/2014	2,113.10	304.94	2,418.0
351828116371202	14N/3E-13M3S	11/06/2014	2,113.80	304.20	2,418.0
351828116371202	14N/3E-13M3S	02/18/2015	2,115.30	302.66	2,418.0
351828116371202	14N/3E-13M3S	05/20/2015	2,118.20	299.85	2,418.0
Local ID: BLA2-3					
351828116371203	14N/3E-13M4S	07/09/1997	2,118.60	299.38	2,418.0
351828116371203	14N/3E-13M4S	07/16/1997	2,117.30	300.70	2,418.0
351828116371203	14N/3E-13M4S	08/19/1997	2,115.60	302.38	2,418.0
351828116371203	14N/3E-13M4S	08/25/1997	2,116.00	302.02	2,418.0

Table 2–1. Water-level data for selected wells in Bicycle Basin, Fort Irwin National Training Center, California, 1955–2015. —Continued

[State well number: See well-numbering system in text. Site identification (ID) is the latitude, longitude, and sequence number of the site.
Abbreviations: mm/dd/yyyy, month/day/year; NAVD 88, North American Vertical Datum of 1988]

Site ID	State well number	Date (mm/dd/yyyy)	Water-surface altitude, feet above NAVD 88	Depth to water, feet below land surface	Land-surface altitude, feet above NAVD 88
Local ID: BLA2-3—Continued					
351828116371203	14N/3E-13M4S	09/03/1997	2,114.60	303.43	2,418.0
351828116371203	14N/3E-13M4S	09/24/1997	2,114.60	303.40	2,418.0
351828116371203	14N/3E-13M4S	10/02/1997	2,114.20	303.83	2,418.0
351828116371203	14N/3E-13M4S	07/09/1999	2,107.40	310.60	2,418.0
351828116371203	14N/3E-13M4S	03/30/2000	2,119.90	298.14	2,418.0
351828116371203	14N/3E-13M4S	07/28/2000	2,124.30	293.73	2,418.0
351828116371203	14N/3E-13M4S	01/30/2002	2,104.00	314.01	2,418.0
351828116371203	14N/3E-13M4S	03/01/2005	2,124.20	293.79	2,418.0
351828116371203	14N/3E-13M4S	11/06/2007	2,130.10	287.93	2,418.0
351828116371203	14N/3E-13M4S	12/19/2007	2,130.20	287.83	2,418.0
351828116371203	14N/3E-13M4S	02/13/2008	2,131.10	286.91	2,418.0
351828116371203	14N/3E-13M4S	04/29/2008	2,131.30	286.74	2,418.0
351828116371203	14N/3E-13M4S	07/29/2008	2,131.30	286.71	2,418.0
351828116371203	14N/3E-13M4S	01/22/2009	2,132.10	285.93	2,418.0
351828116371203	14N/3E-13M4S	01/27/2009	2,131.70	286.34	2,418.0
351828116371203	14N/3E-13M4S	04/08/2009	2,132.20	285.80	2,418.0
351828116371203	14N/3E-13M4S	10/07/2009	2,126.00	292.04	2,418.0
351828116371203	14N/3E-13M4S	06/14/2010	2,128.70	289.27	2,418.0
351828116371203	14N/3E-13M4S	12/13/2010	2,123.20	294.85	2,418.0
351828116371203	14N/3E-13M4S	12/13/2010	2,123.10	294.89	2,418.0
351828116371203	14N/3E-13M4S	04/28/2011	2,122.90	295.07	2,418.0
351828116371203	14N/3E-13M4S	10/24/2011	2,122.10	295.92	2,418.0
351828116371203	14N/3E-13M4S	10/30/2011	2,122.20	295.75	2,418.0
351828116371203	14N/3E-13M4S	02/13/2012	2,121.30	296.73	2,418.0
351828116371203	14N/3E-13M4S	02/21/2012	2,121.90	296.05	2,418.0
351828116371203	14N/3E-13M4S	08/30/2012	2,115.80	302.19	2,418.0
351828116371203	14N/3E-13M4S	04/17/2013	2,117.80	300.23	2,418.0
351828116371203	14N/3E-13M4S	09/10/2013	2,116.30	301.70	2,418.0
351828116371203	14N/3E-13M4S	08/01/2014	2,114.40	303.60	2,418.0
351828116371203	14N/3E-13M4S	11/06/2014	2,113.60	304.45	2,418.0
351828116371203	14N/3E-13M4S	02/18/2015	2,114.90	303.07	2,418.0
351828116371203	14N/3E-13M4S	05/20/2015	2,118.00	300.03	2,418.0
Local ID: B-2					
351830116372601	14N/3E-14H1S	11/14/1964	2,220.60	202.00	2,422.6
351830116372601	14N/3E-14H1S	03/01/1967	2,192.60	230.00	2,422.6
351830116372601	14N/3E-14H1S	01/01/1968	2,193.60	229.00	2,422.6
351830116372601	14N/3E-14H1S	01/01/1969	2,180.60	242.00	2,422.6
351830116372601	14N/3E-14H1S	03/01/1970	2,182.60	240.00	2,422.6
351830116372601	14N/3E-14H1S	02/01/1974	2,185.60	237.00	2,422.6
351830116372601	14N/3E-14H1S	09/01/1978	2,169.60	253.00	2,422.6

Table 2–1. Water-level data for selected wells in Bicycle Basin, Fort Irwin National Training Center, California, 1955–2015. —Continued

[State well number: See well-numbering system in text. Site identification (ID) is the latitude, longitude, and sequence number of the site.
Abbreviations: mm/dd/yyyy, month/day/year; NAVD 88, North American Vertical Datum of 1988]

Site ID	State well number	Date (mm/dd/yyyy)	Water-surface altitude, feet above NAVD 88	Depth to water, feet below land surface	Land-surface altitude, feet above NAVD 88
Local ID: B-2—Continued					
351830116372601	14N/3E-14H1S	01/01/1981	2,159.60	263.00	2,422.6
351830116372601	14N/3E-14H1S	01/26/1993	2,123.40	299.18	2,422.6
351830116372601	14N/3E-14H1S	07/21/1994	2,122.20	300.44	2,422.6
351830116372601	14N/3E-14H1S	09/08/1994	2,121.10	301.53	2,422.6
351830116372601	14N/3E-14H1S	12/20/1994	2,123.20	299.43	2,422.6
351830116372601	14N/3E-14H1S	03/03/1995	2,124.10	298.50	2,422.6
351830116372601	14N/3E-14H1S	08/03/1995	2,126.40	296.20	2,422.6
351830116372601	14N/3E-14H1S	09/18/1996	2,125.50	297.14	2,422.6
351830116372601	14N/3E-14H1S	08/20/1997	2,121.40	301.24	2,422.6
351830116372601	14N/3E-14H1S	09/03/1997	2,119.80	302.75	2,422.6
351830116372601	14N/3E-14H1S	09/08/1997	2,120.40	302.22	2,422.6
351830116372601	14N/3E-14H1S	10/07/1997	2,119.50	303.14	2,422.6
351830116372601	14N/3E-14H1S	07/09/1999	2,115.70	306.93	2,422.6
351830116372601	14N/3E-14H1S	03/30/2000	2,121.30	301.32	2,422.6
351830116372601	14N/3E-14H1S	07/28/2000	2,124.20	298.45	2,422.6
Local ID: B-6					
351810116375701	14N/3E-14P1S	03/01/1988	2,203.90	176.00	2,379.9
351810116375701	14N/3E-14P1S	05/01/1988	2,211.90	168.00	2,379.9
351810116375701	14N/3E-14P1S	01/26/1993	2,205.70	174.20	2,379.9
351810116375701	14N/3E-14P1S	07/21/1994	2,203.30	176.59	2,379.9
351810116375701	14N/3E-14P1S	09/07/1994	2,208.10	171.80	2,379.9
351810116375701	14N/3E-14P1S	11/22/1994	2,202.90	177.00	2,379.9
351810116375701	14N/3E-14P1S	03/03/1995	2,201.70	178.16	2,379.9
351810116375701	14N/3E-14P1S	07/09/1999	2,175.90	203.96	2,379.9
351810116375701	14N/3E-14P1S	02/14/2008	2,130.60	249.30	2,379.9
351810116375701	14N/3E-14P1S	10/27/2011	2,119.00	260.95	2,379.9
351810116375701	14N/3E-14P1S	03/28/2012	2,105.20	274.70	2,379.9
Local ID: TH-7					
351809116375901	14N/3E-14P2S	01/30/1988	2,213.20	166.00	2,379.2
351809116375901	14N/3E-14P2S	05/01/1988	2,212.20	167.00	2,379.2
351809116375901	14N/3E-14P2S	01/26/1993	2,205.70	173.48	2,379.2
351809116375901	14N/3E-14P2S	09/07/1994	2,203.40	175.82	2,379.2
351809116375901	14N/3E-14P2S	11/22/1994	2,203.10	176.08	2,379.2
351809116375901	14N/3E-14P2S	03/03/1995	2,203.10	176.07	2,379.2
351809116375901	14N/3E-14P2S	08/03/1995	2,202.30	176.94	2,379.2
351809116375901	14N/3E-14P2S	09/08/1997	2,144.90	234.31	2,379.2
351809116375901	14N/3E-14P2S	10/07/1997	2,144.10	235.05	2,379.2
351809116375901	14N/3E-14P2S	07/09/1999	2,176.30	202.88	2,379.2
351809116375901	14N/3E-14P2S	03/30/2000	2,124.30	254.92	2,379.2
351809116375901	14N/3E-14P2S	07/28/2000	2,120.00	259.22	2,379.2

Table 2–1. Water-level data for selected wells in Bicycle Basin, Fort Irwin National Training Center, California, 1955–2015. —Continued

[State well number: See well-numbering system in text. Site identification (ID) is the latitude, longitude, and sequence number of the site.
Abbreviations: mm/dd/yyyy, month/day/year; NAVD 88, North American Vertical Datum of 1988]

Site ID	State well number	Date (mm/dd/yyyy)	Water-surface altitude, feet above NAVD 88	Depth to water, feet below land surface	Land-surface altitude, feet above NAVD 88
Local ID: TH-7—Continued					
351809116375901	14N/3E-14P2S	01/30/2002	2,155.70	223.49	2,379.2
351809116375901	14N/3E-14P2S	03/01/2005	2,113.10	266.10	2,379.2
351809116375901	14N/3E-14P2S	03/02/2005	2,130.60	248.59	2,379.2
351809116375901	14N/3E-14P2S	11/06/2007	2,092.00	287.23	2,379.2
351809116375901	14N/3E-14P2S	12/19/2007	2,124.20	255.04	2,379.2
351809116375901	14N/3E-14P2S	02/14/2008	2,130.90	248.28	2,379.2
351809116375901	14N/3E-14P2S	04/29/2008	2,110.40	268.83	2,379.2
351809116375901	14N/3E-14P2S	07/29/2008	2,092.40	286.83	2,379.2
351809116375901	14N/3E-14P2S	01/22/2009	2,101.30	277.93	2,379.2
351809116375901	14N/3E-14P2S	01/27/2009	2,100.00	279.24	2,379.2
351809116375901	14N/3E-14P2S	04/07/2009	2,110.40	268.84	2,379.2
351809116375901	14N/3E-14P2S	10/07/2009	2,089.60	289.61	2,379.2
351809116375901	14N/3E-14P2S	10/09/2009	2,089.50	289.68	2,379.2
351809116375901	14N/3E-14P2S	06/15/2010	2,095.30	283.90	2,379.2
351809116375901	14N/3E-14P2S	12/12/2010	2,110.70	268.48	2,379.2
351809116375901	14N/3E-14P2S	04/28/2011	2,107.20	271.96	2,379.2
351809116375901	14N/3E-14P2S	10/24/2011	2,118.80	260.42	2,379.2
351809116375901	14N/3E-14P2S	10/30/2011	2,119.60	259.62	2,379.2
351809116375901	14N/3E-14P2S	02/13/2012	2,099.40	279.75	2,379.2
351809116375901	14N/3E-14P2S	02/21/2012	2,099.70	279.51	2,379.2
351809116375901	14N/3E-14P2S	08/30/2012	2,085.90	293.34	2,379.2
351809116375901	14N/3E-14P2S	04/17/2013	2,124.80	254.39	2,379.2
351809116375901	14N/3E-14P2S	09/10/2013	2,130.00	249.15	2,379.2
351809116375901	14N/3E-14P2S	08/01/2014	2,096.80	282.45	2,379.2
351809116375901	14N/3E-14P2S	02/18/2015	2,109.10	270.06	2,379.2
Local ID: BA1-1					
351710116392701	14N/3E-22N1S	05/19/1993	2,247.30	170.96	2,418.3
351710116392701	14N/3E-22N1S	09/23/1993	2,246.90	171.41	2,418.3
351710116392701	14N/3E-22N1S	07/21/1994	2,246.90	171.45	2,418.3
351710116392701	14N/3E-22N1S	09/08/1994	2,246.70	171.56	2,418.3
351710116392701	14N/3E-22N1S	09/21/1994	2,246.70	171.56	2,418.3
351710116392701	14N/3E-22N1S	11/22/1994	2,246.60	171.71	2,418.3
351710116392701	14N/3E-22N1S	03/04/1995	2,246.70	171.60	2,418.3
351710116392701	14N/3E-22N1S	08/03/1995	2,246.70	171.62	2,418.3
351710116392701	14N/3E-22N1S	05/22/1996	2,246.80	171.54	2,418.3
351710116392701	14N/3E-22N1S	06/12/1996	2,246.70	171.64	2,418.3
351710116392701	14N/3E-22N1S	07/17/1997	2,246.60	171.74	2,418.3
351710116392701	14N/3E-22N1S	07/07/1999	2,246.30	171.98	2,418.3
351710116392701	14N/3E-22N1S	03/30/2000	2,246.40	171.91	2,418.3

Table 2–1. Water-level data for selected wells in Bicycle Basin, Fort Irwin National Training Center, California, 1955–2015. —Continued

[State well number: See well-numbering system in text. Site identification (ID) is the latitude, longitude, and sequence number of the site.
Abbreviations: mm/dd/yyyy, month/day/year; NAVD 88, North American Vertical Datum of 1988]

Site ID	State well number	Date (mm/dd/yyyy)	Water-surface altitude, feet above NAVD 88	Depth to water, feet below land surface	Land-surface altitude, feet above NAVD 88
Local ID: B-3					
351719116390301	14N/3E-22P1S	01/26/1993	2,243.00	189.18	2,432.0
351719116390301	14N/3E-22P1S	07/21/1994	2,242.00	189.81	2,432.0
351719116390301	14N/3E-22P1S	09/08/1994	2,242.00	190.23	2,432.0
351719116390301	14N/3E-22P1S	11/22/1994	2,241.00	190.63	2,432.0
351719116390301	14N/3E-22P1S	03/04/1995	2,242.00	190.42	2,432.0
351719116390301	14N/3E-22P1S	08/03/1995	2,241.00	190.67	2,432.0
351719116390301	14N/3E-22P1S	09/18/1996	2,240.00	191.51	2,432.0
Local ID: BLA4-1					
351759116374401	14N/3E-23B1S	04/30/2008	2,147.00	229.77	2,377.0
351759116374401	14N/3E-23B1S	07/29/2008	2,141.00	235.86	2,377.0
351759116374401	14N/3E-23B1S	01/22/2009	2,144.00	232.61	2,377.0
351759116374401	14N/3E-23B1S	01/27/2009	2,144.00	233.04	2,377.0
351759116374401	14N/3E-23B1S	04/07/2009	2,140.00	236.59	2,377.0
351759116374401	14N/3E-23B1S	10/08/2009	2,136.00	240.72	2,377.0
351759116374401	14N/3E-23B1S	03/02/2010	2,145.00	232.48	2,377.0
351759116374401	14N/3E-23B1S	03/02/2010	2,144.00	232.52	2,377.0
351759116374401	14N/3E-23B1S	06/15/2010	2,142.00	234.73	2,377.0
351759116374401	14N/3E-23B1S	12/14/2010	2,136.00	240.58	2,377.0
351759116374401	14N/3E-23B1S	12/14/2010	2,136.00	240.51	2,377.0
351759116374401	14N/3E-23B1S	12/17/2010	2,136.00	240.61	2,377.0
351759116374401	14N/3E-23B1S	12/17/2010	2,136.00	240.65	2,377.0
351759116374401	14N/3E-23B1S	04/28/2011	2,134.00	242.51	2,377.0
351759116374401	14N/3E-23B1S	10/24/2011	2,136.00	241.31	2,377.0
351759116374401	14N/3E-23B1S	10/30/2011	2,136.00	241.16	2,377.0
351759116374401	14N/3E-23B1S	02/13/2012	2,139.00	237.86	2,377.0
351759116374401	14N/3E-23B1S	02/21/2012	2,139.00	238.21	2,377.0
351759116374401	14N/3E-23B1S	08/30/2012	2,131.00	245.85	2,377.0
351759116374401	14N/3E-23B1S	04/17/2013	2,138.00	238.92	2,377.0
351759116374401	14N/3E-23B1S	09/10/2013	2,142.00	234.55	2,377.0
351759116374401	14N/3E-23B1S	08/01/2014	2,136.00	241.34	2,377.0
351759116374401	14N/3E-23B1S	11/03/2014	2,135.00	242.37	2,377.0
351759116374401	14N/3E-23B1S	02/10/2015	2,140.00	236.88	2,377.0
351759116374401	14N/3E-23B1S	02/16/2015	2,140.00	236.62	2,377.0
351759116374401	14N/3E-23B1S	5/21/2015	2,140.00	237.05	2,377.0
Local ID: BLA4-2					
351759116374402	14N/3E-23B2S	04/30/2008	2,133.00	243.61	2,377.0
351759116374402	14N/3E-23B2S	07/29/2008	2,109.00	268.07	2,377.0
351759116374402	14N/3E-23B2S	01/22/2009	2,117.00	259.85	2,377.0
351759116374402	14N/3E-23B2S	01/27/2009	2,115.00	262.10	2,377.0
351759116374402	14N/3E-23B2S	04/07/2009	2,109.00	268.28	2,377.0

Table 2–1. Water-level data for selected wells in Bicycle Basin, Fort Irwin National Training Center, California, 1955–2015. —Continued

[State well number: See well-numbering system in text. Site identification (ID) is the latitude, longitude, and sequence number of the site.
Abbreviations: mm/dd/yyyy, month/day/year; NAVD 88, North American Vertical Datum of 1988]

Site ID	State well number	Date (mm/dd/yyyy)	Water-surface altitude, feet above NAVD 88	Depth to water, feet below land surface	Land-surface altitude, feet above NAVD 88
Local ID: BLA4-2—Continued					
351759116374402	14N/3E-23B2S	10/08/2009	2,105.00	272.16	2,377.0
351759116374402	14N/3E-23B2S	03/02/2010	2,134.00	243.05	2,377.0
351759116374402	14N/3E-23B2S	03/02/2010	2,134.00	243.19	2,377.0
351759116374402	14N/3E-23B2S	06/15/2010	2,110.00	266.90	2,377.0
351759116374402	14N/3E-23B2S	12/14/2010	2,109.00	267.57	2,377.0
351759116374402	14N/3E-23B2S	12/14/2010	2,109.00	267.98	2,377.0
351759116374402	14N/3E-23B2S	04/27/2011	2,105.00	272.43	2,377.0
351759116374402	14N/3E-23B2S	10/24/2011	2,118.00	259.04	2,377.0
351759116374402	14N/3E-23B2S	10/30/2011	2,120.00	257.05	2,377.0
351759116374402	14N/3E-23B2S	02/13/2012	2,117.00	259.90	2,377.0
351759116374402	14N/3E-23B2S	02/21/2012	2,113.00	263.97	2,377.0
351759116374402	14N/3E-23B2S	08/30/2012	2,101.00	275.67	2,377.0
351759116374402	14N/3E-23B2S	04/17/2013	2,126.00	250.74	2,377.0
351759116374402	14N/3E-23B2S	09/10/2013	2,131.00	246.12	2,377.0
351759116374402	14N/3E-23B2S	08/01/2014	2,109.00	268.24	2,377.0
351759116374402	14N/3E-23B2S	11/03/2014	2,124.00	253.27	2,377.0
351759116374402	14N/3E-23B2S	02/10/2015	2,130.00	246.80	2,377.0
351759116374402	14N/3E-23B2S	02/16/2015	2,121.00	256.47	2,377.0
351759116374402	14N/3E-23B2S	02/17/2015	2,120.00	257.16	2,377.0
351759116374402	14N/3E-23B2S	05/20/2015	2,130.00	247.05	2,377.0
Local ID: BLA4-3					
351759116374403	14N/3E-23B3S	04/30/2008	2,145.00	231.64	2,377.0
351759116374403	14N/3E-23B3S	07/29/2008	2,144.00	233.17	2,377.0
351759116374403	14N/3E-23B3S	01/22/2009	2,144.00	233.02	2,377.0
351759116374403	14N/3E-23B3S	01/27/2009	2,143.00	233.51	2,377.0
351759116374403	14N/3E-23B3S	04/07/2009	2,143.00	233.95	2,377.0
351759116374403	14N/3E-23B3S	10/08/2009	2,142.00	235.04	2,377.0
351759116374403	14N/3E-23B3S	03/02/2010	2,143.00	234.01	2,377.0
351759116374403	14N/3E-23B3S	03/02/2010	2,143.00	234.05	2,377.0
351759116374403	14N/3E-23B3S	06/15/2010	2,142.00	234.71	2,377.0
351759116374403	14N/3E-23B3S	12/14/2010	2,141.00	235.64	2,377.0
351759116374403	14N/3E-23B3S	12/14/2010	2,141.00	236.10	2,377.0
351759116374403	14N/3E-23B3S	04/28/2011	2,139.00	237.77	2,377.0
351759116374403	14N/3E-23B3S	10/24/2011	2,140.00	237.28	2,377.0
351759116374403	14N/3E-23B3S	10/30/2011	2,140.00	237.42	2,377.0
351759116374403	14N/3E-23B3S	02/13/2012	2,140.00	237.02	2,377.0
351759116374403	14N/3E-23B3S	02/21/2012	2,139.00	237.65	2,377.0
351759116374403	14N/3E-23B3S	08/30/2012	2,138.00	238.87	2,377.0
351759116374403	14N/3E-23B3S	04/17/2013	2,138.00	239.40	2,377.0
351759116374403	14N/3E-23B3S	09/10/2013	2,139.00	238.34	2,377.0

Table 2–1. Water-level data for selected wells in Bicycle Basin, Fort Irwin National Training Center, California, 1955–2015. —Continued

[State well number: See well-numbering system in text. Site identification (ID) is the latitude, longitude, and sequence number of the site.
Abbreviations: mm/dd/yyyy, month/day/year; NAVD 88, North American Vertical Datum of 1988]

Site ID	State well number	Date (mm/dd/yyyy)	Water-surface altitude, feet above NAVD 88	Depth to water, feet below land surface	Land-surface altitude, feet above NAVD 88
Local ID: BLA4-3—Continued					
351759116374403	14N/3E-23B3S	08/01/2014	2,138.00	239.13	2,377.0
351759116374403	14N/3E-23B3S	11/03/2014	2,137.00	239.79	2,377.0
351759116374403	14N/3E-23B3S	02/10/2015	2,138.00	239.04	2,377.0
351759116374403	14N/3E-23B3S	02/15/2015	2,138.00	239.03	2,377.0
351759116374403	14N/3E-23B3S	02/17/2015	2,138.00	239.22	2,377.0
351759116374403	14N/3E-23B3S	05/20/2015	2,138.00	239.15	2,377.0
Local ID: BX-2					
351738116374101	14N/3E-23G1S	10/30/1980	2,205.00	155.60	2,360.6
351738116374101	14N/3E-23G1S	01/26/1993	2,214.90	145.67	2,360.6
351738116374101	14N/3E-23G1S	09/24/1993	2,214.10	146.47	2,360.6
351738116374101	14N/3E-23G1S	07/21/1994	2,213.50	147.11	2,360.6
351738116374101	14N/3E-23G1S	09/08/1994	2,213.40	147.23	2,360.6
351738116374101	14N/3E-23G1S	09/21/1994	2,213.20	147.36	2,360.6
351738116374101	14N/3E-23G1S	11/22/1994	2,212.80	147.78	2,360.6
351738116374101	14N/3E-23G1S	02/02/1995	2,213.00	147.57	2,360.6
351738116374101	14N/3E-23G1S	03/03/1995	2,212.90	147.72	2,360.6
351738116374101	14N/3E-23G1S	09/18/1996	2,211.00	149.57	2,360.6
351738116374101	14N/3E-23G1S	07/08/1997	2,210.10	150.53	2,360.6
351738116374101	14N/3E-23G1S	09/04/1997	2,209.10	151.46	2,360.6
351738116374101	14N/3E-23G1S	09/08/1997	2,209.80	150.75	2,360.6
351738116374101	14N/3E-23G1S	10/07/1997	2,210.10	150.49	2,360.6
351738116374101	14N/3E-23G1S	07/29/1999	2,204.20	156.35	2,360.6
351738116374101	14N/3E-23G1S	03/30/2000	2,201.60	159.02	2,360.6
351738116374101	14N/3E-23G1S	08/01/2000	2,200.40	160.20	2,360.6
351738116374101	14N/3E-23G1S	01/30/2002	2,195.30	165.29	2,360.6
351738116374101	14N/3E-23G1S	03/01/2005	2,186.10	174.52	2,360.6
351738116374101	14N/3E-23G1S	11/06/2007	2,176.80	183.83	2,360.6
351738116374101	14N/3E-23G1S	12/18/2007	2,179.50	181.12	2,360.6
351738116374101	14N/3E-23G1S	02/15/2008	2,179.00	181.58	2,360.6
351738116374101	14N/3E-23G1S	04/29/2008	2,178.80	181.78	2,360.6
351738116374101	14N/3E-23G1S	07/29/2008	2,177.70	182.90	2,360.6
351738116374101	14N/3E-23G1S	01/22/2009	2,176.60	183.98	2,360.6
351738116374101	14N/3E-23G1S	04/07/2009	2,175.90	184.65	2,360.6
351738116374101	14N/3E-23G1S	10/07/2009	2,174.40	186.19	2,360.6
351738116374101	14N/3E-23G1S	06/14/2010	2,172.90	187.65	2,360.6
351738116374101	14N/3E-23G1S	12/14/2010	2,171.70	188.88	2,360.6
351738116374101	14N/3E-23G1S	12/14/2010	2,171.80	188.75	2,360.6
351738116374101	14N/3E-23G1S	04/27/2011	2,170.80	189.75	2,360.6
351738116374101	14N/3E-23G1S	10/24/2011	2,170.20	190.35	2,360.6
351738116374101	14N/3E-23G1S	10/30/2011	2,170.00	190.56	2,360.6

Table 2–1. Water-level data for selected wells in Bicycle Basin, Fort Irwin National Training Center, California, 1955–2015. —Continued

[State well number: See well-numbering system in text. Site identification (ID) is the latitude, longitude, and sequence number of the site.
Abbreviations: mm/dd/yyyy, month/day/year; NAVD 88, North American Vertical Datum of 1988]

Site ID	State well number	Date (mm/dd/yyyy)	Water-surface altitude, feet above NAVD 88	Depth to water, feet below land surface	Land-surface altitude, feet above NAVD 88
Local ID: BX-2—Continued					
351738116374101	14N/3E-23G1S	02/13/2012	2,170.00	190.60	2,360.6
351738116374101	14N/3E-23G1S	02/21/2012	2,169.50	191.06	2,360.6
351738116374101	14N/3E-23G1S	08/30/2012	2,169.00	191.64	2,360.6
351738116374101	14N/3E-23G1S	04/17/2013	2,167.90	192.66	2,360.6
351738116374101	14N/3E-23G1S	09/10/2013	2,167.80	192.77	2,360.6
351738116374101	14N/3E-23G1S	08/01/2014	2,167.00	193.59	2,360.6
351738116374101	14N/3E-23G1S	12/09/2014	2,166.80	193.83	2,360.6
351738116374101	14N/3E-23G1S	02/17/2015	2,166.50	194.11	2,360.6
351738116374101	14N/3E-23G1S	05/20/2015	2,166.40	194.24	2,360.6
Local ID: BX-1					
351742116362401	14N/3E-24H1S	10/30/1980	2,218.90	142.70	2,361.6
351742116362401	14N/3E-24H1S	01/26/1993	2,193.80	167.81	2,361.6
351742116362401	14N/3E-24H1S	07/29/1993	2,192.00	169.56	2,361.6
351742116362401	14N/3E-24H1S	07/21/1994	2,190.00	171.60	2,361.6
351742116362401	14N/3E-24H1S	07/27/1994	2,189.60	171.99	2,361.6
351742116362401	14N/3E-24H1S	09/08/1994	2,189.30	172.30	2,361.6
351742116362401	14N/3E-24H1S	09/19/1994	2,189.30	172.27	2,361.6
351742116362401	14N/3E-24H1S	12/20/1994	2,189.40	172.18	2,361.6
351742116362401	14N/3E-24H1S	01/31/1995	2,189.80	171.84	2,361.6
351742116362401	14N/3E-24H1S	03/03/1995	2,189.60	171.99	2,361.6
351742116362401	14N/3E-24H1S	08/03/1995	2,188.50	173.13	2,361.6
351742116362401	14N/3E-24H1S	09/18/1996	2,183.00	178.57	2,361.6
Local ID: BLA3-1					
351716116363701	14N/3E-24Q1S	07/14/1997	2,151.50	204.17	2,355.7
351716116363701	14N/3E-24Q1S	07/22/1997	2,189.60	166.05	2,355.7
351716116363701	14N/3E-24Q1S	09/08/1997	2,190.70	164.99	2,355.7
351716116363701	14N/3E-24Q1S	07/08/1999	2,186.40	169.31	2,355.7
351716116363701	14N/3E-24Q1S	03/30/2000	2,183.60	172.14	2,355.7
351716116363701	14N/3E-24Q1S	01/30/2002	2,179.30	176.39	2,355.7
351716116363701	14N/3E-24Q1S	03/01/2005	2,168.80	186.93	2,355.7
351716116363701	14N/3E-24Q1S	11/06/2007	2,164.00	191.70	2,355.7
351716116363701	14N/3E-24Q1S	12/19/2007	2,163.60	192.07	2,355.7
351716116363701	14N/3E-24Q1S	02/14/2008	2,163.80	191.85	2,355.7
351716116363701	14N/3E-24Q1S	04/30/2008	2,164.10	191.56	2,355.7
351716116363701	14N/3E-24Q1S	07/28/2008	2,163.00	192.72	2,355.7
351716116363701	14N/3E-24Q1S	01/22/2009	2,162.20	193.48	2,355.7
351716116363701	14N/3E-24Q1S	01/26/2009	2,162.10	193.60	2,355.7
351716116363701	14N/3E-24Q1S	04/08/2009	2,161.20	194.48	2,355.7
351716116363701	14N/3E-24Q1S	10/07/2009	2,159.80	195.86	2,355.7
351716116363701	14N/3E-24Q1S	06/14/2010	2,159.80	195.94	2,355.7

Table 2–1. Water-level data for selected wells in Bicycle Basin, Fort Irwin National Training Center, California, 1955–2015. —Continued

[State well number: See well-numbering system in text. Site identification (ID) is the latitude, longitude, and sequence number of the site.
Abbreviations: mm/dd/yyyy, month/day/year; NAVD 88, North American Vertical Datum of 1988]

Site ID	State well number	Date (mm/dd/yyyy)	Water-surface altitude, feet above NAVD 88	Depth to water, feet below land surface	Land-surface altitude, feet above NAVD 88
Local ID: BLA3-1—Continued					
351716116363701	14N/3E-24Q1S	12/17/2010	2,158.30	197.44	2,355.7
351716116363701	14N/3E-24Q1S	04/27/2011	2,157.10	198.63	2,355.7
351716116363701	14N/3E-24Q1S	10/24/2011	2,155.80	199.85	2,355.7
351716116363701	14N/3E-24Q1S	10/30/2011	2,156.00	199.65	2,355.7
351716116363701	14N/3E-24Q1S	02/13/2012	2,156.30	199.40	2,355.7
351716116363701	14N/3E-24Q1S	02/21/2012	2,156.00	199.69	2,355.7
351716116363701	14N/3E-24Q1S	08/30/2012	2,153.90	201.77	2,355.7
351716116363701	14N/3E-24Q1S	04/17/2013	2,153.70	201.98	2,355.7
351716116363701	14N/3E-24Q1S	09/10/2013	2,154.80	200.92	2,355.7
351716116363701	14N/3E-24Q1S	08/01/2014	2,153.20	202.51	2,355.7
351716116363701	14N/3E-24Q1S	11/04/2014	2,151.90	203.76	2,355.7
351716116363701	14N/3E-24Q1S	02/16/2015	2,152.70	203.04	2,355.7
351716116363701	14N/3E-24Q1S	05/21/2015	2,152.30	203.36	2,355.7
Local ID: BLA3-2					
351716116363702	14N/3E-24Q2S	07/14/1997	2,153.50	202.21	2,355.7
351716116363702	14N/3E-24Q2S	07/23/1997	2,190.20	165.46	2,355.7
351716116363702	14N/3E-24Q2S	09/08/1997	2,190.40	165.29	2,355.7
351716116363702	14N/3E-24Q2S	07/08/1999	2,185.70	169.99	2,355.7
351716116363702	14N/3E-24Q2S	03/30/2000	2,181.90	173.80	2,355.7
351716116363702	14N/3E-24Q2S	01/30/2002	2,178.40	177.30	2,355.7
351716116363702	14N/3E-24Q2S	03/01/2005	2,168.10	187.57	2,355.7
351716116363702	14N/3E-24Q2S	11/06/2007	2,162.80	192.85	2,355.7
351716116363702	14N/3E-24Q2S	12/19/2007	2,162.80	192.95	2,355.7
351716116363702	14N/3E-24Q2S	02/14/2008	2,163.10	192.61	2,355.7
351716116363702	14N/3E-24Q2S	04/30/2008	2,163.60	192.12	2,355.7
351716116363702	14N/3E-24Q2S	07/28/2008	2,161.90	193.78	2,355.7
351716116363702	14N/3E-24Q2S	01/22/2009	2,161.40	194.31	2,355.7
351716116363702	14N/3E-24Q2S	01/26/2009	2,161.20	194.47	2,355.7
351716116363702	14N/3E-24Q2S	04/08/2009	2,160.20	195.48	2,355.7
351716116363702	14N/3E-24Q2S	10/07/2009	2,158.80	196.88	2,355.7
351716116363702	14N/3E-24Q2S	06/14/2010	2,159.00	196.74	2,355.7
351716116363702	14N/3E-24Q2S	12/17/2010	2,157.20	198.46	2,355.7
351716116363702	14N/3E-24Q2S	04/27/2011	2,156.20	199.47	2,355.7
351716116363702	14N/3E-24Q2S	10/24/2011	2,155.10	200.64	2,355.7
351716116363702	14N/3E-24Q2S	10/30/2011	2,155.20	200.45	2,355.7
351716116363702	14N/3E-24Q2S	02/13/2012	2,155.60	200.07	2,355.7
351716116363702	14N/3E-24Q2S	02/21/2012	2,155.20	200.45	2,355.7
351716116363702	14N/3E-24Q2S	08/30/2012	2,152.80	202.90	2,355.7
351716116363702	14N/3E-24Q2S	04/17/2013	2,153.20	202.50	2,355.7
351716116363702	14N/3E-24Q2S	09/10/2013	2,154.40	201.28	2,355.7

Table 2–1. Water-level data for selected wells in Bicycle Basin, Fort Irwin National Training Center, California, 1955–2015. —Continued

[State well number: See well-numbering system in text. Site identification (ID) is the latitude, longitude, and sequence number of the site.
Abbreviations: mm/dd/yyyy, month/day/year; NAVD 88, North American Vertical Datum of 1988]

Site ID	State well number	Date (mm/dd/yyyy)	Water-surface altitude, feet above NAVD 88	Depth to water, feet below land surface	Land-surface altitude, feet above NAVD 88
Local ID: BLA3-2—Continued					
351716116363702	14N/3E-24Q2S	08/01/2014	2,152.20	203.49	2,355.7
351716116363702	14N/3E-24Q2S	11/04/2014	2,151.10	204.57	2,355.7
351716116363702	14N/3E-24Q2S	02/09/2015	2,152.20	203.54	2,355.7
351716116363702	14N/3E-24Q2S	02/16/2015	2,152.00	203.69	2,355.7
351716116363702	14N/3E-24Q2S	05/21/2015	2,151.80	203.95	2,355.7
Local ID: BLA3-3					
351716116363703	14N/3E-24Q3S	07/14/1997	2,165.20	190.46	2,355.7
351716116363703	14N/3E-24Q3S	07/23/1997	2,189.80	165.90	2,355.7
351716116363703	14N/3E-24Q3S	09/08/1997	2,189.20	166.50	2,355.7
351716116363703	14N/3E-24Q3S	07/08/1999	2,184.60	171.10	2,355.7
351716116363703	14N/3E-24Q3S	03/30/2000	2,181.30	174.37	2,355.7
351716116363703	14N/3E-24Q3S	01/30/2002	2,176.90	178.76	2,355.7
351716116363703	14N/3E-24Q3S	03/01/2005	2,166.60	189.14	2,355.7
351716116363703	14N/3E-24Q3S	11/06/2007	2,161.00	194.74	2,355.7
351716116363703	14N/3E-24Q3S	12/19/2007	2,160.90	194.75	2,355.7
351716116363703	14N/3E-24Q3S	02/14/2008	2,161.50	194.21	2,355.7
351716116363703	14N/3E-24Q3S	04/30/2008	2,162.20	193.53	2,355.7
351716116363703	14N/3E-24Q3S	07/28/2008	2,160.20	195.52	2,355.7
351716116363703	14N/3E-24Q3S	01/22/2009	2,159.80	195.89	2,355.7
351716116363703	14N/3E-24Q3S	01/26/2009	2,159.60	196.09	2,355.7
351716116363703	14N/3E-24Q3S	04/08/2009	2,158.50	197.20	2,355.7
351716116363703	14N/3E-24Q3S	10/07/2009	2,157.00	198.65	2,355.7
351716116363703	14N/3E-24Q3S	06/14/2010	2,157.50	198.23	2,355.7
351716116363703	14N/3E-24Q3S	12/17/2010	2,155.50	200.20	2,355.7
351716116363703	14N/3E-24Q3S	04/27/2011	2,154.30	201.42	2,355.7
351716116363703	14N/3E-24Q3S	10/24/2011	2,153.40	202.29	2,355.7
351716116363703	14N/3E-24Q3S	10/30/2011	2,153.60	202.11	2,355.7
351716116363703	14N/3E-24Q3S	02/13/2012	2,154.10	201.60	2,355.7
351716116363703	14N/3E-24Q3S	02/21/2012	2,153.70	201.97	2,355.7
351716116363703	14N/3E-24Q3S	08/30/2012	2,151.00	204.68	2,355.7
351716116363703	14N/3E-24Q3S	04/17/2013	2,151.80	203.88	2,355.7
351716116363703	14N/3E-24Q3S	09/10/2013	2,153.30	202.41	2,355.7
351716116363703	14N/3E-24Q3S	08/01/2014	2,150.60	205.12	2,355.7
351716116363703	14N/3E-24Q3S	11/04/2014	2,149.50	206.19	2,355.7
351716116363703	14N/3E-24Q3S	02/09/2015	2,150.80	204.87	2,355.7
351716116363703	14N/3E-24Q3S	02/16/2015	2,150.80	204.95	2,355.7
351716116363703	14N/3E-24Q3S	05/20/2015	2,150.40	205.29	2,355.7
Local ID: BLA3-4					
351716116363704	14N/3E-24Q4S	07/14/1997	2,175.80	179.89	2,355.7
351716116363704	14N/3E-24Q4S	07/24/1997	2,189.10	166.55	2,355.7

Table 2–1. Water-level data for selected wells in Bicycle Basin, Fort Irwin National Training Center, California, 1955–2015. —Continued

[State well number: See well-numbering system in text. Site identification (ID) is the latitude, longitude, and sequence number of the site.
Abbreviations: mm/dd/yyyy, month/day/year; NAVD 88, North American Vertical Datum of 1988]

Site ID	State well number	Date (mm/dd/yyyy)	Water-surface altitude, feet above NAVD 88	Depth to water, feet below land surface	Land-surface altitude, feet above NAVD 88
Local ID: BLA3-4—Continued					
351716116363704	14N/3E-24Q4S	09/08/1997	2,188.60	167.09	2,355.7
351716116363704	14N/3E-24Q4S	07/08/1999	2,183.80	171.94	2,355.7
351716116363704	14N/3E-24Q4S	03/30/2000	2,180.40	175.32	2,355.7
351716116363704	14N/3E-24Q4S	01/30/2002	2,175.90	179.83	2,355.7
351716116363704	14N/3E-24Q4S	03/01/2005	2,165.50	190.21	2,355.7
351716116363704	14N/3E-24Q4S	11/06/2007	2,159.80	195.92	2,355.7
351716116363704	14N/3E-24Q4S	12/19/2007	2,159.80	195.90	2,355.7
351716116363704	14N/3E-24Q4S	02/14/2008	2,160.40	195.25	2,355.7
351716116363704	14N/3E-24Q4S	04/30/2008	2,161.10	194.55	2,355.7
351716116363704	14N/3E-24Q4S	07/28/2008	2,159.10	196.61	2,355.7
351716116363704	14N/3E-24Q4S	01/22/2009	2,158.70	196.96	2,355.7
351716116363704	14N/3E-24Q4S	01/26/2009	2,158.60	197.14	2,355.7
351716116363704	14N/3E-24Q4S	04/08/2009	2,157.40	198.31	2,355.7
351716116363704	14N/3E-24Q4S	10/07/2009	2,155.90	199.82	2,355.7
351716116363704	14N/3E-24Q4S	06/14/2010	2,156.60	199.10	2,355.7
351716116363704	14N/3E-24Q4S	12/17/2010	2,154.40	201.30	2,355.7
351716116363704	14N/3E-24Q4S	04/27/2011	2,153.20	202.49	2,355.7
351716116363704	14N/3E-24Q4S	10/24/2011	2,152.30	203.38	2,355.7
351716116363704	14N/3E-24Q4S	10/25/2011	2,152.50	203.24	2,355.7
351716116363704	14N/3E-24Q4S	02/13/2012	2,153.10	202.64	2,355.7
351716116363704	14N/3E-24Q4S	02/21/2012	2,152.70	202.96	2,355.7
351716116363704	14N/3E-24Q4S	08/30/2012	2,149.90	205.80	2,355.7
351716116363704	14N/3E-24Q4S	04/17/2013	2,150.90	204.80	2,355.7
351716116363704	14N/3E-24Q4S	09/10/2013	2,152.50	203.22	2,355.7
351716116363704	14N/3E-24Q4S	08/01/2014	2,149.60	206.14	2,355.7
351716116363704	14N/3E-24Q4S	11/04/2014	2,148.60	207.11	2,355.7
351716116363704	14N/3E-24Q4S	02/09/2015	2,150.00	205.66	2,355.7
351716116363704	14N/3E-24Q4S	02/16/2015	2,149.90	205.82	2,355.7
351716116363704	14N/3E-24Q4S	05/20/2015	2,149.50	206.16	2,355.7
Local ID: BLA3-5					
351716116363705	14N/3E-24Q5S	07/14/1997	2,184.60	171.05	2,355.7
351716116363705	14N/3E-24Q5S	07/24/1997	2,189.40	166.26	2,355.7
351716116363705	14N/3E-24Q5S	09/08/1997	2,189.00	166.74	2,355.7
351716116363705	14N/3E-24Q5S	07/08/1999	2,184.40	171.31	2,355.7
351716116363705	14N/3E-24Q5S	03/30/2000	2,181.10	174.64	2,355.7
351716116363705	14N/3E-24Q5S	01/30/2002	2,176.60	179.14	2,355.7
351716116363705	14N/3E-24Q5S	03/01/2005	2,166.00	189.73	2,355.7
351716116363705	14N/3E-24Q5S	11/06/2007	2,160.70	195.00	2,355.7
351716116363705	14N/3E-24Q5S	12/19/2007	2,160.40	195.25	2,355.7
351716116363705	14N/3E-24Q5S	02/14/2008	2,161.00	194.72	2,355.7

Table 2–1. Water-level data for selected wells in Bicycle Basin, Fort Irwin National Training Center, California, 1955–2015. —Continued

[State well number: See well-numbering system in text. Site identification (ID) is the latitude, longitude, and sequence number of the site.
Abbreviations: mm/dd/yyyy, month/day/year; NAVD 88, North American Vertical Datum of 1988]

Site ID	State well number	Date (mm/dd/yyyy)	Water-surface altitude, feet above NAVD 88	Depth to water, feet below land surface	Land-surface altitude, feet above NAVD 88
Local ID: BLA3-5—Continued					
351716116363705	14N/3E-24Q5S	04/30/2008	2,161.60	194.13	2,355.7
351716116363705	14N/3E-24Q5S	07/28/2008	2,159.90	195.76	2,355.7
351716116363705	14N/3E-24Q5S	01/22/2009	2,159.40	196.31	2,355.7
351716116363705	14N/3E-24Q5S	01/26/2009	2,159.20	196.48	2,355.7
351716116363705	14N/3E-24Q5S	04/08/2009	2,158.20	197.47	2,355.7
351716116363705	14N/3E-24Q5S	10/07/2009	2,156.70	198.98	2,355.7
351716116363705	14N/3E-24Q5S	06/14/2010	2,157.30	198.41	2,355.7
351716116363705	14N/3E-24Q5S	12/17/2010	2,155.20	200.54	2,355.7
351716116363705	14N/3E-24Q5S	04/27/2011	2,154.00	201.68	2,355.7
351716116363705	14N/3E-24Q5S	10/24/2011	2,152.90	202.83	2,355.7
351716116363705	14N/3E-24Q5S	10/30/2011	2,153.00	202.69	2,355.7
351716116363705	14N/3E-24Q5S	02/13/2012	2,153.60	202.14	2,355.7
351716116363705	14N/3E-24Q5S	02/21/2012	2,153.30	202.37	2,355.7
351716116363705	14N/3E-24Q5S	08/30/2012	2,150.80	204.94	2,355.7
351716116363705	14N/3E-24Q5S	04/17/2013	2,151.20	204.47	2,355.7
351716116363705	14N/3E-24Q5S	09/10/2013	2,152.70	202.98	2,355.7
351716116363705	14N/3E-24Q5S	08/01/2014	2,150.40	205.32	2,355.7
351716116363705	14N/3E-24Q5S	11/04/2014	2,149.10	206.59	2,355.7
351716116363705	14N/3E-24Q5S	02/09/2015	2,150.30	205.37	2,355.7
351716116363705	14N/3E-24Q5S	02/16/2015	2,150.40	205.34	2,355.7
351716116363705	14N/3E-24Q5S	05/20/2015	2,150.00	205.69	2,355.7
Local ID: BLA5-1					
351638116374301	14N/3E-26K1S	04/25/2011	2,160.00	185.15	2,345.0
351638116374301	14N/3E-26K1S	10/25/2011	2,159.00	186.08	2,345.0
351638116374301	14N/3E-26K1S	10/31/2011	2,159.00	186.24	2,345.0
351638116374301	14N/3E-26K1S	02/13/2012	2,158.00	186.54	2,345.0
351638116374301	14N/3E-26K1S	03/27/2012	2,158.00	187.01	2,345.0
351638116374301	14N/3E-26K1S	11/05/2014	2,154.00	190.94	2,345.0
351638116374301	14N/3E-26K1S	12/04/2014	2,154.00	190.97	2,345.0
351638116374301	14N/3E-26K1S	12/10/2014	2,154.00	190.90	2,345.0
351638116374301	14N/3E-26K1S	05/20/2015	2,153.00	191.54	2,345.0
351638116374301	14N/3E-26K1S	07/02/2015	2,153.00	191.90	2,345.0
Local ID: BLA5-3					
351638116374303	14N/3E-26K3S	04/25/2011	2,161.00	184.20	2,345.0
351638116374303	14N/3E-26K3S	10/25/2011	2,160.00	185.08	2,345.0
351638116374303	14N/3E-26K3S	10/31/2011	2,160.00	185.26	2,345.0
351638116374303	14N/3E-26K3S	02/13/2012	2,159.00	185.64	2,345.0
351638116374303	14N/3E-26K3S	03/27/2012	2,159.00	186.17	2,345.0
351638116374303	14N/3E-26K3S	11/03/2014	2,155.00	189.92	2,345.0
351638116374303	14N/3E-26K3S	12/04/2014	2,155.00	189.97	2,345.0

Table 2–1. Water-level data for selected wells in Bicycle Basin, Fort Irwin National Training Center, California, 1955–2015. —Continued

[State well number: See well-numbering system in text. Site identification (ID) is the latitude, longitude, and sequence number of the site.
Abbreviations: mm/dd/yyyy, month/day/year; NAVD 88, North American Vertical Datum of 1988]

Site ID	State well number	Date (mm/dd/yyyy)	Water-surface altitude, feet above NAVD 88	Depth to water, feet below land surface	Land-surface altitude, feet above NAVD 88
Local ID: BLA5-3—Continued					
351638116374303	14N/3E-26K3S	12/04/2014	2,143.00	201.53	2,345.0
351638116374303	14N/3E-26K3S	05/20/2015	2,154.00	190.70	2,345.0
351638116374303	14N/3E-26K3S	07/02/2015	2,154.00	190.91	2,345.0
Local ID: BLA5B-1					
351638116374304	14N/3E-26K4S	04/25/2011	2,160.00	184.87	2,345.0
351638116374304	14N/3E-26K4S	10/25/2011	2,159.00	185.93	2,345.0
351638116374304	14N/3E-26K4S	10/31/2011	2,159.00	186.10	2,345.0
351638116374304	14N/3E-26K4S	02/13/2012	2,159.00	186.42	2,345.0
351638116374304	14N/3E-26K4S	03/27/2012	2,158.00	186.84	2,345.0
351638116374304	14N/3E-26K4S	11/05/2014	2,154.00	190.81	2,345.0
351638116374304	14N/3E-26K4S	12/04/2014	2,154.00	190.84	2,345.0
351638116374304	14N/3E-26K4S	05/20/2015	2,154.00	191.44	2,345.0
351638116374304	14N/3E-26K4S	07/02/2015	2,153.00	191.76	2,345.0
Local ID: BP-2, MW-12					
351654116393301	14N/3E-27E1S	01/26/1993	2,325.80	75.60	2,401.4
351654116393301	14N/3E-27E1S	09/24/1993	2,321.10	80.29	2,401.4
351654116393301	14N/3E-27E1S	08/15/1994	2,325.00	76.38	2,401.4
351654116393301	14N/3E-27E1S	09/08/1994	2,324.50	76.88	2,401.4
351654116393301	14N/3E-27E1S	02/08/1995	2,326.10	75.27	2,401.4
351654116393301	14N/3E-27E1S	05/04/1995	2,327.90	73.50	2,401.4
351654116393301	14N/3E-27E1S	08/09/1995	2,327.70	73.68	2,401.4
351654116393301	14N/3E-27E1S	11/07/1995	2,327.40	73.96	2,401.4
Local ID: BP-3, MW-13					
351656116393101	14N/3E-27E2S	01/26/1993	2,325.80	75.65	2,401.4
351656116393101	14N/3E-27E2S	09/23/1993	2,326.80	74.64	2,401.4
351656116393101	14N/3E-27E2S	08/15/1994	2,325.00	76.42	2,401.4
351656116393101	14N/3E-27E2S	09/08/1994	2,324.70	76.72	2,401.4
351656116393101	14N/3E-27E2S	02/08/1995	2,326.20	75.22	2,401.4
351656116393101	14N/3E-27E2S	05/04/1995	2,327.90	73.50	2,401.4
351656116393101	14N/3E-27E2S	08/09/1995	2,327.70	73.66	2,401.4
351656116393101	14N/3E-27E2S	11/07/1995	2,327.50	73.92	2,401.4
Local ID: BP-4, MW-14					
351656116392901	14N/3E-27E3S	01/26/1993	2,324.90	76.48	2,401.4
351656116392901	14N/3E-27E3S	09/24/1993	2,320.40	81.00	2,401.4
351656116392901	14N/3E-27E3S	08/15/1994	2,324.20	77.15	2,401.4
351656116392901	14N/3E-27E3S	09/08/1994	2,324.10	77.33	2,401.4
351656116392901	14N/3E-27E3S	02/08/1995	2,325.40	76.00	2,401.4
351656116392901	14N/3E-27E3S	05/04/1995	2,326.90	74.54	2,401.4
351656116392901	14N/3E-27E3S	08/08/1995	2,327.00	74.43	2,401.4
351656116392901	14N/3E-27E3S	11/07/1995	2,326.70	74.66	2,401.4

Table 2–1. Water-level data for selected wells in Bicycle Basin, Fort Irwin National Training Center, California, 1955–2015. —Continued

[State well number: See well-numbering system in text. Site identification (ID) is the latitude, longitude, and sequence number of the site.
Abbreviations: mm/dd/yyyy, month/day/year; NAVD 88, North American Vertical Datum of 1988]

Site ID	State well number	Date (mm/dd/yyyy)	Water-surface altitude, feet above NAVD 88	Depth to water, feet below land surface	Land-surface altitude, feet above NAVD 88
Local ID: BP-4, MW-14—Continued					
351656116392901	14N/3E-27E3S	01/30/2002	2,327.80	73.56	2,401.4
351656116392901	14N/3E-27E3S	03/01/2005	2,329.20	72.25	2,401.4
351656116392901	14N/3E-27E3S	11/06/2007	2,330.50	70.95	2,401.4
351656116392901	14N/3E-27E3S	12/18/2007	2,331.00	70.39	2,401.4
351656116392901	14N/3E-27E3S	02/16/2008	2,330.20	71.25	2,401.4
351656116392901	14N/3E-27E3S	04/30/2008	2,329.20	72.25	2,401.4
351656116392901	14N/3E-27E3S	07/29/2008	2,328.50	72.90	2,401.4
351656116392901	14N/3E-27E3S	01/22/2009	2,328.50	72.92	2,401.4
351656116392901	14N/3E-27E3S	01/27/2009	2,328.40	73.02	2,401.4
351656116392901	14N/3E-27E3S	04/07/2009	2,328.80	72.57	2,401.4
351656116392901	14N/3E-27E3S	06/15/2010	2,328.10	73.27	2,401.4
351656116392901	14N/3E-27E3S	12/14/2010	2,328.40	73.01	2,401.4
351656116392901	14N/3E-27E3S	12/14/2010	2,328.40	72.98	2,401.4
351656116392901	14N/3E-27E3S	10/25/2011	2,328.10	73.26	2,401.4
351656116392901	14N/3E-27E3S	02/13/2012	2,327.30	74.08	2,401.4
351656116392901	14N/3E-27E3S	02/21/2012	2,327.10	74.30	2,401.4
351656116392901	14N/3E-27E3S	08/30/2012	2,326.10	75.33	2,401.4
351656116392901	14N/3E-27E3S	04/17/2013	2,327.20	74.25	2,401.4
351656116392901	14N/3E-27E3S	09/10/2013	2,325.80	75.64	2,401.4
351656116392901	14N/3E-27E3S	08/01/2014	2,324.90	76.54	2,401.4
351656116392901	14N/3E-27E3S	05/20/2015	2,325.80	75.64	2,401.4
Local ID: BP-MW22					
351659116393801	14N/3E-28A1S	09/24/1993	2,327.10	83.73	2,410.8
351659116393801	14N/3E-28A1S	02/09/1995	2,333.70	77.08	2,410.8
351659116393801	14N/3E-28A1S	05/05/1995	2,336.50	74.29	2,410.8
351659116393801	14N/3E-28A1S	08/09/1995	2,336.30	74.52	2,410.8
351659116393801	14N/3E-28A1S	11/08/1995	2,335.90	74.93	2,410.8
351659116393801	14N/3E-28A1S	07/01/1999	2,332.90	77.87	2,410.8
351659116393801	14N/3E-28A1S	07/28/2000	2,332.10	78.68	2,410.8
351659116393801	14N/3E-28A1S	01/30/2002	2,334.90	75.90	2,410.8
351659116393801	14N/3E-28A1S	03/01/2005	2,334.60	76.24	2,410.8
351659116393801	14N/3E-28A1S	11/06/2007	2,338.30	72.48	2,410.8
351659116393801	14N/3E-28A1S	02/16/2008	2,338.60	72.17	2,410.8
351659116393801	14N/3E-28A1S	04/29/2008	2,337.30	73.47	2,410.8
351659116393801	14N/3E-28A1S	07/29/2008	2,336.10	74.68	2,410.8
351659116393801	14N/3E-28A1S	01/22/2009	2,335.60	75.23	2,410.8
351659116393801	14N/3E-28A1S	04/08/2009	2,336.30	74.52	2,410.8
351659116393801	14N/3E-28A1S	12/14/2010	2,337.00	73.79	2,410.8
351659116393801	14N/3E-28A1S	10/25/2011	2,336.00	74.82	2,410.8
351659116393801	14N/3E-28A1S	02/13/2012	2,334.60	76.21	2,410.8

Table 2–1. Water-level data for selected wells in Bicycle Basin, Fort Irwin National Training Center, California, 1955–2015. —Continued

[State well number: See well-numbering system in text. Site identification (ID) is the latitude, longitude, and sequence number of the site.
Abbreviations: mm/dd/yyyy, month/day/year; NAVD 88, North American Vertical Datum of 1988]

Site ID	State well number	Date (mm/dd/yyyy)	Water-surface altitude, feet above NAVD 88	Depth to water, feet below land surface	Land-surface altitude, feet above NAVD 88
Local ID: BP-1, MW-11					
351635116393601	14N/3E-28H1S	01/26/1993	2,330.70	76.67	2,407.4
351635116393601	14N/3E-28H1S	09/24/1993	2,332.60	74.80	2,407.4
351635116393601	14N/3E-28H1S	08/15/1994	2,330.20	77.19	2,407.4
351635116393601	14N/3E-28H1S	09/08/1994	2,330.10	77.27	2,407.4
351635116393601	14N/3E-28H1S	02/09/1995	2,334.00	73.42	2,407.4
351635116393601	14N/3E-28H1S	05/05/1995	2,336.80	70.64	2,407.4
351635116393601	14N/3E-28H1S	08/09/1995	2,336.40	71.03	2,407.4
351635116393601	14N/3E-28H1S	11/08/1995	2,335.80	71.64	2,407.4
Local ID: BP-MW21					
351656116393401	14N/3E-28H2S	09/24/1993	2,329.10	71.79	2,400.9
351656116393401	14N/3E-28H2S	02/09/1995	2,330.70	70.21	2,400.9
351656116393401	14N/3E-28H2S	05/05/1995	2,334.70	66.16	2,400.9
351656116393401	14N/3E-28H2S	08/09/1995	2,332.60	68.34	2,400.9
351656116393401	14N/3E-28H2S	11/08/1995	2,332.10	68.80	2,400.9
Local ID: B-9_Aprt					
351611116380201	14N/3E-35C1S	04/10/1963	2,225.00	127.00	2,352.0
351611116380201	14N/3E-35C1S	02/02/1993	2,331.00	21.15	2,352.0
351611116380201	14N/3E-35C1S	07/22/1994	2,209.00	143.05	2,352.0
351611116380201	14N/3E-35C1S	03/08/1995	2,202.00	149.69	2,352.0
351611116380201	14N/3E-35C1S	08/11/1995	2,203.00	148.79	2,352.0
351611116380201	14N/3E-35C1S	07/07/1999	2,194.00	158.31	2,352.0
351611116380201	14N/3E-35C1S	02/14/2008	2,172.00	179.55	2,352.0
351611116380201	14N/3E-35C1S	07/29/2008	2,165.00	186.95	2,352.0
Local ID: BLA1-1					
351610116380201	14N/3E-35C2S	07/28/1994	2,207.73	149.67	2,357.4
351610116380201	14N/3E-35C2S	09/08/1994	2,207.42	149.98	2,357.4
351610116380201	14N/3E-35C2S	12/13/1994	2,207.50	149.90	2,357.4
351610116380201	14N/3E-35C2S	03/04/1995	2,207.27	150.13	2,357.4
351610116380201	14N/3E-35C2S	08/11/1995	2,205.00	152.40	2,357.4
351610116380201	14N/3E-35C2S	07/07/1999	2,199.34	158.06	2,357.4
351610116380201	14N/3E-35C2S	03/30/2000	2,197.72	159.68	2,357.4
351610116380201	14N/3E-35C2S	07/28/2000	2,195.21	162.19	2,357.4
351610116380201	14N/3E-35C2S	01/30/2002	2,193.01	164.39	2,357.4
351610116380201	14N/3E-35C2S	03/01/2005	2,183.69	173.71	2,357.4
Local ID: BLA1-2					
351610116380501	14N/3E-35C4S	01/30/2002	2,189.32	162.68	2,352.0
351610116380501	14N/3E-35C4S	03/01/2005	2,180.16	171.84	2,352.0
351610116380501	14N/3E-35C4S	11/06/2007	2,176.16	175.84	2,352.0
351610116380501	14N/3E-35C4S	12/20/2007	2,175.87	176.13	2,352.0
351610116380501	14N/3E-35C4S	02/14/2008	2,176.03	175.97	2,352.0

Table 2–1. Water-level data for selected wells in Bicycle Basin, Fort Irwin National Training Center, California, 1955–2015. —Continued

[State well number: See well-numbering system in text. Site identification (ID) is the latitude, longitude, and sequence number of the site.
Abbreviations: mm/dd/yyyy, month/day/year; NAVD 88, North American Vertical Datum of 1988]

Site ID	State well number	Date (mm/dd/yyyy)	Water-surface altitude, feet above NAVD 88	Depth to water, feet below land surface	Land-surface altitude, feet above NAVD 88
Local ID: BLA1-2—Continued					
351610116380501	14N/3E-35C4S	04/30/2008	2,175.65	176.35	2,352.0
351610116380501	14N/3E-35C4S	07/29/2008	2,174.37	177.63	2,352.0
351610116380501	14N/3E-35C4S	12/15/2010	2,170.57	181.43	2,352.0
351610116380501	14N/3E-35C4S	12/17/2010	2,170.49	181.51	2,352.0
351610116380501	14N/3E-35C4S	12/17/2010	2,170.49	181.51	2,352.0
351610116380501	14N/3E-35C4S	10/24/2011	2,169.14	182.86	2,352.0
351610116380501	14N/3E-35C4S	10/31/2011	2,169.10	182.90	2,352.0
351610116380501	14N/3E-35C4S	02/13/2012	2,168.99	183.01	2,352.0
351610116380501	14N/3E-35C4S	02/21/2012	2,168.82	183.18	2,352.0
351610116380501	14N/3E-35C4S	08/30/2012	2,167.60	184.40	2,352.0
351610116380501	14N/3E-35C4S	04/17/2013	2,167.34	184.66	2,352.0
351610116380501	14N/3E-35C4S	09/10/2013	2,166.96	185.04	2,352.0
351610116380501	14N/3E-35C4S	08/12/2014	2,166.16	185.84	2,352.0
351610116380501	14N/3E-35C4S	05/20/2015	2,165.00	186.73	2,352.0
Local ID: B-5					
351811116361801	14N/4E-18N1S	01/26/1993	2,187.90	190.13	2,378.0
351811116361801	14N/4E-18N1S	07/21/1994	2,183.20	194.76	2,378.0
351811116361801	14N/4E-18N1S	12/20/1994	2,191.90	186.08	2,378.0
351811116361801	14N/4E-18N1S	03/01/2005	2,151.20	226.85	2,378.0
351811116361801	14N/4E-18N1S	10/27/2011	2,141.00	237.00	2,378.0
Local ID: B-5A					
351811116361701	14N/4E-18N2S	12/03/1992	2,170.20	209.27	2,379.5
351811116361701	14N/4E-18N2S	01/26/1993	2,189.00	190.50	2,379.5
351811116361701	14N/4E-18N2S	09/07/1994	2,161.70	217.80	2,379.5
351811116361701	14N/4E-18N2S	11/22/1994	2,181.70	197.83	2,379.5
351811116361701	14N/4E-18N2S	03/03/1995	2,176.00	203.51	2,379.5
351811116361701	14N/4E-18N2S	08/03/1995	2,159.90	219.58	2,379.5
351811116361701	14N/4E-18N2S	09/18/1996	2,153.40	226.08	2,379.5
351811116361701	14N/4E-18N2S	07/08/1997	2,179.90	199.59	2,379.5
351811116361701	14N/4E-18N2S	09/03/1997	2,180.30	199.15	2,379.5
351811116361701	14N/4E-18N2S	09/08/1997	2,177.40	202.12	2,379.5
351811116361701	14N/4E-18N2S	07/09/1999	2,150.70	228.76	2,379.5
351811116361701	14N/4E-18N2S	03/30/2000	2,146.00	233.53	2,379.5
351811116361701	14N/4E-18N2S	07/28/2000	2,142.70	236.83	2,379.5
351811116361701	14N/4E-18N2S	01/30/2002	2,158.70	220.81	2,379.5
351811116361701	14N/4E-18N2S	03/01/2005	2,151.40	228.11	2,379.5
351811116361701	14N/4E-18N2S	11/06/2007	2,127.30	252.15	2,379.5
351811116361701	14N/4E-18N2S	12/19/2007	2,145.40	234.06	2,379.5
351811116361701	14N/4E-18N2S	02/14/2008	2,147.70	231.82	2,379.5
351811116361701	14N/4E-18N2S	04/29/2008	2,136.20	243.29	2,379.5

Table 2–1. Water-level data for selected wells in Bicycle Basin, Fort Irwin National Training Center, California, 1955–2015. —Continued

[State well number: See well-numbering system in text. Site identification (ID) is the latitude, longitude, and sequence number of the site.
Abbreviations: mm/dd/yyyy, month/day/year; NAVD 88, North American Vertical Datum of 1988]

Site ID	State well number	Date (mm/dd/yyyy)	Water-surface altitude, feet above NAVD 88	Depth to water, feet below land surface	Land-surface altitude, feet above NAVD 88
Local ID: B-5A—Continued					
351811116361701	14N/4E-18N2S	07/29/2008	2,127.40	252.14	2,379.5
351811116361701	14N/4E-18N2S	01/22/2009	2,128.90	250.55	2,379.5
351811116361701	14N/4E-18N2S	01/27/2009	2,128.30	251.21	2,379.5
351811116361701	14N/4E-18N2S	04/08/2009	2,126.00	253.54	2,379.5
351811116361701	14N/4E-18N2S	10/07/2009	2,124.20	255.33	2,379.5
351811116361701	14N/4E-18N2S	06/15/2010	2,127.40	252.11	2,379.5
351811116361701	14N/4E-18N2S	12/13/2010	2,124.70	254.85	2,379.5
351811116361701	14N/4E-18N2S	12/13/2010	2,124.70	254.83	2,379.5
351811116361701	14N/4E-18N2S	10/24/2011	2,139.60	239.93	2,379.5
351811116361701	14N/4E-18N2S	10/30/2011	2,140.10	239.41	2,379.5
351811116361701	14N/4E-18N2S	02/13/2012	2,126.50	252.97	2,379.5
351811116361701	14N/4E-18N2S	02/21/2012	2,138.50	241.03	2,379.5
351811116361701	14N/4E-18N2S	08/30/2012	2,119.30	260.23	2,379.5
351811116361701	14N/4E-18N2S	04/17/2013	2,140.90	238.59	2,379.5
351811116361701	14N/4E-18N2S	09/10/2013	2,144.30	235.20	2,379.5
351811116361701	14N/4E-18N2S	08/01/2014	2,120.10	259.37	2,379.5
351811116361701	14N/4E-18N2S	02/16/2015	2,123.20	256.33	2,379.5
351811116361701	14N/4E-18N2S	05/21/2015	2,139.20	240.26	2,379.5

Appendix 3. Water-Quality Data for Selected Wells in Bicycle Basin at Fort Irwin National Training Center, California, 1993–2011

Table 3–1. Water-quality data for selected wells in Bicycle Basin at Fort Irwin National Training Center, California, 1993–2011.

[E, estimated; ft, feet; hhmm, hour minute; ID, identification; mm/dd/yyyy, month/day/year; R, reported by the U.S. Geological Survey (USGS) Stable Isotope and Tritium Laboratory; TU, tritium units; <, less than; —, no data]

State well number	Date (mm/dd/yyyy)	Site ID	Local ID	Time (hhmm)	Depth of well, in ft below land surface (P72008)	Depth to water level, in ft below land surface (P72019)	Altitude of land surface, in feet (P72000)	Carbon dioxide, water, unfiltered, in milligrams per liter (P00405)	pH, water, field (P00400)	pH, water, lab (P00403)
14N/3E-13K1S	06/03/1993	351830116364501	B-1	1515	600	—	2,398	—	—	8.1
14N/3E-13M1S	05/21/1993	351829116371201	B-4	0915	600	—	2,419	2.8	8.1	8.1
14N/3E-13M1S	06/03/1993	351829116371201	B-4	1510	600	—	2,419	—	—	8.1
14N/3E-13M1S	09/14/1994	351829116371201	B-4	1015	600	—	2,419	4.4	7.8	7.8
14N/3E-13M2S	07/14/1997	351828116371201	BLA2 580-600	1200	600	319.95	2,418	5.7	7.8	7.9
14N/3E-13M2S	09/23/1997	351828116371201	BLA2 580-600	1430	600	—	2,418	3.3	8.0	8.1
14N/3E-13M2S	07/30/2000	351828116371201	BLA2 580-600	1200	600	—	2,418	2.8	8.1	8.0
14N/3E-13M3S	07/14/1997	351828116371202	BLA2 420-440	1700	440	301.07	2,418	13.0	7.4	7.7
14N/3E-13M3S	09/23/1997	351828116371202	BLA2 420-440	1800	440	—	2,418	16.0	7.4	7.4
14N/3E-13M3S	07/31/2000	351828116371202	BLA2 420-440	1145	440	—	2,418	3.9	7.9	7.7
14N/3E-13M4S	09/24/1997	351828116371203	BLA2 310-330	1240	330	—	2,418	6.4	7.7	7.9
14N/3E-13M4S	07/30/2000	351828116371203	BLA2 310-330	1530	330	—	2,418	4.7	7.8	7.6
14N/3E-13M4S	12/02/2010	351828116371203	BLA2 310-330	1314	330	—	2,418	3.2	7.9	8.1
14N/3E-14H1S	06/03/1993	351830116372601	B-2	1500	602	—	2,423	—	—	8.1
14N/3E-14H1S	07/29/1993	351830116372601	B-2	1030	602	—	2,423	3.3	8.0	8.1
14N/3E-14P1S	03/28/2000	351810116375701	B-6	1230	535	—	2,380	3.5	7.9	8.0
14N/3E-22N1S	05/19/1993	351710116392701	BA1	1830	260	170.96	2,418	2.7	8.1	8.1
14N/3E-22N1S	09/23/1993	351710116392701	BA1	1225	260	171.41	2,418	4.3	7.9	7.6
14N/3E-22N1S	09/21/1994	351710116392701	BA1	1300	260	171.56	2,418	5.7	7.8	7.8
14N/3E-22N1S	05/22/1996	351710116392701	BA1	1500	260	171.54	2,418	4.9	7.9	—
14N/3E-22N1S	06/12/1996	351710116392701	BA1	1035	260	171.64	2,418	3.9	7.9	7.8
14N/3E-22N1S	07/17/1997	351710116392701	BA1	1200	260	—	2,418	5.4	7.8	7.9
14N/3E-23B1S	03/02/2010	351759116374401	BLA4-1	1530	850	—	2,375	1.3	8.3	8.3
14N/3E-23B2S	03/02/2010	351759116374402	BLA4-2	1315	460	—	2,375	3.1	8.0	8.1
14N/3E-23B2S	12/05/2011	351759116374402	BLA4-2	1635	460	—	2,375	3.0	8.1	8.1
14N/3E-23B3S	03/02/2010	351759116374403	BLA4-3	1450	280	—	2,375	3.2	8.0	8.0
14N/3E-23B3S	12/05/2011	351759116374403	BLA4-3	1600	280	—	2,375	3.6	8.0	8.1
14N/3E-23G1S	09/24/1993	351738116374101	BX-2	0930	747	146.47	2,361	2.7	8.1	8.1
14N/3E-23G1S	09/21/1994	351738116374101	BX-2	1730	747	147.36	2,361	3.0	8.1	7.9
14N/3E-23G1S	12/02/2010	351738116374101	BX-2	2100	747	—	2,361	2.7	8.1	8.2

Table 3–1. Water-quality data for selected wells in Bicycle Basin at Fort Irwin National Training Center, California, 1993–2011.—Continued

[E, estimated; ft, feet; hhmm, hour minute; ID, identification; mm/dd/yyyy, month/day/year; R, reported by the U.S. Geological Survey (USGS) Stable Isotope and Tritium Laboratory; TU, tritium units; <, less than; —, no data]

State well number	Date (mm/dd/yyyy)	Site ID	Local ID	Time (hhmm)	Depth of well, in ft below land surface (P72008)	Depth to water level, in ft below land surface (P72019)	Altitude of land surface, in feet (P72000)	Carbon dioxide, water, unfiltered, in milligrams per liter (P00405)	pH, water, field (P00400)	pH, water, lab (P00403)
14N/3E-24H1S	07/29/1993	351742116362401	BX-1	1640	413	169.56	2,362	4.3	7.8	7.9
14N/3E-24H1S	09/20/1994	351742116362401	BX-1	1245	413	—	2,362	4.8	7.8	7.7
14N/3E-24Q1S	07/22/1997	351716116363701	BLA3 878-898	1400	898	—	2,356	4.8	7.7	7.8
14N/3E-24Q1S	09/08/1997	351716116363701	BLA3 878-898	1230	898	—	2,356	3.4	7.8	7.8
14N/3E-24Q1S	07/28/2000	351716116363701	BLA3 878-898	1330	898	—	2,356	3.4	7.8	7.8
14N/3E-24Q2S	07/23/1997	351716116363702	BLA3 725-734	1130	745	—	2,356	6.8	7.5	7.6
14N/3E-24Q2S	09/09/1997	351716116363702	BLA3 725-734	1100	745	—	2,356	4.9	7.6	7.6
14N/3E-24Q2S	07/29/2000	351716116363702	BLA3 725-734	1240	745	—	2,356	2.8	7.8	7.7
14N/3E-24Q3S	07/23/1997	351716116363703	BLA3 590-610	1700	610	—	2,356	13.0	7.5	7.7
14N/3E-24Q3S	09/10/1997	351716116363703	BLA3 590-610	1630	610	—	2,356	9.7	7.6	7.7
14N/3E-24Q3S	07/27/2000	351716116363703	BLA3 590-610	1645	610	—	2,356	3.8	8.0	8.1
14N/3E-24Q4S	07/24/1997	351716116363704	BLA3 430-450	1130	450	—	2,356	8.7	7.6	7.9
14N/3E-24Q4S	09/10/1997	351716116363704	BLA3 430-450	1030	450	—	2,356	6.1	7.8	7.9
14N/3E-24Q4S	07/29/2000	351716116363704	BLA3 430-450	1600	450	—	2,356	3.8	8.0	8.0
14N/3E-24Q5S	07/24/1997	351716116363705	BLA3 290-310	1600	310	—	2,356	15.0	7.4	7.6
14N/3E-24Q5S	09/08/1997	351716116363705	BLA3 290-310	1600	310	—	2,356	13.0	7.5	7.6
14N/3E-24Q5S	07/28/2000	351716116363705	BLA3 290-310	1615	310	—	2,356	7.8	7.7	7.7
14N/3E-24Q5S	12/06/2011	351716116363705	BLA3 290-310	1300	310	—	2,356	5.6	7.8	8.0
14N/3E-26K1S	05/12/2011	351638116374301	BLA5 1	1250	360	—	2,343	0.9	8.5	8.6
14N/3E-26K3S	12/08/2011	351638116374303	BLA5 3	1630	210	—	2,343	0.6	8.9	8.9
14N/3E-26K4S	05/12/2011	351638116374304	BLA5B 1	1420	270	—	2,343	2.4	8.1	8.2
14N/3E-27E1S	11/29/1994	351654116393301	BP-2, MW-12	1100	—	—	2,399	5.5	7.5	—
14N/3E-27E1S	02/08/1995	351654116393301	BP-2, MW-12	1600	—	75.27	2,399	3.2	7.7	—
14N/3E-27E1S	05/04/1995	351654116393301	BP-2, MW-12	1640	—	73.50	2,399	2.6	7.8	—
14N/3E-27E1S	05/08/1995	351654116393301	BP-2, MW-12	1800	—	73.50	2,399	3.0	7.7	7.2
14N/3E-27E1S	08/09/1995	351654116393301	BP-2, MW-12	1120	—	73.70	2,399	3.9	7.6	—
14N/3E-27E1S	11/07/1995	351654116393301	BP-2, MW-12	1510	—	73.96	2,399	4.7	7.5	—
14N/3E-27E2S	11/29/1994	351656116393101	BP-3, MW-13	1000	—	—	2,399	3.1	7.7	—
14N/3E-27E2S	02/08/1995	351656116393101	BP-3, MW-13	1330	—	75.22	2,399	3.1	7.8	—
14N/3E-27E2S	05/04/1995	351656116393101	BP-3, MW-13	1400	—	73.50	2,399	2.3	7.8	—
14N/3E-27E2S	08/09/1995	351656116393101	BP-3, MW-13	0920	—	73.70	2,399	2.6	7.8	—

Table 3–1. Water-quality data for selected wells in Bicycle Basin at Fort Irwin National Training Center, California, 1993–2011.—Continued

[E, estimated; ft, feet; hhmm, hour minute; ID, identification; mm/dd/yyyy, month/day/year; R, reported by the U.S. Geological Survey (USGS) Stable Isotope and Tritium Laboratory; TU, tritium units; <, less than; —, no data]

State well number	Date (mm/dd/yyyy)	Site ID	Local ID	Time (hhmm)	Depth of well, in ft below land surface (P72008)	Depth to water level, in ft below land surface (P72019)	Altitude of land surface, in feet (P72000)	Carbon dioxide, water, unfiltered, in milligrams per liter (P00405)	pH, water, field (P00400)	pH, water, lab (P00403)
14N/3E-27E2S	11/07/1995	351656116393101	BP-3, MW-13	1300	—	73.92	2,399	3.1	7.7	—
14N/3E-27E3S	11/28/1994	351656116392901	BP-4, MW-14	1400	—	—	2,399	1.5	8.1	—
14N/3E-27E3S	02/08/1995	351656116392901	BP-4, MW-14	1000	—	76.00	2,399	1.4	8.1	—
14N/3E-27E3S	05/04/1995	351656116392901	BP-4, MW-14	1345	—	74.50	2,399	1.5	8.1	—
14N/3E-27E3S	08/08/1995	351656116392901	BP-4, MW-14	1930	—	74.40	2,399	1.5	8.0	—
14N/3E-27E3S	11/07/1995	351656116392901	BP-4, MW-14	1045	—	74.66	2,399	2.3	7.8	—
14N/3E-28A1S	11/29/1994	351659116393801	BP-MW22	1700	151.28	—	2,411	3.6	7.8	—
14N/3E-28A1S	02/09/1995	351659116393801	BP-MW22	1515	151.28	77.08	2,411	3.7	7.8	—
14N/3E-28A1S	05/05/1995	351659116393801	BP-MW22	1500	151.28	74.29	2,411	2.5	7.9	7.6
14N/3E-28A1S	08/09/1995	351659116393801	BP-MW22	1950	151.28	74.50	2,411	3.4	7.8	—
14N/3E-28A1S	11/08/1995	351659116393801	BP-MW22	1520	151.28	74.93	2,411	3.3	7.8	7.7
14N/3E-28H1S	11/29/1994	351635116393601	BP-1, MW-11	1440	—	75.57	2,405	11.0	7.4	—
14N/3E-28H1S	02/09/1995	351635116393601	BP-1, MW-11	1230	—	73.42	2,405	14.0	7.3	—
14N/3E-28H1S	05/05/1995	351635116393601	BP-1, MW-11	1140	—	70.64	2,405	5.1	7.7	—
14N/3E-28H1S	08/09/1995	351635116393601	BP-1, MW-11	1420	—	71.00	2,405	8.6	7.5	—
14N/3E-28H1S	11/08/1995	351635116393601	BP-1, MW-11	1320	—	71.64	2,405	8.5	7.5	—
14N/3E-28H2S	11/29/1994	351656116393401	BP-MW21	1400	164.32	72.04	2,401	5.2	7.6	—
14N/3E-28H2S	02/09/1995	351656116393401	BP-MW21	0945	164.32	70.21	2,401	3.8	7.7	—
14N/3E-28H2S	05/05/1995	351656116393401	BP-MW21	1320	164.32	66.16	2,401	2.7	7.8	—
14N/3E-28H2S	08/09/1995	351656116393401	BP-MW21	1220	164.32	68.30	2,401	4.2	7.6	—
14N/3E-28H2S	11/08/1995	351656116393401	BP-MW21	1030	164.32	68.80	2,401	4.9	7.5	—
14N/3E-35C1S	03/29/2000	351611116380201	AIRPORT	1215	245	—	2,350	1.7	8.4	8.3
14N/3E-35C2S	07/31/2000	351610116380201	BLA1-1	1550	175	—	2,355	3.1	8.2	7.6
14N/4E-18N1S	05/21/1993	351811116361801	B-5	0800	800	—	2,378	4.0	7.8	7.9
14N/4E-18N1S	06/03/1993	351811116361801	B-5	1520	800	—	2,378	—	—	7.9
14N/4E-18N1S	09/23/1993	351811116361801	B-5	1000	800	—	2,378	6.5	7.5	7.6
14N/4E-18N1S	09/14/1994	351811116361801	B-5	1430	800	—	2,378	7.7	7.5	7.6
14N/4E-18N1S	03/28/2000	351811116361801	B-5	0915	800	—	2,378	3.7	7.8	7.9
14N/4E-18N1S	12/09/2008	351811116361801	B-5	1350	800	—	2,378	5.4	7.6	7.8
14N/4E-18N1S	12/01/2010	351811116361801	B-5	1130	800	—	2,378	3.0	7.9	7.9

Table 3–1. Water-quality data for selected wells in Bicycle Basin at Fort Irwin National Training Center, California, 1993–2011.—Continued

[E, estimated; ft, feet; hhmm, hour minute; ID, identification; mm/dd/yyyy, month/day/year; R, reported by the U.S. Geological Survey (USGS) Stable Isotope and Tritium Laboratory; TU, tritium units; <, less than; —, no data]

State well number	Date (mm/dd/[yyyy)	Specific conductance, lab, in microsiemens per centimeter at 25 degrees Celsius (P90095)	Specific conductance, in microsiemens per centimeter at 25 degrees Celsius (P00095)	Temperature, air, in degrees Celcius (P00020)	Temperature, water, in degrees Celcius (P00010)	Calcium, in milligrams per liter (P00915)	Magnesium, in milligrams per liter (P00925)	Potassium, in milligrams per liter (P00935)	Sodium, in milligrams per liter (P00930)
14N/3E-13K1S	06/03/1993	—	—	—	—	36.0	7.10	13.5	122
14N/3E-13M1S	05/21/1993	876	870	24.5	28.5	19.0	3.60	14.0	150
14N/3E-13M1S	06/03/1993	—	—	—	—	25.5	5.20	13.1	138
14N/3E-13M1S	09/14/1994	877	882	—	27.5	19.0	3.70	15.0	150
14N/3E-13M2S	07/14/1997	972	980	34.8	29.3	12.6	2.49	14.9	182
14N/3E-13M2S	09/23/1997	935	977	33.8	28.5	14.0	2.82	14.8	186
14N/3E-13M2S	07/30/2000	968	984	39.0	30.3	14.3	2.85	14.4	175
14N/3E-13M3S	07/14/1997	904	908	36.9	29.2	12.8	3.75	14.2	168
14N/3E-13M3S	09/23/1997	953	981	32.5	28.1	9.35	3.19	10.8	200
14N/3E-13M3S	07/31/2000	838	857	—	29.3	23.0	4.53	14.6	137
14N/3E-13M4S	09/24/1997	799	838	34.0	28.0	21.1	4.63	15.3	140
14N/3E-13M4S	07/30/2000	923	942	41.5	30.7	29.4	5.82	16.4	142
14N/3E-13M4S	12/02/2010	821	814	18.0	23.2	25.3	4.98	15.1	133
14N/3E-14H1S	06/03/1993	—	—	—	—	23.7	7.40	13.1	154
14N/3E-14H1S	07/29/1993	871	888	—	29.0	20.0	3.70	16.0	150
14N/3E-14P1S	03/28/2000	839	825	—	27.4	22.6	4.63	14.9	137
14N/3E-22N1S	05/19/1993	939	946	29.0	27.0	17.0	6.70	11.0	160
14N/3E-22N1S	09/23/1993	906	909	28.0	26.5	18.0	7.60	11.0	160
14N/3E-22N1S	09/21/1994	901	931	—	29.0	19.0	7.60	12.0	160
14N/3E-22N1S	05/22/1996	—	907	29.0	25.9	—	—	—	—
14N/3E-22N1S	06/12/1996	890	897	31.5	26.3	20.0	7.60	12.0	150
14N/3E-22N1S	07/17/1997	874	884	—	27.9	18.7	7.10	11.4	150
14N/3E-23B1S	03/02/2010	840	837	18.6	28.3	9.63	0.940	15.9	150
14N/3E-23B2S	03/02/2010	1,840	1,890	19.1	27.3	20.4	4.45	21.6	340
14N/3E-23B2S	12/05/2011	1,780	1,820	18.0	23.5	23.3	5.06	19.9	335
14N/3E-23B3S	03/02/2010	868	864	18.4	23.6	18.9	3.29	14.7	151
14N/3E-23B3S	12/05/2011	837	847	10.5	15.0	21.9	3.86	14.3	149
14N/3E-23G1S	09/24/1993	880	872	—	24.5	18.0	3.30	13.0	160
14N/3E-23G1S	09/21/1994	872	856	29.0	26.0	17.0	3.20	14.0	160
14N/3E-23G1S	12/02/2010	1,200	1,200	7.0	22.0	11.2	1.79	12.9	237

Table 3–1. Water-quality data for selected wells in Bicycle Basin at Fort Irwin National Training Center, California, 1993–2011.—Continued

[E, estimated; ft, feet; hhmm, hour minute; ID, identification; mm/dd/yyyy, month/day/year; R, reported by the U.S. Geological Survey (USGS) Stable Isotope and Tritium Laboratory; TU, tritium units; <, less than; —, no data]

State well number	Date (mm/dd/[yyyy)	Specific conductance, lab, in microsiemens per centimeter at 25 degrees Celsius (P90095)	Specific conductance, in microsiemens per centimeter at 25 degrees Celsius (P00095)	Temperature, air, in degrees Celcius (P00020)	Temperature, water, in degrees Celcius (P00010)	Calcium, in milligrams per liter (P00915)	Magnesium, in milligrams per liter (P00925)	Potassium, in milligrams per liter (P00935)	Sodium, in milligrams per liter (P00930)
14N/3E-24H1S	07/29/1993	820	838	34.5	24.5	31.0	10.0	4.90	120
14N/3E-24H1S	09/20/1994	773	780	32.0	26.0	32.0	10.0	5.30	110
14N/3E-24Q1S	07/22/1997	1,440	1,430	—	25.8	40.8	14.3	5.70	217
14N/3E-24Q1S	09/08/1997	1,290	1,450	—	28.1	42.2	15.8	5.34	227
14N/3E-24Q1S	07/28/2000	1,470	1,490	40.0	28.6	45.4	16.7	4.64	219
14N/3E-24Q2S	07/23/1997	1,810	1,820	—	26.2	50.3	18.5	10.0	268
14N/3E-24Q2S	09/09/1997	1,770	1,850	—	27.7	62.0	22.9	7.49	265
14N/3E-24Q2S	07/29/2000	1,850	1,890	40.5	28.8	71.2	25.7	6.24	253
14N/3E-24Q3S	07/23/1997	1,020	1,050	—	26.3	9.92	4.30	5.90	198
14N/3E-24Q3S	09/10/1997	896	942	—	28.1	10.8	4.29	4.32	182
14N/3E-24Q3S	07/27/2000	845	861	39.5	28.4	12.9	4.39	3.13	159
14N/3E-24Q4S	07/24/1997	928	949	—	26.6	13.2	4.05	5.50	179
14N/3E-24Q4S	09/10/1997	849	894	—	26.5	14.3	4.04	4.51	170
14N/3E-24Q4S	07/29/2000	874	895	41.0	28.6	14.8	4.19	4.33	166
14N/3E-24Q5S	07/24/1997	934	955	—	26.2	24.1	8.90	6.10	157
14N/3E-24Q5S	09/08/1997	888	940	—	27.8	27.7	10.0	5.57	156
14N/3E-24Q5S	07/28/2000	915	931	40.5	27.1	34.9	12.5	5.02	140
14N/3E-24Q5S	12/06/2011	992	1,030	10.0	21.5	39.1	14.1	5.41	156
14N/3E-26K1S	05/12/2011	810	837	27.5	25.0	5.62	1.46	6.48	166
14N/3E-26K3S	12/08/2011	944	969	11.0	21.5	2.54	0.344	3.40	215
14N/3E-26K4S	05/12/2011	759	781	29.5	24.5	18.1	4.36	10.6	143
14N/3E-27E1S	11/29/1994	—	1,420	—	22.1	—	—	—	—
14N/3E-27E1S	02/08/1995	—	1,420	15.5	21.3	—	—	—	—
14N/3E-27E1S	05/04/1995	—	1,450	22.8	22.7	—	—	—	—
14N/3E-27E1S	05/08/1995	1,450	1,440	23.1	22.7	86.0	12.0	19.0	170
14N/3E-27E1S	08/09/1995	—	1,500	40.5	23.5	—	—	—	—
14N/3E-27E1S	11/07/1995	—	1,530	24.6	22.0	—	—	—	—
14N/3E-27E2S	11/29/1994	—	1,440	—	22.2	—	—	—	—
14N/3E-27E2S	02/08/1995	—	1,440	16.2	21.9	—	—	—	—
14N/3E-27E2S	05/04/1995	—	1,470	24.6	23.3	—	—	—	—

Table 3–1. Water-quality data for selected wells in Bicycle Basin at Fort Irwin National Training Center, California, 1993–2011.—Continued

[E, estimated; ft, feet; hhmm, hour minute; ID, identification; mm/dd/yyyy, month/day/year; R, reported by the U.S. Geological Survey (USGS) Stable Isotope and Tritium Laboratory; TU, tritium units; <, less than; —, no data]

State well number	Date (mm/dd/[yyyy)	Specific conductance, lab, in microsiemens per centimeter at 25 degrees Celsius (P90095)	Specific conductance, in microsiemens per centimeter at 25 degrees Celsius (P00095)	Temperature, air, in degrees Celcius (P00020)	Temperature, water, in degrees Celcius (P00010)	Calcium, in milligrams per liter (P00915)	Magnesium, in milligrams per liter (P00925)	Potassium, in milligrams per liter (P00935)	Sodium, in milligrams per liter (P00930)
14N/3E-27E2S	08/09/1995	—	1,510	36.5	24.5	—	—	—	—
14N/3E-27E2S	11/07/1995	—	1,480	25.1	22.0	—	—	—	—
14N/3E-27E3S	11/28/1994	—	1,120	—	22.0	—	—	—	—
14N/3E-27E3S	02/08/1995	—	1,090	14.3	18.6	—	—	—	—
14N/3E-27E3S	05/04/1995	—	1,180	25.3	23.2	—	—	—	—
14N/3E-27E3S	08/08/1995	—	1,400	38.5	24.5	—	—	—	—
14N/3E-27E3S	11/07/1995	—	1,520	22.4	22.2	—	—	—	—
14N/3E-28A1S	11/29/1994	—	1,470	—	21.6	—	—	—	—
14N/3E-28A1S	02/09/1995	—	1,590	15.6	21.6	—	—	—	—
14N/3E-28A1S	05/05/1995	1,780	1,780	18.6	22.1	58.0	6.80	21.0	280
14N/3E-28A1S	08/09/1995	—	1,840	37.0	24.0	—	—	—	—
14N/3E-28A1S	11/08/1995	1,780	1,740	26.5	22.4	53.0	6.40	19.0	270
14N/3E-28H1S	11/29/1994	—	1,830	—	23.4	—	—	—	—
14N/3E-28H1S	02/09/1995	—	1,620	16.8	22.0	—	—	—	—
14N/3E-28H1S	05/05/1995	—	1,490	17.0	20.8	—	—	—	—
14N/3E-28H1S	08/09/1995	—	1,550	43.3	24.5	—	—	—	—
14N/3E-28H1S	11/08/1995	—	1,560	24.0	22.0	—	—	—	—
14N/3E-28H2S	11/29/1994	—	1,800	—	22.3	—	—	—	—
14N/3E-28H2S	02/09/1995	—	1,700	16.3	21.5	—	—	—	—
14N/3E-28H2S	05/05/1995	—	1,630	17.5	22.7	—	—	—	—
14N/3E-28H2S	08/09/1995	—	1,810	42.0	24.5	—	—	—	—
14N/3E-28H2S	11/08/1995	—	1,800	23.2	22.0	—	—	—	—
14N/3E-35C1S	03/29/2000	1,010	986	—	22.8	8.89	3.18	6.69	202
14N/3E-35C2S	07/31/2000	1,040	1,060	39.5	27.8	9.35	3.67	6.05	212
14N/4E-18N1S	05/21/1993	1,210	1,210	19.5	24.5	58.0	10.0	8.50	170
14N/4E-18N1S	06/03/1993	—	—	—	—	70.5	11.7	8.50	178
14N/4E-18N1S	09/23/1993	1,180	1,190	21.0	27.5	61.0	10.0	8.00	160
14N/4E-18N1S	09/14/1994	1,190	1,200	—	27.5	57.0	9.90	8.20	160
14N/4E-18N1S	03/28/2000	1,180	1,170	—	25.6	55.8	10.0	8.53	163
14N/4E-18N1S	12/09/2008	1,340	1,370	13.0	28.0	67.4	10.7	9.35	186

Table 3–1. Water-quality data for selected wells in Bicycle Basin at Fort Irwin National Training Center, California, 1993–2011.—Continued

[E, estimated; ft, feet; hhmm, hour minute; ID, identification; mm/dd/yyyy, month/day/year; R, reported by the U.S. Geological Survey (USGS) Stable Isotope and Tritium Laboratory; TU, tritium units; <, less than; —, no data]

State well number	Date (mm/dd/[yyyy)	Specific conductance, lab, in microsiemens per centimeter at 25 degrees Celsius (P90095)	Specific conductance, in microsiemens per centimeter at 25 degrees Celsius (P00095)	Temperature, air, in degrees Celcius (P00020)	Temperature, water, in degrees Celcius (P00010)	Calcium, in milligrams per liter (P00915)	Magnesium, in milligrams per liter (P00925)	Potassium, in milligrams per liter (P00935)	Sodium, in milligrams per liter (P00930)
14N/4E-18N1S	12/01/2010	1,340	1,320	8.0	27.0	64.7	10.5	8.64	180

State well number	Date (mm/dd/yyyy)	Alkalinity, fixed endpoint (pH 4.5) titration, field, in milligrams per liter as calcium carbonate (P39036)	Alkalinity, fixed endpoint (pH 4.5) titration, laboratory, in milligrams per liter as calcium carbonate (P90410)	Alkalinity, inflection-point titration method (incremental titration method), field, in milligrams per liter as calcium carbonate (P29801)	Bromide, in milligrams per liter (P71870)	Chloride, in milligrams per liter (P00940)	Fluoride, in milligrams per liter (P00950)	Iodide, in milligrams per liter (P71865)	Silica, in milligrams per liter as silica (P00955)	Sulfate, in milligrams per liter (P00945)
14N/3E-13K1S	06/03/1993	—	153	—	—	78.6	1.90	—	—	108
14N/3E-13M1S	05/21/1993	160	—	164	0.350	80.0	2.50	0.034	90.0	120
14N/3E-13M1S	06/03/1993	—	111	—	—	103	2.50	—	—	130
14N/3E-13M1S	09/14/1994	140	—	142	0.340	80.0	2.70	0.037	92.0	120
14N/3E-13M2S	07/14/1997	180	—	—	0.370	82.2	3.48	0.042	99.7	146
14N/3E-13M2S	09/23/1997	170	—	—	0.360	79.5	3.21	0.053	104	152
14N/3E-13M2S	07/30/2000	—	184	—	0.360	80.6	3.53	0.026	98.7	139
14N/3E-13M3S	07/14/1997	160	—	166	0.320	73.9	2.23	0.053	90.7	136
14N/3E-13M3S	09/23/1997	190	—	—	0.320	67.7	1.54	0.054	85.1	139
14N/3E-13M3S	07/31/2000	—	159	—	0.320	70.4	1.83	0.033	88.8	119
14N/3E-13M4S	09/24/1997	—	160	—	0.310	60.6	2.09	0.031	97.6	122
14N/3E-13M4S	07/30/2000	—	153	—	0.350	101	1.84	0.037	91.3	116
14N/3E-13M4S	12/02/2010	150	159	144	0.380	63.1	0.19	0.006	92.4	123
14N/3E-14H1S	06/03/1993	—	170	—	—	71.7	2.70	—	—	128
14N/3E-14H1S	07/29/1993	170	—	172	0.330	69.0	2.40	0.023	65.0	130
14N/3E-14P1S	03/28/2000	140	21.0	144	0.330	65.3	3.50	0.018	97.5	119
14N/3E-22N1S	05/19/1993	180	182	—	0.270	74.0	3.20	0.084	28.0	160
14N/3E-22N1S	09/23/1993	170	—	172	0.290	70.0	3.00	0.078	31.0	150
14N/3E-22N1S	09/21/1994	170	—	177	0.280	64.0	2.70	0.074	31.0	140
14N/3E-22N1S	05/22/1996	180	—	—	—	—	—	—	—	—
14N/3E-22N1S	06/12/1996	170	—	—	0.250	60.0	2.60	0.078	31.0	150
14N/3E-22N1S	07/17/1997	180	—	181	0.230	60.4	2.60	0.085	31.7	144
14N/3E-23B1S	03/02/2010	140	160	142	0.350	73.5	3.18	0.070	111	125
14N/3E-23B2S	03/02/2010	180	194	175	0.880	307	7.25	0.149	94.3	225

Table 3–1. Water-quality data for selected wells in Bicycle Basin at Fort Irwin National Training Center, California, 1993–2011.—Continued

[E, estimated; ft, feet; hhmm, hour minute; ID, identification; mm/dd/yyyy, month/day/year; R, reported by the U.S. Geological Survey (USGS) Stable Isotope and Tritium Laboratory; TU, tritium units; <, less than; —, no data]

State well number	Date (mm/dd/yyyy)	Alkalinity, fixed endpoint (pH 4.5) titration, field, in milligrams per liter as calcium carbonate (P39036)	Alkalinity, fixed endpoint (pH 4.5) titration, laboratory, in milligrams per liter as calcium carbonate (P90410)	Alkalinity, inflection-point titration method (incremental titration method), field, in milligrams per liter as calcium carbonate (P29801)	Bromide, in milligrams per liter (P71870)	Chloride, in milligrams per liter (P00940)	Fluoride, in milligrams per liter (P00950)	Iodide, in milligrams per liter (P71865)	Silica, in milligrams per liter as silica (P00955)	Sulfate, in milligrams per liter (P00945)
14N/3E-23B2S	12/05/2011	—	191	—	0.786	300	7.81	0.139	94.4	220
14N/3E-23B3S	03/02/2010	170	178	169	0.310	68.4	3.41	0.018	86.4	121
14N/3E-23B3S	12/05/2011	—	178	—	0.296	67.1	3.52	0.007	92.2	117
14N/3E-23G1S	09/24/1993	160	—	158	0.310	70.0	5.80	0.045	88.0	110
14N/3E-23G1S	09/21/1994	170	—	172	0.320	67.0	6.00	0.028	87.0	110
14N/3E-23G1S	12/02/2010	180	192	182	0.490	145	5.74	0.372	92.6	144
14N/3E-24H1S	07/29/1993	140	—	141	0.350	94.0	2.00	0.012	52.0	98.0
14N/3E-24H1S	09/20/1994	140	—	139	0.300	84.0	1.90	0.011	57.0	80.0
14N/3E-24Q1S	07/22/1997	110	—	110	0.690	270	1.55	0.055	29.5	133
14N/3E-24Q1S	09/08/1997	110	—	108	0.660	294	1.35	0.053	27.5	138
14N/3E-24Q1S	07/28/2000	—	112	—	0.740	294	1.23	0.023	28.9	128
14N/3E-24Q2S	07/23/1997	100	—	101	0.900	371	1.37	0.059	32.5	176
14N/3E-24Q2S	09/09/1997	95	—	94	0.910	408	1.13	0.048	29.8	174
14N/3E-24Q2S	07/29/2000	—	92.0	—	0.910	396	1.26	0.034	32.1	170
14N/3E-24Q3S	07/23/1997	200	—	204	0.360	116	2.57	0.046	35.3	101
14N/3E-24Q3S	09/10/1997	190	—	190	0.350	127	2.46	0.053	32.3	62.7
14N/3E-24Q3S	07/27/2000	—	195	—	0.290	105	2.30	0.025	31.1	53.4
14N/3E-24Q4S	07/24/1997	200	—	196	0.310	78.6	2.10	0.045	45.7	118
14N/3E-24Q4S	09/10/1997	190	—	190	0.310	71.6	2.10	0.044	46.7	112
14N/3E-24Q4S	07/29/2000	—	196	—	0.320	69.0	2.62	0.031	47.2	105
14N/3E-24Q5S	07/24/1997	190	—	194	0.310	75.3	1.59	0.047	56.2	125
14N/3E-24Q5S	09/08/1997	200	—	198	0.350	75.7	1.70	0.035	54.8	129
14N/3E-24Q5S	07/28/2000	—	201	—	0.360	76.8	1.64	0.020	54.6	118
14N/3E-24Q5S	12/06/2011	180	193	178	0.431	124	1.92	0.005	54.0	111
14N/3E-26K1S	05/12/2011	160	169	—	0.328	67.4	2.97	0.008	68.3	117
14N/3E-26K3S	12/08/2011	250	251	248	0.317	62.4	4.30	0.010	80.5	116
14N/3E-26K4S	05/12/2011	140	151	—	0.324	64.5	3.06	0.005	79.6	113
14N/3E-27E1S	11/29/1994	91	—	93	—	—	—	—	—	—
14N/3E-27E1S	02/08/1995	90	—	90	—	—	—	—	—	—
14N/3E-27E1S	05/04/1995	84	—	84	—	—	—	—	—	—

Table 3–1. Water-quality data for selected wells in Bicycle Basin at Fort Irwin National Training Center, California, 1993–2011.—Continued

[E, estimated; ft, feet; hhmm, hour minute; ID, identification; mm/dd/yyyy, month/day/year; R, reported by the U.S. Geological Survey (USGS) Stable Isotope and Tritium Laboratory; TU, tritium units; <, less than; —, no data]

State well number	Date (mm/dd/yyyy)	Alkalinity, fixed endpoint (pH 4.5) titration, field, in milligrams per liter as calcium carbonate (P39036)	Alkalinity, fixed endpoint (pH 4.5) titration, laboratory, in milligrams per liter as calcium carbonate (P90410)	Alkalinity, inflection-point titration method (incremental titration method), field, in milligrams per liter as calcium carbonate (P29801)	Bromide, in milligrams per liter (P71870)	Chloride, in milligrams per liter (P00940)	Fluoride, in milligrams per liter (P00950)	Iodide, in milligrams per liter (P71865)	Silica, in milligrams per liter as silica (P00955)	Sulfate, in milligrams per liter (P00945)
14N/3E-27E1S	05/08/1995	84	—	84	—	220	2.40	—	50.0	180
14N/3E-27E1S	08/09/1995	85	—	86	—	—	—	—	—	—
14N/3E-27E1S	11/07/1995	83	—	83	—	—	—	—	—	—
14N/3E-27E2S	11/29/1994	87	—	87	—	—	—	—	—	—
14N/3E-27E2S	02/08/1995	93	—	95	—	—	—	—	—	—
14N/3E-27E2S	05/04/1995	81	—	81	—	—	—	—	—	—
14N/3E-27E2S	08/09/1995	80	—	80	—	—	—	—	—	—
14N/3E-27E2S	11/07/1995	74	—	74	—	—	—	—	—	—
14N/3E-27E3S	11/28/1994	95	—	94	—	—	—	—	—	—
14N/3E-27E3S	02/08/1995	97	—	94	—	—	—	—	—	—
14N/3E-27E3S	05/04/1995	89	—	89	—	—	—	—	—	—
14N/3E-27E3S	08/08/1995	83	—	84	—	—	—	—	—	—
14N/3E-27E3S	11/07/1995	78	—	80	—	—	—	—	—	—
14N/3E-28A1S	11/29/1994	120	—	119	—	—	—	—	—	—
14N/3E-28A1S	02/09/1995	110	—	111	—	—	—	—	—	—
14N/3E-28A1S	05/05/1995	100	—	101	—	280	3.20	—	52.0	180
14N/3E-28A1S	08/09/1995	98	—	99	—	—	—	—	—	—
14N/3E-28A1S	11/08/1995	97	—	99	—	270	4.20	—	54.0	190
14N/3E-28H1S	11/29/1994	140	—	138	—	—	—	—	—	—
14N/3E-28H1S	02/09/1995	130	—	131	—	—	—	—	—	—
14N/3E-28H1S	05/05/1995	130	—	132	—	—	—	—	—	—
14N/3E-28H1S	08/09/1995	130	—	134	—	—	—	—	—	—
14N/3E-28H1S	11/08/1995	130	—	128	—	—	—	—	—	—
14N/3E-28H2S	11/29/1994	98	—	96	—	—	—	—	—	—
14N/3E-28H2S	02/09/1995	91	—	92	—	—	—	—	—	—
14N/3E-28H2S	05/05/1995	89	—	88	—	—	—	—	—	—
14N/3E-28H2S	08/09/1995	88	—	89	—	—	—	—	—	—
14N/3E-28H2S	11/08/1995	87	—	88	—	—	—	—	—	—
14N/3E-35C1S	03/29/2000	220	154	219	0.090	70.7	5.37	0.024	47.5	128
14N/3E-35C2S	07/31/2000	—	259	—	0.290	63.7	5.16	0.035	38.8	139

Table 3–1. Water-quality data for selected wells in Bicycle Basin at Fort Irwin National Training Center, California, 1993–2011.—Continued

[E, estimated; ft, feet; hhmm, hour minute; ID, identification; mm/dd/yyyy, month/day/year; R, reported by the U.S. Geological Survey (USGS) Stable Isotope and Tritium Laboratory; TU, tritium units; <, less than; —, no data]

State well number	Date (mm/dd/yyyy)	Alkalinity, fixed endpoint (pH 4.5) titration, field, in milligrams per liter as calcium carbonate (P39036)	Alkalinity, fixed endpoint (pH 4.5) titration, laboratory, in milligrams per liter as calcium carbonate (P90410)	Alkalinity, inflection-point titration method (incremental titration method), field, in milligrams per liter as calcium carbonate (P29801)	Bromide, in milligrams per liter (P71870)	Chloride, in milligrams per liter (P00940)	Fluoride, in milligrams per liter (P00950)	Iodide, in milligrams per liter (P71865)	Silica, in milligrams per liter as silica (P00955)	Sulfate, in milligrams per liter (P00945)
14N/4E-18N1S	05/21/1993	120	—	124	0.490	200	1.10	0.019	49.0	130
14N/4E-18N1S	06/03/1993	—	114	—	—	228	1.50	—	—	166
14N/4E-18N1S	09/23/1993	120	—	118	0.590	200	1.20	0.016	52.0	130
14N/4E-18N1S	09/14/1994	120	—	122	0.510	200	1.20	0.022	51.0	130
14N/4E-18N1S	03/28/2000	120	231	119	0.460	193	1.20	0.013	50.8	125
14N/4E-18N1S	12/09/2008	—	118	—	0.250	248	1.00	0.007	43.6	137
14N/4E-18N1S	12/01/2010	110	120	113	0.670	245	0.96	0.003	45.2	140

State well number	Date (mm/dd/yyyy)	Dissolved solids, sum of constituents, in milligrams per liter (P70301)	Ammonia, in milligrams per liter as nitrogen (P00608)	Nitrate plus nitrite, in milligrams per liter as nitrogen (P00631)	Nitrate, in milligrams per liter as nitrogen (P00618)	Nitrite, in milligrams per liter as nitrogen (P00613)	Organic nitrogen, in milligrams per liter (P00607)	Total nitrogen, in milligrams per liter (P00602)	Ortho-phosphate, in milligrams per liter (P00660)	Orthophosphate, in milligrams per liter as phosphorus (P00671)
14N/3E-13K1S	06/03/1993	480	<0.020	4.70	—	—	—	—	—	—
14N/3E-13M1S	05/21/1993	601	<0.020	4.80	—	<0.010	—	—	—	<0.010
14N/3E-13M1S	06/03/1993	510	0.010	5.80	—	—	—	—	—	—
14N/3E-13M1S	09/14/1994	592	<0.020	5.00	—	<0.010	—	—	—	<0.010
14N/3E-13M2S	07/14/1997	669	<0.020	3.14	3.12	0.019	—	—	1.19	0.390
14N/3E-13M2S	09/23/1997	677	0.020	3.11	—	<0.010	—	—	0.56	0.180
14N/3E-13M2S	07/30/2000	655	<0.020	3.27	—	<0.010	—	—	0.07	0.020
14N/3E-13M3S	07/14/1997	630	<0.010	4.55	4.39	0.160	—	—	7.29	2.38
14N/3E-13M3S	09/23/1997	711	<0.010	5.15	—	<0.010	—	—	57.6	18.8
14N/3E-13M3S	07/31/2000	574	<0.010	3.79	—	<0.010	—	—	0.17	0.050
14N/3E-13M4S	09/24/1997	594	<0.010	6.16	—	<0.010	—	—	5.28	1.72
14N/3E-13M4S	07/30/2000	618	<0.020	4.66	—	<0.010	—	—	0.11	0.040
14N/3E-13M4S	12/02/2010	572	<0.020	6.08	6.08	<0.001	<0.05	<6.1	0.13	0.043
14N/3E-14H1S	06/03/1993	521	0.015	4.20	—	—	—	—	—	—
14N/3E-14H1S	07/29/1993	584	<0.020	5.00	—	<0.010	—	—	—	<0.010
14N/3E-14P1S	03/28/2000	579	<0.020	5.87	—	<0.010	—	—	—	<0.010
14N/3E-22N1S	05/19/1993	577	<0.010	1.20	1.18	0.020	—	—	0.49	0.160

Table 3–1. Water-quality data for selected wells in Bicycle Basin at Fort Irwin National Training Center, California, 1993–2011.—Continued

[E, estimated; ft, feet; hhmm, hour minute; ID, identification; mm/dd/yyyy, month/day/year; R, reported by the U.S. Geological Survey (USGS) Stable Isotope and Tritium Laboratory; TU, tritium units; <, less than; —, no data]

State well number	Date (mm/dd/yyyy)	Dissolved solids, sum of constituents, in milligrams per liter (P70301)	Ammonia, in milligrams per liter as nitrogen (P00608)	Nitrate plus nitrite, in milligrams per liter as nitrogen (P00631)	Nitrate, in milligrams per liter as nitrogen (P00618)	Nitrite, in milligrams per liter as nitrogen (P00613)	Organic nitrogen, in milligrams per liter (P00607)	Total nitrogen, in milligrams per liter (P00602)	Ortho-phosphate, in milligrams per liter (P00660)	Orthophosphate, in milligrams per liter as phosphorus (P00671)
14N/3E-22N1S	09/23/1993	561	<0.020	1.10	1.09	0.010	—	—	0.74	0.240
14N/3E-22N1S	09/21/1994	553	<0.020	0.98	0.95	0.030	—	—	3.99	1.30
14N/3E-22N1S	05/22/1996	—	—	—	—	—	—	—	—	—
14N/3E-22N1S	06/12/1996	544	<0.020	1.10	1.08	0.020	—	—	2.51	0.820
14N/3E-22N1S	07/17/1997	541	<0.010	1.09	1.07	0.022	—	—	1.07	0.350
14N/3E-23B1S	03/02/2010	E583	<0.020	1.74	1.71	0.029	—	—	0.16	0.052
14N/3E-23B2S	03/02/2010	E1,130	<0.020	0.98	0.91	0.068	—	—	0.42	0.136
14N/3E-23B2S	12/05/2011	1,130	<0.020	1.10	1.02	0.085	<0.16	<1.2	0.27	0.088
14N/3E-23B3S	03/02/2010	E575	<0.020	5.29	—	<0.002	—	E5.4	0.19	0.061
14N/3E-23B3S	12/05/2011	601	<0.010	5.30	5.29	0.004	<0.26	<5.4	0.14	0.046
14N/3E-23G1S	09/24/1993	603	<0.020	8.70	—	<0.010	—	—	0.06	0.020
14N/3E-23G1S	09/21/1994	606	<0.020	8.40	—	<0.010	—	—	—	<0.010
14N/3E-23G1S	12/02/2010	789	<0.020	6.71	6.71	<0.001	<0.07	6.8	0.11	0.037
14N/3E-24H1S	07/29/1993	529	<0.020	7.00	—	<0.010	—	—	—	<0.010
14N/3E-24H1S	09/20/1994	498	0.010	7.50	—	<0.010	—	—	—	<0.010
14N/3E-24Q1S	07/22/1997	799	<0.020	3.91	3.77	0.147	—	—	1.75	0.570
14N/3E-24Q1S	09/08/1997	836	<0.020	3.63	3.54	0.081	—	—	1.15	0.370
14N/3E-24Q1S	07/28/2000	E822	<0.020	3.43	—	<0.010	—	—	0.16	0.050
14N/3E-24Q2S	07/23/1997	1,020	<0.020	4.38	4.12	0.267	—	—	6.31	2.06
14N/3E-24Q2S	09/09/1997	1,050	0.020	4.47	4.46	0.014	—	—	2.23	0.730
14N/3E-24Q2S	07/29/2000	E1,030	0.020	4.39	—	<0.010	—	—	0.040	0.010
14N/3E-24Q3S	07/23/1997	628	<0.010	3.56	3.16	0.402	—	—	14.1	4.58
14N/3E-24Q3S	09/10/1997	561	—	2.04	2.02	0.017	—	—	10.9	3.54
14N/3E-24Q3S	07/27/2000	E499	0.040	1.76	—	<0.010	—	—	1.28	0.420
14N/3E-24Q4S	07/24/1997	599	<0.020	6.04	5.89	0.154	—	—	6.81	2.22
14N/3E-24Q4S	09/10/1997	569	<0.020	5.63	5.62	0.012	—	—	3.29	1.07
14N/3E-24Q4S	07/29/2000	557	0.020	5.51	—	<0.010	—	—	0.074	0.020
14N/3E-24Q5S	07/24/1997	601	<0.020	5.39	5.35	0.045	—	—	4.30	1.40
14N/3E-24Q5S	09/08/1997	614	0.040	5.72	—	<0.010	—	—	8.45	2.76
14N/3E-24Q5S	07/28/2000	590	<0.020	5.30	—	<0.010	—	—	0.337	0.110
14N/3E-24Q5S	12/06/2011	636	<0.020	5.10	5.10	<0.001	<0.31	<5.2	0.063	0.020

Table 3–1. Water-quality data for selected wells in Bicycle Basin at Fort Irwin National Training Center, California, 1993–2011.—Continued

[E, estimated; ft, feet; hhmm, hour minute; ID, identification; mm/dd/yyyy, month/day/year; R, reported by the U.S. Geological Survey (USGS) Stable Isotope and Tritium Laboratory; TU, tritium units; <, less than; —, no data]

State well number	Date (mm/dd/yyyy)	Dissolved solids, sum of constituents, in milligrams per liter (P70301)	Ammonia, in milligrams per liter as nitrogen (P00608)	Nitrate plus nitrite, in milligrams per liter as nitrogen (P00631)	Nitrate, in milligrams per liter as nitrogen (P00618)	Nitrite, in milligrams per liter as nitrogen (P00613)	Organic nitrogen, in milligrams per liter (P00607)	Total nitrogen, in milligrams per liter (P00602)	Ortho-phosphate, in milligrams per liter (P00660)	Orthophosphate, in milligrams per liter as phosphorus (P00671)
14N/3E-26K1S	05/12/2011	551	0.020	4.64	4.63	0.004	<0.07	4.7	0.215	0.070
14N/3E-26K3S	12/08/2011	645	<0.020	5.26	5.26	0.002	—	<5.3	0.248	0.081
14N/3E-26K4S	05/12/2011	545	<0.020	4.67	4.66	0.003	<0.06	4.7	0.138	0.045
14N/3E-27E1S	11/29/1994	—	<0.020	19.0	19.0	0.010	—	—	—	<0.010
14N/3E-27E1S	02/08/1995	—	<0.020	20.0	20.0	0.030	—	—	—	<0.010
14N/3E-27E1S	05/04/1995	—	<0.020	20.0	—	<0.010	—	—	—	<0.010
14N/3E-27E1S	05/08/1995	879	<0.020	20.0	20.0	0.010	0.18	20.0	0.031	0.010
14N/3E-27E1S	08/09/1995	—	<0.020	22.0	—	<0.010	—	—	0.031	0.010
14N/3E-27E1S	11/07/1995	—	<0.020	22.0	—	<0.010	—	—	0.031	0.010
14N/3E-27E2S	11/29/1994	—	<0.010	20.0	—	<0.010	—	—	—	<0.010
14N/3E-27E2S	02/08/1995	—	<0.010	21.0	21.0	0.020	—	—	0.031	0.010
14N/3E-27E2S	05/04/1995	—	0.010	21.0	—	<0.010	—	—	0.031	0.010
14N/3E-27E2S	08/09/1995	—	<0.010	22.0	—	<0.010	—	—	0.031	0.010
14N/3E-27E2S	11/07/1995	—	<0.010	20.0	—	<0.010	—	—	0.031	0.010
14N/3E-27E3S	11/28/1994	—	<0.010	25.0	—	<0.010	—	—	0.031	0.010
14N/3E-27E3S	02/08/1995	—	<0.020	14.0	14.0	0.020	—	—	0.092	0.030
14N/3E-27E3S	05/04/1995	—	<0.020	15.0	—	<0.010	—	—	—	<0.010
14N/3E-27E3S	08/08/1995	—	<0.010	19.0	—	<0.010	—	—	—	<0.010
14N/3E-27E3S	11/07/1995	—	<0.020	22.0	—	<0.010	—	—	—	<0.010
14N/3E-28A1S	11/29/1994	—	<0.010	21.0	21.0	0.010	0.19	21.0	0.031	0.010
14N/3E-28A1S	02/09/1995	—	<0.020	23.0	23.0	0.020	—	—	0.031	0.010
14N/3E-28A1S	05/05/1995	1,080	0.020	30.0	—	<0.010	—	—	0.031	0.010
14N/3E-28A1S	08/09/1995	—	—	31.0	—	<0.010	—	—	—	<0.010
14N/3E-28A1S	11/08/1995	1,060	0.010	30.0	—	<0.010	—	—	—	<0.010
14N/3E-28H1S	11/29/1994	—	<0.010	20.0	—	<0.010	—	—	—	<0.010
14N/3E-28H1S	02/09/1995	—	<0.020	16.0	—	<0.010	—	—	0.031	0.010
14N/3E-28H1S	05/05/1995	—	<0.020	13.0	—	<0.010	—	—	—	<0.010
14N/3E-28H1S	08/09/1995	—	—	14.0	—	<0.010	—	—	0.061	0.020
14N/3E-28H1S	11/08/1995	—	<0.010	14.0	—	<0.010	—	—	0.031	0.010
14N/3E-28H2S	11/29/1994	—	<0.020	26.0	—	<0.010	—	—	—	<0.010
14N/3E-28H2S	02/09/1995	—	<0.020	23.0	—	<0.010	—	—	—	<0.010

Table 3–1. Water-quality data for selected wells in Bicycle Basin at Fort Irwin National Training Center, California, 1993–2011.—Continued

[E, estimated; ft, feet; hhmm, hour minute; ID, identification; mm/dd/yyyy, month/day/year; R, reported by the U.S. Geological Survey (USGS) Stable Isotope and Tritium Laboratory; TU, tritium units; <, less than; —, no data]

State well number	Date (mm/dd/yyyy)	Dissolved solids, sum of constituents, in milligrams per liter (P70301)	Ammonia, in milligrams per liter as nitrogen (P00608)	Nitrate plus nitrite, in milligrams per liter as nitrogen (P00631)	Nitrate, in milligrams per liter as nitrogen (P00618)	Nitrite, in milligrams per liter as nitrogen (P00613)	Organic nitrogen, in milligrams per liter (P00607)	Total nitrogen, in milligrams per liter (P00602)	Ortho-phosphate, in milligrams per liter (P00660)	Orthophosphate, in milligrams per liter as phosphorus (P00671)
14N/3E-28H2S	05/05/1995	—	<0.020	21.0	—	<0.010	—	—	—	<0.010
14N/3E-28H2S	08/09/1995	—	<0.020	21.0	—	<0.010	—	—	—	<0.010
14N/3E-28H2S	11/08/1995	—	<0.020	23.0	—	<0.010	—	—	—	<0.010
14N/3E-35C1S	03/29/2000	637	<0.020	7.04	—	<0.010	—	—	0.034	0.010
14N/3E-35C2S	07/31/2000	E654	<0.020	4.25	—	<0.010	—	—	0.095	0.030
14N/4E-18N1S	05/21/1993	727	<0.020	5.40	—	<0.010	—	—	—	<0.010
14N/4E-18N1S	06/03/1993	758	<0.010	5.60	—	—	—	—	—	—
14N/4E-18N1S	09/23/1993	719	0.010	5.30	—	<0.010	—	—	0.031	0.010
14N/4E-18N1S	09/14/1994	717	—	5.60	—	<0.010	—	—	—	<0.010
14N/4E-18N1S	03/28/2000	706	<0.010	5.53	—	<0.010	—	—	—	<0.010
14N/4E-18N1S	12/09/2008	798	—	4.94	—	<0.002	—	—	0.090	0.029
14N/4E-18N1S	12/01/2010	786	<0.010	4.96	4.96	<0.001	<0.06	5.0	0.069	0.023

State well number	Date (mm/dd/yyyy)	Phosphorus, milligrams per liter as phosphorus (P00666)	Aluminum, micrograms per liter (P01106)	Arsenic, micrograms per liter (P01000)	Barium, micrograms per liter (P01005)	Boron, micrograms per liter (P01020)	Chromium, micrograms per liter (P01030)	Iron, micrograms per liter (P01046)	Lithium, micrograms per liter (P01130)	Manganese, micrograms per liter (P01056)	Strontium, micrograms per liter (P01080)
14N/3E-13K1S	06/03/1993	—	—	—	—	—	—	—	—	<30.0	—
14N/3E-13M1S	05/21/1993	<0.01	<10.0	29.0	36.0	1,200	—	9.0	48.0	<1.00	400
14N/3E-13M1S	06/03/1993	—	—	—	—	—	—	—	—	<30.0	—
14N/3E-13M1S	09/14/1994	0.01	—	37.0	36.0	1,200	—	<3.0	49.0	<1.00	390
14N/3E-13M2S	07/14/1997	1.58	—	35.0	26.5	1,130	—	7.0	—	12.6	347
14N/3E-13M2S	09/23/1997	0.21	—	39.0	34.0	1,190	—	<3.0	—	2.50	423
14N/3E-13M2S	07/30/2000	<0.05	<20.0	41.7	35.2	1,110	—	<10.0	42.0	<2.20	414
14N/3E-13M3S	07/14/1997	7.95	—	45.0	9.0	1,130	—	179.0	—	59.9	225
14N/3E-13M3S	09/23/1997	21.0	—	72.0	10.2	1,220	—	122	—	139	169
14N/3E-13M3S	07/31/2000	E0.04	<20.0	36.1	32.1	1,110	—	<10.0	44.0	<2.20	402
14N/3E-13M4S	09/24/1997	2.95	—	29.0	25.5	1,260	—	41.0	—	7.10	365
14N/3E-13M4S	07/30/2000	E0.04	<20.0	24.6	39.1	1,210	—	<10.0	58.0	<2.20	472
14N/3E-13M4S	12/02/2010	<0.02	<5.1	24.6	31.9	1,110	—	<3.0	73.0	0.20	407
14N/3E-14H1S	06/03/1993	—	—	—	—	—	—	—	—	<30.0	—

Table 3–1. Water-quality data for selected wells in Bicycle Basin at Fort Irwin National Training Center, California, 1993–2011.—Continued

[E, estimated; ft, feet; hhmm, hour minute; ID, identification; mm/dd/yyyy, month/day/year; R, reported by the U.S. Geological Survey (USGS) Stable Isotope and Tritium Laboratory; TU, tritium units; <, less than; —, no data]

State well number	Date (mm/dd/yyyy)	Phosphorus, milligrams per liter as phosphorus (P00666)	Aluminum, micrograms per liter (P01106)	Arsenic, micrograms per liter (P01000)	Barium, micrograms per liter (P01005)	Boron, micrograms per liter (P01020)	Chromium, micrograms per liter (P01030)	Iron, micrograms per liter (P01046)	Lithium, micrograms per liter (P01130)	Manganese, micrograms per liter (P01056)	Strontium, micrograms per liter (P01080)
14N/3E-14H1S	07/29/1993	<0.01	4.0	29.0	35.0	1,200	10.0	8.0	50.0	2.00	390
14N/3E-14P1S	03/28/2000	<0.05	<20.0	19.0	32.2	1,110	—	<10.0	45.0	<2.20	264
14N/3E-22N1S	05/19/1993	0.17	—	3.0	8.0	1,000	—	7.0	31.0	28.0	400
14N/3E-22N1S	09/23/1993	0.23	12.0	3.0	9.0	1,100	<1.00	<3.0	30.0	32.0	430
14N/3E-22N1S	09/21/1994	1.30	—	7.0	8.0	1,000	—	<3.0	31.0	38.0	430
14N/3E-22N1S	05/22/1996	—	—	—	—	—	—	—	—	—	—
14N/3E-22N1S	06/12/1996	0.81	—	4.0	<100	1,040	—	<3.0	28.0	34.0	490
14N/3E-22N1S	07/17/1997	0.33	—	3.0	8.5	994	—	<3.0	—	32.7	477
14N/3E-23B1S	03/02/2010	<0.04	E7.7	103	30.3	1,040	5.10	<6.0	45.0	2.40	260
14N/3E-23B2S	03/02/2010	0.09	E2.4	45.7	23.8	1,230	E0.11	<6.0	44.0	11.8	464
14N/3E-23B2S	12/05/2011	0.06	<11.0	39.2	25.4	1,310	—	14.2	47.5	15.1	493
14N/3E-23B3S	03/02/2010	E0.02	E6.8	73.7	29.3	1,090	41.0	<6.0	80.0	0.20	231
14N/3E-23B3S	12/05/2011	0.03	6.8	24.4	30.1	1,160	—	4.7	89.0	0.87	260
14N/3E-23G1S	09/24/1993	0.05	17.0	22.0	33.0	1,200	11.0	24.0	60.0	1.00	240
14N/3E-23G1S	09/21/1994	<0.01	—	24.0	29.0	1,200	—	<3.0	53.0	<1.00	210
14N/3E-23G1S	12/02/2010	<0.02	4.0	21.3	12.5	1,370	—	<3.0	71.0	0.40	152
14N/3E-24H1S	07/29/1993	<0.01	3.0	6.0	44.0	860	4.00	12.0	30.0	3.00	390
14N/3E-24H1S	09/20/1994	<0.01	—	7.0	42.0	780	—	25.0	35.0	2.00	380
14N/3E-24Q1S	07/22/1997	1.20	—	5.0	15.6	794	—	<3.0	—	51.3	559
14N/3E-24Q1S	09/08/1997	0.38	—	3.0	14.9	808	—	<3.0	—	45.9	582
14N/3E-24Q1S	07/28/2000	0.06	E10.0	E1.0	12.8	777	—	<10.0	35.0	18.6	612
14N/3E-24Q2S	07/23/1997	2.95	—	6.0	15.6	792	—	5.0	—	128	617
14N/3E-24Q2S	09/09/1997	0.76	—	2.0	19.5	745	—	5.0	—	62.4	781
14N/3E-24Q2S	07/29/2000	<0.05	<20.0	E0.5	16.8	726	—	<10.0	43.0	<2.20	811
14N/3E-24Q3S	07/23/1997	9.88	—	13.0	3.0	934	—	148	—	121	138
14N/3E-24Q3S	09/10/1997	6.08	—	8.0	4.6	896	—	74.0	—	96.2	183
14N/3E-24Q3S	07/27/2000	0.51	<20.0	2.7	9.3	846	—	<10.0	21.0	E1.30	160
14N/3E-24Q4S	07/24/1997	4.18	—	21.0	6.8	924	—	67.0	—	62.6	203
14N/3E-24Q4S	09/10/1997	1.44	—	12.0	10.4	919	—	<3.0	—	21.1	230
14N/3E-24Q4S	07/29/2000	<0.05	<20.0	6.7	13.3	889	—	<10.0	27.0	<2.20	212
14N/3E-24Q5S	07/24/1997	4.71	—	11.0	6.7	876	—	138	—	55.3	337

Table 3–1. Water-quality data for selected wells in Bicycle Basin at Fort Irwin National Training Center, California, 1993–2011.—Continued

[E, estimated; ft, feet; hhmm, hour minute; ID, identification; mm/dd/yyyy, month/day/year; R, reported by the U.S. Geological Survey (USGS) Stable Isotope and Tritium Laboratory; TU, tritium units; <, less than; —, no data]

State well number	Date (mm/dd/yyyy)	Phosphorus, milligrams per liter as phosphorus (P00666)	Aluminum, micrograms per liter (P01106)	Arsenic, micrograms per liter (P01000)	Barium, micrograms per liter (P01005)	Boron, micrograms per liter (P01020)	Chromium, micrograms per liter (P01030)	Iron, micrograms per liter (P01046)	Lithium, micrograms per liter (P01130)	Manganese, micrograms per liter (P01056)	Strontium, micrograms per liter (P01080)
14N/3E-24Q5S	09/08/1997	2.85	—	13.0	7.9	916	—	16.0	—	42.9	409
14N/3E-24Q5S	07/28/2000	0.13	<20.0	2.0	29.0	902	—	<10.0	38.0	<2.20	439
14N/3E-24Q5S	12/06/2011	0.03	<2.2	3.0	29.2	874	—	4.6	58.7	0.54	466
14N/3E-26K1S	05/12/2011	0.03	28.4	33.3	2.9	999	—	11.8	18.4	0.73	94.2
14N/3E-26K3S	12/08/2011	0.05	28.9	51.9	3.6	967	—	18.5	14.8	0.62	45.4
14N/3E-26K4S	05/12/2011	0.02	5.1	14.5	21.0	995	—	4.7	33.9	0.81	306
14N/3E-27E1S	11/29/1994	<0.01	—	—	—	—	—	—	—	—	—
14N/3E-27E1S	02/08/1995	<0.01	—	—	—	—	—	—	—	—	—
14N/3E-27E1S	05/04/1995	0.01	—	—	—	—	—	—	—	—	—
14N/3E-27E1S	05/08/1995	0.01	—	—	—	1,100	—	<3.0	—	<1.00	—
14N/3E-27E1S	08/09/1995	<0.01	—	—	—	—	—	—	—	—	—
14N/3E-27E1S	11/07/1995	0.02	—	—	—	—	—	—	—	—	—
14N/3E-27E2S	11/29/1994	<0.01	—	—	—	—	—	—	—	—	—
14N/3E-27E2S	02/08/1995	<0.01	—	—	—	—	—	—	—	—	—
14N/3E-27E2S	05/04/1995	0.03	—	—	—	—	—	—	—	—	—
14N/3E-27E2S	08/09/1995	<0.01	—	—	—	—	—	—	—	—	—
14N/3E-27E2S	11/07/1995	<0.01	—	—	—	—	—	—	—	—	—
14N/3E-27E3S	11/28/1994	<0.01	—	—	—	—	—	—	—	—	—
14N/3E-27E3S	02/08/1995	0.02	—	—	—	—	—	—	—	—	—
14N/3E-27E3S	05/04/1995	<0.01	—	—	—	—	—	—	—	—	—
14N/3E-27E3S	08/08/1995	<0.01	—	—	—	—	—	—	—	—	—
14N/3E-27E3S	11/07/1995	0.01	—	—	—	—	—	—	—	—	—
14N/3E-28A1S	11/29/1994	0.01	—	—	—	—	—	—	—	—	—
14N/3E-28A1S	02/09/1995	<0.01	—	—	—	—	—	—	—	—	—
14N/3E-28A1S	05/05/1995	0.01	—	—	—	1,400	—	<3.0	—	<1.00	—
14N/3E-28A1S	08/09/1995	0.02	—	—	—	—	—	—	—	—	—
14N/3E-28A1S	11/08/1995	<0.01	—	—	—	1,500	—	<3.0	—	<1.00	—
14N/3E-28H1S	11/29/1994	<0.01	—	—	—	—	—	—	—	—	—
14N/3E-28H1S	02/09/1995	<0.01	—	—	—	—	—	—	—	—	—
14N/3E-28H1S	05/05/1995	0.01	—	—	—	—	—	—	—	—	—
14N/3E-28H1S	08/09/1995	<0.01	—	—	—	—	—	—	—	—	—

Table 3–1. Water-quality data for selected wells in Bicycle Basin at Fort Irwin National Training Center, California, 1993–2011.—Continued

[E, estimated; ft, feet; hhmm, hour minute; ID, identification; mm/dd/yyyy, month/day/year; R, reported by the U.S. Geological Survey (USGS) Stable Isotope and Tritium Laboratory; TU, tritium units; <, less than; —, no data]

State well number	Date (mm/dd/yyyy)	Phosphorus, milligrams per liter as phosphorus (P00666)	Aluminum, micrograms per liter (P01106)	Arsenic, micrograms per liter (P01000)	Barium, micrograms per liter (P01005)	Boron, micrograms per liter (P01020)	Chromium, micrograms per liter (P01030)	Iron, micrograms per liter (P01046)	Lithium, micrograms per liter (P01130)	Manganese, micrograms per liter (P01056)	Strontium, micrograms per liter (P01080)
14N/3E-28H1S	11/08/1995	<0.01	—	—	—	—	—	—	—	—	—
14N/3E-28H2S	11/29/1994	<0.01	—	—	—	—	—	—	—	—	—
14N/3E-28H2S	02/09/1995	<0.01	—	—	—	—	—	—	—	—	—
14N/3E-28H2S	05/05/1995	<0.01	—	—	—	—	—	—	—	—	—
14N/3E-28H2S	08/09/1995	<0.01	—	—	—	—	—	—	—	—	—
14N/3E-28H2S	11/08/1995	<0.01	—	—	—	—	—	—	—	—	—
14N/3E-35C1S	03/29/2000	<0.05	<20.0	29.0	4.2	1,570	—	45.0	17.0	<2.20	294
14N/3E-35C2S	07/31/2000	E0.04	<20.0	30.0	5.6	1,990	—	<10.0	20.0	E1.80	310
14N/4E-18N1S	05/21/1993	<0.01	<10.0	5.0	39.0	810	—	10.0	55.0	<1.00	630
14N/4E-18N1S	06/03/1993	—	—	—	—	—	—	—	—	<30.0	—
14N/4E-18N1S	09/23/1993	0.02	5.0	5.0	43.0	790	3.00	<3.0	60.0	<1.00	630
14N/4E-18N1S	09/14/1994	0.01	—	6.0	37.0	770	—	<3.0	54.0	<1.00	600
14N/4E-18N1S	03/28/2000	<0.05	<20.0	5.0	40.7	761	—	<10.0	54.0	<2.20	626
14N/4E-18N1S	12/09/2008	—	<4.0	3.4	35.0	719	2.70	9.0	57.1	0.60	688
14N/4E-18N1S	12/01/2010	<0.02	1.7	3.5	38.4	672	—	8.0	92.0	0.60	716

State well number	Date (mm/dd/yyyy)	Carbon-14 counting error, percent modern carbon (P49934)	Carbon-14, percent modern carbon (P49933[1])	Tritium, in picocuries per liter (P07000)	Tritium, in TU	Carbon-13/carbon-12 ratio, per mil (P82081)	Deuterium/protium ratio, per mil (P82082)	Oxygen-18/oxygen-16 ratio, per mil (P82085)
14N/3E-13K1S	06/03/1993	—	—	—	—	—	—	—
14N/3E-13M1S	05/21/1993	—	—	—	—	—	–96.4	–12.42
14N/3E-13M1S	06/03/1993	—	—	—	—	—	—	—
14N/3E-13M1S	09/14/1994	—	[1]5.3	—	—	–8.80	–96.8	–12.38
14N/3E-13M2S	07/14/1997	—	—	—	—	—	–100.0	–12.53
14N/3E-13M2S	09/23/1997	0.08	1.3	<0.30	<0.09	–6.02	–98.7	–12.43
14N/3E-13M2S	07/30/2000	0.06	1.7	<0.30	<0.09	–5.98	–98.2	–12.48
14N/3E-13M3S	07/14/1997	—	—	—	—	—	–96.4	–12.15
14N/3E-13M3S	09/23/1997	0.18	9.5	<0.30	<0.09	–7.41	–94.5	–11.90
14N/3E-13M3S	07/31/2000	0.11	6.4	<0.30	<0.09	–6.31	–92.5	–12.21
14N/3E-13M4S	09/24/1997	—	—	—	—	—	–94.8	–11.76
14N/3E-13M4S	07/30/2000	0.12	6.0	<0.30	<0.09	–6.99	–93.6	–12.36

Table 3–1. Water-quality data for selected wells in Bicycle Basin at Fort Irwin National Training Center, California, 1993–2011.—Continued

[E, estimated; ft, feet; hhmm, hour minute; ID, identification; mm/dd/yyyy, month/day/year; R, reported by the U.S. Geological Survey (USGS) Stable Isotope and Tritium Laboratory; TU, tritium units; <, less than; —, no data]

State well number	Date (mm/dd/yyyy)	Carbon-14 counting error, percent modern carbon (P49934)	Carbon-14, percent modern carbon (P49933[1])	Tritium, in picocuries per liter (P07000)	Tritium, in TU	Carbon-13/carbon-12 ratio, per mil (P82081)	Deuterium/protium ratio, per mil (P82082)	Oxygen-18/oxygen-16 ratio, per mil (P82085)
14N/3E-13M4S	12/02/2010	—	—	—	—	—	–94.2	–11.83
14N/3E-14H1S	06/03/1993	—	—	—	—	—	—	—
14N3E-14H1S	07/29/1993	—	—	—	—	—	–98.0	–12.48
14N/3E-14P1S	03/28/2000	0.15	6.6	<0.30	<0.09	–7.21	–94.5	–11.90
14N/3E-22N1S	05/19/1993	—	—	—	—	—	–88.6	–11.24
14N/3E-22N1S	09/23/1993	—	[1]12.7	—	—	–6.40	–88.5	–11.24
14N/3E-22N1S	09/21/1994	—	—	—	—	—	–87.8	–11.20
14N/3E-22N1S	05/22/1996	—	—	—	—	—	—	—
14N/3E-22N1S	06/12/1996	—	—	—	—	—	—	—
14N/3E-22N1S	07/17/1997	0.19	12.1	<–0.16	<–0.05	–5.81	–89.3	–11.05
14N/3E-23B1S	03/02/2010	0.03	0.7	R0.10	R0.03	–6.22	–97.3	–12.13
14N/3E-23B2S	03/02/2010	0.04	1.7	0.70	0.22	–5.74	–96.5	–12.07
14N/3E-23B2S	12/05/2011	—	—	—	—	—	–97.9	–12.03
14N/3E-23B3S	03/02/2010	0.09	5.4	R–0.20	R–0.06	–6.45	–93.7	–11.77
14N/3E-23B3S	12/05/2011	—	—	—	—	—	–93.7	–11.79
14N/3E-23G1S	09/24/1993	—	[1]8.6	<0.30	<0.09	–7.10	–89.6	–11.43
14N/3E-23G1S	09/21/1994	—	[1]4.7	—	—	–7.40	–90.1	–11.38
14N/3E-23G1S	12/02/2010	—	—	—	—	—	–92.8	–11.50
14N/3E-24H1S	07/29/1993	—	—	—	—	—	–94.7	–12.22
14N/3E-24H1S	09/20/1994	—	[1]14.3	—	—	–9.00	–95.6	–12.46
14N/3E-24Q1S	07/22/1997	—	—	—	—	—	–99.7	–12.78
14N/3E-24Q1S	09/08/1997	0.12	5.6	<0.30	<0.09	–8.58	–101.0	–12.94
14N/3E-24Q1S	07/28/2000	0.09	4.2	<0.30	<0.09	–8.12	–100.0	–13.00
14N/3E-24Q2S	07/23/1997	—	—	—	—	—	–100.0	–12.72
14N/3E-24Q2S	09/09/1997	0.11	5.0	<0.30	<0.09	–8.82	–99.4	–12.76
14N/3E-24Q2S	07/29/2000	0.10	4.2	<0.30	<0.09	–8.21	–97.8	–12.74
14N/3E-24Q3S	07/23/1997	—	—	—	—	—	–99.7	–12.75
14N/3E-24Q3S	09/10/1997	0.12	3.6	<0.30	<0.09	–8.74	–102.0	–13.25
14N/3E-24Q3S	07/27/2000	0.09	2.8	<0.30	<0.09	–8.11	–101.0	–13.41
14N/3E-24Q4S	07/24/1997	—	—	—	—	—	–94.8	–12.08

Table 3–1. Water-quality data for selected wells in Bicycle Basin at Fort Irwin National Training Center, California, 1993–2011.—Continued

[E, estimated; ft, feet; hhmm, hour minute; ID, identification; mm/dd/yyyy, month/day/year; R, reported by the U.S. Geological Survey (USGS) Stable Isotope and Tritium Laboratory; TU, tritium units; <, less than; —, no data]

State well number	Date (mm/dd/yyyy)	Carbon-14 counting error, percent modern carbon (P49934)	Carbon-14, percent modern carbon (P49933[1])	Tritium, in picocuries per liter (P07000)	Tritium, in TU	Carbon-13/carbon-12 ratio, per mil (P82081)	Deuterium/protium ratio, per mil (P82082)	Oxygen-18/oxygen-16 ratio, per mil (P82085)
14N/3E-24Q4S	09/10/1997	0.18	8.4	<0.30	<0.09	–8.51	–94.0	–12.01
14N/3E-24Q4S	07/29/2000	0.14	8.1	<0.30	<0.09	–7.42	–94.3	–12.11
14N/3E-24Q5S	07/24/1997	—	—	—	—	—	–95.0	–12.02
14N/3E-24Q5S	09/08/1997	0.14	7.1	<0.30	<0.09	–7.42	–94.4	–12.02
14N/3E-24Q5S	07/28/2000	0.11	6.1	<0.30	<0.09	–7.24	–92.9	–12.05
14N/3E-24Q5S	12/06/2011	—	—	—	—	—	–95.4	–11.97
14N/3E-26K1S	05/12/2011	0.10	10.8	R0.30	R0.09	–8.12	–95.1	–12.00
14N/3E-26K3S	12/08/2011	0.14	6.9	R–0.30	R–0.09	–7.11	–94.7	–11.87
14N/3E-26K4S	05/12/2011	0.10	11.3	R0.00	R0.00	–8.30	–95.0	–12.02
14N/3E-27E1S	11/29/1994	—	—	—	—	—	—	—
14N/3E-27E1S	02/08/1995	—	—	—	—	—	—	—
14N/3E-27E1S	05/04/1995	—	—	—	—	—	—	—
14N/3E-27E1S	05/08/1995	—	—	—	—	—	–85.6	–10.43
14N/3E-27E1S	08/09/1995	—	—	—	—	—	—	—
14N/3E-27E1S	11/07/1995	—	—	—	—	—	—	—
14N/3E-27E2S	11/29/1994	—	—	—	—	—	—	—
14N/3E-27E2S	02/08/1995	—	—	—	—	—	—	—
14N/3E-27E2S	05/04/1995	—	—	—	—	—	—	—
14N/3E-27E2S	08/09/1995	—	—	—	—	—	—	—
14N/3E-27E2S	11/07/1995	—	—	—	—	—	—	—
14N/3E-27E3S	11/28/1994	—	—	—	—	—	—	—
14N/3E-27E3S	02/08/1995	—	—	—	—	—	—	—
14N/3E-27E3S	05/04/1995	—	—	—	—	—	—	—
14N/3E-27E3S	08/08/1995	—	—	—	—	—	—	—
14N/3E-27E3S	11/07/1995	—	—	—	—	—	—	—
14N/3E-28A1S	11/29/1994	—	—	—	—	—	—	—
14N/3E-28A1S	02/09/1995	—	—	—	—	—	—	—
14N/3E-28A1S	05/05/1995	—	—	—	—	—	—	—
14N/3E-28A1S	08/09/1995	—	—	—	—	—	—	—
14N/3E-28A1S	11/08/1995	—	—	—	—	—	–87.5	–10.61

Table 3–1. Water-quality data for selected wells in Bicycle Basin at Fort Irwin National Training Center, California, 1993–2011.—Continued

[E, estimated; ft, feet; hhmm, hour minute; ID, identification; mm/dd/yyyy, month/day/year; R, reported by the U.S. Geological Survey (USGS) Stable Isotope and Tritium Laboratory; TU, tritium units; <, less than; —, no data]

State well number	Date (mm/dd/yyyy)	Carbon-14 counting error, percent modern carbon (P49934)	Carbon-14, percent modern carbon (P49933[1])	Tritium, in picocuries per liter (P07000)	Tritium, in TU	Carbon-13/carbon-12 ratio, per mil (P82081)	Deuterium/protium ratio, per mil (P82082)	Oxygen-18/oxygen-16 ratio, per mil (P82085)
14N/3E-28H1S	11/29/1994	—	—	—	—	—	—	—
14N/3E-28H1S	02/09/1995	—	—	—	—	—	—	—
14N/3E-28H1S	05/05/1995	—	—	—	—	—	—	—
14N/3E-28H1S	08/09/1995	—	—	—	—	—	—	—
14N/3E-28H1S	11/08/1995	—	—	—	—	—	—	—
14N/3E-28H2S	11/29/1994	—	—	—	—	—	—	—
14N/3E-28H2S	02/09/1995	—	—	—	—	—	—	—
14N/3E-28H2S	05/05/1995	—	—	—	—	—	—	—
14N/3E-28H2S	08/09/1995	—	—	—	—	—	—	—
14N/3E-28H2S	11/08/1995	—	—	—	—	—	—	—
14N/3E-35C1S	03/29/2000	0.20	11.5	<0.30	<0.09	–6.60	–92.3	–11.54
14N/3E-35C2S	07/31/2000	0.12	7.7	<0.30	<0.09	–5.43	–90.4	–11.06
14N/4E-18N1S	05/21/1993	—	—	—	—	—	–96.1	–12.49
14N/4E-18N1S	06/03/1993	—	—	—	—	—	—	—
14N/4E-18N1S	09/23/1993	—	[1]9.1	<0.30	<0.09	–9.20	–96.7	–12.49
14N/4E-18N1S	09/14/1994	—	[1]10.4	—	—	–8.50	–96.5	–12.44
14N/4E-18N1S	03/28/2000	—	—	—	—	—	–96.9	–12.32
14N/4E-18N1S	12/09/2008	0.09	8.2	R0.00	R0.00	–8.31	–97.5	–12.43
14N/4E-18N1S	12/01/2010	—	—	—	—	—	–97.7	–12.43

[1]Parameter code P82172, used prior to 1995, is described in the National Water Information System (NWIS) as carbon-14 age, apparent, dissolved, by liquid scintillation (analysis by University of Waterloo Isotope Lab).

Publishing support provided by the U.S. Geological Survey
Science Publishing Network, Sacramento Publishing Service Center

For more information concerning the research in this report, contact the
Director, California Water Science Center
U.S. Geological Survey
6000 J Street, Placer Hall
Sacramento, California 95819
https://ca.water.usgs.gov

ISSN 2328-0328 (online)
https://doi.org/10.3133/sir20185067

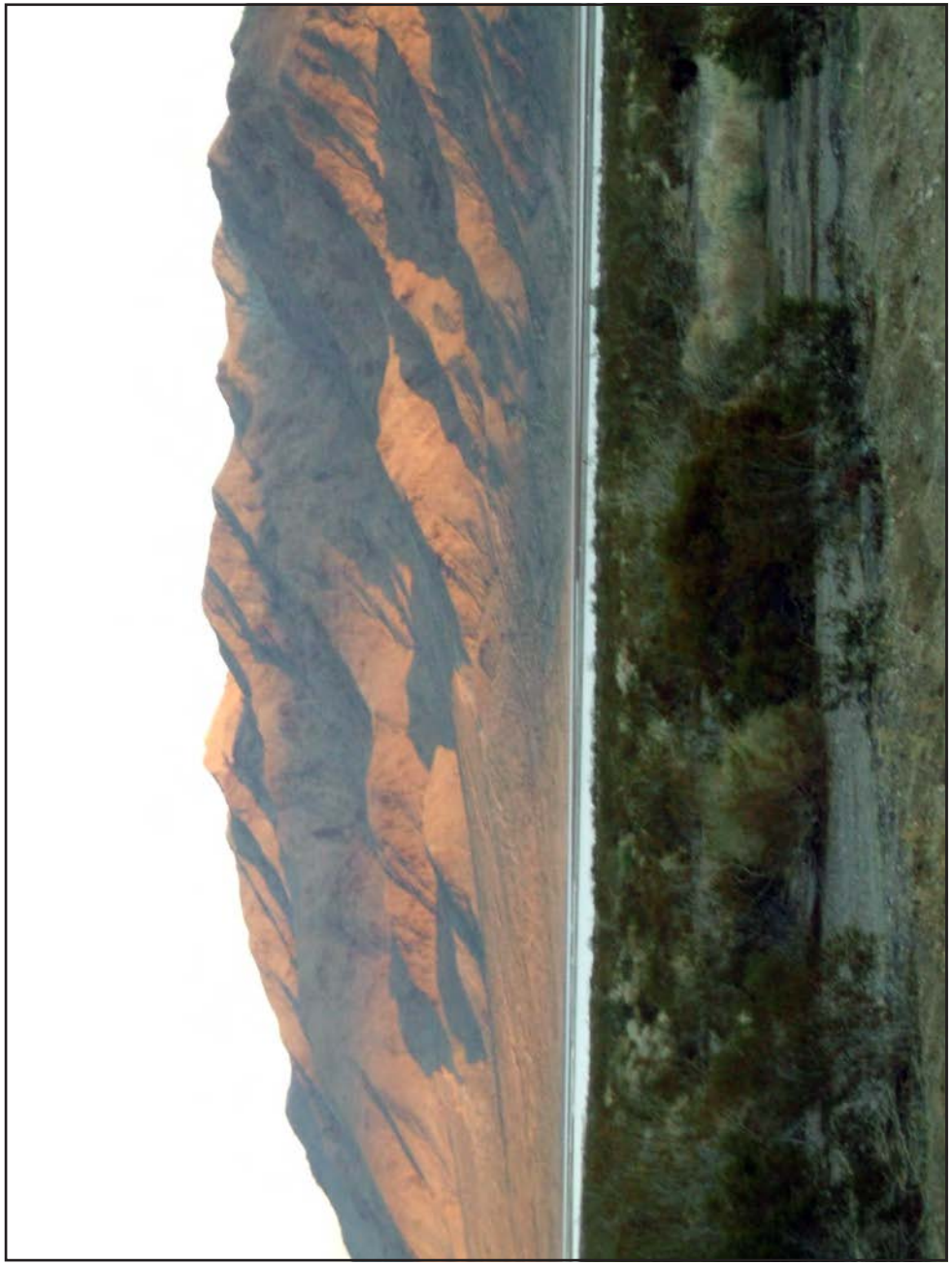

ISSN 2328-0328 (online)
https://doi.org/10.3133/sir20185067